ENERGY-FREE SYSTEMS

THEORY CONDITIONS AND DESIGN OF STRUCTURES THROUGH SEEKING MECHANISMS

JESSE FERBER

Energy-free Systems

Theory, conception, and design of
statically balanced spring mechanisms

Just Herder

Just as he was placing his camera in position, the sand at his feet began to move with a rustle. He drew his foot back, shuddering, but the flow of the sand did not stop for some time. What a delicate, dangerous balance!
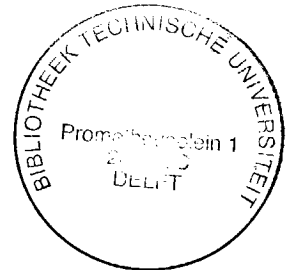
Kobo Abe, 1924

Energy-free Systems

Theory, conception and design of
statically balanced spring mechanisms

Proefschrift

ter verkrijging van de graad van doctor
aan de Technische Universiteit Delft,
op gezag van de Rector Magnificus prof. ir K.F. Wakker,
voorzitter van het College voor Promoties,
in het openbaar te verdedigen op dinsdag 27 november 2001 om 16:00 uur
door Justus Laurens HERDER,
werktuigkundig ingenieur,
geboren te Hengelo (O.)

iii

Dit proefschrift is goedgekeurd door de promotor:
Prof. ir J.C. Cool

Samenstelling promotiecommissie:
Rector Magnificus, voorzitter
Prof. ir J.C. Cool, Technische Universiteit Delft, promotor
Prof. dr ir A. de Boer, Universiteit Twente
Prof. dr ir J. van Eijk, Technische Universiteit Delft
Prof. dr C.M. Gosselin, Université Laval, Quebec, Canada
Ir P.V. Pistecky, Technische Universiteit Delft
Prof. dr ir C.J. Snijders, Technische Universiteit Delft
Prof. dr ir K. van der Werff, Technische Universiteit Delft

to my father

who was the spring to my technical interest. A dentist himself, he was known for his golden hands with which he fixed anything from a multisegmented bridge to an antique carriage clock, all with no apparent difficulty and remarkable quality. I never equaled his excellent marks for mechanics at highschool, yet he advised me to study mechanical engineering rather than follow his steps. So I did, and am now to become a doctor after all.

Contents

Preface

Es gibt Menschen, die immer nur wissen werden, was sein könnte, während die andren wie Detektive wissen, was ist. Die etwas Bewegliches bergen, wo die andren fest sind. Eine Ahnung von Andersseinkönnen. Ein richtungsloses Gefühl ohne Neigung und Abneigung zwischen den Erhebungen und Gewohnheiten der Welt. Ein Heimweh, aber ohne Heimat. Das macht alles möglich!

There are people, who will always only know, what 'could be', whereas the others know, like detectives, what 'is'. Who incorporate something agile, while the others are rigid. A notion of the different. An aimless feeling without preference or aversion between the world's elevations and the ordinary. A homesickness, but without a home. That makes everything possible!

Robert Musil, 1921

During numerous discussions with my supervisor Prof. ir Jan C. Cool, one thing became readily clear: there are always other possibilities. This holds true for the solutions to a particular problem, but, perhaps more importantly, also for the perspectives to regard this problem. For instance, in the analysis of the *spring butterfly* (figure 4.23), the approaches seemed innumerable. There we sat again around the low table in his office, on the edge of our seats, alternately surprised about yet another view to the same problem. A different force resolution yielded new insight, expressing moment-of-force in terms of area provided additional proof, a kinematic principle opened opportunities, geometry revealed another regularity prompting us to remark that had the Ancient Greeks known the helical spring and Newton's force, this thesis might have been written some twenty-two centuries ago. This process continued even when finding alternate perspectives seemed to have become something of a goal in itself. The conventional wells running dry, our paths drifted away, in a natural manner, into the unexplored; daydreaming about the yet non-existent rather than the application of established science and knowledge, exploring conceivable possibilities rather than sticking to reality. Sometimes even excursions into the impossible were useful to arrive at alternate solutions. This provided the breeding ground for the ideas and the objectives for the theoretical treatise in chapter three. Our goals inspired by the above process, a solid foundation was developed from well-accepted mechanics.

Perhaps rebelling against the conventions, but certainly with the conviction that it would yield simpler and lighter results, Jan advocated with passion, and

continues to do so, the essence of forces in mechanisms, and a force perspective in the design process. It takes time and effort to depart from education and habit dominated by a kinematic view, and to get a grip on its complementary part of mechanics. It was during the discussions at the low table, this time leaning back in the comfortable chairs, that this new ground was slowly developed. Again, the challenge was to break into the capacity of thinking anything that *could be*, and to value that what *is*, not more important than that what *is not*, a capacity Musil (1930) called Möglichkeitssinn (sense of the possible). His views on art: "Das Prinzip der Kunst ist unaufhörliche Variation", and on 'Menşch sein' (being human): "Die Aufgabe ist: immer neue Lösungen, Zusammenhänge, Konstellationen, Variablen zu entdecken, Prototypen von Geschehensabläufen hinzustellen, lockende Vorbilder, wie man Mensch sein kann", are readily paraphrased towards a design paradigm: 'The principle of design is ceaseless variation; the task is to discover ever new solutions, relations, arrangements, variables, to pursue prototypical lines of thought, to find attractive examples, about how a design could be made'. Sometimes, after a fortunate change of perspectives, the result came almost as a surprise. Rephrasing the question of eliminating the pivot in the basic equilibrator as: how to exchange the pivot *force* by a spring *force,* led to a solution (figure 5.13) within a week. The force directed design approach may be slightly overemphasized in this thesis, but this is justified by its simultaneous promise and underdevelopment to date.

I enjoyed the opportunity to learn regarding a problem from different perspectives while at the same time being receptive for the unexpected. Of course, now that some of the ideas have been put to paper, reality is gained and (day)dream is lost (Man hat Wirklichkeit gewonnen und Traum verloren; Musil, 1930). The sheets of this thesis reflect mainly results, rather than the mental excursions behind them, yet it is hoped they will stimulate similar undertakings on the verge of the known and the unknown, the possible and the impossible, the real and the surreal. This thesis aims at taking mechanical design a step further, perhaps a small one, certainly not the only one possible, but on reclaimed land.

Und der Detektivmensch hat sein Gesicht an seinen Fährten und braucht es nicht aufwärts zu heben. Aber Ich? Und du? Einer ist ein Narr, zwei eine neue Menschheit!

And the detective-person has his eye on his tracks and need not raise his look. But I? And you? One is a fool, two a new humankind!

Robert Musil, 1921

Reader's Guide

Although this thesis is primarily aimed at the design of statically balanced spring mechanisms and presents a framework for their conception, a theoretical treatise of statically balanced systems was developed in the course of this work. To obtain a logical order, the theoretical part is placed in the early chapters. However, the chapters are reasonably self-contained, so those readers who are initially more interested in the conceptional design may wish to omit chapter 3 and section 4.6 on first reading and can do so without reducing their enjoyment of the rest. Other readers may wish to read the chapters in the presented order. Anyhow, one will find that the earlier chapters provide the groundwork for chapter five, where most of the design takes place. Gravity equilibrators, spring force balancers, with or without fixed pivots, few or many degrees of freedom, as well as some remarkable geometric propositions will be derived in the course of this report.

The work presented in this thesis is to be attributed to the author, unless otherwise indicated. Work of others and contributions by others to this work have been referenced as conscientiously as possible. For instance, many of the working models have been detailed and manufactured by others, among them many students, while the working principle was conceived by the author. In these cases, the explanation of the working principle contains no references, while the desciption of the working model is referenced. Without any degradation of either's efforts, the cooperation in many of the graduation projects was such that the result can safely be called a co-production. In these cases, references to both the MSc-thesis and the scientific paper are included. To compromise the readability of the text no more than necessary, most references are included in endnotes at the end of this thesis, referred to by numbers between square brackets. For example, [3.2] would refer to endnote two of chapter three, to be found at the end of this volume, in this case page 197. Generally, endnotes provide background, detailed additional information, and justification, which is not essential for the continuation of reading.

All examples are depicted schematically and with exaggerated dimensions. To reduce the number of symbols in a sequence of drawings within one figure, the symbols of unchanged parameters are often omitted. Normal springs are mostly drawn as a zigzag line with circular loops at the ends of the spring. The special zero-free-length springs are drawn without spring loops to easily distinguish them from normal springs.

Each chapter is concluded with a short summary, highlighting the line of argument and the results of each chapter. Some of the individual chapters, especially chapters three and six, contain unanswered questions or issues not exhaustively treated, providing great scope for further work. Chapter seven will tie these leads together, highlight the relations between the chapters, and evaluate the design appoach used in this thesis.

Nomenclature

a	distance from a grounded pivot to a grounded spring attachment point
a_i	postion vector of a grounded spring attachment point relative to a fixed reference frame
$a_{i/c}$	position vector of a grounded spring attachment point relative to a local reference frame
A	fixed spring attachment point
A	matrix used to effect the planar form of vector multiplication
b	translation vector, translational dilatation
C	pivot point, origin of local reference frame
d	wire diameter of helical spring
D	diameter of circle, coil diameter of helical spring
e	unit vector
F	magnitude of force
F	force vector
g	accelleration of gravity
h	elevation over reference plane or datum
i	index, counter
I_c	mass moment of inertia with respect to point C
I_i	identity matrix of rank i
j	counter
k	spring stiffness
K	constant, amplitude of sine function
ℓ	actual length of spring
l	actual length vector
ℓ_0	free length of spring
L_0	initial length of spring
m	mass
M	mass matrix
n	number, total number
O	origin of fixed reference frame
p	fraction, spatial target trajectory of potential field
q	target trajectory in ground plane
P	point, pole
Q	point, coupler point

r	link length, distance from pivot to spring attachment point on the link
r_i	postion vector of a moving spring attachment point relative to a fixed reference frame
$r_{i/c}$	postion vector of a moving spring attachment point relative to a local reference frame
R	radius
$\boldsymbol{R}$	orthogonal rotation matrix
$\boldsymbol{S}$	tangent stiffness matrix
T	intersection of force action lines
u	skew coordinate
v	skew coordinate
V	potential, potential energy
W	work
x	orthogonal coordinate (abscissa)
y	orthogonal coordinate (ordinate)
z	orthogonal coordinate, vertical deflection
α	fixed angle, rotational dilatation, inclination angle
β	fixed angle, rotational dilatation
γ	angle between lines of action of forces, phase angle of sine function
θ	variable angle
κ	ratio of force magnitudes
λ	translational dilatation factor, magnification factor
π	polode
ρ	variable imaginary link length
Σ	summation from $i = 1$ to n
φ	variable angle
ϕ	variable angle
ψ	variable angle

1   Introduction

in which the aim of this study is stated, the design approach is introduced, the principle of static balance is elucidated, the importance of a force directed design approach is emphasized, limitations are indicated, and the structure of this thesis is outlined.

1.1   Motivation and objective

There is a delicate three-way balance between (i) a problem and its very nature, (ii) the inescapable principles that govern the problem and (iii) the method used to obtain a solution. So often we take the nature of the problem for granted and place it in too broad a category; then we uncritically accept some favourite method because some authority persuades us that it is foolproof and universal; so we can hop on a band-wagon named "routine", and we are spared the task of examining the relevant principles, even when they turn out to be extraordinary simple.

K. H. Hunt, 1986

A great number of mechanical devices use their energy inefficiently. This not only results in excessive energy consumption, but also in other undesired aspects of system behavior. For instance, an anthropomorphic robot arm with actuators at each joint will spend most of its energy on carrying its own weight [1.1]. Furthermore, heavy actuators are required, presenting an additional load to the arm, and challenging the safety of the system.

Great improvements in system behavior are possible when the energy flows and the configurations of forces are considered more carefully. It is unfortunate that the power systems in the appliances and machines around us are so common that their use is unquestioned, even though very often much more subtle and elegant solutions are possible. This thesis will investigate opportunities to conserve energy in mechanical systems, not only aiming at a reduction of energy consumption but also at the improvement of other aspects of system behavior, such as the force transmission quality, and the reduction of overall weight.

The study is motivated by the special demands imposed on assistive devices in rehabilitation technology, where decreased mechanical efficiency not only raises energy consumption, but also reduces the transmission of forces for the benefit of force feedback. An example from hand prosthesis design may elucidate the fact that rehabilitation aids often need unconventional solutions to make them operable. Hand prostheses (as all assistive devices, and indeed all

tools) should interact with their user in a natural way. To achieve this goal, they should simultaneously have good cosmetics, high wearing comfort and be easy to operate [1.2]. Ease of operation implies that they should function well (*i.e.* silent, fast, and with reliable motoric function), with low operating effort (in terms of energy, force, and excursion, but also in terms of mental load), and with good force feedback. The prevailing design solution for motoric function, an electric power system, is not satisfactory, firstly due to the weight of the motors, transmissions, and the battery, which conflicts with the demand for high wearing comfort, and secondly because feedback of the pinch force is absent, which complicates intuitive control. For these reasons, *body powered* prostheses are preferable, where healthy muscle groups operate the prosthesis and provide feedback [1.3].

Selecting a good principle, though essential, is not sufficient. Care must be taken that the forces are transferred from the prosthetic fingers via a transmission mechanism to the operating interface without distortion and that the operating effort remains within reason. Therefore, friction is to be avoided. Again, a conventional solution, *i.e.* the application of ball bearings to reduce friction, is undesirable in hand prosthetics, due to their weight and the limited space available, and secondly because playing with water and sand, among the favorite activities of many children, is disastrous for even sealed ball bearings. In addition to avoiding friction, the (visco-) elastic counteraction of the cosmetic covering should be eliminated [1.4]. This undesired spring force both raises energy consumption and reduces the force feedback because a component is added to the operating force, which has no relation with the pinch force. Unlike friction, the glove force is predominantly a *conservative* force and can therefore in principle be compensated (similar to the static balancing of undesired mass by means of a counterweight).

Although inspired by design in the field of rehabilitation technology, it will become clear that there is great application potential in general mechanical engineering for the approach assumed in this thesis, since systems with reduced energy consumption and pure transmission of forces will generally perform better, while control is simplified, accuracy is improved, manufacturing cost is cut, weight is reduced, and safety is easier guaranteed. It is expected that each of these features will rapidly gain importance not only due to natural resources running out, globalization and increasing competition, but also due to the growing attention for the user-friendliness of appliances.

In summary, the approach in this thesis follows from the desire to design mechanical systems with exceptional energy-efficiency. To this end, the forces are to be transferred without loss or distortion, undesired non-conservative

forces for instance due to friction should be eliminated, while undesired conservative forces such as elastic counteraction, magnetic influences or gravity should be compensated. Simultaneously, care must be taken that the result will be lightweight, simple, and reliable. These and similar considerations (both product and use-related) have led to the line of thought assumed throughout this thesis. The next section will outline the main guiding principles of the proposed design approach.

1.2   Design approach

Quale è stato il principio fondamentale di tutte le mie realizzazioni? Si spiega con una sola parola: -Semplicità- portata all'estremo possibile.

What is the fundamental principle of all my creations? That comes down to a single motto: -Simplicity- pushed to the farthest extremes.

Fabio Taglioni, In: Cathcart 1983

This section will present the main principles guiding the design in this thesis: the principle of statically balanced mechanisms incorporating springs will be introduced; the concept of force directed design will be outlined; and it will be argued that rather than one method, the alternation between the different perspectives of energy, force, and stability, and between general and particular approaches is vital to arrive at good designs.

Statically balanced systems

Particularly suited to serve the objectives of this thesis are statically balanced mechanisms [1.5, 1.6]. A statically balanced system is a system in static equilibrium throughout its range of motion, rather than in a single position or a limited number of positions only, under the condition of the absence of friction. Different kinds of statically balanced systems can be distinguished (see chapter two). This thesis will prefer the use of springs to other energy storage devices, as these seem most appropriate to arrive at lightweight and low-friction solutions. Even though helical extension springs may lack safety in case of coil breakage, they are preferred to compression springs for their less cumbersome mounting, and because of the low-friction rolling contact on the inside of the spring loop when arranged properly [1.14].

Statically balanced systems can be investigated from three different perspectives. The *continuous equilibrium* as mentioned in the definitions is a first one. Secondly, the continuous equilibrium results in *constant total potential energy* as the system moves. Consequently, quasistatic (or kinetostatic) motion requires no operating effort, even though the system

3

behavior is dominated by forces and energy flows. Thirdly, it is noted that although not unstable, a statically balanced system cannot be considered stable either, as it has no preferred position. It is just in between stable and unstable, a state also called *neutral equilibrium* or *neutral stability*. These three features (continuous equilibrium, constant potential, and neutral stability), are equivalent in that they comply with the same principles of mechanics, yet provide different valuable perspectives, which will all be used in this thesis.

In reality, quasistatic motion and friction-free mechanisms can only be approximated. Therefore, even systems with perfectly constant potential energy will require operating effort for acceleration and deceleration, and for overcoming the resistance due to friction or viscosity. When friction is present, the existence of many equilibrium positions does not necessarily imply a constant potential energy function. When the aim of a design is to attain many equilibrium positions, such as in cheap desk lamps, friction can be very useful. This thesis, however, will be devoted to those applications such as in rehabilitation technology, where friction is to be avoided since low operating effort and pure force transmission are principal issues. To emphasize this main interest, the term *energy-free system* is introduced, indicating the idealized situation of friction-free mechanical systems with perfectly constant potential energy. However, the terms statically balanced, indifferent, neutral equilibrium, and energy-free are used indiscriminately throughout this thesis denoting the same kind of idealized system behavior: systems with constant potential energy, considered in quasistatic motion, without friction or other energy dissipating phenomena.

Force directed design

Another prominent notion will be the consideration of forces early in the conceptional design phase. Classically, in the design of mechanisms, desired motion characteristics are specified first. Then a topology of the mechanism is selected (*e.g.* a four-bar linkage or a cam) and the dimensions of the elements are determined by kinematic synthesis or optimization techniques [1.7]. Finally, actuators are added to effect the desired motion under loaded conditions. The distribution of internal forces is calculated only to avoid overloading or excessive deformations. As desired motion is taken as point of departure, this approach can be called *motion directed design*. In substantial parts of the mechanical design practice, this approach is undisputed.

In rehabilitation technology, or more generally in application fields where humans interact with machines, it is virtually inevitable to consider the forces in an early phase of the design. Precise motions are often of less concern than

matters like stability, low force levels, force distribution, force transmission and force feedback. Matching the characteristics of human and machine requires a comprehensive approach in which forces play an essential role. Furthermore, weight and energy-efficiency, especially in rehabilitation aids, are of primary concern. Since in classical mechanism design the matter of adding actuators is often implicitly considered trivial (required torques are calculated and suitable actuators are selected after the design of the motion mechanism) this is not likely to result in the most lightweight and energy-efficient design. For these reasons, it is more natural to start the design with the specification of profitable configurations of forces or desired force transmission characteristics. This approach, taking profitable configurations of forces as the point of departure, is called *force directed design* [1.8]. Several projects in the medical field have demonstrated the usefulness of the force directed design approach [1.9]. However, it is evident that force directed design has wider application potential and yields similar advantages outside rehabilitation technology, as will be illustrated by a number of examples in the following chapters.

Force directed design is not and is not intended to be a method in the sense of a recipe that needs only to be followed to end up with a solution. It is a *way of thinking* which by no means aims to exclude the designer's creativity from the design process. On the contrary, it requires the ability of assuming an unusual perspective, which in turn tends to enhance the generation of alternative solutions, and often favors simplicity and efficiency of the resulting products. The usual tendency to neglect friction is substantially reduced, and undesired forces are less likely taken for granted. Instead, it becomes obvious to introduce forces in the design, for instance to oppose these undesired forces, or to perform certain tasks such as providing a contact force or eliminating backlash.

Not a general method

The third guiding principle adopted in this thesis is *not* to strive for a *general design method*. Essentially, one may argue, the design of statically balanced mechanisms comes down to matching the energy characteristics of the potential energy storage devices involved. Indeed, calculating the energy transfer function required to match these characteristics usually is fairly straightforward, but this is not at all true for deriving a mechanism fulfilling this required transfer function. Methods generating a mechanism from given specifications tend to come up with complex linkages incorporating many links or cams, usually unsuitable for the application in rehabilitation aids [1.10]. This approach may be characterized as top-down: finding *particular* solutions from a *general* theory.

Tempting as it may be, this approach as a *design* perspective is disregarded here in favor of the opposite approach.

This thesis will start with the derivation of very elementary *particular* arrangements of statically balanced systems and investigate their behavior at a fundamental level. To this end, a specific branch of mechanics will be investigated closely. The approach in this *analytical* phase may be regarded top-down, but one should bear in mind that the aim of this phase is to gain insight in the nature of energy-free systems. Subsequently, the path of *design* is treaded, where a bottom-up approach will be employed. In this synthetical phase, a number of logical rules are derived to modify, simplify or expand the original elementary configuration, for instance to be able to match other potential energy characteristics. Thus, the family of working designs is expanded. This approach may be characterized as bottom-up, *generalizing* from *particular* solutions. It is argued that the bottom-up way of working yields more basic insight, and results in much simpler designs. Primarily based on a potential energy perspective, a framework for the design of energy-free systems is put up. However, following the conception in this manner, a force analysis will prove to be essential for the design, and in many cases lead to more profitable embodiments. Thus, the conceptional designs come to being by alternating synthesis and analysis efforts, potential energy and force perspectives.

As argued previously, the approach assumed in this thesis is not intended as a method in the sense of a recipe but merely as a line of thought. The insight in the coherence of the elements of a particular solution, or of a composition of particular solutions, is used to modify, expand or simplify a certain configuration. In this thesis, energy, force and stability perspectives will alternate continuously. In fact, this is part of the creative aspect of the design approach proposed. Consequently, there are no recipe-rules for this, but many examples are provided to illustrate possible procedures.

Limitations

This section will elaborate on a number of restrictions imposed on this thesis. The issues of static balancing, linear extension springs, low friction solutions, and simplicity will be addressed successively.

Static balancing should be well distinguished from *dynamic balancing* or *(shaking) force balancing*, where the aim is to eliminate the reaction forces and torques transmitted to the frame of a machine due to the motion of a constituent mechanism [1.11]. This kind of dynamic balancing indeed implies static balancing. However, if dynamic balance is not required, static balancing alone allows much more profitable engineering solutions. For instance, shaking force

balancing generally requires the addition of counterweights or at least the redistribution of system weight, whereas static balance can be achieved by the use of springs, which results in a more lightweight and compact system. It is also immediately admitted that there are many phenomena and applications in the dynamic domain that could benefit from the design for constant energy, such as the design of oscillating systems [1.12]. Although the term energy-free is not restricted to static systems, its dynamic equivalent will not be considered.

It is also readily acknowledged that statically balanced spring mechanisms may very well be realized by using other than helical extension springs. Several applications of torsion springs are known to give good results [1.6]. Furthermore, an ocean of opportunities for spring force compensation is waiting to be explored in the rapidly developing field of *compliant mechanisms* [1.13]. Many of these mechanisms are begging to be balanced. In principle, any element with potential energy storage capacity can be used to realize statically balanced systems. However, it is felt that one step should be taken at a time. The complexity of compliant mechanism design, for instance, might otherwise throw a veil over the clear principle of static balancing. This thesis is therefore constrained to linear springs, as these provide the simplest working principles.

Due to the nature of neutral equilibrium, the focus of attention will be on conservative forces, such as elastic and gravitational forces, but non-conservative forces will not be neglected. Especially Coulomb friction is consistently taken into account. Low friction is essential for the proper functioning of energy-free systems. For instance, a passive spring force compensation system which eliminates one undesired influence (the parasitic spring force) while introducing another (friction) is not of much use. The practical consequences of this obvious statement are easily underestimated, yet it is probably one of the main reasons for the scarse application of even the simplest gravity equilibrators [1.15]. Whenever hinges are indispensable, the application of low-friction *rolling-link mechanisms* will be considered [1.14]. The application of rolling links in balanced spring mechanisms is particularly fruitful as the forces present can be used to secure the contact between the members of the rolling mechanism.

For a variety of reasons, such as reliability, low friction, low weight and low cost, balanced spring mechanism should be simple, especially the compensation type [1.10]. When it is assumed that the task of an engineer consists of creating a *concept*, determining optimal *forms* for the parts, and selecting appropriate *materials* and associated production techniques [1.16], the term simplicity can be used as a subjective measure incorporating the number of parts and their practical embodiment, the complexity of the parts' shapes, the manufacturing

difficulty, and the exoticness of the materials used. A four-bar linkage, for instance, simple as it may seem in a diagram, should already be considered too complex for the application in a hand prosthesis: in practice it incorporates a multiple of four parts, while the bearings with fork-shaped supports require more space and material than is desirable, and lead to unfavorable force transmission paths (see also endnote [1.14]). In the case of balanced systems, the *simplicity* of the design (in terms of number, complexity and material of the parts) will have to be weighed against the balancing *accuracy* (in terms of theoretical transfer function as well as deviation due to friction) and the *reliability* (in terms of wear and risk of breakdown). Sometimes a simple but approximate balancing mechanism is preferable to a complex one with closer to perfect balance. This is not always a regrettable compromise, as sometimes function or control benefits from non-perfect balance, see for instance the Wilmer arm orthosis described in the next chapter (figure 2.6). As another example, in balancing the hood of a car, the spring mechanism is usually designed such that it approximately counterbalances the weight of the hood in the middle range of its motion. When the hood is up, the spring overcounterbalances, and when the hood is down the spring undercounterbalances [1.17]. Thus, although this study concentrates on perfect or optimal balancing, it should be kept in mind that this might be too much of a good thing in many cases. Yet, it seems a good idea to start with the design of a perfect balancer and deviate from this as desired.

1.3   Outline

It was as though the world no longer contained anything certain. There were only unstable elements; everything had been cut free, was floating.

Paul Bowles, 1967, p131

Although design was the principal goal of this thesis, ideas of a more general nature emerged in the course of the project, which eventually led to a theory on equivalent forces. This theory has developed simultaneously with the conception of particular designs, or even lagged behind. However, the sequence of subjects in this thesis will be logical, rather than chronological.

Chapter two will start with an overview of some interesting examples of energy-free systems from literature. This overview does not claim completeness but aims to demonstrate the often-unexpected phenomena which can be realized using the concept of static balance. Subsequently, chapter three will treat static

balance as a special state of motion, investigate the fundamental principles governing static balance, and derive a particular solution of an energy-free system. Chapter four will review this particular solution and use it as the basis for a framework of design rules. The framework will be put to use in chapter five, which will present a variety of perfectly balanced spring mechanisms. Chapter six will be devoted to situations where approximate static balance is obtained. Finally, chapter seven will summarize the findings of this thesis.

1.4　Summary

The present thesis is primarily concerned with the design of *statically balanced systems*, briefly defined as friction-free mechanical systems with perfectly constant potential energy. These systems are in static equilibrium throughout their range of motion and can therefore be operated quasistatically without operating effort. For this reason, they will be called *energy-free systems*.

The study is motivated by the special demands made on assistive devices in rehabilitation technology. The design approach in this thesis stems from the desire to design mechanical systems with high energy-efficiency and good force-transmission quality, and is characterized by several principles. One basic consideration to obtain simple designs adopted in this thesis is *not* to strive for a *general design method*. Fundamental understanding often is facilitated and inspired by the close inspection of particular solutions or working prototypes. This thesis will therefore start with the derivation of a very elementary *particular* arrangement of a statically balanced system and investigate neutral equilibrium at a fundamental level. Subsequently, a number of logical rules are derived to modify, simplify or expand the original arrangement. Another consideration is that in rehabilitation technology, or more generally, in application fields where humans interact with machines, or in fact, mechanical engineering in general, it is worthwhile to consider *force directed design*. Matching the characteristics of human and machine requires a comprehensive approach in which forces play a key role. It is a *way of thinking* which by no means aims to exclude the designer's creativity from the design process.

Based on the notions mentioned above, energy-free systems incorporating helical springs will be concerned, aiming at simple low-friction mechanisms with perfect or near perfect static balance. The fundamental principles will be investigated, a framework for the conceptional design will be put up, and perfect as well as approximate energy-free systems will be designed.

2 Balancers

in which known examples of statically balanced systems are given, ranging from ancient gravity equilibrators, via magnetic force balancers, to the spring force compensators which are the main subject of this thesis, while at the end a listing of principal features is provided.

2.1 Introduction

I play with arrangements of weight and distance that lie on the brink of instability to achieve slow, lyrical motions; a one-way swing in one of my sculptures takes 20 seconds or longer. Such arrangements possess another noteworthy attribute: when the distribution of weight approaches instability, the forces needed to set the pendulum in motion diminish to almost nothing. A breeze that softly stirs leaves can also move a sculpture weighing 500 kilograms. Control of weight and balance - and also of time - gives me a means of expression comparable to color for a painter or sound for a composer.

George Rickey, 1993

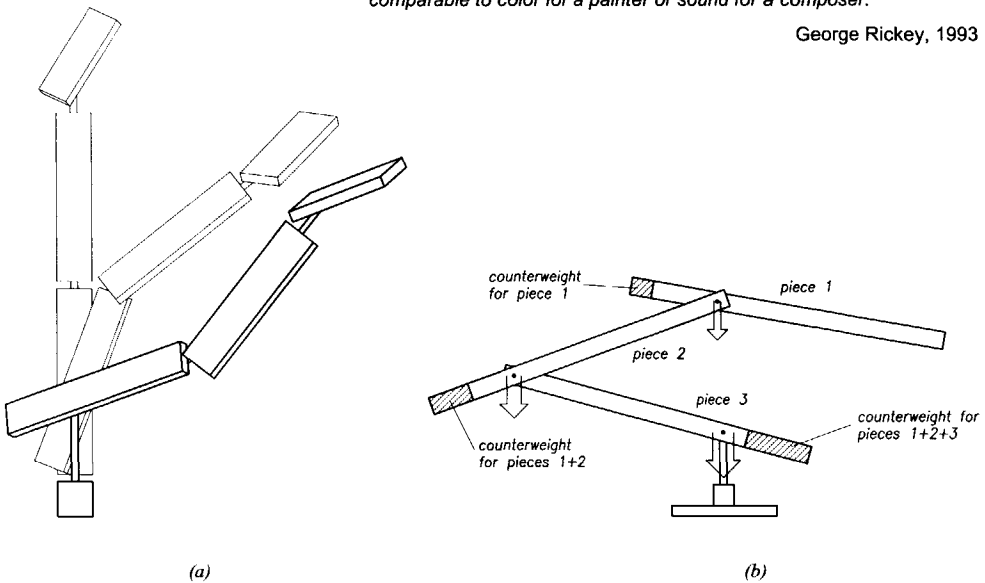(a)   (b)

Figure 2.1   George Rickey's Breaking Column incorporates three counterbalanced pieces that trace out conical motions. An almost exactly even distribution of weight allows them to respond to the slightest wafts of air, tracing slow, unpredictable but expressive convolutions [2.1]: *(a) three respective positions of the Breaking Column, (b) schematic representation of the working principle.*

The continuous equilibrium of energy-free systems has induced many applications. Once part of our daily life, statically balanced systems are hardly

noticed, since they make many appliances function as they should. Almost without notice we adjust our desk lamps or open the hood of an automobile. Newly confronted with them however, many are surprised and fascinated by their working principle. Stunned by the *Kinetic Art* of George Rickey (figure 2.1, see also section 2.2 and [2.1]), for instance, many spectators wonder where the motors are hidden. Yet, the gentle movement of all of these mechanisms is based on the redistribution of potential energy *within* the system, because of which only little external energy is required (see next section). This chapter will give some examples, not aiming at completeness, but to stir the imagination.

Static balancers can be categorized according to the forces to be balanced (weight, spring force, other conservative forces) and the balancing principle (counterweight, springs and others). Section 2.2 will be concerned with balancing undesired weigth by means of counterweigths. Section 2.3 will give examples of balancing undesired weigth by other means, such as springs, and will also discuss static balancing of undesired forces other than weight, such as magnetic forces. Finally, section 2.4 will concentrate on balancing undesired spring forces by means of springs.

2.2   Counterweighting

Also, the linkage has the ability to support a weight from the moving point of interest with an equal balance as the point moves along [a straight line]. "This gives the mechanism powers of neutral equilibrium".

J. Daniel, cited in N. P. Chironis, 1961

There are numerous examples of statically balanced mechanisms, most of which make use of counterweights to equilibrate undesired weight [1.5]. With the proper counterweight, the system is in equilibrium in any position. When a counterbalanced beam rotates non-horizontally in the gravity field, gravity potential is exchanged between the balanced mass and the counterweight. When the mass is lifted, the counterweight will drop, and vice versa, resulting in constant potential energy.

One of the oldest examples reported from ancient history is the *mechane*. This device was used in the classic Greek theater to bring, as by miracle, the gods or the heroes of the tragedy on stage. It has long been a mystery how the proverbial *Deus ex Machina* actually worked, since the appearance of the hero was supposed to come as a complete surprise for the audience in the amphitheater. According to the reconstruction by Dimarogonas (figure 2.2
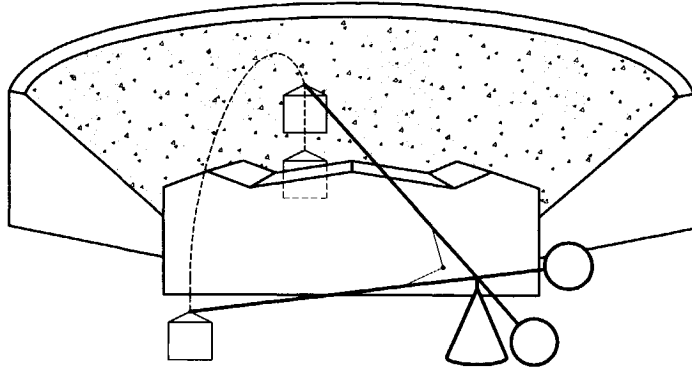
12

Figure 2.2   Deus ex Machina. Reconstruction of the 'mechane' for the Athens theater of Dionysos [2.2].

and [2.2]), the mechane most likely comprised of a beam, pivoted behind the *scene*-buildings so that it was invisible until the desired moment. A single person could operate it since it was balanced by a counterweight, and guided in its movement by ropes. In all its simplicity, the mechane incorporates all the features of statically balanced systems, and illustrates their merits.

In Rickey's *Kinetic Art* (1993), several balanced beams are stacked on one another. The counterweight of each beam needs to be sufficient to balance its own weight as well as the total weight of the beam(s) it is supporting (figure 2.1b). Smart use is made of the fact that the supporting force for each beam is constant, regardless of the orientation of the beam, and can therefore be considered a constant additional load to the beam underneath. As a
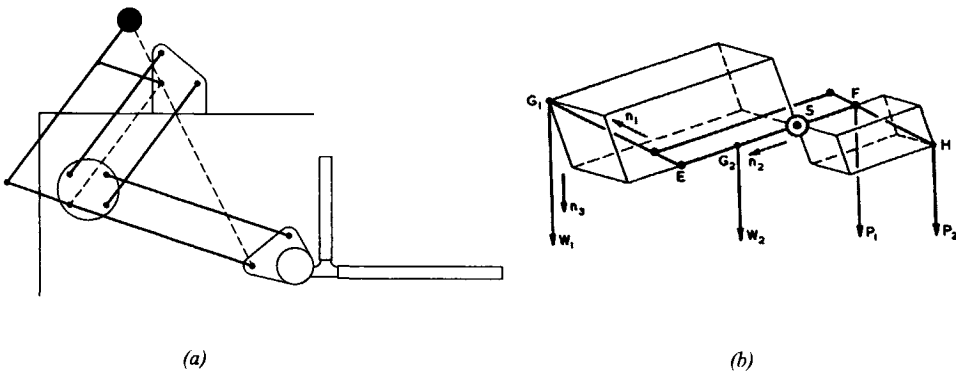

(a)   *(b)*

Figure 2.3   Counterweighting of a moving mass: (a) drafting machine [2.3], *where link mass is neglected, (b) spatial balance* [2.4].
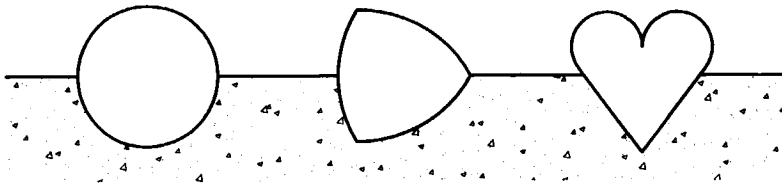
Figure 2.4   Prismatic bodies with specially shaped cross-sections exhibit neutral-equilibrium behavior when floating in a fluid. For the cylinder (or ball), the density of the fluid may have any value, for the other shapes, the fluid density must be twice the density of the floating body [2.5].

consequence, the successive beams from top to base must be increasingly heavy, yet all pieces are shaped with similar outward appearance to delude the spectator.

A well-known balancing mechanism is present in classic drafting machines, where the planar movement of the mass of the rules and their rotating and guiding mechanism is completely balanced by a single counterweight (figure 2.3a, [2.3]). The same principle is applied in other embodiments, such as the spatial balance in figure 2.3b, designed for use as a mobile arm support for people with reduced muscular ability [2.4]. Here, the parallelogram linkage is materialized in a spatial form. In both cases, the working principle is based on the kinematic action of a pantograph linkage (see also chapter five and endnote [5.8]). The moment arms of the weight forces, though variable, keep a constant ratio. Therefore, equilibrium is maintained throughout its range of motion.

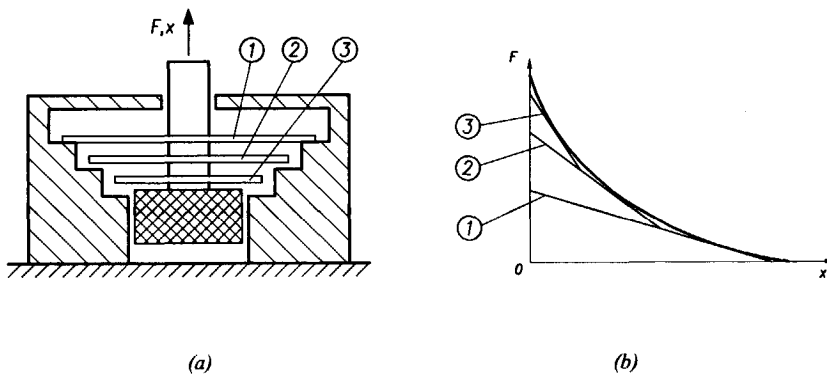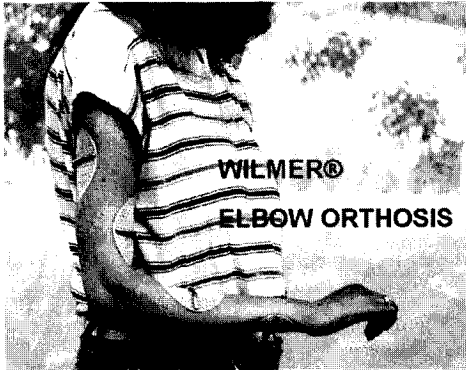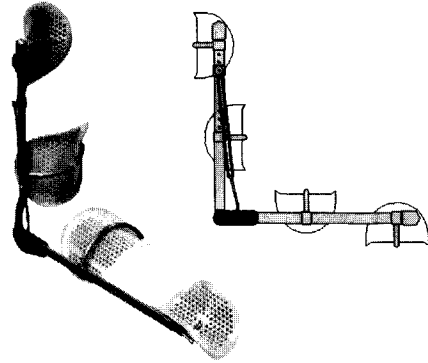(a)   (b)

Figure 2.5   Internally-balanced magnet: (a) basic structure, (b) force-displacement relationship of the multi-stage spring unit compared to the magnet's characteristic [2.6].

14

(a) *(b)* *(c)*

Figure 2.6   Elbow orthosis [2.7], [5.1]: *(a) hardly visible when worn by a user, (b) orthosis in locked position, (c) diagram of working principle, showing the O-ring spring.*

2.3   Other balancing principles

A cylinder of density 0.5 having one of the above cross-sections will float without turning over, in whichever postion it may be.

R. D. Mauldin, In: Wells, 1995

Although balancing of masses by means of counterweights is most common, many more physical phenomena and mechanical components can, in the appropriate arrangement, provide statically balanced systems. In these cases energy is exchanged between various kinds of energy storage devices, rather than between masses only. A well-known principle is the balancing of weight by means of springs [1.6]. This section will present a number of examples incorporating less common balancing principles.

Perhaps a special case of mass balancing is realized by floating prismatic bodies with specially shaped cross-sections and with half the density of the fluid they are floating in. They can be oriented arbitrarily and rotated with no effort, despite the continuously changing pressure distribution on their surfaces, due to their constant 'diameter' (figure 2.4, [2.5]).

An unusual example of static balancing is the *internally-balanced magnet,* intended for robots climbing metal walls (figure 2.5, [2.6]). This design was triggered by the desire to avoid energy-consuming electromagnets in favor of permanent magnets. In combination with a balancing mechanism, the strong action of the permanent magnet can easily be switched on (or off) by moving

15

Figure 2.7 Anglepoise desk lamp [2.8]: (a) original type 1227 version, (b) historical advertisement emphasizing effortless operation.

the magnet towards (or from) the metal wall with negligible operating effort. The apparent contradiction of strong sticking force between the foot and the wall, and low operation force F is understood if one realizes that when the device has been switched on, the magnet's sticking force is transmitted from the wall via the springs to the climbing robot's foot. As the magnet is released towards the wall, the plate springs are stressed. The energy stored in the springs is recovered when the magnet is pulled back, thus assisting the operator.

An important field of application of balanced systems is present in rehabilitation aids, where weight and low operating effort are essential features. Based on the simple principle of balancing the forearm weight by means of a rubber spring, a highly appreciated elbow orthosis has been developed (figure 2.6, [2.7], [5.1]). Advantage has been taken from the phenomenon that in the equilibration of a mass by means of a spring, the orientation of the spring system with respect to the acceleration of gravity affects the balance. Due to a slight underbalance and an automatic locking mechanism, the movement of the elbow can be controlled by the shoulder: lifting the arm sideways reduces the influence of gravity on the forearm so that the spring now overcompensates and moves the arm until it is locked at a 90 degrees position. Lifting the arm again releases the elbow lock and the arm can be stretched again. Noteworthy is the
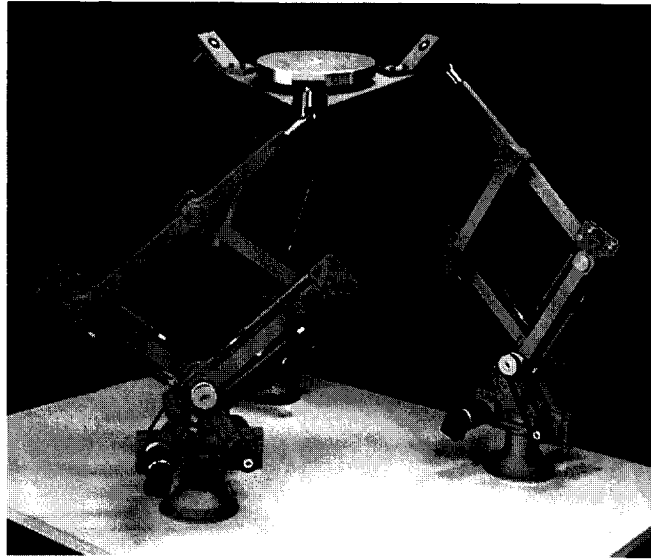
*Figure 2.8   Statically balanced parallel manipulator* [2.9].

fact that, because the external forces are in a single plane, the elbow joint is not loaded by torsional moments in spite of the single-sided construction, which both reduces weight, takes away statical indeterminacy, improves its cosmetic appearance and wearing comfort, and facilitates putting on the device and taking it off.

An example of the exact spring balancing of weight is the *Anglepoise* desk lamp (figure 2.7, [2.8]). Under the proper conditions regarding the link geometry and the choice of the springs (to be explained in section 5.2), this lamp can be moved with negligible effort to any position, where it will remain, in spite of its low friction. If the lamp, for instance, is lowered, gravity potential of the links and the lampshade is converted into elastic energy in the springs, which is released again when the lamp is raised. Unlike many other spring-balanced desk lamps, this design functions almost perfectly, so much so that it tends to act as a leveling instrument.

A similar balancing principle was applied in a six degree-of-freedom parallel manipulator (figure 2.8, [2.9]), which was developed for use in motion simulators. The moving platform is carried in any position by the three spring-actuated legs using parallelogram linkages, so that the actuators only need to accelerate and decelerate the system. As the desired accelerations are considerable, springs were preferred to the use of counterweights.
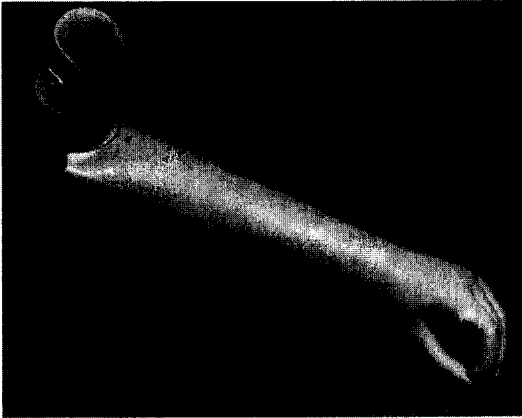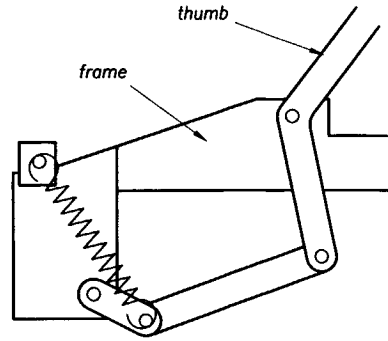
(a)   *(b)*

Figure 2.9   Cosmetic glove compensation: (a) prosthesis for hand and forearm, with cosmetic glove [1.2; 1.4], *(b) working principle compensation mechanism* [1.6; 2.10].

2.4   Spring force compensation

Why it wasn't invented sooner is a question that will never be answered. But why and how it works can be determined from elementary mechanics.

Arthur D. Brickman, 1976

This thesis particularly aims at the design of systems in which one spring statically balances another, or several other springs. This kind of balancing is called spring force compensation or spring-to-spring balancing. Although less in number than counterweighting systems, several interesting examples of this balancing principle exist.

To attain an inconspicuous appearance, hand prostheses are supplied with a flexible covering, the *cosmetic glove*. Unfortunately, this glove counteracts the movement of the prosthesis' fingers so forcefully, that many children are not able to entirely open their artificial hand (figure 2.9). The glove counteraction consists of an elastic and a viscous component [1.4]. In principle, the elastic component of this counteraction can be balanced by a spring mechanism. This *compensation device* is to deliver the energy required to open the prosthesis against the action of the glove, and to recover the elastic potential that is released by the glove when the prosthesis closes again. Perfect compensation would thus cancel the need for operating energy during free movement of the

18
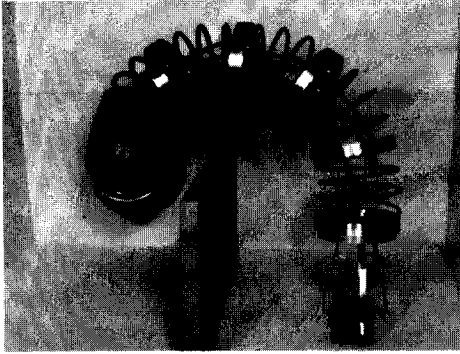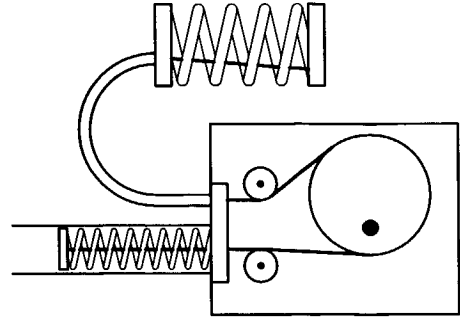
(a)   (b)

Figure 2.10   Elastor, serpentine flexible robot arm: (a) curved arm with gripper, (b) working principle of the compensation mechanism [2.11].

prosthesis: the elastic influence of the glove would be fully eliminated, as if there were no glove present. Although practical applications are impeded by the viscoelastic properties of the glove's material and the strongly non-linear glove characteristics, the operating effort can be reduced significantly [2.10].

A second example of a spring-to-spring balancing arrangement is found in the *Elastor,* a biologically inspired robot design (figure 2.10, [2.11]). The *Elastor* is a compliant structure, consisting of a series of eight helical compression springs, separated by metal rings. Each compression spring can be buckled in any direction by pulling one or two of three strings attached to each ring. Thus, by pulling the appropriate strings, the whole column can assume almost any desired shape. Relatively small actuators (three for each segment) with low power consumption suffice, thanks to the fact that the buckling force of the helical compression spring is compensated. To realize this, each string is connected to a compensatory spring via an adjustment mechanism, consisting of an eccentrically pivoted pulley. This mechanism provides approximate balance.

A special case of spring-to-spring balancing is present in the redistribution of elastic tension in special construction elements. In the following examples, elastic potential is not exchanged between distinct elements but redistributed within a single element (figure 2.11). A loop in an otherwise stretched hose can be moved back and forth effortlessly, regardless of the pressure inside the hose [2.12]. A similar phenomenon is applied in the Rolamite [2.13], a configuration of two rollers and two parallel support planes, kept together by a flexible band. The moments due to the bending of the band around the rollers
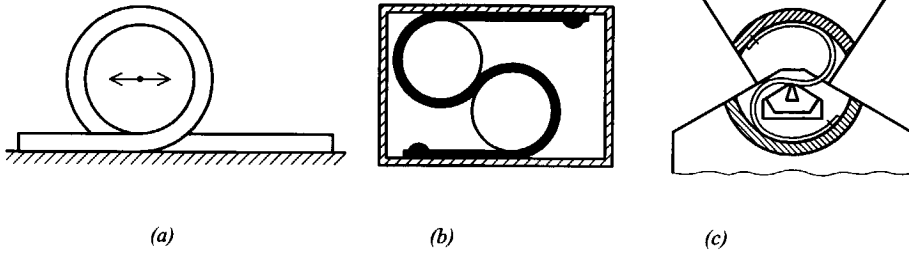
19

<div align="center">(a)   (b)   (c)</div>

Figure 2.11   Redistribution of elastic tension: (a) hose with a loop [2.12], *(b) the Rolamite* [2.13], *(c) pre-loaded knife edge pivot* [2.14].

cancel out and a low-friction neutral-equilibrium mechanism remains. A similar principle is used to obtain electrical continuity and a constant preload in a knife edge pivot [2.14]. Also neutral equilibrium compliant mechanisms can be regarded as spring mechanisms that redistribute elastic tension during motion [2.15].

2.5   Features

> *Although there are many advantages, the inclusion of compliance provides several challenges in mechanism analysis and design. Because energy is stored in the flexible members, energy is no longer conserved between the input and output ports of the mechanism.*
>
> M.D. Murphy, A. Midha, L.L. Howell, 1996

The explorative journey above yields a listing of the distinctive features of statically balanced systems, as presented below.

Compensation of undesired forces. A first feature is the possibility to eliminate the influence of previously existing undesired conservative forces, such as the weight of a robot arm, the counteraction of the cosmetic glove in hand prostheses, or the elastic forces in compliant mechanisms [1.13]. The undesired force is not eliminated but its effect is offset. Therefore, this feature will be denoted by the term *compensation*.

Energy-free motion. Statically balanced systems can be moved in the presence of considerable conservative forces, and yet they require no operating force or energy. Energy exchange between the energy storage elements within the system is perfect, so the only external energy demand is to make up for losses, and to accelerate and decelerate the mechanism. In many mechanical systems, such as industrial robots, the static gravity load takes up the major part
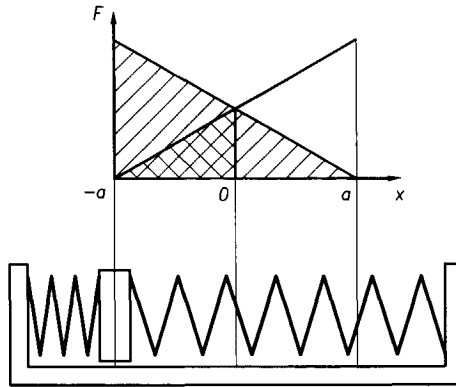
Figure 2.12   Energy exchange between two springs in a parallel arrangement. The area with the /// hatching represents the elastic energy present in the left spring in the drawn situation of the springs, whereas the area with the \\\ hatching represents the energy transferred into the previously relaxed spring in the central position. Note that in an idealized dynamic situation, with a mass between the springs, the system will oscillate.

of the energy consumption [1.1]. Also for people with reduced muscular capacity, assistive devices taking up the gravity forces allow them to employ their remaining force for useful tasks, rather than carry their own weight.

Full energy exchange. To state it explicitly, balanced mechanisms make possible the full energy exchange between several energy storage devices, with no operating effort during quasistatic motion. This is not at all trivial. For instance, consider two equal springs, arranged according to figure 2.12 rather than in a neutral equilibrium configuration. When one spring, containing energy, is quasistatically released against the other, unloaded spring, only a quarter of the loaded spring's elastic potential is transferred to the unloaded spring, while half of the original elastic energy is dissipated (or transformed into kinetic energy [1.12]).

Improved information transmission. In manually operated instruments, such as body powered hand prostheses and surgical forceps, the elimination of undesired forces, such as weight or undesired spring forces, not only reduces operating effort, but also improves feedback: analogue information present in the magnitude of the forces is transmitted without distortion through the mechanism.

Energy-free force control. A balanced spring mechanism can be moved without effort under the influence of a number of springs. The forces in the fixed points of the springs can be put to use, for instance in a clamp function. As the clamping force can be controlled without any operating effort (neither

force nor energy), a balanced spring mechanism can provide infinite force amplification $F_{out} / F_{in} = F_{clamp} / F_{operate} = \infty$. Thus, energy-free force control is possible when the attachment point of the force controlled is stationary (as is the case when clamping a rigid object).

Elimination of backlash. In specific cases it is advantageous to introduce forces to prestress a mechanism or to secure contact between parts [2.16]. In particular, rolling-link mechanisms [1.14] can benefit from the addition of springs in a statically balanced arrangement. Spring forces can be added in a neutral equilibrium configuration so that they have no influence on the force transfer function, yet keep the rollers together.

Zero stiffness. Another feature of statically balanced systems is that they possess zero stiffness, which makes them useful in vibration isolation [2.17]. By non-complete balancing, a system's natural frequency can be altered, which can be useful in the tuning of ballistic systems [2.18].

Neutral buoyancy. By using gravity equilibrators, forces due to gravity are compensated. This allows zero-gravity simulation, for instance for space research applications. Often neutral buoyancy is achieved in special water tanks but the inertia and viscosity of water can drastically affect system dynamics, while the solution of a control scheme to compensate for gravity requires the system designed for space to be strong enough to operate under 1-g conditions [2.19].

Improved performance. In general, precision of operation is enhanced if loading characteristics are reduced [2.20]. Furthermore, if undesired forces are eliminated, smaller actuators are needed (if any), the whole construction can become more light-weight, and control is simplified, which all leads to improved performance, decreased power consumption and reduced heat rise [2.21].

Inherent safety. Finally, the fact that statically balanced mechanisms are in equilibrium when unactuated presents a form of safety. For instance, in an electrically powered robot arm with passive gravity balancing, a power failure does not result in a dramatic breakdown of the mechanism.

Disadvantages may be that in the case of balancing pre-existing systems, additional parts will be introduced. It is therefore proposed to incorporate static balance from the start of the design process. A disadvantage of using springs rather than counterweights in the case of gravity compensation may be the fact that a vertical reference is needed. Furthermore, the pivot force in mass-to-mass balancing is always vertical, which reduces the need for a large, heavy, or fixed support. In some applications, the potential energy present in the system is increased, which may be undesirable.

2.6 Summary

This chapter illustrated the wide variety of applications for static balancing. While far from complete, a number of often unexpected possibilities were reviewed. Numerous instruments, machines and appliances benefit from static balance. They share natural behavior and self-evident operation. Due to their comforting and reassuring action, their working principle is easily overlooked or undervalued. Simultaneously, the application of static balance sometimes seems to have been forgotten. Undesired counteraction, for instance due to system mass, remains unquestioned while static balancing allows the effortless lifting of weights. In principle, any conservative force can be equilibrated. Static balancing can thus solve many problems which initially may seem unsolvable, as for instance in the internally balanced magnet.

Advantageous features of statically balanced systems include the following: compensation of undesired forces, energy-free motion, full energy exchange, improved information transmission, energy-free force control, elimination of backlash, zero stiffness, neutral buoyancy, improved performance, and inherent safety.

3   Fundamentals

in which the governing principles of planar neutral-equilibrium force systems are investigated by considering the contribution of forces to the state of motion of a rigid body, both to the nominal state and to the stability of the nominal state, resulting in a method for finding dynamically equivalent resultant forces, as well as an elementary neutral equilibrium spring mechanism which will serve as starting point for the conception framework as presented in chapter four [3.1].

3.1   Introduction

Vectors are equal if both vectors have the same magnitude and both are pointing in the same direction. (...) Note that we do not demand that both vectors are in exactly the same position in space. This definition is strictly only valid for free vectors. (...) It is unfortunate, but nonetheless a fact, that forces cannot generally be considered as free vectors.

P.E. Lewis and J.P. Ward, 1989, p6/15

Neutral equilibrium is a special state of motion, where every configuration of a system is a static equilibrium position, and hence stability is zero. This can be illustrated by the equilibrium of two forces. It is well known that a system of two forces is in equilibrium when these forces are equal in magnitude, opposite in direction, and share their line of action, irrespective of the location of their points of application on this line. However, when concerned with stability, the application points gain vital importance. Therefore, forces cannot be considered as free vectors, not even as sliding vectors, but need to be considered as bound vectors. This chapter will investigate the stability of rigid bodies in 2D.

The important role of the points of application of forces regarding the stability will be illustrated by considering an unconstrained rigid body, subject to two forces (figure 3.1a). The Newton-Euler equations of motion for this body read:

$$\Sigma F_i = m\ddot{r}_c \tag{3.1}$$

$$\Sigma\left(Ar_{i/c}\right)^T F_i = I_c\ddot{\varphi} \tag{3.2}$$

where F_i is an external force acting on the body, m is the mass of the rigid body, $\ddot{r}_c$ is the acceleration of the center of mass, I_c is the mass moment of inertia about C, and $\ddot{\varphi}$ is the rotational acceleration of the rigid body. The vector notation is as follows. A vector r_i is the position vector of the point of application P_i of the force F_i, expressed in the global coordinate system,
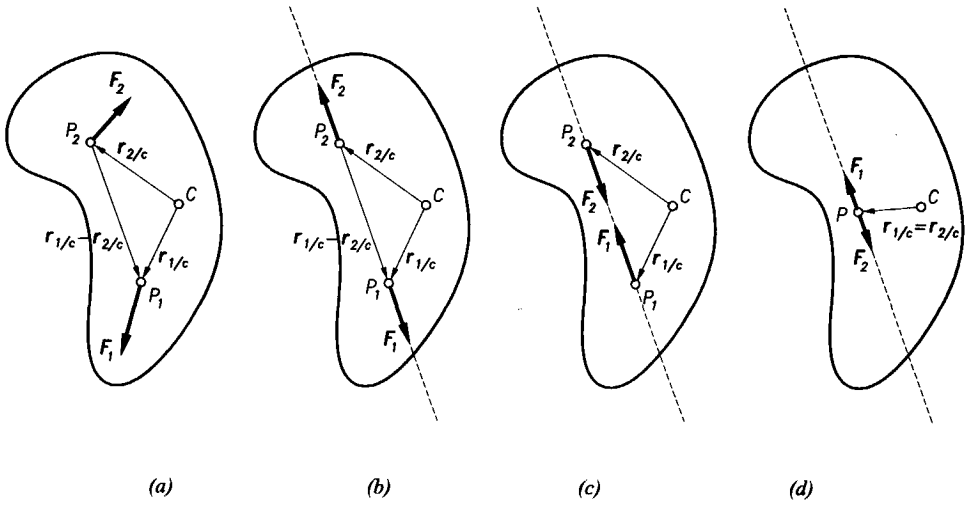
Figure 3.1   Two-force systems: (a) general case, (b) stable equilibrium, (c) unstable equilibrium, (d) neutral equilibrium.

whereas $r_{i/c}$ denotes a postion vector relative to a point C of the rigid body. In this example, the center of mass is taken for point C. The subscript ^{T} denotes transposition, and the matrix A, which reads:

$$A = \begin{bmatrix} 0 & -1 \\ 1 & 0 \end{bmatrix} \tag{3.3}$$

is used to effect the planar form of the vector multiplication $r_i \times F_i$. It is noted that the summation convention is not used, but individual variables are considered. Furthermore it is noted that vectors and matrices are typed in boldface, in the text as well as in the figures.

For equilibrium, the accelerations $\ddot{r}_c$ and $\ddot{\varphi}$ need to be zero. This results in the following set of equations:

$$F_1 + F_2 = 0 \tag{3.4}$$

$$\left(Ar_{1/c}\right)^T F_1 + \left(Ar_{2/c}\right)^T F_2 = 0 \tag{3.5}$$

From equation 3.4 it is seen that $F_1 = -F_2$. Substituting this into equation 3.5 yields:

$$\left(A\left(r_{1/c} - r_{2/c}\right)\right)^T F_1 = 0 \tag{3.6}$$

This expression is true if F_1 and therefore also F_2 are directed along the vector connecting their application points $r_{1/c} - r_{2/c}$. However, the sense of the forces is still undetermined, so different equilibrium configurations are possible: the

26

one where the forces point away from each other (figure 3.1b), the one where the forces point towards each other (figure 3.1c), and also the one where the points of application coincide (figure 3.1d).

To investigate the stability of the obtained equilibrium configurations, small variations about the equilibrium position are considered. The equations of motion for variations about the equilibrium position follow from the equations 3.1 and 3.2 through expansion according to:

$$\Sigma F_i + \left(\Sigma F_i\right)_{,r_c} \Delta r_c + \left(\Sigma F_i\right)_{,\varphi} \Delta\varphi = m\ddot{r}_c + m\Delta\ddot{r}_c \tag{3.7}$$

$$\Sigma\left(Ar_{i/c}\right)^T F_i + \left(\Sigma\left(Ar_{i/c}\right)^T F_i\right)_{,r_c} \Delta r_c + \left(\Sigma\left(Ar_{i/c}\right)^T F_i\right)_{,\varphi} \Delta\varphi = I_c\ddot{\varphi} + I_c\Delta\ddot{\varphi} \tag{3.8}$$

where the comma in the index denotes differentiation, for instance $_{,\varphi}$ is short for $\partial/\partial\varphi$. As the equilibrium is characterized by equations 3.1 and 3.2, the equations for the small variations alone read:

$$\left(\Sigma F_i\right)_{,r_c} \Delta r_c + \left(\Sigma F_i\right)_{,\varphi} \Delta\varphi = m\Delta\ddot{r}_c \tag{3.9}$$

$$\left(\Sigma\left(Ar_{i/c}\right)^T F_i\right)_{,r_c} \Delta r_c + \left(\Sigma\left(Ar_{i/c}\right)^T F_i\right)_{,\varphi} \Delta\varphi = I_c\Delta\ddot{\varphi} \tag{3.10}$$

where Σ indicates summation, in this case from $i = 1$ to 2. These equations show that the forces and moments must be differentiated with respect to the position and orientation of the rigid body, r_c and φ, respectively, implying that the *character* of these forces affects the result. Considering forces of constant magnitude and direction simplifies the equations considerably. Each term F_i is independent of r_c and φ, while each term $\left(Ar_{i/c}\right)^T F_i$ is dependent on φ only. Consequently, equations 3.9 and 3.10 reduce to:

$$m\Delta\ddot{r}_c = 0 \tag{3.11}$$

$$I_c\Delta\ddot{\varphi} - \left(\Sigma\left(Ar_{i/c}\right)^T F_i\right)_{,\varphi} \Delta\varphi = 0 \tag{3.12}$$

Evidently, translations about the equilibrium position have no influence. However, rotations do affect the equilibrium. Using the coordinate systems in figure 3.2, any point of the rigid body P_i can be expressed relative to an arbitrary point C of the rigid body:

$$r_i = r_c + r_{i/c} = r_c + R r'_{i/c} \tag{3.13}$$

where the accent-mark $'$ indicates that a vector is expressed in the local coordinate system associated with the rigid body (figure 3.3); and where R is the orthogonal rotation matrix:

$$R(\varphi) = \begin{bmatrix} \cos\varphi & -\sin\varphi \\ \sin\varphi & \cos\varphi \end{bmatrix} \tag{3.14}$$
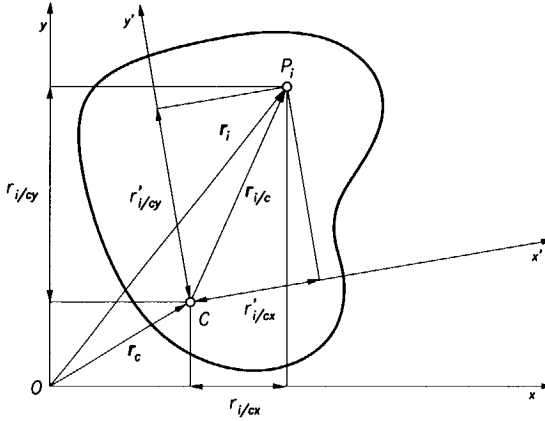
Figure 3.2   Local (x', y') and global (x, y) coordinate systems.

The term $-\left(\Sigma(A\mathbf{r}_{i/c})^T \mathbf{F}_i\right)_{,\varphi}$ can now be elaborated as follows:

$$-\left(\Sigma(A\mathbf{r}_{i/c})^T \mathbf{F}_i\right)_{,\varphi} = -\Sigma\left(\mathbf{F}_i^T R_{,\varphi}\mathbf{r}'_{i/c}\right)_{,\varphi} = -\Sigma \mathbf{F}_i^T R_{,\varphi\varphi}\mathbf{r}'_{i/c}$$

$$= -\Sigma \mathbf{F}_i^T R_{,\varphi\varphi} R^{-1} \mathbf{r}_{i/c} = \Sigma \mathbf{F}_i^T \mathbf{r}_{i/c} \qquad (3.15)$$

where the identities $R_{,\varphi\varphi} = -R$, $R^{-1} = R^T$, and $RR^T = I$ are used. For the two forces in the example of figure 3.1bc, where the forces are equal, opposite, and collinear, this term becomes:

$$\Sigma \mathbf{F}_i^T \mathbf{r}_{i/c} = \mathbf{F}_1^T \mathbf{r}_{1/c} + \mathbf{F}_2^T \mathbf{r}_{2/c} = \mathbf{F}_1^T\left(\mathbf{r}_{1/c} - \mathbf{r}_{2/c}\right) = \pm Fr \qquad (3.16)$$

where $F = |\mathbf{F}_1|$ and $r = |(\mathbf{r}_{1/c} - \mathbf{r}_{2/c})|$. Depending on the sense of the forces, this term can be positive or negative. When $\mathbf{F}_1$ and $\mathbf{r}_{1/c} - \mathbf{r}_{2/c}$ have the same sense, as in figure 3.1b, the term is positive. Hence, the solution of the harmonic equation 3.12 is a harmonic function having a natural frequency:

$$\omega_n = \sqrt{\frac{Fr}{I_c}} \qquad (3.17)$$

which implies a stable equilibrium. When $\mathbf{F}_1$ and $\mathbf{r}_{1/c} - \mathbf{r}_{2/c}$ have opposite senses, the term $\Sigma \mathbf{F}_i^T \mathbf{r}_{i/c}$ is negative, which introduces an exponential function with a negative and a positive power of ω_n in the solution of equation 3.12, resulting in unstable equilibrium. In the case of coincident points of application (figure 3.1d), the term $\Sigma \mathbf{F}_i^T \mathbf{r}_{i/c}$ reduces to zero, yielding indifferent equilibrium for rotation, in addition to the indifference for translation as previously found. Hence, the equilibrium is indifferent for translations and rotations, a state called
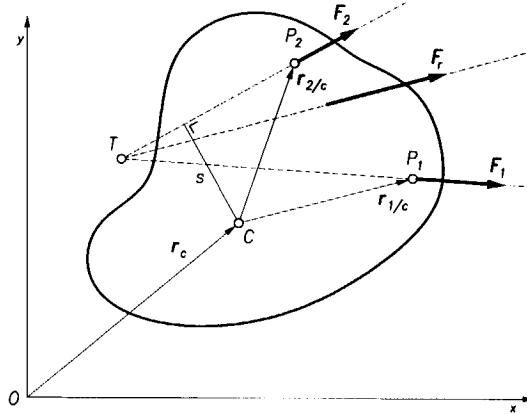
28

Figure 3.3   The resultant force F_r of two forces F_1 and F_2 may apply anywhere on its line of action to yield instantaneous equivalence.

neutral equilibrium. The above treatise clearly illustrates that the points of application of the forces determine the stability of the equilibrium.

The systems dealt with in this thesis typically incorporate at least three forces: two external forces (spring forces or gravity forces) and a support force. One way of investigating the stability of such a three-spring system is to compose two of these three forces into one resultant force. This would yield one of the force systems of figure 3.1, so the stability can be determined. Clearly, for this approach to be effective, the point of application of the resultant force needs to be determined. However, even though in planar mechanics it is common practice to compose two forces acting on a rigid body into a single resultant force (figure 3.3 [3.2]), this procedure does not yield a point of application for the resultant force, because usually the contribution of this force to the *equilibrium* is considered, rather than the contribution of this force to the *stability of the equilibrium*. For this reason, a force composition technique will be derived in this chapter, which is not only equivalent with respect to the *instantaneous* or static influence of a force on a rigid body, but also for the *dynamic* influence or the stability contribution. The resultant force found will be called the *dynamically equivalent (resultant) force* (DEF), while its application point will be called the *dynamically equivalent application point* (DEP) [3.3].

From the notion that the dynamically equivalent resultant force should have the same contribution to the stability of a rigid body as the original forces, additional conditions will emerge which uniquely pinpoint the dynamically

29

equivalent force on its line of action. This chapter will first review the conventional static force composition from the perspective of *same contribution* (section 3.2). Static equilibrium will be regarded as a special case of the *nominal state* of motion of a rigid body in the planar case, which will be described using the Newton-Euler equations of motion, the principle of virtual work, and the energy potential [3.4]. Although principally equivalent, all of the three methods mentioned will be used, as each provides specific advantages. Subsequently, section 3.3 will consider small variations about the nominal state, in order to investigate *the stability of the nominal state*. Again the stability of static equilibrium will be treated as a special case of motion, and the contribution of forces to this state of motion will be investigated. This will lead to a procedure for the composition of two forces into a resultant force which is equivalent to the original two forces with respect to stability, including equations for the point of application of the dynamically equivalent force for the cases of constant forces and central linear forces. In addition to this, section 3.3 will present the derivation of an elementary statically balanced spring mechanism. Finally, section 3.4 will present a graphical interpretation of the findings.

3.2   Statically equivalent force

Befindet sich der Körper im Gleichgewicht, so ist die Resultierende gleich Null, und daher muss bei einer gedachten unendlich kleinen Verrückung, welche mit den geometrischen Bedingungen des Systems zu vereinbaren (virtuell) ist, die Arbeit der äusseren Kräfte gleich Null sein. Dieser Satz darf auf endliche Verrückungen ausgedehnt werden wenn der Körper auch in der neuen Lage im Gleichgewicht ist.

When the body is in equilibrium, the resultant force is equal to zero. Therefore, the work done by the external forces due to a infinitesimal displacement, which is in accordance with the geometric constraints of the system (virtual), must be zero. This principle may be extended to finite displacements when the body is in equilibrium also in the new position.

K. Lachmann, 1929

In statics, a force F_r is called the resultant force of two forces F_1 and F_2 if, firstly, its contribution to the force system acting on a rigid body is equal to the contribution of the original forces and, secondly, the moment contribution of the resultant force about an arbitrary point C of the rigid body is the same as the contribution of the original forces [3.4]:

$$F_r = F_1 + F_2 \tag{3.18}$$

$$\left(A\mathbf{r}_{r/c}\right)^T \mathbf{F}_r = \left(A\mathbf{r}_{1/c}\right)^T \mathbf{F}_1 + \left(A\mathbf{r}_{2/c}\right)^T \mathbf{F}_2 \qquad (3.19)$$

The use of the well-known equations 3.18 and 3.19 is usually restricted to situations of static equilibrium, as in section 3.1. However, the remainder of this section will use these not only to investigate the equilibrium situation, but any nominal state of motion, including dynamic motion. To this end, the *contributions* of a force $\mathbf{F}_i$ to the equations of motion of a rigid body, the virtual work done on the rigid body, and the potential energy of this force will be regarded successively. At this stage, the use of three approaches may seem overdone, but the following section will follow up on all of them. Furthermore, in particular cases the one approach will turn out to be more convenient than the other.

Equations of motion

Equations 3.18 and 3.19 are valid with respect to any point C on the rigid body. If now the center of mass of the rigid body is selected for C, the Newton-Euler equations of motion can be used to investigate the conditions under which a force $\mathbf{F}_r$ is equivalent to the two forces $\mathbf{F}_1$ and $\mathbf{F}_2$ together. In matrix form, the equations of motion for a rigid body due to n forces yield:

$$\begin{bmatrix} m\mathbf{I}_2 & 0 \\ 0 & I_c \end{bmatrix}\begin{bmatrix} \ddot{\mathbf{r}}_c \\ \ddot{\varphi} \end{bmatrix} - \begin{bmatrix} \Sigma \mathbf{F}_i \\ \Sigma (A\mathbf{r}_{i/c})^T \mathbf{F}_i \end{bmatrix} = 0 \qquad (3.20)$$

Suppose that $\Sigma \mathbf{F}_i$ includes $\mathbf{F}_1$ and $\mathbf{F}_2$ among other forces, and $\Sigma (A\mathbf{r}_{i/c})^T \mathbf{F}_i$ includes their moment contributions $(A\mathbf{r}_{1/c})^T \mathbf{F}_1$ and $(A\mathbf{r}_{2/c})^T \mathbf{F}_2$, among other terms. Then a single force $\mathbf{F}_r$ has the same contribution to the nominal state of motion, as represented by equation 3.20, under the following conditions:

$$\mathbf{F}_r = \mathbf{F}_1 + \mathbf{F}_2 \qquad (3.21)$$

$$\left(A\mathbf{r}_{r/c}\right)^T \mathbf{F}_r = \left(A\mathbf{r}_{1/c}\right)^T \mathbf{F}_1 + \left(A\mathbf{r}_{2/c}\right)^T \mathbf{F}_2 \qquad (3.22)$$

Clearly, this results in the conditions already given in equations 3.18 and 3.19. This prooves that the resultant force $\mathbf{F}_r$ found above is indeed equivalent to $\mathbf{F}_1$ and $\mathbf{F}_2$ together, not only in static equilibrium but also in any nominal (dynamic) state of motion. To emphasize this capacity, the resultant force $\mathbf{F}_r$ will be called the *instantaneously equivalent force*, rather than the statically equivalent force.

Virtual work

Equations 3.18 and 3.19 can also be derived using the principle of virtual work. This is particularly illustrative as the moment equation 3.19 manifests itself in a

very natural manner. The virtual work δW_i done by a force F_i acting at point P_i amounts to:

$$\delta W_i = F_i^T \delta r_i \tag{3.23}$$

where δr_i is the virtual displacement. Expressed in the virtual displacement of the center of mass δr_c and the virtual rotation $\delta \varphi$ of the body, the virtual displacement reads:

$$\delta r_i = \delta r_c + R_{,\varphi} r'_{i/c} \delta \varphi = \delta r_c + R_{,\varphi} R^{-1} r_{i/c} \delta \varphi = \delta r_c + A r_{i/c} \delta \varphi \tag{3.24}$$

where it is noted that $\partial r'_{i/c} = 0$ for a rigid body.

A force F_r is instantaneously equivalent to two forces F_1 and F_2 if the virtual work done by F_r is equal to the virtual work done by F_1 and F_2 together:

$$F_r^T \delta r_r = F_1^T \delta r_1 + F_2^T \delta r_2 \tag{3.25}$$

Substituting equation 3.24 gives:

$$F_r^T \delta r_c + F_r^T A r_{r/c} \delta \varphi = F_1^T \delta r_c + F_1^T A r_{1/c} \delta \varphi + F_2^T \delta r_c + F_2^T A r_{2/c} \delta \varphi \tag{3.26}$$

As this equation must be valid for any possible δr_c and $\delta \varphi$, the following set of relations results:

$$F_r = F_1 + F_2 \tag{3.27}$$

$$F_r^T A r_{r/c} = F_1^T A r_{1/c} + F_2^T A r_{2/c} \tag{3.28}$$

Rearranging the latter expression gives:

$$\left(A r_{r/c}\right)^T F_r = \left(A r_{1/c}\right)^T F_1 + \left(A r_{2/c}\right)^T F_2 \tag{3.29}$$

Thus, together with equation 3.27, a set of equations equal to the set of equations 3.18 and 3.19 results.

Potential energy

In a third and final way, the instantaneously equivalent force can also be found using the potential energy method, which in some cases leads to a solution in a more direct and convenient way. Using this method, the motion of a rigid body is investigated by examining the total potential of the forces acting on the body. The potential exists only in case the forces are conservative. In the case of a rigid body, only the potential of the external forces is to be concerned, so the equations of motion can be written as follows:

$$\begin{bmatrix} m I_2 & 0 \\ 0 & I_c \end{bmatrix} \begin{bmatrix} \ddot{r}_c \\ \ddot{\varphi} \end{bmatrix} - \begin{bmatrix} V_{,r_c} \\ V_{,\varphi} \end{bmatrix} = 0 \tag{3.30}$$

where V is the total potential, and $V,_{r_c} = \Sigma F_i$ and $V,_\varphi = \Sigma (A r_{i/c})^T F_i$. When V_i is the potential due to an external force F_i, the following expression can be formulated:

$$dV_i = F_i^T dr_i = F_i^T (dr_c + R,_\varphi r'_{i/c} d\varphi) = F_i^T (dr_c + A r_{i/c} d\varphi)$$

$$= F_i^T dr_c + F_i^T A r_{i/c} d\varphi \qquad (3.31)$$

By definition, this implies that the contribution to the state of motion of the force F_i with respect to translation and rotation, respectively, is given as:

$$(V_i),_{r_c^T} = F_i \qquad (3.32)$$

$$(V_i),_\varphi = F_i^T A r_{i/c} = (A r_{i/c})^T F_i \qquad (3.33)$$

In case it is now desired that the contribution to the state of motion of a resultant force F_r is equal to the contribution of two given forces F_1 and F_2, then the contributions $(V_r),_{r_c}$ and $(V_r),_\varphi$ due to F_r must equal the contributions $(V_1),_{r_c} + (V_2),_{r_c}$ and $(V_1),_\varphi + (V_2),_\varphi$ due to F_1 and F_2, respectively, which leads to:

$$F_r = F_1 + F_2 \qquad (3.34)$$

$$(A r_{r/c})^T F_r = (A r_{1/c})^T F_1 + (A r_{2/c})^T F_2 \qquad (3.35)$$

These equations are equal to the equations derived using the equations of motion and the principle of virtual work.

3.3   Dynamically equivalent force

The principle of transmissibility states that the conditions of equilibrium or motion of a rigid body will remain unchanged if a force F acting at a given point of the rigid body is replaced by a force F' of the same magnitude and same direction, but acting at a different point, provided that the two forces have the same line of action. The two forces F and F' have the same effect on the rigid body and are said to be equivalent.

F.P. Beer and E.R. Johnston Jr., 1997, p73

In the previous section, three approaches were used to find two conditions for a force F_r to be *instantaneously* equivalent to two given forces F_1 and F_2: the vector equation 3.18 determines the magnitude and direction of the force F_r, whereas the line of action of the force F_r is determined by the scalar equation 3.19. However, equations 3.18 and 3.19 do *not* determine the point of application of the force F_r (figure 3.3). This is not important for the

contribution to the nominal state, but for the *stability* of the nominal state, the point of application of a force is essential. In addition to the example of figure 3.1, this is demonstrated in the equilibrium position of a pendulum, which is stable, whereas the equilibrium position of the inverted pendulum is unstable. Yet the lines of action of the forces are identical for both of the equilibrium positions, and equations 3.18 and 3.19 apply in both systems. Therefore, it is essential that (*instantaneous*) equivalence (as considered in many textbooks) is well distinguished from *dynamic* equivalence. A resultant force will be considered dynamically equivalent to a system of forces acting on a rigid body if the contributions of the resultant force and the original system of forces to the *stability* of the body are equal.

To investigate the stability of the nominal state of a rigid body in the two-dimensional case, this section will consider small variations about the nominal state of the body. Again, different methods will be used to assess the conditions under which a single force is equivalent to two given forces, this time with respect to stability. Conditions will be found, additional to equations 3.18 and 3.19, which will be called the *stability equations*.

The equations of motion for variations about the nominal state of motion were given in equations 3.7 and 3.8. The equations for the variations alone, in matrix form, read:

$$\begin{bmatrix} mI_2 & 0 \\ 0 & I_c \end{bmatrix}\begin{bmatrix} \Delta\ddot{r}_c \\ \Delta\ddot{\varphi} \end{bmatrix} + \begin{bmatrix} -(\Sigma F_i)_{,r_c} & -(\Sigma F_i)_{,\varphi} \\ -\Sigma\left((Ar_{i/c})^T F_i\right)_{,r_c} & -\left(\Sigma(Ar_{i/c})^T F\right)_{,\varphi} \end{bmatrix}\begin{bmatrix} \Delta r_c \\ \Delta\varphi \end{bmatrix} = 0 \qquad (3.36)$$

where the first matrix is the mass matrix *M*, and the second is the tangent stiffness matrix *S*.

Alternatively, the variations about the nominal state of motion can be investigated using the potential energy method. To this end, equation 3.30 can be expanded according to:

$$\begin{bmatrix} mI_2 & 0 \\ 0 & I_c \end{bmatrix}\begin{bmatrix} \Delta\ddot{r}_c \\ \Delta\ddot{\varphi} \end{bmatrix} + \begin{bmatrix} -V_{,r_c r_c} & -V_{,r_c \varphi} \\ -V_{,\varphi r_c} & -V_{,\varphi\varphi} \end{bmatrix}\begin{bmatrix} \Delta r_c \\ \Delta\varphi \end{bmatrix} = 0 \qquad (3.37)$$

The tangent stiffness matrix *S* found this way must be symmetric, otherwise the system is non-conservative and the potential does not exist. This way, the existence of the potential of any kind of force can be investigated, and therewith provides a check on the application of this procedure.

As noted previously, the differentiation in the equations 3.36 and 3.37 shows that the character of these forces becomes relevant. In the following sections, two kinds of forces will be addressed which play an important role

throughout this thesis: constant forces, such as gravity forces, and central linear forces, such as the forces due to zero-free-length springs.

Constant forces

In our natural habitat, gravity forces can be approximated as forces of invariant magnitude and direction. For these forces, most of the elements in the tangent stiffness matrix S (equation 3.36) vanish. Consequently, the only relevant term in the matrix S is $-\left(\Sigma\left(A r_{i/c}\right)^T F_i\right)_{,\varphi}$. It was shown in equation 3.15 that this term, for constant forces, is equal to $F_i^T r_{i/c}$. Consequently, the stiffness matrix of a constant force F_i acting on point P_i of a rigid body reduces to:

$$S = \begin{bmatrix} 0 & 0 \\ 0 & F_i^T r_{i/c} \end{bmatrix} \tag{3.38}$$

Apparently, the contribution to the stability of a constant force is characterized by the scalar product of the force vector and its position vector. If it is now desired to find the dynamically equivalent force F_r of two constant forces F_1 and F_2, their contributions to the tangent stiffness matrix S of equation 3.38 must be equal, leading to the following equation:

$$F_r^T r_{r/c} = F_1^T r_{1/c} + F_2^T r_{2/c} \tag{3.39}$$

Thus a scalar equation is found, which, together with the equations 3.18 and 3.19, uniquely defines the application point of the dynamically equivalent force F_r, when constant forces are assumed. This equation will be called the *stability equation* for the case of constant forces. The application point found in this manner will be called the *dynamically equivalent application point* (*DEP*) of the resultant force. In case the resultant force F_r applies at the dynamically equivalent point of application, this force will be called the *dynamically equivalent force* (*DEF*). So in order to find the dynamically equivalent force, three equations must be satisfied: the force equation (3.18), dealing with the force vectors; the moment equation (3.19), containing the vector products of the force vectors and their position vectors; and the stability equation (3.39), which comprises the scalar products of the force vectors and their position vectors.

This result can also be obtained using the potential method. To illustrate this, the contributions of a force F_i to the terms of the tangent stiffness matrix S in equation 3.37 are derived by differentiating equations 3.32 and 3.33:

$$-\left(V_i\right)_{,r_c r_c} = \begin{bmatrix} 0 & 0 \\ 0 & 0 \end{bmatrix}; \quad -\left(V_i\right)_{,r_c \varphi} = \begin{bmatrix} 0 & 0 \end{bmatrix}; \quad -\left(V_i\right)_{,\varphi r_c^T} = \begin{bmatrix} 0 \\ 0 \end{bmatrix}; \tag{3.40}$$

$$-\left(V_i\right)_{,\varphi\varphi} = \left(-F_i^T R_{,\varphi} r_{i/c}'\right)_{,\varphi} = -F_i^T R_{,\varphi\varphi} r_{i/c}' = -F_i^T R_{,\varphi\varphi} R^{-1} r_{i/c} = F_i^T r_{i/c} \quad (3.41)$$

It is noted that the two mixed partial derivatives are each other's transposed. Therefore the tangent stiffness matrix is symmetric and the potential exists for constant forces, as was expected.

Examples

Two examples will be given next. First, reconsidering the pendulum, it is seen that in the hanging pendulum the above measure for the stability is equal to:

$$F_r^T r_{r/c} = \begin{bmatrix} 0 & -mg \end{bmatrix} \begin{bmatrix} \ell \sin\varphi \\ -\ell \cos\varphi \end{bmatrix} = mg\ell \cos\varphi \quad (3.42)$$

where ℓ is the length of the pendulum, φ the angular deviation from the hanging equilibrium position, m the point mass at its end, and g the acceleration of gravity. For $\varphi = 0$, the expression is positive and therefore this equilibrium position is stable. For the inverted pendulum ($\varphi = \pi$), the expression is negative and therefore the upright equilibrium position is unstable:

$$F_r^T r_{r/c} = \begin{bmatrix} 0 & -mg \end{bmatrix} \begin{bmatrix} \ell \sin\varphi \\ -\ell \cos\varphi \end{bmatrix} = -mg\ell \quad (3.43)$$

The second example concerns two gravity forces $F_1 = \begin{bmatrix} 0 & -m_1 g \end{bmatrix}^T$ and $F_2 = \begin{bmatrix} 0 & -m_2 g \end{bmatrix}^T$, acting on a rigid body at P_1 and P_2, respectively (figure 3.4). For the dynamically equivalent force, the following force, moment, and stability equations are applicable:

$$F_r = F_1 + F_2 \quad (3.44)$$

$$\left(A r_{r/c}\right)^T F_r = \left(A r_{1/c}\right)^T F_1 + \left(A r_{2/c}\right)^T F_2 \quad (3.45)$$

$$F_r^T r_{r/c} = F_1^T r_{1/c} + F_2^T r_{2/c} \quad (3.46)$$

where point C is an arbitrary point of the rigid body (not the center of mass). Substituting the expressions for the forces into these three equations gives the following set of three equations:

$$F_r = -m_1 g \begin{bmatrix} 0 & 1 \end{bmatrix}^T - m_2 g \begin{bmatrix} 0 & 1 \end{bmatrix}^T = -\left(m_1 g + m_2 g\right) \begin{bmatrix} 0 & 1 \end{bmatrix}^T \quad (3.47)$$

$$-\left(m_1 g + m_2 g\right) \begin{bmatrix} -r_{ry/c} & r_{rx/c} \end{bmatrix} \begin{bmatrix} 0 \\ 1 \end{bmatrix} = -m_1 g \begin{bmatrix} -r_{1y/c} & r_{1x/c} \end{bmatrix} \begin{bmatrix} 0 \\ 1 \end{bmatrix}$$
$$-m_2 g \begin{bmatrix} -r_{2y/c} & r_{2x/c} \end{bmatrix} \begin{bmatrix} 0 \\ 1 \end{bmatrix} \quad (3.48)$$

$$-\left(m_1 g + m_2 g\right) \begin{bmatrix} 0 & 1 \end{bmatrix} \begin{bmatrix} r_{rx/c} \\ r_{ry/c} \end{bmatrix} = -m_1 g \begin{bmatrix} 0 & 1 \end{bmatrix} \begin{bmatrix} r_{1x/c} \\ r_{1y/c} \end{bmatrix} - m_2 g \begin{bmatrix} 0 & 1 \end{bmatrix} \begin{bmatrix} r_{2x/c} \\ r_{2y/c} \end{bmatrix} \quad (3.49)$$
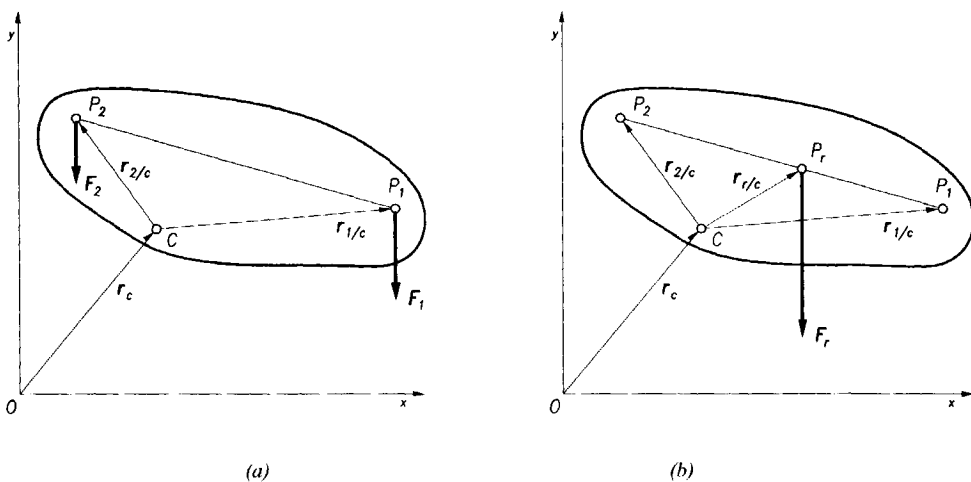
36

Figure 3.4   The dynamically equivalent force of two gravity forces applies at the intersection of its action line and the line connecting the application points of the original forces: (a) two given gravity forces, (b) dynamically equivalent resultant.

Working out the second and third equation gives, respectively:

$$r_{rx/c} = \frac{m_1 g}{m_1 g + m_2 g} \; r_{1x/c} + \frac{m_2 g}{m_1 g + m_2 g} \; r_{2x/c} \tag{3.50}$$

$$r_{ry/c} = \frac{m_1 g}{m_1 g + m_2 g} \; r_{1y/c} + \frac{m_2 g}{m_1 g + m_2 g} \; r_{2y/c} \tag{3.51}$$

Thus the application point $P_r = (r_{rx/c}, r_{ry/c})$ of the dynamically equivalent force is found to be located on the line connecting P_1 and P_2, so that $P_1 P_r / P_r P_2 = m_2 / m_1$. Although this example may be considered trivial in the sense that many will intuitively pinpoint the application point of the resultant force on this location, the above derivation shows that this is justified from the perspective of equivalent dynamics.

Evidently, applying the procedure of finding dynamically equivalent forces to the special case of gravity forces yields the combined center of mass, which indeed is the dynamically equivalent point of application of the gravity forces, or indeed the mass forces in general. It can therefore be concluded that the proposed procedure for finding dynamically equivalent resultant forces is the generalization of the commonly accepted procedure for finding the combined center of mass.

The fact that the resultant force at this location yields the same stability as the original forces is readily verified by deriving a statically balanced system from this example. If the rigid body of figure 3.4 is supported at the

37

dynamically equivalent application point P_r by a force $F_s = -F_r$, neutral equilibrium results. In the case the DEF F_r is considered, this force and the support force act at the same point, as the forces in figure 3.1d do, so clearly this is a situation of neutral equilibrium. If, instead, the original forces and the support force are considered, the familiar case of the counterweighted beam results. One could say that the DEF F_r can be resolved in a dynamically equivalent way into F_1 and F_2. In both cases, the contributions to the stability of the forces acting on the body, (F_r and F_s) and (F_1, F_2 and F_s), respectively, cancel each other out, and neutral equilibrium is the result.

Central linear forces

Where the preceding section dealt with constant forces, such as gravity forces, this section is concerned with forces of a different nature: central linear forces. These are forces generated by a central linear force field. One special type of central linear forces consists of the forces generated by zero-free-length springs (see also section 4.2), which will prove to be of great benefit in this thesis. Due to the nature of these forces, their magnitude and direction varies as a function of position or orientation. Therefore, the tangent stiffness matrix S will contain more non-zero elements than is the case with constant forces. This section will derive the conditions for the dynamically equivalent force of two central linear forces, or, in particular, two zero-free-lengths springs.

As zero-free-length springs generate zero force when their ends coincide, such a spring force can be written as:

$$F_i = k_i(a_i - r_i) = k_i(a_{i/c} - r_{i/c}) = k_i(a_i - r_c - r_{i/c}) = k_i(a_i - r_c - Rr'_{i/c}) \quad (3.52)$$

where k_i is the spring stiffness; a_i is the position vector of the one end of the spring; and r_i is the position vector of the other end of the spring. If one end of the spring is fixed, a_i will be associated with the fixed end (and will then be the origin of the central linear force field). The vector r_i will then be associated with the moving end. The moment contribution of such a force with respect to an arbitrary point C of the body is found to be:

$$(Ar_{i/c})^T F_i = F_i^T R_{,\varphi} r'_{i/c} = k_i(a_i - r_c - Rr'_{i/c})^T R_{,\varphi} r'_{i/c} \quad (3.53)$$

From these equations, the contributions due to this force to the elements of the stiffness matrix S (equation 3.36) can be derived:

$$-(F_i)_{,r_c} = k_i I_2 \quad (3.54)$$

$$-(F_i)_{,\varphi} = k_i R_{,\varphi} r'_{i/c} \quad (3.55)$$

$$-\left(\left(A\boldsymbol{r}_{i/c}\right)^T \boldsymbol{F}_i\right)_{,r_c}^T = k_i\left(\boldsymbol{R}_{,\varphi}\boldsymbol{r}'_{i/c}\right)^T \tag{3.56}$$

$$-\left(\left(A\boldsymbol{r}_{i/c}\right)^T \boldsymbol{F}_i\right)_{,\varphi}^T = k_i\left(\boldsymbol{R}_{,\varphi}\boldsymbol{r}'_{i/c}\right)^T \boldsymbol{R}_{,\varphi}\boldsymbol{r}'_{i/c} - \boldsymbol{F}_i^T \boldsymbol{R}_{,\varphi\varphi}\boldsymbol{r}'_{i/c} \tag{3.57}$$

Using $\boldsymbol{R}_{,\varphi} = A\boldsymbol{R}$, equation 3.55 and 3.56 become:

$$-\left(\boldsymbol{F}_i\right)_{,\varphi} = k_i\boldsymbol{R}_{,\varphi}\boldsymbol{r}'_{i/c} = k_iA\boldsymbol{R}\boldsymbol{r}'_{i/c} = k_iA\boldsymbol{r}_{i/c} \tag{3.58}$$

$$-\left(\left(A\boldsymbol{r}_{i/c}\right)^T \boldsymbol{F}_i\right)_{,r_c}^T = k_i\left(\boldsymbol{R}_{,\varphi}\boldsymbol{r}'_{i/c}\right)^T = k_i\left(A\boldsymbol{R}\boldsymbol{r}'_{i/c}\right)^T = k_i\left(A\boldsymbol{r}_{i/c}\right)^T \tag{3.59}$$

With $\boldsymbol{R}_{,\varphi}^T \boldsymbol{R}_{,\varphi} = \boldsymbol{I}$, $\left|\boldsymbol{r}'_{i/c}\right| = \left|\boldsymbol{r}_{i/c}\right|$, and $\boldsymbol{R}_{,\varphi\varphi} = -\boldsymbol{R}$, equation 3.57 becomes:

$$-\left(\left(A\boldsymbol{r}_{i/c}\right)^T \boldsymbol{F}_i\right)_{,\varphi}^T = k_i\boldsymbol{r}'^T_{i/c}\boldsymbol{r}'_{i/c} + \boldsymbol{F}_i^T \boldsymbol{R}\boldsymbol{r}'_{i/c} = k_i\boldsymbol{r}_{i/c}^T\boldsymbol{r}_{i/c} + \boldsymbol{F}_i^T \boldsymbol{r}_{i/c} \tag{3.60}$$

So the tangent stiffness matrix S for central linear forces evolves into:

$$S = \begin{bmatrix} k_i\boldsymbol{I}_2 & k_iA\boldsymbol{r}_{i/c} \\ k_i\left(A\boldsymbol{r}_{i/c}\right)^T & k_i\boldsymbol{r}_{i/c}^T\boldsymbol{r}_{i/c} + \boldsymbol{F}_i^T \boldsymbol{r}_{i/c} \end{bmatrix} \tag{3.61}$$

As compared to the constant-force stiffness matrix (equation 3.38), the following differences are apparent. Two additional terms $k_iA\boldsymbol{r}_{i/c}$ and $k_i\left(A\boldsymbol{r}_{i/c}\right)^T$ are present. Consequently, the system is no longer indifferent with respect to arbitrary displacements. Pure translation is associated with a stiffness k_i due to the term $k_i\boldsymbol{I}_2$. Furthermore, the lower right term is expanded with the terms $k_i\boldsymbol{r}_{i/c}^T\boldsymbol{r}_{i/c}$. Hence, different stability equations result as compared to the constant-force case.

Using the potential energy method, the same result is obtained as follows. Taking the partial derivatives of equations 3.32 and 3.33, and substituting $\boldsymbol{F}_i = k_i\left(\boldsymbol{a}_i - \boldsymbol{r}_c - \boldsymbol{R}\boldsymbol{r}'_{i/c}\right)$ gives the contributions to the tangent stiffness matrix S as given in equation 3.37 as:

$$-V_{,r_c^T r_c} = -\left(\boldsymbol{F}_i\right)_{,r_c} = k_i\boldsymbol{I}_2 \tag{3.62}$$

$$-V_{,r_c^T \varphi} = -\left(\boldsymbol{F}_i\right)_{,\varphi} = k_i\boldsymbol{R}_{,\varphi}\boldsymbol{r}'_{i/c} = k_iA\boldsymbol{r}_{i/c} \tag{3.63}$$

$$-V_{,\varphi r_c} = -\left(\boldsymbol{F}_i^T \boldsymbol{R}_{,\varphi}\boldsymbol{r}'_{i/c}\right)_{,r_c} = -\left(\boldsymbol{F}_i^T A\boldsymbol{r}_{i/c}\right)_{,r_c} \tag{3.64}$$

$$= -\left(k_i\left(\boldsymbol{a}_i - \boldsymbol{r}_c - \boldsymbol{R}\boldsymbol{r}'_{i/c}\right)^T A\boldsymbol{r}_{i/c}\right)_{,r_c} = k_i\left(A\boldsymbol{r}_{i/c}\right)^T$$

$$-V_{,\varphi\varphi} = -\left(\boldsymbol{F}_i^T \boldsymbol{R}_{,\varphi}\boldsymbol{r}'_{i/c}\right)_{,\varphi} = -\left(\boldsymbol{F}_i^T\right)_{,\varphi}\boldsymbol{R}_{,\varphi}\boldsymbol{r}'_{i/c} - \boldsymbol{F}_i^T\left(\boldsymbol{R}_{,\varphi}\boldsymbol{r}'_{i/c}\right)_{,\varphi} \tag{3.65}$$

$$= k_i\boldsymbol{R}_{,\varphi}\boldsymbol{r}'_{i/c}\boldsymbol{R}_{,\varphi}\boldsymbol{r}'_{i/c} - \boldsymbol{F}_i^T \boldsymbol{R}_{,\varphi\varphi}\boldsymbol{r}'_{i/c} = k_i A\boldsymbol{r}_{i/c}^T A\boldsymbol{r}_{i/c} + \boldsymbol{F}_i^T \boldsymbol{R}\boldsymbol{r}'_{i/c}$$

$$= k_i\boldsymbol{r}_{i/c}^T\boldsymbol{r}_{i/c} + \boldsymbol{F}_i^T \boldsymbol{r}_{i/c}$$

As was the case with constant forces, comparing equations 3.63 and 3.64 shows that also in this case the tangent stiffness matrix is symmetric, so central linear forces have a potential as well, and are therefore conservative too.

If now two central linear forces are to be replaced by a single equivalent one, the contribution to the stiffness matrix S due to the equivalent central linear force (index r) must be equal to the contribution due to the two original forces. Considering equations 3.62 through 3.65 respectively, this leads to the following conditions for equal stability (stability equations):

$$k_r = k_1 + k_2 \tag{3.66}$$

$$k_r A r_{r/c} = k_1 A r_{1/c} + k_2 A r_{2/c} \tag{3.67}$$

$$k_r r_{r/c}^T r_{r/c} + F_r^T r_{r/c} = k_1 r_{1/c}^T r_{1/c} + F_1^T r_{1/c} + k_2 r_{2/c}^T r_{2/c} + F_2^T r_{2/c} \tag{3.68}$$

Thus, when replacing two central linear forces by one, a total of seven equations are found: the vector equations 3.18 and 3.67, and the scalar equations 3.19, 3.66, and 3.68, which are to be solved for five unknowns (one scalar, k_r, and two vectors, r_r and a_r). Consequently, no solutions are found in general: two central linear forces cannot generally be substituted by a single one in a dynamically equivalent manner.

Special solutions

As was pointed out, it is generally not possible to replace two central linear forces by a single dynamically equivalent one. This is unfortunate in the design of spring mechanisms where zero-free-length springs are used as central linear forces. However, there are at least two ways to arrive at a solution. The first one is to restrict the motion to rotation only, and to replace the two zero-free-length springs not by a resultant zero-free-length spring but by a constant force. Under these conditions, a solution can be found as follows. Due to the restriction to rotation, equations 3.63 and 3.64 do not apply; and due to the comparison of two central linear forces with a constant force, dynamic equivalence is characterized by:

$$F_r^T r_{r/c} = k_1 r_{1/c}^T r_{1/c} + F_1^T r_{1/c} + k_2 r_{2/c}^T r_{2/c} + F_2^T r_{2/c} \tag{3.69}$$

where the left side corresponds to the expression for constant forces. Now, together with the equations 3.18 and 3.19, a total of four equations (one vector equation and two scalar equations) are found to solve for four unknowns (two vectors, F_r and $r_{r/c}$). The physical interpretation of this solution is still an open question, however an example confirming this phenomenon is given in chapter five, section 5.2 (the Floating Suspension).
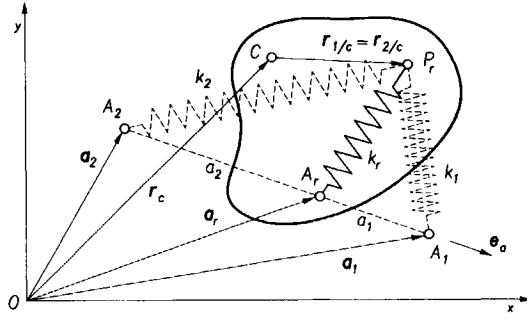
40

Figure 3.5 Two zero-free-length springs, acting at the same point of the rigid body, can be composed into a single dynamically equivalent one.

Another special solution is possible when the zero-free-length springs are attached to the rigid body at the same position. Then $r_1 = r_2$, or equivalently $r_{1/c} = r_{2/c}$ which, substituted in equations 3.18 and 3.19 and using equation 3.13, leads to $r_{r/c} = r_{1/c} = r_{2/c}$, or equivalently $r_r = r_1 = r_2$. Together with equation 3.66, this immediately satisfies equation 3.67, while equation 3.68 now becomes:

$$(k_1 + k_2)r_{r/c}^T r_{r/c} + F_r^T r_{r/c} = k_1 r_{r/c}^T r_{r/c} + F_1^T r_{r/c} + k_2 r_{r/c}^T r_{r/c} + F_2^T r_{r/c} \qquad (3.70)$$

As the $r_{r/c}^T r_{r/c}$ terms cancel out, the following relation remains:

$$(k_1 + k_2)(a_r - r_r)^T r_{r/c} = k_1(a_1 - r_r)^T r_{r/c} + k_2(a_2 - r_r)^T r_{r/c} \qquad (3.71)$$

Rearranging gives:

$$\left((k_1 + k_2)a_r^T - k_1 a_1^T - k_2 a_2^T\right) r_{r/c} = 0 \qquad (3.72)$$

This should be valid for any $r_{r/c}$, and therefore, introducing the unit vector e_a and using the relations $a_1 - a_2 = ae_a$ and $a_1 + a_2 = a$ (see figure 3.5):

$$a_r = \frac{k_1}{k_1 + k_2}a_1 + \frac{k_2}{k_1 + k_2}a_2 \qquad (3.73)$$

$$= \frac{k_1}{k_1 + k_2}a_1 - \frac{k_1}{k_1 + k_2}a_2 + \frac{k_1}{k_1 + k_2}a_2 + \frac{k_2}{k_1 + k_2}a_2$$

$$= \frac{k_1}{k_1 + k_2}(a_1 - a_2) + a_2$$

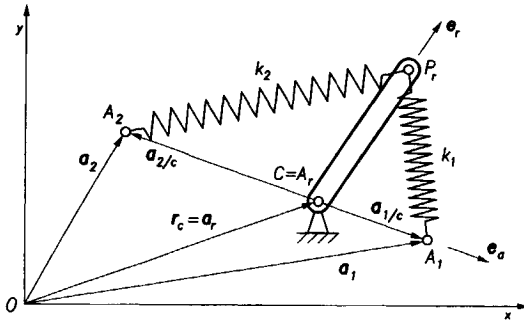$$= a_2 + \frac{k_1}{k_1 + k_2}ae_a$$

41

Figure 3.6   A neutral equilibrium spring mechanism is obtained when the rigid body is hinged at the fixed attachment point of the resultant spring.

From this result it is seen that a_r traces the line $A_1 A_2$ as the stiffnesses k_1 and k_2 vary. It is also seen that $a_2 = ak_1/(k_1 + k_2)$ and $a_1 = ak_2/(k_1 + k_2)$. Consequently, the relation $a_1/a_2 = k_2/k_1$, or $k_1 a_1 = k_2 a_2$, defines the location of point A_r on the line $A_1 A_2$.

So, two zero-free-length springs, k_1 and k_2, each attached with one end to a first rigid body and with the other end to a second rigid body, can be composed into a single zero-free-length spring k_r in a dynamically equivalent way for any movement of the rigid body, under the following conditions. Firstly, k_r must equal $k_1 + k_2$ (due to equation 3.66), secondly, the free ends of the springs must be attached to the same point of application P_r, so $r_{r/c} = r_{1/c} = r_{2/c}$ (assumed earlier); and thirdly, the fixed end A_r of the dynamically equivalent zero-free-length spring must be located on the line connecting A_1 and A_2, so that $k_1 a_1 = k_2 a_2$ (resulting from equation 3.77). Inversely, these equations can be used to resolve a single spring into two springs, where it is noted that this does not give a unique solution.

Basic spring force balancer

One way to design a neutral equilibrium system is to use the procedure for the composition of zero-free-length springs by first finding a zero-stability solution for one spring k_r attached between point P_r on the moving body and the grounded point A_r, and then resolve this spring in a dynamically equivalent way into two springs, k_1 and k_2. As was found earlier, a solution exists under the condition that only rotation is considered (so that equation 3.67 can be disregarded), where the contribution to the stability (equation 3.68) must equal zero:

$$k_r \boldsymbol{r}_{r/c}^T \boldsymbol{r}_{r/c} + \boldsymbol{F}_r^T \boldsymbol{r}_{r/c} = 0 \qquad (3.74)$$

or:

$$\left(k_r \boldsymbol{r}_{r/c}^T + k_r (\boldsymbol{a}_r - \boldsymbol{r}_c - \boldsymbol{r}_{r/c})^T\right) \boldsymbol{r}_{r/c} = 0 \qquad (3.75)$$

This is true for any $\boldsymbol{r}_{r/c}$ if:

$$\boldsymbol{r}_c = \boldsymbol{a}_r \qquad (3.76)$$

So the rigid body is indifferent for rotation if its pivot point coincides with the grounded spring attachment point, regardless of the length r_r of the vector $\boldsymbol{r}_{r/c} = r_r \boldsymbol{e}_r$, where $\boldsymbol{e}_r$ is the unit vector in the direction of $\boldsymbol{r}_{r/c}$. Obviously, this is true for the system with the dynamically equivalent spring k_r, since the length of a spring hinged in this fashion will not change during motion. However, since two springs k_1 and k_2 can be found, which are dynamically equivalent to spring k_r, the system with these springs k_1 and k_2 is also statically balanced. The conditions for these springs are that they both attach to the rotatable body at point P_r; that $k_r = k_1 + k_2$; and that the grounded attachment points comply with equation 3.73. Therefore, a link connecting point P_r with pivot point C turns the spring system of figure 3.5 into a statically balanced mechanism (figure 3.6).

Alternatively, the mechanism in figure 3.6 is found when the resultant force associated with the two-spring system of figure 3.5 is considered. This force, using equation 3.52, is given by:

$$\boldsymbol{F}_r = k_1 (\boldsymbol{a}_{1/c} - \boldsymbol{r}_{1/c}) + k_2 (\boldsymbol{a}_{2/c} - \boldsymbol{r}_{2/c}) = (k_1 a_1 - k_2 a_2) \boldsymbol{e}_a - (k_1 r_1 + k_2 r_2) \boldsymbol{e}_r \qquad (3.77)$$

where $\boldsymbol{a}_{1/c} = a_1 \boldsymbol{e}_a$ and $\boldsymbol{a}_{2/c} = -a_2 \boldsymbol{e}_a$, and where $\boldsymbol{e}_a$ is the unit vector in the direction of $\boldsymbol{a}_{1/c}$. Substituting $k_1 a_1 = k_2 a_2$ and $r_1 = r_2 = r$ into equation 3.77, the expression for the force $\boldsymbol{F}_r$ becomes:

$$\boldsymbol{F}_r = -(k_1 + k_2) r \boldsymbol{e}_r \qquad (3.78)$$

As the $\boldsymbol{e}_a$ component cancels, it is seen that this force is always directed towards the pivot C. Therefore, interpositioning a link between point P_r and pivot C yields the same statically balanced mechanism. This arrangement will be called the *basic spring force balancer* for statically balanced spring mechanisms (see also section 4.3). Taking this particular mechanism as a starting point, a framework for the modification, extension and simplification of statically balanced zero-free-length spring mechanisms will be put up in the following chapter, but prior to this, a graphical representation of some of the above will be given.
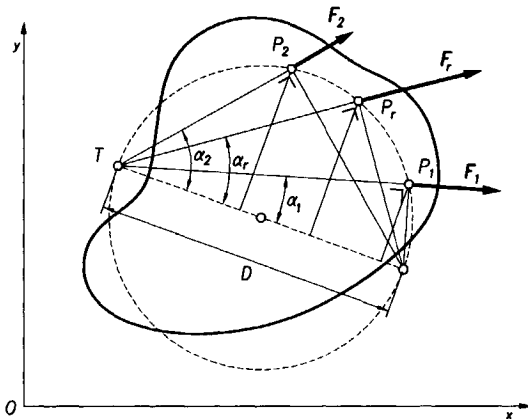
Figure 3.7   For constant forces, the application point of the dynamically equivalent force is located on the circle circumscribing the application points of the two original forces and the intersection of their action lines [3.5].

3.4   Graphical representation

Since the time of F. Commandino (1509-1575) who translated the works of Archimedes, Apollonius, and Pappus, many other theorems in the same spirit have been discovered. Such results were studied in great detail during the nineteenth century. As the present tendency is to abandon them in favor of other branches of mathematics, we shall be content to mention a few that seem particularly interesting.

H. S. M. Coxeter, 1969, p3

In the example of figure 3.4, a quick geometric construction was found for the application point of the dynamically equivalent force of two constant forces with parallel lines of action, which was already known from the procedure of determining the combined center of mass. This raises the question whether a similar procedure exists for finding the dynamically equivalent application point of two non-parallel forces, such as in the case of the forces F_1 and F_2 in figure 3.3. This section will provide such a construction for the case of constant forces, and will investigate its use in the case of central linear forces.

Constant forces
The graphical construction of the DEP of two non-parallel constant forces turns out to be very elegant. The DEP is located on the circle defined by the application points of the original forces and the intersection of their lines of
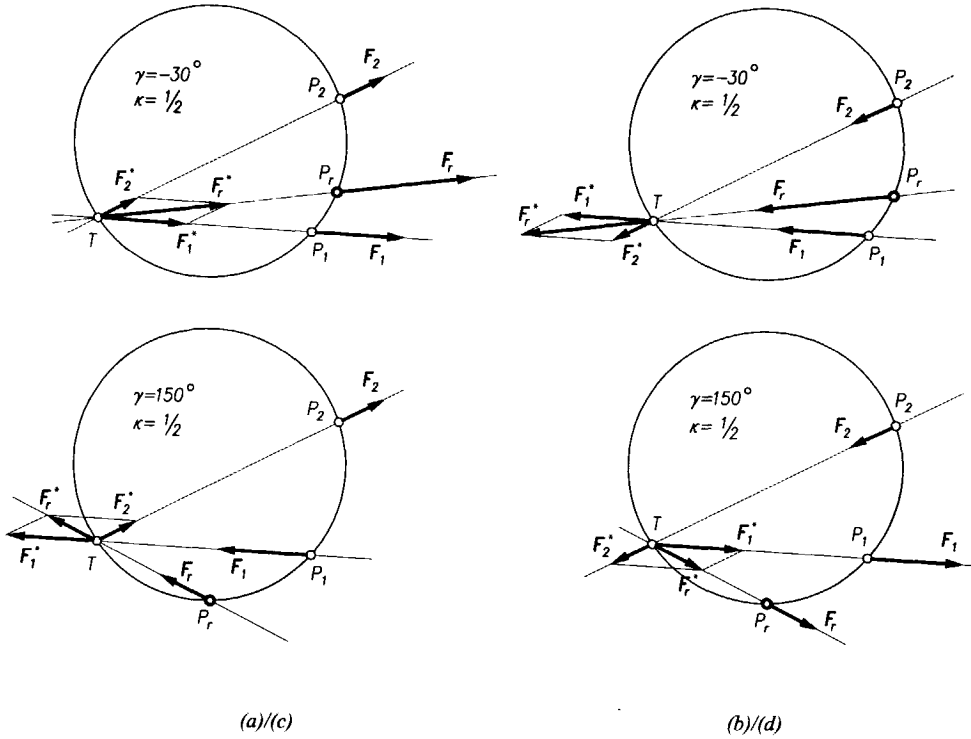
44

$$(a)/(c) \qquad\qquad\qquad (b)/(d)$$

Figure 3.8   Dependent on the polarity of the forces, with given action lines and magnitudes of the original constant forces, one of two dynamically equivalent points of application is found.

action (figure 3.7 [3.5]). This section will prove this remarkable fact by assuming that the four points are indeed on a circle and showing that equation 3.39 results.

First it is realized that the projection of the vector summation $(F_1 + F_2)$, or F_r, on any line through the intersection T of the action lines of the forces F_1 and F_2, is equal to the summation of the individual projections of the forces F_1 and F_2. Assuming that P_1, P_2, T, and P_r are located on a circle and projecting the forces on the diameter of the circle through T, one can write:

$$F_r \cos\alpha_r = F_1 \cos\alpha_1 + F_2 \cos\alpha_2 \qquad\qquad (3.79)$$

where F_i is short for $|F_i|$. Multiplying by the diameter D gives:

$$F_r D \cos\alpha_r = F_1 D \cos\alpha_1 + F_2 D \cos\alpha_2 \qquad\qquad (3.80)$$

When T is selected as point C, the terms $D\cos\alpha_i$ are equal to $r_{i/c}$ (short for $|r_{i/c}|$). Furthermore, the vectors $r_{i/c}$ and F_i are collinear. Consequently, equation 3.80 reduces to:
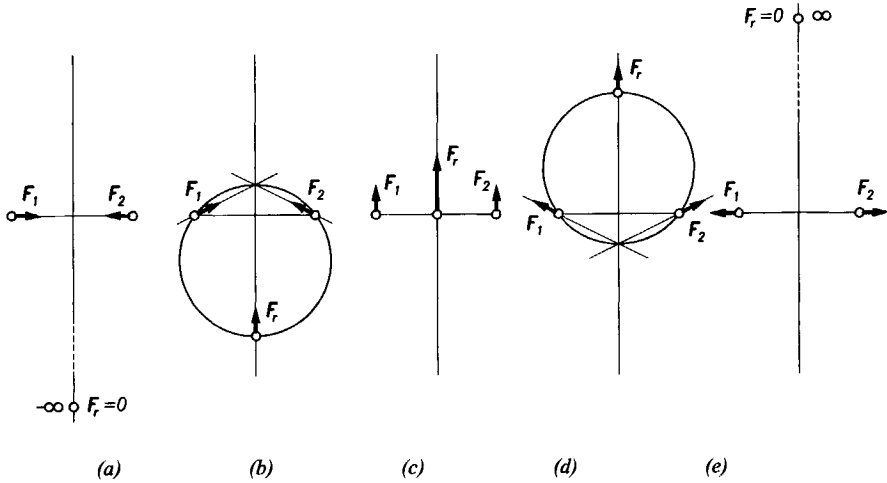
Figure 3.9 Illustration of the influence of the inclined angle between the original forces on the location of the dynamically equivalent point of application: (a) $\gamma = -\pi$, (b) $\gamma = -2\pi/3$, (c) $\gamma = 0$, (d) $\gamma = 2\pi/3$, (e) $\gamma = \pi$.

$$F_r r_{r/t} = F_1 r_{1/t} + F_2 r_{2/t} \tag{3.81}$$

or:

$$\boldsymbol{F}_r^T \boldsymbol{r}_{r/t} = \boldsymbol{F}_1^T \boldsymbol{r}_{1/t} + \boldsymbol{F}_2^T \boldsymbol{r}_{2/t} \tag{3.82}$$

Since $\boldsymbol{F}_r = \boldsymbol{F}_1 + \boldsymbol{F}_2$, equation 3.82 is valid with respect to any point C of the rigid body. Consequently, equation 3.82 becomes equal to equation 3.39, which concludes the proof. Appendix 3.1 presents a geometrical proof.

To become familiar with the graphical representation, figure 3.8 displays four different configurations of forces. The angle γ between the lines of action is defined as the angle about T from F_2 counterclockwise to F_1, while the symbol κ is used for the absolute ratio of the forces: $\kappa = |F_2|/|F_1|$. In all configurations, the original points of application P_1 and P_2 are the same, as are the magnitudes F and lines of action of the forces F_1 and F_2. Only the senses are varied. Changing the sense of one of the forces results in a different dynamically equivalent application point. However, when both signs are changed, the original dynamically equivalent application point is found again. It appears that two dynamically equivalent application points are possible with given lines of action and magnitudes. The angle γ defines which of the two possible locations is appropriate. In figure 3.9, the case of equal forces ($\kappa = 1$) is considered in some detail. The inclined angle γ is varied, and the symmetrical situation (*i.e.* point T is located on the perpendicular bisector of P_1
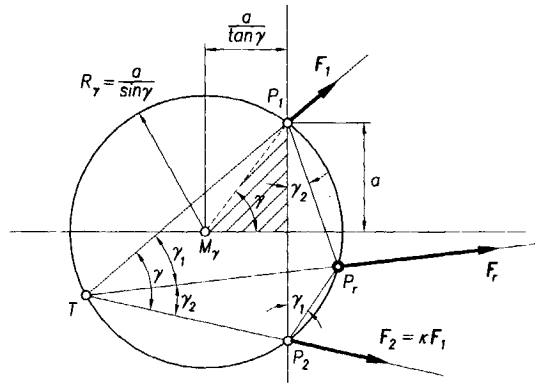
46

Figure 3.10 Circle of constant inclination angle.

and P_2) is considered. As γ is varied from $-\pi$ to π, the resultant point of application runs on the perpendicular bisector of P_1P_2 from $-\infty$ to ∞, while the magnitude of the resultant force rises from zero to a maximum of $2F$ and then falls to zero again.

The procedure of dynamically equivalent composition of constant forces incorporates a great deal of regularity. Several phenomena will be presented here. It has already been shown that the dynamically equivalent application point of two constant forces F_1 and F_2 with inclined angle γ is found on the circle through P_1, P_2, and T. It is interesting to note that, as long as γ is constant, *every* dynamically equivalent application point of these forces, regardless of their magnitudes and directions, is located on this same circle. This is due to the fact that this circle is the locus of points T from which P_1P_2 subtends the angle γ, as is illustrated in figure 3.10. So, given γ, points T, P_1, and P_2 always put up the same circle on which the dynamically equivalent application point is located. This circle will be called the *circle of constant γ*, or γ-*circle* for short. From the hatched triangle, it can be shown that the radius of the circle is $R_\gamma = a / \sin\gamma$, and that its center is located on the perpendicular bisector of P_1P_2, at a distance of $a / \tan\gamma$ from the midpoint of P_1P_2 (see also appendix 3.2). Noteworthy is the fact that the triangle $P_1P_2P_r$, put up by the original application points and the dynamically equivalent application point, is similar to the mirrored triangle of forces.

Thus, the inclination angle γ alone already defines the circle on which the DEP is to be found. The location of the DEP on this circle is determined by the ratio of force magnitudes $\kappa = |F_2|/|F_1|$, as will be shown next. From applying
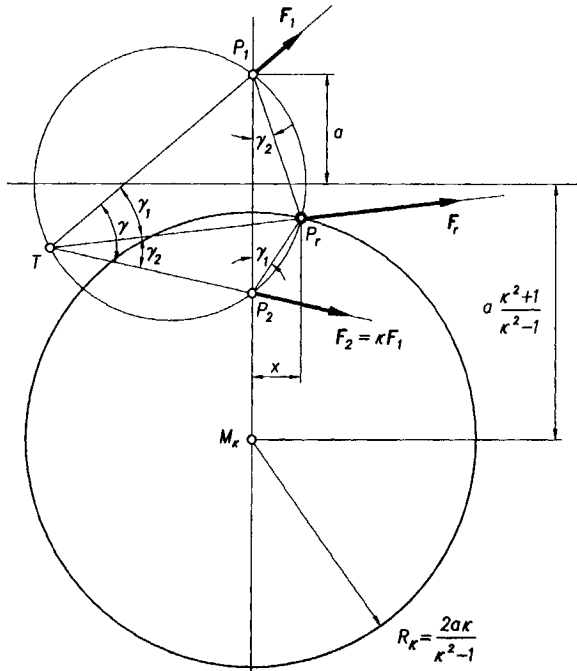
47

Figure 3.11   Circle of constant magnitude ratio.

the sine rule to the triangle of forces it is seen that κ divides the inclination angle γ into two parts, γ_1 and γ_2, according to the equation $\kappa = |F_2|/|F_1| = \sin\gamma_1 / \sin\gamma_2$. The inscribed angles P_2TP_r and $P_2P_1P_r$ in figure 3.10 subtend the same arc P_2P_r and are therefore congruent. Likewise, angle $P_1P_2P_r$ equals angle P_1TP_r. Thus, it is seen that, for example in case $\kappa = 1$ (*i.e.* $\gamma_1 = \gamma_2$), the dynamically equivalent application point lies on the intersection of the γ-circle and the positive x-axis, regardless of the location of T on the γ-circle. Furthermore, as γ is divided in two constant parts γ_1 and γ_2 by the given ratio κ, the location of the dynamically equivalent application point on the arc P_2P_1 is independent on the location of point T on the circle, because P_1P_r and P_2P_r always subtend the constant angles γ_1 and γ_2, respectively, from point T.

It is now interesting, when γ is given, to assess the influence of variation of κ on the location of the DEP (figure 3.11). With the definition of κ in mind, the challenge is to find the locus of points such that the ratio $\sin\gamma_1 / \sin\gamma_2$ in triangle $P_1P_2P_r$ is constant. As $\sin\gamma_1 = x / P_2P_r$ and $\sin\gamma_2 = x / P_1P_r$, the ratio $\sin\gamma_1 / \sin\gamma_2$ must equal P_1P_r / P_2P_r. So the problem can be reformulated as finding the locus of a point whose distances from two fixed points P_1 and P_2
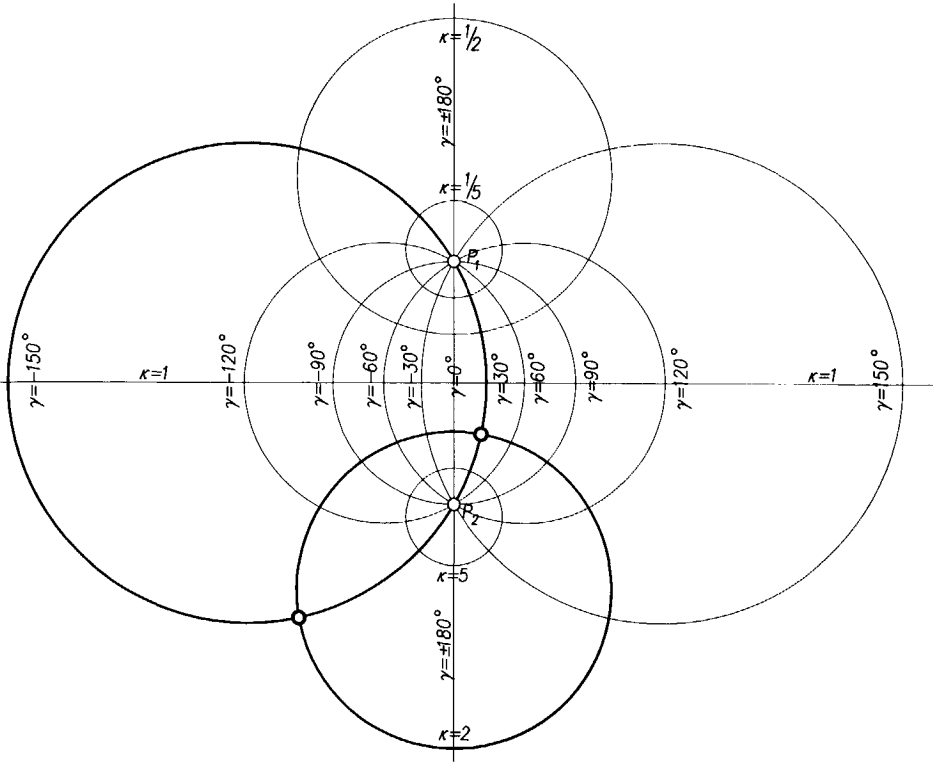
48

Figure 3.12 The circles of constant inclination angle and constant magnitude ratio are orthogonal.

have a constant ratio κ. This is the definition of a circle according to Apollonius [3.6]. The center of this circle is located on the line P_1P_2 at a distance $-a(\kappa^2+1)/(\kappa^2-1)$ from the midpoint of P_1P_2, while its radius is $R_\kappa = 2a\kappa/(\kappa^2-1)$, as shown in figure 3.11, see also appendix 3.2. Thus, the locus of all DEPs associated with a constant κ is a circle, which will be called the *circle of constant κ*, or κ-*circle* for short.

The dynamically equivalent application points can now quickly be found as the intersection points of the appropriate γ- and κ-circles. These circles are only dependent on the distance between the original points of application, a, the internal angle of the lines of action, γ, and the ratio of force magnitudes, κ. In figure 3.12, the circles are sketched for several values of γ and κ. The γ-circles, for various values of γ, form an *intersecting pencil of coaxal circles*, whereas the κ-circles, for various values of κ, form a *nonintersecting pencil of*
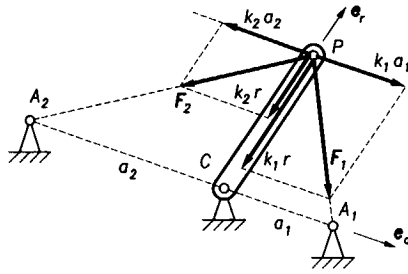
Figure 3.13   Faulty application of constant-force circle construction to central linear forces yields a constant distance between the application point found and the pivot.

coaxal circles [3.6]. Since P_1 and P_2 are the *common points* for the (intersecting) pencil of γ-circles, as well as the *limiting points* for the (nonintersecting) pencil of κ-circles, the γ- and κ-pencils are orthogonal [3.6].

The correct one of the two intersection points of the appropriate γ- and κ-circles follows from the senses of the forces, as illustrated in figures 3.9 and 3.10, or, when the line of action of the resultant force has been constructed, the correct dynamically equivalent application point is found as the point of intersection of the γ-circle and this line, which is not point T. Alternatively, by using the definition of γ as the angle about T from F_2 counterclockwise to F_1, each circle of constant γ is divided by the original points of application (the *common* points of the γ-pencil) into two arcs. By way of example, the arcs for $\gamma = 30°$ and $\gamma = -150°$, and the circle for $\kappa = 2$ are drawn in bold style. Note that the circle for $\kappa = 1$ reduces to a line, the horizontal axis of the figure, as has already been derived in figure 3.9.

Central linear forces

For central linear forces, a procedure as elegant as the circle for constant forces has not yet been found. Clearly, the faulty application of the constant force construction to central linear forces results in an error. It will be shown that this error is a constant term, which can be represented graphically. Therefore, this issue will be addressed briefly.

The contributions to the stability of two constant forces, and two central linear forces, respectively, are given by:

$$\left(-V_{,\varphi\varphi}\right)_{const} = F_1^T r_{1/c} + F_2^T r_{2/c} \tag{3.83}$$

$$\left(-V_{,\varphi\varphi}\right)_{centr.lin.} = k_1 r_{1/c}^T r_{1/c} + F_1^T r_{1/c} + k_2 r_{2/c}^T r_{2/c} + F_2^T r_{2/c} \tag{3.84}$$

The difference, and therewith the error made when applying the constant force construction to central linear forces is equal to $k_1 r_{1/c}^T r_{1/c} + k_2 r_{2/c}^T r_{2/c}$ which is a constant term. This error term will be investigated for the case of the basic spring force balancer (figure 3.13). By introducing a unit vector e_r with respect to the local reference frame, so that $r_{1/c} = r_{2/c} = r_{r/c} = r e_r$, the error expression becomes:

$$k_1 r_{1/c}^T r_{1/c} + k_2 r_{2/c}^T r_{2/c} = (k_1 + k_2) r^2 \qquad (3.85)$$

This is a constant term, originating from a vector e_r running along with the link, thus representing a shift along this vector towards the pivot.

In the example of the basic spring force balancer, the circle through the spring force application points and the intersection of the action lines degenerates into point P. The DEP of the resultant force is therefore found to be at point P, the moving end of the link, rather than the pivot where it should be. Due to the consideration of the spring forces as constant forces, a correction is needed. One interesting correction for the DEP to end up at C is found when the stability contribution of the resultant force is investigated. According to equation 3.78, the resultant force is equal to $F_r = -(k_1 + k_2) r e_r$. Therefore the stability contribution of this force, regarded as a constant force, is:

$$F_r^T r_{r/c} = -(k_1 + k_2) r e_\varphi^T r e_\varphi = -(k_1 + k_2) r^2 \qquad (3.86)$$

which is the opposite of the expression in equation 3.85. Evidently, the correct DEP is found when the spring forces are considered constant forces, as long as the DEP found is corrected by a shift over a distance r, where r is calculated from equation 3.86, in the direction of e_r, where $F_r = |F_r|$.

3.5   Summary

This chapter has regarded forces acting on a rigid body from the perspective of their contribution to its state of motion. It was found that the resultant force of two forces not only yields equal contribution in situations of static equilibrium but in any (dynamic) nominal state of motion. The force equation (equation 3.18) determines the magnitude and direction of the resultant (free vector), while the moment equation (equation 3.19) confines the resultant force vector to act along the line through the intersection of the action lines of the original forces (sliding vector). Thus, the instantaneously (statically) equivalent force of two arbitrary forces is determined.

For dynamic equivalence, it was argued that the contribution of the forces to the stability was to be analyzed. Therefore, variations about the nominal state

were considered. Due to the differentiation involved, the character of the forces had to be taken into account. For the equivalent force of two *constant* forces, an additional scalar equation was found, called the *stability equation* (for constant forces), which uniquely locates the resultant force on the previously found line of action (bound vector). Thus, the *dynamically equivalent resultant force* (DEF) of two arbitrary but constant forces, given as bound vectors, is uniquely defined by the force equation (equation 3.18), the moment equation (equation 3.19) and the stability equation (equation 3.39), together a set of one vector equation, two scalar equations, and four unknowns (magnitude, direction, and the x- and y-coordinates of the application point). The application point of the DEF was called the *dynamically equivalent point of application* (DEP).

Graphical inspection of the stability equation revealed the most notable phenomenon that the DEP, the application points of the original forces, and the intersection of the action lines of the original forces, are all located on the same *circle*. This yielded a convenient graphical way to find the dynamically equivalent of two constant forces. In the special case of constant forces of equal direction, for instance two gravity forces, the DEF was found to apply between the application points of the original forces at distances proportional to the magnitudes of the original forces. In the case of gravity forces, this is exactly at the combined center of mass. Clearly, the center of mass is the dynamically equivalent application point of mass forces. It can therefore be concluded that the proposed procedure for finding dynamically equivalent resultant forces is the generalization of the commonly accepted procedure for finding the center of mass.

As regards central linear forces, such as zero-free-length spring forces, three conditions (stability equations) for dynamic equivalence are found in addition to the force and the moment equations: two scalar equations and one vector equation (equations 3.66 through 3.68). As there are five unknowns, no solution is found in general. However, two special solutions are possible. The first one was found by restricting the motion to rotation and substituting the two central linear forces by a resultant constant force, rather than a resultant central linear force. The second solution was found in case the central linear forces apply at the same point of the rigid body. As to the latter solution, it was found that two zero-free-length springs, connected to the same moving point, can be composed into a single zero-free-length spring, hinged between the moving point and a stationary fixed point. A graphical construction for the DEP of two central linear forces was not found. However, a correction was proposed to compensate

for the error introduced in case the circle-construction for constant forces would be applied to a situation with central linear forces.

Finally, demanding zero stability for the two-spring system where the springs attach at the same point of the movable body yielded the solution of a link connecting the ends of the dynamically equivalent one, which is a statically balanced mechanism of a rather trivial kind. However, by replacing the resultant spring by two dynamically equivalent springs in one of infinitely many ways, neutral stability was maintained, yet now in a most useful design. This spring mechanism was called the *basic spring force balancer*.

4 Conception framework

in which a simple balanced spring mechanism incorporating zero-free-length springs is adopted as a basic spring force balancer; elementary rules for its modification are derived; and the combination of the basic spring force balancer and the modification rules is proposed as a framework for the conceptual design of statically balanced spring mechanisms.

4.1 Introduction

Counterweights or springs can only rarely act directly on the system which is to be balanced. Therefore it is usually necessary to have a special mechanism which transmits the forces into the system and, by reason of its transmission ratio, establishes equilibrium in the system. Such a mechanism, to be known as an adjustment mechanism, has therefore special importance, and the determination of its dimensions becomes of great importance when concerning oneself with force balancing.

H. Hilpert, 1968

Principally, in order to achieve a statically balanced system, at least two conservative forces are required, which must be associated in such a way that they yield zero stability. In other words, at least two potential energy storage devices (*e.g.* springs and masses) are required, which must be coupled in such a way that their energy characteristics as a function of the degrees of freedom add up to a constant value. When balancing pre-existing unbalanced systems, an *adjustment mechanism* connecting the potential energy storage devices will generally be required to connect for instance the compensation spring to the mechanism to be balanced. As this adjustment mechanism may have to accommodate strongly non-linear characteristics, it may be accordingly complicated. However, when the design of energy-free systems is commenced from scratch, much less complicated, inherently balanced systems can be designed. Then the characteristics can be adjusted to one another employing as little of an *adjustment mechanism* in between as possible. This kind of systems is aimed at in this thesis. Indeed, this approach of starting a design with a balanced system, even when the ultimate goal is a non-zero-stiffness mechanism, may very well be favorable for system behavior in general.

By way of illustration of the effect of even a simple adjustment mechanism, figure 4.1 displays two situations of the connection of two equal zero-free-length springs of stiffness k. The direct connection in figure 4.1a yields a resultant (translational) stiffness of twice the individual stiffness of the separate
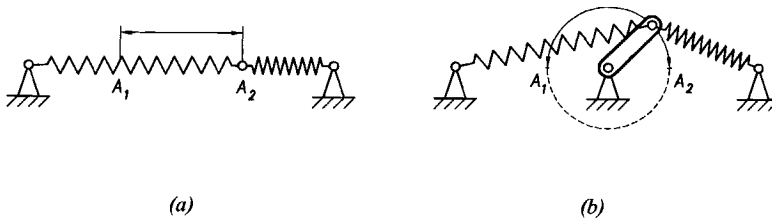
(a)   *(b)*

Figure 4.1   Adjustment mechanisms between two zero free length springs: (a) direct in-line connection, (b) connection through rotatable link. With equal zero free length springs of stiffness k, the direct in-line connection results in a stiffness of 2k, whereas the connection through a rotatable link yields a balanced mechanism.

springs, whereas the connection through the crank in figure 4.1b yields zero (rotational) stiffness and therefore perfect balance. Apparently, when the task is to move a point under the influence of two zero-free-length springs from A_1 to A_2, a stiffness range from $2k$ (direct in-line connection of the springs) to zero (by applying the basic spring force balancer) can be covered by adjusting the parameters of two springs and a single link.

The previous chapter arrived at the system of figure 4.1b via inspection of the equations for the composition of two zero-free-length springs, from a synthetical perspective. However, as it is against all probability that the solutions for a specific problem can be derived from the theory in this way, this chapter will employ a different approach. The spring mechanism of figure 4.1b will be adopted as the *basic spring force balancer*, the starting point for the conception of statically balanced spring mechanisms, to be put up in this chapter. The approach differs from the classical mechanism synthesis methods [4.1] in that the already statically balanced basic spring force balancer is developed into a mechanism of desired specifications, rather than that an adjustment mechanism is synthesized to match the required transfer function between the energy storage devices. The result is more a lucid and logical framework than a general method, yet it is perceived to give a great deal more insight into the conceptional design.

This chapter will start with a brief deliberation on zero-free-length springs, as these will play an important role in the approach proposed (section 4.2). Subsequently, the basic spring force balancer will be discussed in section 4.3, followed by an investigation of several ways to modify the basic spring force balancer in section 4.4. This will result in a set of *modification rules* and directives on how to use them (section 4.5). The combination of basic spring force balancer and modification rules will be denoted as the *framework* for the conception of balanced spring mechanisms. This framework will function as the
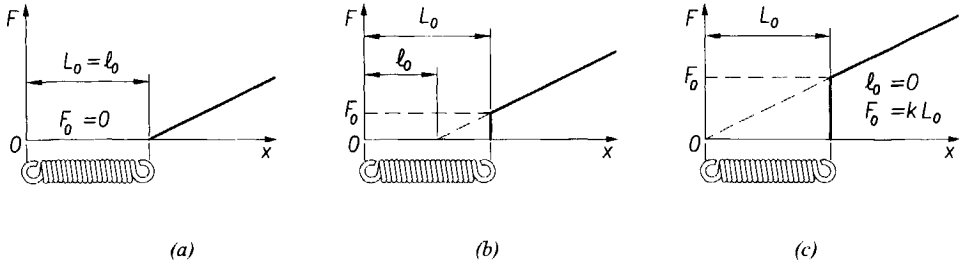
Figure 4.2 Spring characteristics: (a) extension spring with zero initial tension so that free length equals initial length, (b) extension spring with some initial tension so that the free length is smaller than the initial length, (c) spring with zero-free-length due to an initial tension of kL_0.

design toolbox for chapter five. As the framework has been put up from the perspective of potential energy, it is interesting to investigate the influence of the modification rules on the stability. This will be done in a separate section, section 4.6. The chapter will conclude with an overview of the modification rules.

4.2   Ideal springs

Correct Anglepoising spring are characterised by the feature that the force exerted by them is always proportional to their length and the length of an Anglepoising spring is considered to be the distance separating the centres of the pins by which they are anchored to the machine.

George Carwardine, ca 1932

Principle

It will become clear in the next sections that the design of statically balanced mechanisms is favored by the use of *zero-free-length springs* [4.2]. The free length of a linear spring should be well distinguished from the initial length. To illustrate this, definitions are given and a special diagram is used. The *initial length* L_0 is the distance between the insides of the spring loops when no external load is present. The *initial tension* F_0 is the force needed to separate the coils at all. The diagram of three springs characteristics will now be discussed: without initial tension, with some initial tension (as most helical extension springs have), and with increased initial tension. When there is no initial tension and the spring is stretched along a straight line, the origin of the diagram is in fact set at the neutral position of the free end of the spring. The initial length in these cases is of no concern. However, in applications where the spring rotates when stretched, it becomes more logical to select the fixed end as
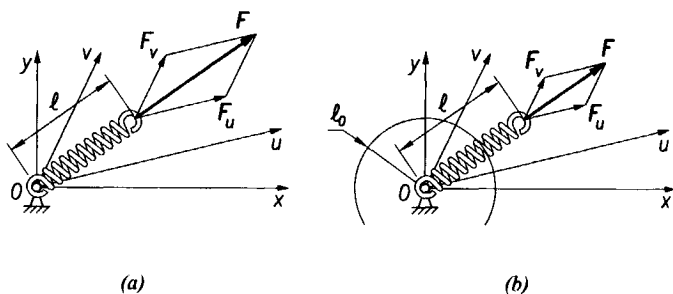
Figure 4.3   Resolution of spring forces in u and v direction: (a) ideal spring, where $F_u=ku$ and $F_v=kv$, (b) normal spring, where $F_u=k(u-\ell_0e_u)$ and $F_v=k(v-\ell_0e_v)$.

the origin. Thus, a force-length diagram results, rather than the usual force deflection diagram.

Figure 4.2a shows the force-length characteristic of a spring of which the coils do not (or only just) touch one another. Deflection will linearly increase when force builds up. The spring in figure 4.2b is coiled with some initial tension. Although the stiffness and the initial length do not change, the force needed for a given deflection does change, and the characteristic appears to intersect the length-axis at a point closer to the origin of the graph. The *free length* ℓ_0 of a linear spring is defined as the distance from the origin to the intersection of the (extension of the) characteristic and the length-axis in the force-length diagram. Thus, the free length of a spring with initial tension is smaller than the initial length, and is calculated as $\ell_0 = L_0 - F_0/k$. As the initial tension increases, the intersection of the characteristic extension approaches the origin.

A special case emerges for $F_0 = kL_0$, when the intersection coincides with the origin of the force-length diagram. The free length is zero and the force has become proportional to the length of the spring, rather than to its deflection only. Springs or spring arrangements exhibiting this behavior are called *zero-free-length springs*. Extension springs with zero free length, constant spring rate, limitless strain, zero mass, and forces acting along their centerline are termed *ideal springs* in this thesis. Springs with a free length greater than zero will be called *normal springs*.

Usually, the free length of extension springs is greater than zero. The force due to deflection of the spring yields:

$$F_i = k_i\left(l_i - \ell_{0i}\right) = k_i\left(a_i - r_i - \ell_{0i}\right) = k_i\left(a_{i/c} - r_{i/c} - \ell_{0i}\right) \qquad (4.1)$$

where F_i is the spring force, k_i is the spring stiffness; l_i is the actual length of the spring; ℓ_{0i} is the free length; a_i is the position vector of the one end of the
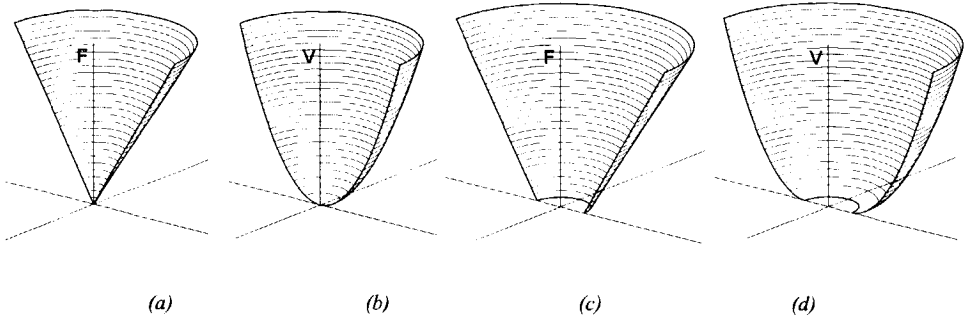
58

(a)   *(b)*   *(c)*   *(d)*

Figure 4.4   Force and potential functions of ideal and normal springs of equal stiffness, restricted to moving in the x-y-plane: (a) ideal spring force characteristic: cone, (b) ideal spring potential function: paraboloid, (c) normal spring force characteristic: chopped cone, (d) normal spring potential function: note that this is not a chopped paraboloid [4.3].

spring; and r_i is the position vector of the other end of the spring. If one end of the spring is fixed, a_i will be associated with the fixed end, and r_i with the moving end. In extension springs with initial tension, the free length ℓ_0 should be well distinguished from the initial length L_0. In ideal springs, the free length is zero and equation 4.1 reduces to:

$$F_i = k_i l_i = k_i \left(a_i - r_i \right) = k_i \left(a_{i/c} - r_{i/c} \right) \tag{4.2}$$

Thus, the force vector of an ideal spring is equal to the difference of the position vectors of its ends, multiplied by the spring constant. This feature will prove to be most useful in the treatment of forces in ideal spring mechanisms, especially because the components in any directions u and v are equal to the excursions in these directions multiplied by the spring stiffness, as is illustrated in figure 4.3. The resolution of the spring force in skew components, rather than in orthogonal directions, will be termed *skew resolution*.

   In an x-y-F-graph, an ideal spring, fixed at the origin, is characterized by an upside-down cone with its apex in the origin of the diagram, while the potential energy function shows a paraboloid that touches the origin (figure 4.4ab). Normal springs are somewhat more complex. The cone in the x-y-F-graph has an imaginary apex below zero, and the x-y-V graph has a flat circular zero-region (figure 4.4cd). In both graphs, the area inside the free-length circle (the intersection of the cone with the ground plane), or indeed inside the initial-length circle, is of no practical significance.
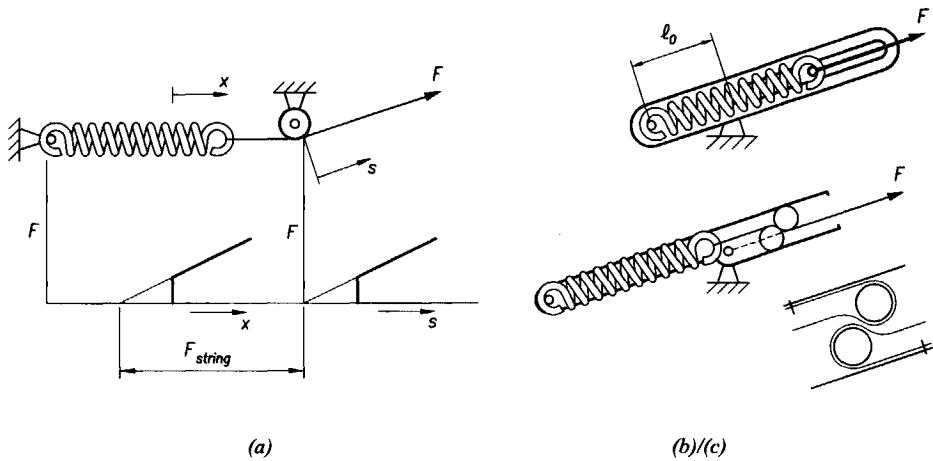
Figure 4.5   Practical embodiments of zero free length springs (additional versions included in appendix 4.1): (a) pulley and string [4.2], (b) storing the free length away behind the pivot using a guiding element [4.2], (c) similar, with rolling-link guide.

Practical embodiment

Unfortunately, zero-free-length springs are not readily available. The free length ℓ_0 of off-the-shelf springs usually amounts to 70 to 90 percent of the initial length L_0. There are, however, several ways to achieve zero-free-length behavior. The practical embodiments can be classified into two groups: one group with increased initial tension, and another that hides the free length (references included in [4.2], additional embodiments are given in appendix 4.1).

One way to increase initial tension is to employ a special coiling process, where the wire is twisted while being coiled (appendix 4.1, [4.2]). As a result, the coils are pressed together due to initial tension in the wire. As was argued in figure 4.2c, the free length ℓ_0 of a helical extension spring becomes zero when the initial tension is increased to the value kL_0. This yields ideal spring behavior in the range from L_0 to the maximum deflection. It is noted that the maximum deflection is decreased as compared to a similar spring without initial tension. Increased initial tension can also be achieved using a compression spring with two internal brackets (appendix 4.1, [4.2]).

A second way to achieve ideal spring behavior is to store the free length behind a guiding element. One example is a string passing through a guide eye or a pulley, configured such that the free end of the string starts building up force as soon as it leaves the guide eye or the pulley (figure 4.5a). Another way to store the free length of the spring is to devise a physical point on the action
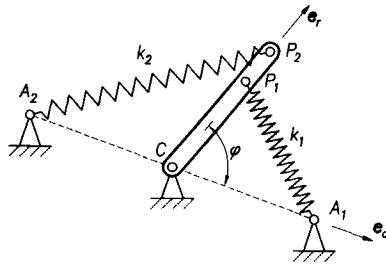
Figure 4.6   Basic spring force balancer in slightly generalized form.

line of the ideal spring, and align this point by a guiding element (such as for example the one in figure 4.5b, see also appendix 4.1 and [4.2]). In this class of ideal spring emulators, a guiding element is needed to avoid instability. Hence, some friction is involved in most practical embodiments of ideal springs. A special alignment arrangement is the one using a Rolamite with a modified flexible band arrangement shown in figure 4.5c.

Other ideal spring emulators include out-of-plane bending elements and special materials (appendix 4.1). Due to their practical inconvenience, they will not be discussed further.

4.3   Basic spring force balancer

> For all tasks of balancing, one will make an effort to bring the balancing back to those cases, since they result in the simplest principles of action.
>
> H. Hilpert, 1968

Figure 4.1b showed the balanced spring mechanism derived earlier (section 3.3) from zero stability considerations. As this particular mechanism, especially in the symmetrical version with $k_1 = k_2$ and $a_1 = a_2 = r_1 = r_2$, probably is the simplest (non-trivial) statically balanced spring mechanism, it will be adopted as the starting point for the approach used in this thesis, and be called the *basic spring force balancer*. This system will now be analyzed in some more detail, to derive the conditions for static balance and to investigate the forces in the mechanism. To this end, the potential will be derived, first for one spring, then for the complete mechanism. A slightly more general diagram will be used, with different indices for each spring (figure 4.6).
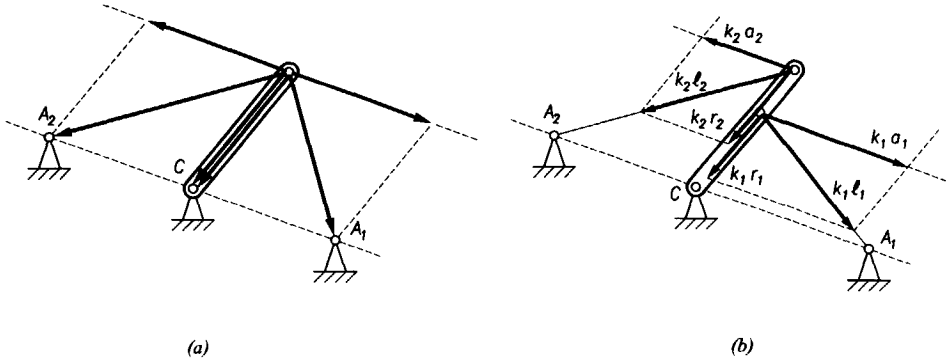
Figure 4.7   Skew resolution of forces: (a) symmetric basic spring force balancer, (b) slightly
generalized basic spring force balancer.

A configuration of a spring, attached between ground and the end of a
rotatable link, for example the triangle CP_1A_1 for spring k_1, will be called a
spring-lever element. The moving end of the spring is located on the line
carried by the unit vector e_r, which moves along with the link. Another unit
vector $e_a = a_{1/c}/|a_{1/c}|$ is introduced, and the following vectors are defined:
$r_{1/c} = r_1 e_r$, $r_{2/c} = r_2 e_r$, $a_{1/c} = a_1 e_a$ and $a_{2/c} = -a_2 e_a$. Then the potential of the
spring-lever element i is:

$$V_i = \tfrac{1}{2} k_i (a_{i/c} - r_{i/c})^T (a_{i/c} - r_{i/c}) + K \tag{4.3}$$

where K is a constant value, dependent on the choice of the potential datum.
Since the potential of a relaxed spring is zero, it is reasonable to select $K = 0$ in
this case. Consequently:

$$V_i = \tfrac{1}{2} k_i (a_{i/c} - r_{i/c})^T (a_{i/c} - r_{i/c}) = \tfrac{1}{2} k_i (a_i e_a - r_i e_\varphi)^T (a_i e_a - r_i e_\varphi)$$

$$= \tfrac{1}{2} k_i (a_i^2 - 2 a_i r_i \cos\varphi + r_i^2) = \tfrac{1}{2} k_i (a_i^2 + r_i^2) - k_i a_i r_i \cos\varphi \tag{4.4}$$

where φ is the angle between e_r and e_a. Therefore, the total potential
$V = V_1 + V_2$ of the system in figure 4.6 yields:

$$V = \tfrac{1}{2} k_1 (a_1^2 + r_1^2) + \tfrac{1}{2} k_2 (a_2^2 + r_2^2) - k_1 a_1 r_1 \cos\varphi - k_2 a_2 r_2 \cos(\pi - \varphi) \tag{4.5}$$

From this equation, the moment equation can be derived:

$$V_{,\varphi} = k_1 a_1 r_1 \sin\varphi - k_2 a_2 r_2 \sin\varphi \tag{4.6}$$

One solution for moment equilibrium is $\varphi = 0$ (the action lines of both spring
forces pass through the pivot), but to achieve moment equilibrium for any φ,
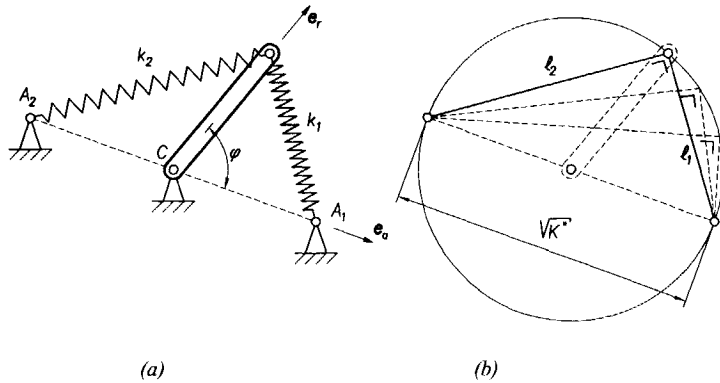
62

Figure 4.8   Basic spring force balancer: (a) symmetrical case with $k_1=k_2$ and $a_1=a_2=r_1=r_2$, (b) diagram explaining the use of Pythagoras' theorem to obtain the basic spring force balancer.

and under the condition that both A_1, C, A_2 and C, P_1, P_2 are collinear, the following condition must be satisfied:

$$k_1 a_1 r_1 = k_2 a_2 r_2 \qquad (4.7)$$

The same result is obtained by demanding that the total potential energy (equation 4.5) is constant, which happens when the cosine terms cancel. From the condition in equation 4.7, it is seen that the parameters k_i, a_i, and r_i can be chosen somewhat arbitrarily, as long as their product $k_i a_i r_i$ remains constant. Thus, more convenient combinations of spring attachment points and stiffness can be selected [4.4]. In the next section, this capacity will be used to modify the basic spring force balancer while maintaining its neutral stability.

Although the above treatise using the potential is very convenient, it will throughout this thesis prove worthwhile (from a scientific perspective) if not essential (from an engineering point of view) to consider the configuration of forces in the design of balanced spring mechanisms as well. The skew resolution of each spring force in a component parallel to the base, and a component along the lever, yields a simple proof of the perfect balance as well as an easy way to determine the design parameters as follows. The component of each spring force F_i parallel to the base equals $k_i a_i$, which acts on the link at a moment arm $r_i \sin \varphi$ about the pivot, while the component along the link equals $k_i r_i$ and does not have a moment contribution about the pivot (figure 4.7b). Setting the moments of either springs equal yields $k_1 a_1 r_1 = k_2 a_2 r_2$, as found earlier. The reaction force in the pivot is the vector summation of the spring force components along the link, which add up to a force of constant magnitude $k_1 r_1 + k_2 r_2$ directed along the link, and the difference of the
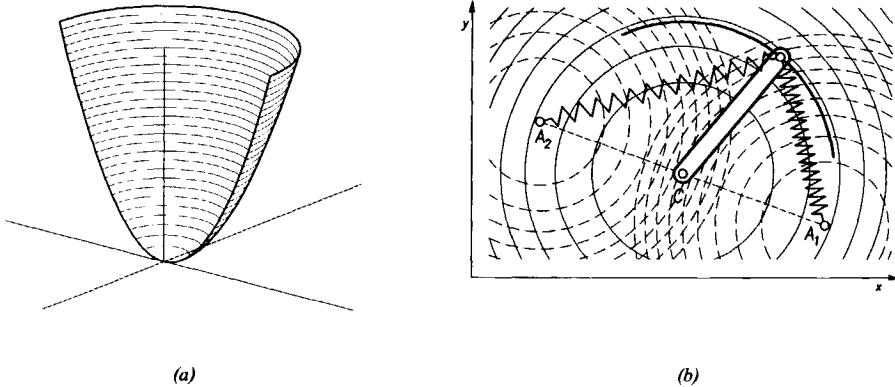
Figure 4.9   Energy fields: (a) energy paraboloid of ideal spring [4.3], *(b) conception of basic spring force balancer through tracing a contour line of the combined energy field of two ideal springs. The dashed circles are the contour lines of the ideal springs attached at A₁ and A₂, respectively, the continuous circles are the contours of the combined energy field, see also figure 4.19.*

components parallel to the base, $k_1a_1 - k_2a_2$. In the special case when $r_1 = r_2 = r$, the components parallel to the base are equal, and the resultant is equal to $(k_1 + k_2)r$, always directed along the lever (figure 4.7a). In this expression, the character of an ideal spring of stiffness $(k_1 + k_2)$ is recognized, as was previously found in chapter three. The dynamically equivalent resultant forces will be treated in section 4.6.

Before presenting rules for the modification of the basic spring force balancer, two more perspectives for the conception, analysis and proof of the basic spring force balancer will be given, to indicate that the possible perspectives are by no means exhausted with equilibrium and potential energy. Firstly, for the symmetrical case with $k_1 = k_2$ and $a_1 = a_2 = r_1 = r_2$ (figure 4.8a), the question how to find an adjustment mechanism which effects constant potential energy may be rephrased as follows. For a system incorporating two equal ideal springs, the total potential must be $\frac{1}{2}k\ell_1^2 + \frac{1}{2}k\ell_2^2 = K$, or $\ell_1^2 + \ell_2^2 = K^*$, where k is the spring constant of either spring, ℓ_i is the actual length of spring k_i, and where K and K^* are constants. One may recognize the theorem of Pythagoras in this expression, and imagine a set of right-angled triangles, all having the same hypotenuse $\sqrt{K^*}$ (figure 4.8b). The locus of the right-angled corners of these triangles forms a circle for all allowable combinations of ℓ_1 and ℓ_2. Therefore, a crank tracing this circle constitutes a suitable physical realization [4.5].
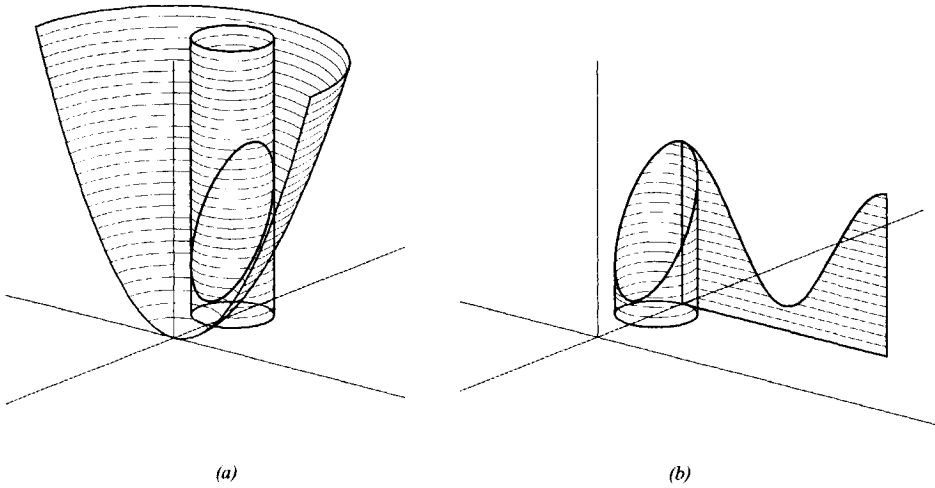
64

(a)   *(b)*

Figure 4.10 Graphical interpretation of the energy function of a rotatable link: (a) the intersection of a cylinder and a paraboloid with parallel center lines is an ellipse, (b) the ellipse corresponds with a sine function on the cylinder wall [4.3].

Secondly, the three-dimensional energy functions (figure 4.9a) can be used as follows. Figure 4.9b gives contour plots of two equal ideal springs, attached at A_1 and A_2. The circular contour lines about A_1 indicate the elastic potential due to spring k_1 as a function of the position of its free end. The same holds for the spring attached at A_2. When the free ends of both springs are connected to one moving point, the energy functions are to be added up. The result is another paraboloid, indicated schematically in the figure (see also figure 4.19). If the moving point traces any of the contour lines of this combined energy function, the potential will remain constant. As the contour lines of the combined energy field are circles, a link suffices as the adjustment mechanism. In case of equal springs, the link is to rotate about the midpoint of line A_1A_2. The case of unequal (ideal) springs is treated later in the next section, while chapter six is concerned with the case of non-ideal springs.

Yet another graphical approach is suggested in figure 4.10. The circle in the ground plane of figure 4.10a is traced by the moving end of a rotatable link. This trajectory cuts off a shape from the energy paraboloid of an ideal spring. It was found that the intersection of a paraboloid and a cylinder with parallel lines of symmetry is situated in an inclined flat plane, and has the shape of an ellipse (this remarkable fact is proved in appendix 4.2). Consequently, the height of the cylinder wall as a function of the rotation angle of the link is a sine function (figure 4.10b). This provides another way of deriving the basic spring force

65

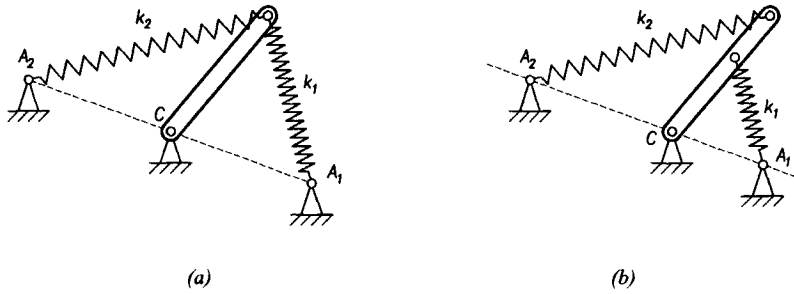*(a)*   *(b)*

Figure 4.11   Modification rule 1: variation of parameters: (a) basic spring force balancer, (b) reduced arm lengths and increased stiffness of spring-lever element labeled 1. Note that the potential and the pivot force are affected.

compensator. The total energy becomes constant by placing two of these sine functions in opposite phase, which implies two ideal springs diametrically opposed with respect to the fixed pivot of the link (some additional peculiarities are given in appendix 4.2).

4.4   Modification operations

> *This means that, if desired, a spring may be attached between a kinematic constraint link and the fixed reference. In this special case, the physical location of the spring becomes somewhat more arbitrary, and more convenient locations for spring attachment may be used.*
>
> G. K. Matthew, D. Tesar, 1976

The basic spring force balancer can be modified without distorting its balance to serve many purposes, including efficient use of available space, the use of off-the-shelf springs with prescribed spring rate, and the design of mechanisms with a specific function. In this section, seven modification rules will be derived (references are included in endnote [4.4]).

Variation of parameters (rule 1)

It has already been proved (equations 4.5 through 4.7) that the basic spring force balancer is statically balanced for rotation about the pivot under the conditions that $k_1 a_1 r_1 = k_2 a_2 r_2$ and A_1, C and A_2 are collinear. Figure 4.11 illustrates a modification of the basic spring force balancer according to the latitude in design granted by this condition. The parameters k_i, a_i, and r_i of a spring-lever element can be chosen as appropriate as long as their product $k_i a_i r_i$ remains constant. Thus, a compact compensation unit can be made, or link lengths can be adjusted to the exact spring specifications.
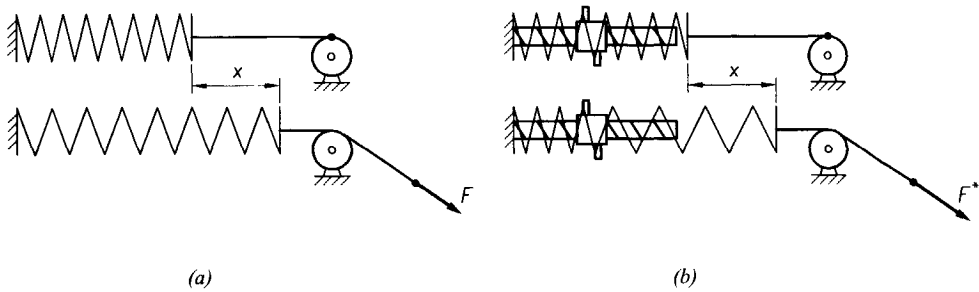
(a)   *(b)*

Figure 4.12 Adjustable ideal spring arrangement: (a) helical spring with sufficient pitch used as extension spring in zero-free-length configuration, (b) nut with extension on threaded rod with pitch equal to the pitch of the unloaded spring allows disengagement of coils, thus effecting increased stiffness [4.6].

In addition to the geometric modification of the parameters a and r, also the stiffness k can be adjusted. A profitable way of achieving this is by using the mechanism in figure 4.12b. Inside a helical spring, of which the coils do not touch when unloaded, a threaded pin is mounted with a pitch equaling the springs pitch. By turning a bolt with extensions holding one coil, the number of coils engaged is changed. When n_{tot} is the total number of coils and n_{eff} the number of active coils, the resulting stiffness has become $k^* = \left(n_{tot} / n_{eff}\right)k$. Thus, the stiffness of the spring can be adjusted, not only when no load is present but also when loaded, without changing the free length [4.6].

One remark should be made. Changing the parameters k_i, a_i, and r_i, even when their product is invariant, generally does require energy. The variable terms of the energy functions in equation 4.5 still cancel under this modification operation, but the constant terms are changed. Therefore, in general, this operation yields a mechanism with altered total energy, so the modification cannot be effected in an energy-free manner.

Rotation (rule 2)

Similar to the translation of forces along their line of action, moments can be rotated about a pivot. Thus, considering a spring-lever element as a moment generator, it can be rotated as a whole about the pivot. The procedure as applied to the basic spring force balancer can be imagined as follows. First the springs are frozen. The lever is duplicated and the resulting individual spring-lever elements are rotated about the fixed pivot by an angle of β (figure 4.13). Then the springs are fixed to ground again, the levers are synchronized by connecting them by a link so that a rotatable body is formed, and finally the springs are thawed. The resulting generalized basic spring force balancer is called the *spring butterfly*. The potential of the spring-lever elements essentially remains
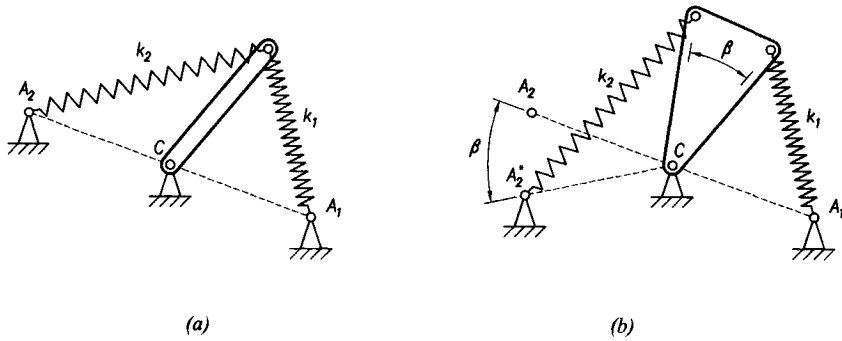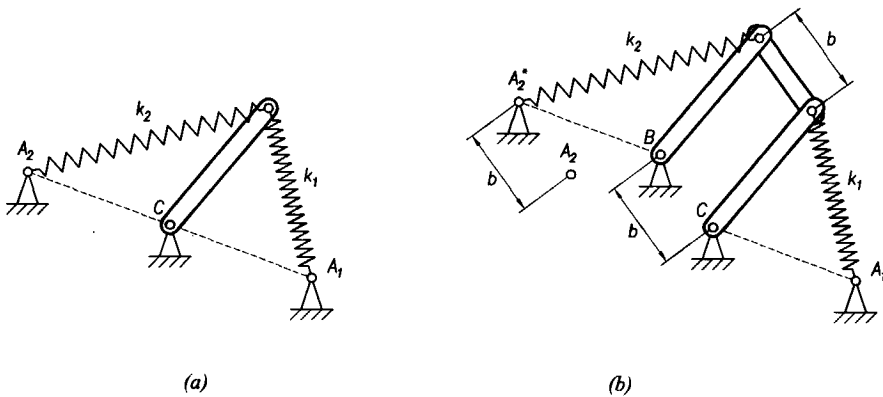
Figure 4.13 Modification rule 2: rotation of spring-lever elements: (a) basic spring force balancer, (b) result after element labeled 2 was frozen, rotated counterclockwise by an angle β, and thawed. This arrangement is called the spring butterfly.

unchanged under this procedure so the state of static balance is maintained. Indeed, unlike rule 1, rotation has no influence on the total potential and can therefore be effected in an energy-free manner.

Shift (rule 3)

A third modification is to shift the individual spring-lever elements apart by a shift vector $b = be_b$, where e_b is the unit vector in shift direction, and connecting the levers by a link into a parallelogram arrangement (figure 4.14). Although a number of additional links is introduced, this operation does not influence the potential energy functions of the springs. Therefore, under this operation, the mechanism remains perfectly balanced, and the modification can

Figure 4.14 Modification rule 3: shift of spring-lever elements: (a) basic spring force balancer, (b) result after element labeled 2 was shifted by the vector $b=be_b$.

(a)   *(b)*
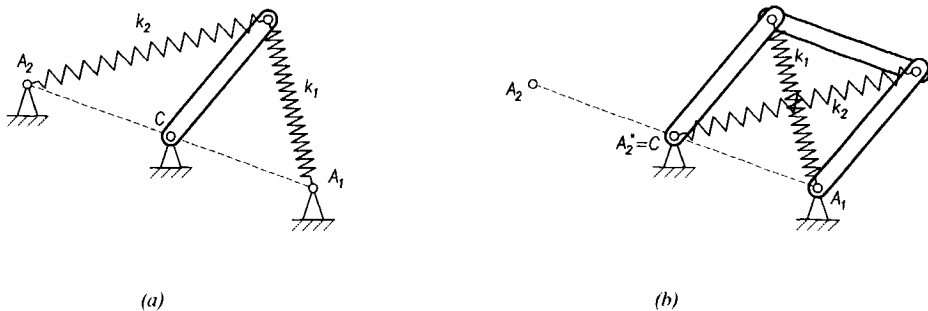
Figure 4.15 Special shift modification: (a) basic spring force balancer, (b) balanced parallelogram.

be carried out energy-free. Note that shifting in any direction is allowed, even into the third dimension, as long as the spring-lever elements remain in parallel planes, and reasonable transmission angles are maintained.

When the two equal spring-lever elements of the symmetric basic spring force balancer are shifted towards each other along their common base, the *balanced parallelogram* results (figure 4.15). This conveniently demonstrates that any parallelogram, with equal ideal springs on its diagonals, yields a statically balanced spring mechanism, as may be verified by inspection of the potential. With equal springs, $k_1 = k_2 = k$, the total potential reads:

$$V = \tfrac{1}{2}k_1\ell_1^2 + \tfrac{1}{2}k_2\ell_2^2 = \tfrac{1}{2}k\left(\ell_1^2 + \ell_2^2\right) \tag{4.8}$$

In a parallelogram, the lengths of the sides relate to the lengths of the diagonals according to:

$$\ell_1^2 + \ell_2^2 = 2\left(r_1^2 + r_2^2\right) \tag{4.9}$$

where r_1 and r_2 are the sides, and ℓ_1 and ℓ_2 are the diagonals. Substituting this expression into equation 4.9 learns that the potential is constant, which concludes the proof.

Kinematic inversion (rule 4)

Clearly, kinematic inversion of the whole mechanism has no effect on relative motion of the elements, including the springs (figure 4.16). Therefore, the system behavior is unchanged, and the modification can be effected energy-free. Interesting is that the resultant force of the springs acting on the moving part now yield a constant force with unchanging direction relative to the fixed reference system.
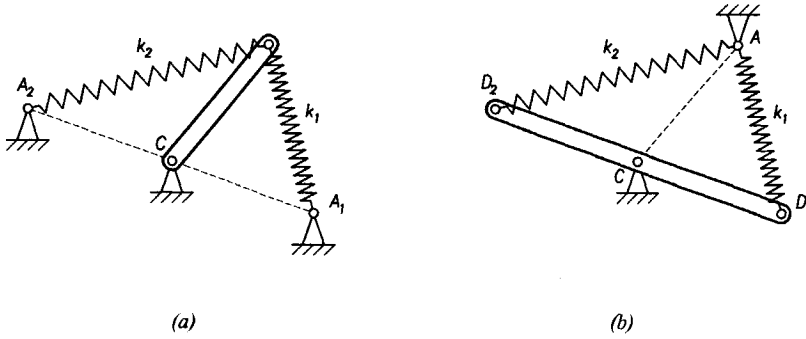
(a)   *(b)*

Figure 4.16 Modification rule 4: kinematic inversion: (a) basic spring force balancer, (b) result after kinematic inversion.

In addition to kinematic inversion, another kind of inversion is sometimes possible with interesting results: the exchange of springs and links. This inversion is allowed when the links are axially loaded only. For instance, in the balanced rhombus (figure 4.17a), which is the symmetric version of the balanced parallelogram (figure 4.15b), interchanging springs and links yields another statically balanced system (figure 4.17b). This system can be regarded as a back-to-back assembly of two basic spring force balancers. As the springs and dimensions are selected equal, the pivot reaction forces due to each basic spring force balancer cancel. Consequently, the pivot can be omitted, which can be a great practical advantage. Chapter five will further develop this principle of floating suspension.

Composition and resolution of ideal springs (rule 5)

In section 3.3, it was demonstrated that two ideal springs, each fixed to the same member with one end and attached to the same moving point with their other end, can be substituted by a single one, and that this resultant spring is
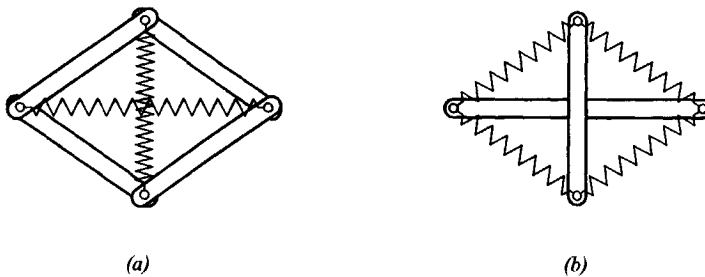

(a)   *(b)*

Figure 4.17 Another kind of inversion: (a) symmetric version of balanced parallelogram (balanced rhombus), (b) result after interchanging springs and links.
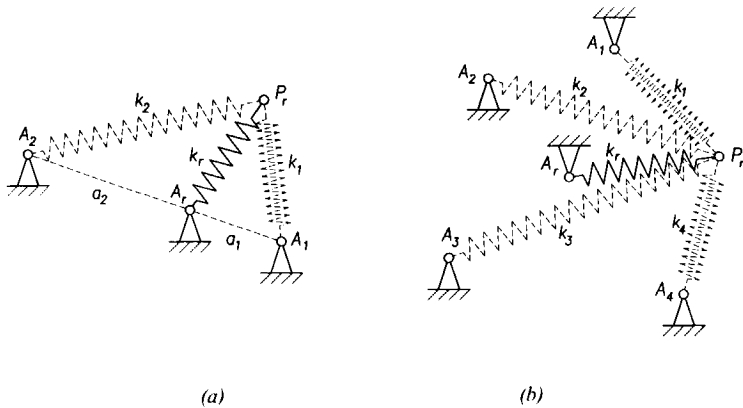
70

Figure 4.18 Modification rule 5: composition of ideal springs: (a) composition of two springs, (b) composition of more springs.

dynamically equivalent with the original springs. The composition of springs can be very convenient in the design of spring mechanisms, for instance when an additional spring is desired or when a spring mechanism is to be simplified. The procedure of section 3.3 is illustrated in figure 4.18a. The substitute spring is located on the line connecting A_1 and A_2, so that $k_1 a_1 = k_2 a_2$, while its stiffness amounts to $k_1 + k_2$.

For the case of n springs attached to the same point P_r, equation 3.64 can be generalized into the following expression:

$$\left(\Sigma k_i\right)\left(a_r - r_r\right)^T r_{r/c} = \Sigma k_i\left(a_i - r_r\right)^T r_{r/c} \tag{4.10}$$

Rearranging gives:

$$a_r = \frac{\Sigma k_i a_i}{\Sigma k_i} \tag{4.11}$$

Thus, an arbitrary number of ideal springs, fixed to a common link, and all acting on a single movable point (figure 4.18b), can be composed into a single ideal spring, with its fixed point located at the position A_r (the position where the movable point is in equilibrium under the influence of the original springs), and with a spring rate k_r equal to the sum of the spring rates of the original springs.

This rule can easily be verified by adding the energy paraboloids of the springs, since the result is another paraboloid. Taking the derivative of this function yields the force-length relationship of an ideal spring of summed stiffness. Note however, that the sum-paraboloid does not touch the ground plane (figure 4.19), which means that the composed spring possesses increased
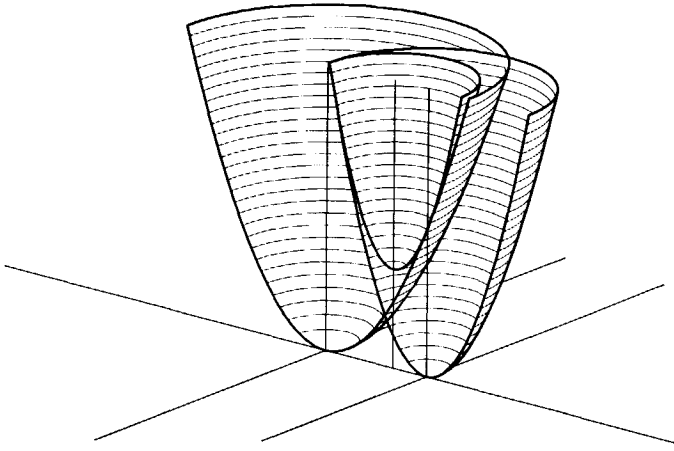
71

Figure 4.19 The addition of two paraboloids is another paraboloid, however this sum-paraboloid does not touch the ground plane [4.3].

energy. This energy is equal to the energy required to stretch the original springs from their fixed points A_i to the equilibrium position A_r, the *assembly potential* V_a of the system, so to speak, where $V_a = \frac{1}{2} k_1 a_1^2 + \frac{1}{2} k_2 a_2^2$. Consequently, this modification is not energy-free.

Composition and resolution of ideal spring-lever elements (rule 6)

Similar to the composition or resolution of ideal springs, ideal spring-lever elements can be composed or resolved as appropriate. Figure 4.20 suggests the composition of elements $A_1 P_1 C$ and $A_2 P_2 C$ into the substitute element $A_r P_r C$. In fact, a sequence of previous rules is applied: first the spring-lever elements are rotated (from $A_1 P_1 C$ and $A_2 P_2 C$ into $C A_1^* P_1^*$ and $C A_2^* P_2^*$, by the clockwise angles β_1 of and β_2 respectively, according to rule 2), then the arm lengths are adjusted (from $C A_1^*$ and $C A_2^*$, both to $C P_r$) together with the spring rates in order to maintain balance (rule 1), and finally the springs (now acting on the same point A_r) are composed into spring k_r using rule 5. Naturally, the resulting substitute element can be altered using rule 1.

From this procedure with two springs, the equations for the n-spring case are readily derived. When n spring-lever elements are to be replaced by a single one, the potential of both systems must be equal:

$$\frac{1}{2} k_r (a_{r/c} - r_{r/c})^T (a_{r/c} - r_{r/c}) = \sum \frac{1}{2} k_i (a_{i/c} - r_{i/c})^T (a_{i/c} - r_{i/c}) \qquad (4.12)$$
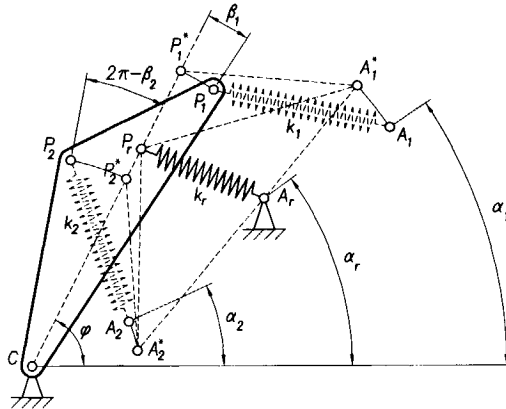
72

Figure 4.20 Modification rule 6: composition of spring-lever elements.

where index r denotes the substitute spring-lever element. Using the symbols of figure 4.20, and defining α_i as the angle between the horizontal and the line CA_i, and the angle β_i as the clockwise rotation angle of spring-lever element $A_i P_i C$, the equation becomes:

$$\tfrac{1}{2}k_r\left(a_r^2+r_r^2\right)-k_r a_r r_r \cos(\varphi-\alpha_r)=\sum\left(\tfrac{1}{2}k_i\left(a_i^2+r_i^2\right)-k_i a_i r_i \cos(\varphi-(\alpha_i-\beta_i))\right)$$

(4.13)

Demanding equality for any φ, and elaboration reveals that this equation is equivalent with the set:

$$k_r a_r r_r = \sum k_i a_i r_i \cos(\alpha_r-(\alpha_i-\beta_i))$$

(4.14)

$$0 = \sum k_i a_i r_i \sin(\alpha_r-(\alpha_i-\beta_i))$$

(4.15)

The line on which the grounded point of the spring of the resultant spring-lever element is to be located (defined by point C and angle α_r) is obtained using the latter equation. It is interesting to note that the latter equation is the moment equilibrium equation about C, which indeed gives zero for $\varphi=\alpha_r$. Application of trigonometry and extracting the α_r-terms from the latter equation gives the criterion for the orientation of the substitute element:

$$\tan\alpha_r = \frac{\sum k_i a_i r_i \sin(\alpha_i-\beta_i)}{\sum k_i a_i r_i \cos(\alpha_i-\beta_i)}$$

(4.16)

The substitution of multiple springs acting on a rotatable body by a single equivalent spring can be summarized as follows. When the point of
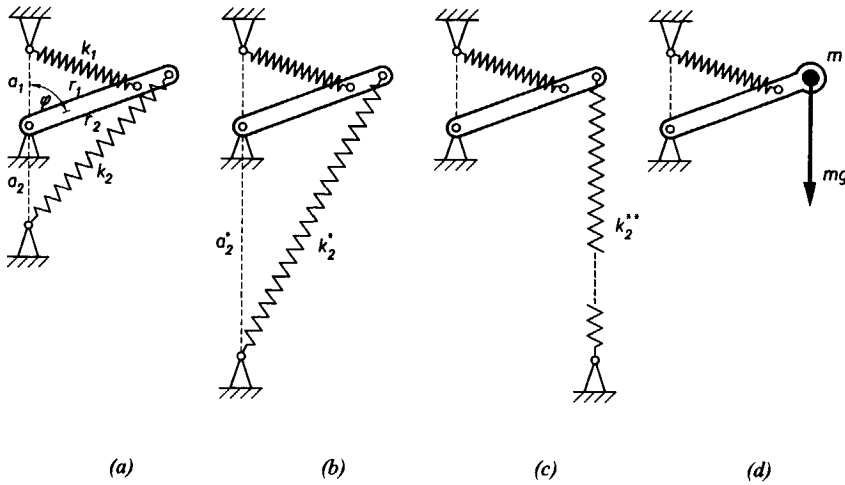
73

Figure 4.21 Modification rule 7: interchange of mass-lever and spring-lever element, illustrated by limit transition.

attachment P_r for the equivalent spring is chosen, the line on which the point of attachment A_r must be placed follows from equation 4.16, equivalent moment is reached if equation 4.15 is satisfied, and equivalent energy is realized if equation 4.13 is used additionally. If equation 4.13 is not satisfied, the left and right sides differ by a constant term. This means that the potential, though still constant, has changed: in the potential equation (equation 4.3) of the substitute spring-lever element, the constant K is no longer zero. The graphical procedure already showed this: since both rules 1 and 5 are used, the total energy of the modified configuration is altered as compared to the original configuration.

Similarity of mass-lever and spring-lever elements (rule 7)

A seventh rule is derived from the apparent similarity in the behavior of mass-lever and spring-lever elements (see also chapter two). A slightly closer examination reveals that a mass-lever element may very well be regarded as the limit case of a spring-lever element. In figure 4.21, the transition of a spring-lever element into a mass-lever element is illustrated. Following rule 2, the base a_2 of the spring-lever element is enlarged. Simultaneously, the spring rate k_2 is decreased, so that the product $k_2 a_2$ remains constant and balance is preserved. As a_2^* approaches infinity, k_2^* reduces to zero. When the spring force is resolved into a component along the lever arm F_{lever} and a vertical component F_{vert}, two things are observed: the vertical component keeps the constant value $k_2 a_2$, and the component along the lever arm F_{lever} has no moment contribution (keep in mind, however, that it *is* present). Hence, in the
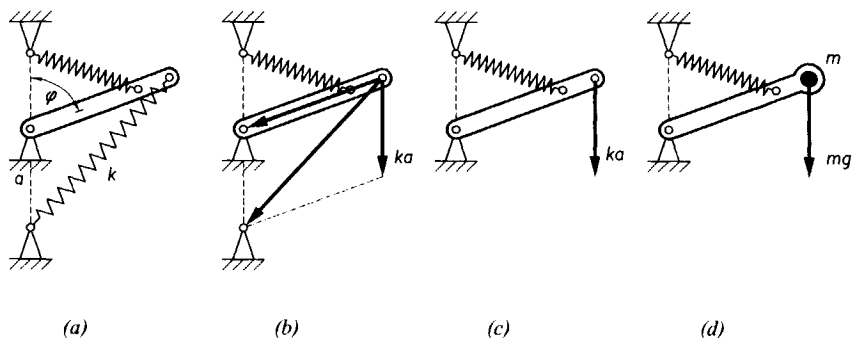
74

Figure 4.22 Modification rule 7: interchange of mass-lever and spring-lever element, illustrated using skew resolution of forces.

limit case, and under the condition $mg = k_2 a_2$, the behavior of the spring-lever element and the mass-lever element have become identical. Gravity balancing often is called *equilibration*, the system in figure 4.21d will be called the *basic gravity equilibrator*.

Naturally, the fact that a balanced mechanism is obtained can also be demonstrated using the potential. Taking the pivot as the datum for the gravity potential, the total potential is:

$$V = \tfrac{1}{2} k_1 \left(a_1^2 + r_1^2\right) - r_1 k_1 a_1 \cos\varphi + mgr_2 \cos\varphi_2 \tag{4.17}$$

This yields the condition $r_1 k_1 a_1 = mgr_2$, and since in the original configuration the condition $r_1 k_1 a_1 = r_2 k_2 a_2$ was true, the condition $mg = k_2 a_2$ results.

Alternatively, the spring force can be resolved in a skew manner (figure 4.22). The vertical component is constant and therefore behaves as a mass. The component along the link has no moment contribution about the pivot and can therefore be disregarded. This also shows the similarity in the behavior of the two systems.
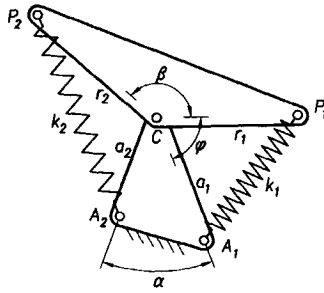
Figure 4.23   Spring butterfly.

4.5   Combination of modifications

Indeed, it is clear, from the equations, that infinitely many statically balanced mechanisms exist, for each of the architectures studied here. Moreover, it is also found, by inspection of the equations, that balancing is always possible for any given value of the geometric parameters. This is an interesting result since it allows the kinematic design of a mechanism to be completed using any criterion and the balancing to be performed a posteriori.

CM Gosselin, J Wang, 2000

What greatly adds to the versatility of the modification rules, is the fact that they can be combined in many ways, due to the linearity of the equations of motion. This capacity was already observed in the graphical procedure of the composition of spring-lever elements. The creative combination of the basic operations in fact constitutes the core of the conception of statically balanced spring mechanisms as proposed in this thesis. Two important phenomena related to the combination of modification rules are described next.

First, it is noted that *order and grouping* of the modification operations are not important in the sequential application of the rules (they are commutative and associative). Thus, the rules can be sequenced to transform the basic spring force balancer into a desired configuration, almost without computations. For instance, the springs in the balanced parallelogram need not be attached to the pivots, but may be moved along their respective links following rule 1. Similarly, by combining rules 1 and 2, spring butterflies of countless shapes can be made (figure 4.23). As a consequence, any spring butterfly with $\alpha + \beta = \pi$ and $k_1 a_1 r_1 = k_2 a_2 r_2$ is statically balanced [4.4].

A sequence of rules was already applied in rule 6. It is interesting to note that the procedure of rule 6 was illustrated using a system that is not balanced.
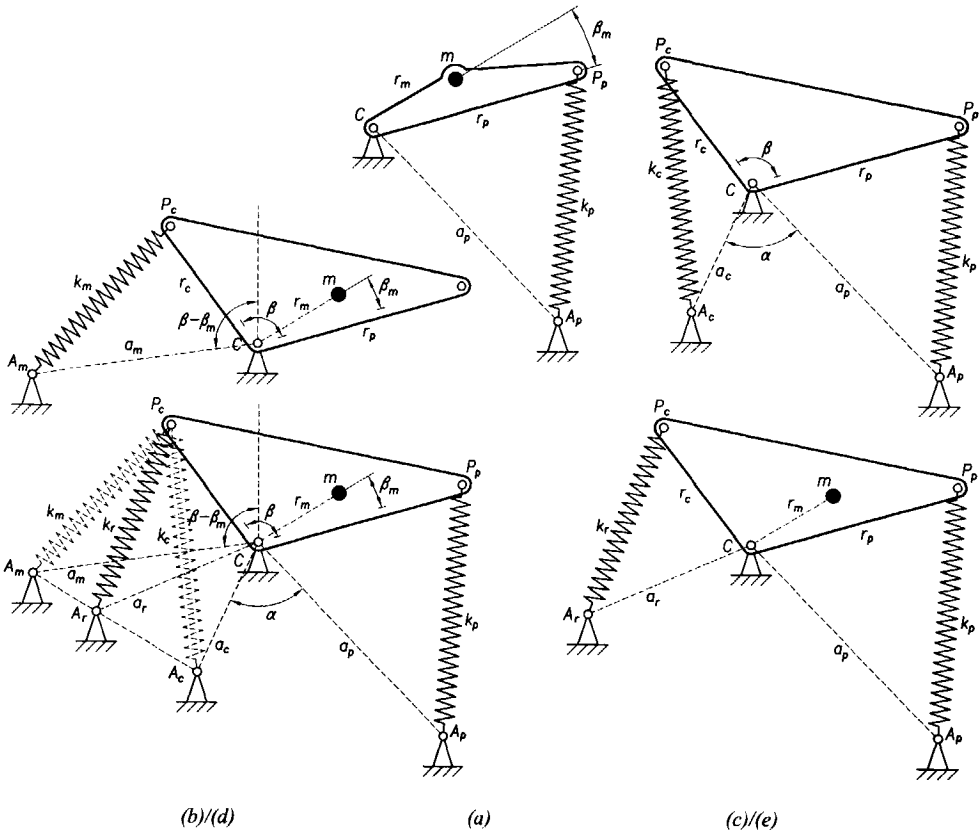
76

Figure 4.24 Combined balancer for undesired spring and mass: (a) rotatable body hampered by mass and spring, (b) gravity equilibrator, (c) spring force balancer, (d) combined balancers, (e) simplified version.

When composing the two spring-lever elements of a statically balanced configuration, such as the spring butterfly in figure 4.23, a rotatable body results with a spring attached between a selected point P_r and the pivot C. This is due to the fact that rotating the spring-lever elements to the line CP_r makes A_1, C, and A_2 collinear. Next, P_1^* and P_2^* are modified to P_r which requires the spring stiffnesses to be changed according to $r_1 k_1 = r_r k_1^*$ and $r_2 k_2 = r_r k_2^*$. Consequently, $a_1 k_1^* = a_2 k_2^*$, which implies that the substitute spring is to be attached at the pivot (see rule 5), and a trivial statically balanced spring mechanism results.

Secondly, *superposition* is allowed, which is a powerful tool in the design of balanced spring mechanisms. If, for instance, a single degree of freedom system is hampered by multiple masses and/or springs, the spring systems required to
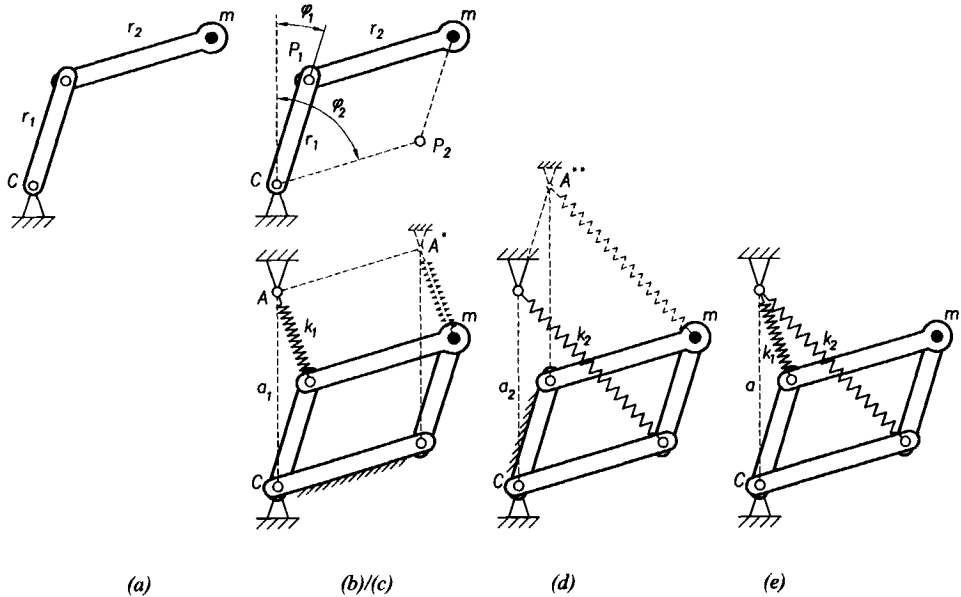
77

Figure 4.25 Two degree-of-freedom gravity balancer: (a) principal problem: balancing a mass at the end of a two-link open loop chain, (b) augmentative links in parallelogram configuration, (c) balancing the first degree of freedom, (d) balancing the second degree of freedom, (e) combining the balancing systems.

balance each of them can be designed independently and applied simultaneously. Furthermore, if a multiple degree of freedom system is to be balanced, it is allowed to design balancers for each single degree of freedom while 'freezing' the other ones, provided that parameters of the balancer for a specific degree of freedom are not affected by the other degrees of freedom. In both of these cases, the resulting balancing systems may be combined into a single one. Two examples will be given next.

A first example illustrates the principle of superposition, as well as the similarity of spring-lever and mass-lever elements. Figure 4.24a shows a rotatable body, hampered by a mass m and a spring k_p. The spring systems required to balance each of them can be designed independently and applied simultaneously, due to the linearity of the governing equations of motion. One of many possibilities is given in the diagram. Neglecting the mass, spring k_c is designed to balance undesired spring k_p (figure 4.24c, recognize a spring butterfly). Neglecting spring k_p, mass m is equilibrated by spring k_m by the subsequent application of rules 7 and 2 (figure 4.24b). The two balancers are combined (figure 4.24d), and finally, the springs are composed into a single one, which balances the mass and the spring simultaneously (figure 4.24e). In

this example, the parameters were chosen such that springs k_m and k_c act at the same point P_c to facilitate their composition into spring k_r, according to rule 5.

A second example demonstrates the handling of more degrees of freedom (figure 4.25). Suppose that a mass supported by a two-link open chain is to be balanced. This problem cannot be solved by straightforward application of one of the modification rules. However, an elegant solution is possible using superposition. To this end, it is useful to construct a parallelogram according to figure 4.25b. This mechanism is sometimes called a five-bar parallelogram linkage, where the fifth link is the frame, which has zero length because the two fixed pivots of links CP_1 and CP_2 coincide. The two-dimensional position of the mass is defined by the angles φ_1 and φ_2. Using the principle of superposition, φ_2 can be frozen while an equilibrator is designed for φ_1 by recognizing the basic gravity balancer in the triangle $P_2 M A^*$ (figure 4.25c). By inspection, the balancing condition is: $mg = k_1 a_1$. However, when φ_2 is released, the spring is not attached adequately with respect to point P_2, which will move with φ_2. To avoid this problem, the spring is shifted along link r_2 so that point A is right above point C. This shift ensures that the system is statically balanced for φ_1 in any configuration of φ_2. The same procedure is followed for φ_2 (figure 4.25d), resulting in $mg = k_2 a_2$. Now the two balancing systems are merged, simply by thawing both angles, and the two degree-of-freedom equilibrator of figure 4.25e results. Proof of this is straightforward by writing down the potential:

$$V = mg(r_1 \cos\varphi_1 + r_2 \cos\varphi_2) + \tfrac{1}{2}k_1\left(a_1^2 + r_1^2\right) - k_1 a_1 r_1 \cos\varphi_1 \qquad (4.18)$$

$$+ \tfrac{1}{2}k_2\left(a_2^2 + r_2^2\right) - k_2 a_2 r_2 \cos\varphi_2$$

$$= \tfrac{1}{2}k_1\left(a_1^2 + r_1^2\right) + \tfrac{1}{2}k_2\left(a_2^2 + r_2^2\right) + (mgr_1 - k_1 a_1 r_1)\cos\varphi_1 + (mgr_2 - k_2 a_2 r_2)\cos\varphi_2$$

For the potential to be constant, the cosine terms need to cancel out, which leads to the balancing conditions found previously. These conditions are independent, which is due to the shift operations performed during the conception. In the special case of $a_1 = a_2 = a$, as displayed in the figure, equal springs are required, regardless of link lengths. It is tempting to compose the springs into a single one, attached at the center of the parallelogram, according to rule 5, but this is not allowed due to the varying distance $P_1 P_2$. In fact, the assembly energy (see rule 5), would then be overlooked. Making up for this would require an additional spring, which conflicts with the desire for a single spring.
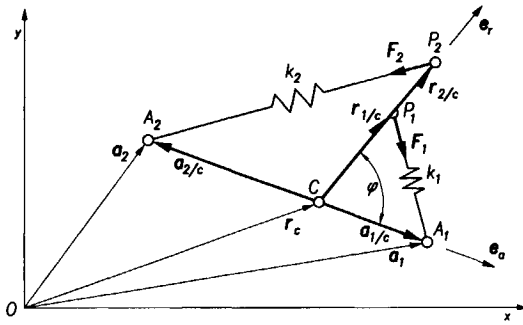
Figure 4.26   Dynamically equivalent force of the spring forces acting on the moving link.

4.6   Stability of modifications

Ja gut, die Gedanken, welche schlaflos vor Glück machen, die dich treiben, dass du tagelang vor dem Wind läufst wie ein Boot, müssen immer etwas falsch sein.

All right, the thoughts, which give you sleepless nights, which drive you, let you sail before the wind for days like a ship, always need to be somewhat faulty.

Robert Musil, 1921

In the previous section, the basic spring force balancer was modified following the potential energy approach. In order to investigate the influence of these modifications on the stability, the theory of chapter three will be applied. In section 3.3, it was found that when motion was restricted to rotation, two central linear forces are to be substituted by a resultant constant force, rather than a resultant central linear force. This remarkable phenomenon will be investigated somewhat further in this section by inspecting the dynamically equivalent forces in the configurations modified according to rules one through four.

Variation of parameters

First, the basic spring force balancer modified by rule 1 will be reviewed. Figure 4.26 reconsiders the neutral equilibrium configuration of chapter three, slightly generalized as compared to figures 3.6, in that P_1 and P_2 are no longer coincidental (as in figure 4.6). However, the points C, P_1 and P_2 are still collinear, located on the line carried by the unit vector $e_r = (\cos\phi \quad \sin\phi)^T$, where ϕ is the angle between the link and the horizontal. It has already been

80

proved (equations 4.4 through 4.6) that the system is statically balanced for rotation about the pivot under the condition that $k_1 a_1 r_1 = k_2 a_2 r_2$. Now the resultant of the spring forces will be investigated to verify the stability condition. The force equation, derived from equation 4.4, yields:

$$V_{,r_c} = -k_1 (a_{1/c} - r_{1/c}) - k_2 (a_{2/c} - r_{2/c}) = -(k_1 a_1 - k_2 a_2) e_a + (k_1 r_1 + k_2 r_2) e_r$$

(4.19)

As in section 4.3, the skew resolution is recognized in this expression, $k_i a_i$ being the component parallel to the base CA_i, and $k_i r_i$ the component parallel to the lever CP_i. This way of resolution, rather than into orthogonal components, will turn out to be of great use. Equilibrium of moments was found for any φ under the condition $r_1 k_1 a_1 = r_2 k_2 a_2$.

Lastly, the application point of the dynamically equivalent force is investigated using the stability equation for rotation about the pivot, derived from equation 4.6:

$$V_{,\varphi\varphi} = k_1 a_1 r_1 \cos \varphi - k_2 a_2 r_2 \cos \varphi$$

(4.20)

a result which can also be found using equation 3.68. For static balance, this expression must always equal zero. This implies the following for the dynamically equivalent application point of the resultant force F_r.

Were F_r to be regarded as a central linear force, its contribution to the stability, according to equation 3.68, amounts to $k_r r_{r/c}^T r_{r/c} + F_r^T r_{r/c}$, which is demanded to be zero. As F_r passes through C, the vectors F_r and $(a_{r/c} - r_{r/c})$ are collinear. Therefore, using e_r as the unit vector in the direction of F_r, one can write $a_{r/c} = a_r e_r$ and $r_{r/c} = r_r e_r$, so

$$k_r r_{r/c}^T r_{r/c} + F_r^T r_{r/c} = k_r r_{r/c}^T r_{r/c} + k_r (a_{r/c} - r_{r/c})^T r_{r/c}$$

$$= k_r a_{r/c}^T r_{r/c} = k_r a_r r_r = 0$$

(4.21)

There are three solutions to this equation. The first one is $k_r = 0$, which is not valid since $|F_r| \neq 0$. The other solutions are that either $a_r = 0$ or $r_r = 0$. This means that at least one end of the resultant spring must be attached at the pivot and that the other end is hinged on the line carried by e_r, at a distance r_r or a_r, respectively, from the pivot. Considering the appearance of the expression for the resultant force (equation 4.19), this is only valid if $k_1 a_1 = k_2 a_2$, or $r_1 = r_2$. This result is in agreement with section 3.3, where it was found that a resultant spring does not generally exist, except under specific conditions, one of them being $r_1 = r_2$.

The other solution suggested in section 3.3 is to replace the two spring forces by a constant force, which will be done next. Were F_r to be regarded as a constant force, then its contribution to the stability, according to
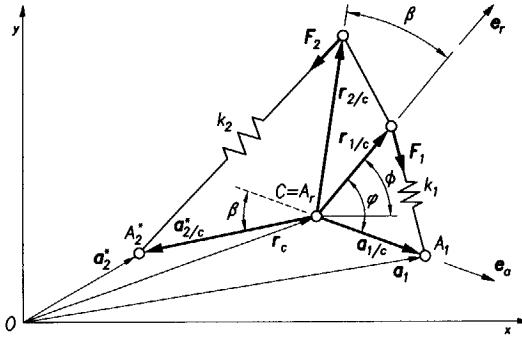
Figure 4.27   Dynamically equivalent force of the spring forces acting on the moving link of the spring butterfly.

equation 3.38, amounts to $F_r^T r_{r/c}$, which must be zero for neutral equilibrium. As F_r passes through C, the vectors F_r and $r_{r/c}$ are collinear. Therefore, using e_r as the unit vector in the direction of F_r:

$$F_r^T r_{r/c} = F_r^T r_r e_r = F_r^T r_r \frac{F_r}{|F_r|} = r_r |F_r| = 0 \qquad (4.22)$$

Knowing that $|F_r| \neq 0$, it follows that r_r must be zero. Consequently, the dynamically equivalent application point of F_r coincides with point C. Apparently, substituting the two spring forces by a constant force yields satisfactory results with respect to dynamic equivalence.

Rotation

Similar considerations apply to the spring butterfly. From figure 4.27, the following expressions for the arm lengths are derived:

$$r_{1/c} = r_1 e_r, \quad r_{2/c} = r_2 R(\beta)e_r, \quad a_{1/c} = a_1 e_a, \quad a_{2/c} = -a_2 R(\beta)e_a \qquad (4.23)$$

The potential of the modified basic spring force balancer is given by:

$$V = \tfrac{1}{2} k_1 (a_1 e_a - r_1 e_r)^T (a_1 e_a - r_1 e_r) \qquad (4.24)$$

$$+ \tfrac{1}{2} k_2 (-a_2 R(\beta)e_a - r_2 R(\beta)e_r)^T (-a_2 R(\beta)e_a - r_2 R(\beta)e_r)$$

The resultant force and moment are, respectively:

$$V_{,r_c} = -k_1(a_1 e_a - r_1 e_r) - k_2(-a_2 R(\beta)e_a - r_2 R(\beta)e_r) \qquad (4.25)$$

$$V_{,\varphi} = -k_1(A r_1 e_r)^T (a_1 e_a - r_1 e_r) - k_2(A r_2 R(\beta)e_r)^T (-a_2 R(\beta)e_a - r_2 R(\beta)e_r)$$

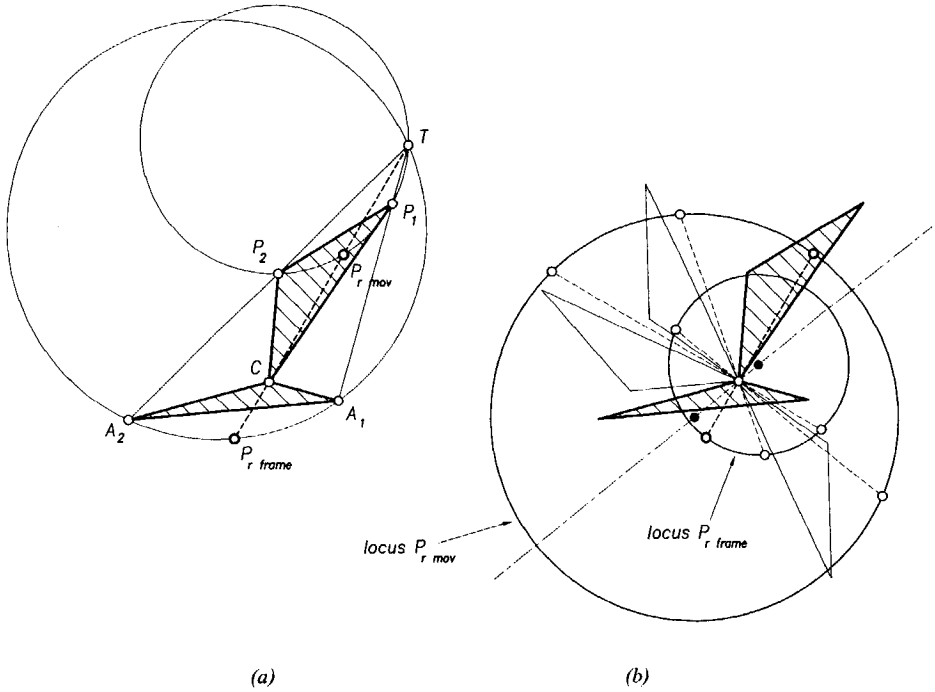$$= -r_1 k_1 a_1 \left(A e_r\right)^T e_a + k_1 r_1^2 \left(A e_r\right)^T e_r + r_2 k_2 a_2 \left(A R(\beta) e_r\right)^T R(\beta) e_a$$
$$+ k_2 r_2^2 \left(A R(\beta) e_r\right)^T R(\beta) e_r$$
$$= \left(r_1 k_1 a_1 - r_2 k_2 a_2\right) \sin \varphi \tag{4.26}$$

where the equality $\left(A R(\beta) e_r\right)^T R(\beta) e_a = \left(A e_r\right)^T e_a$ is used. It is seen that the same condition for neutral equilibrium results, as for any φ the resultant moment must vanish. The stability condition for rotation about the pivot yields:

$$V_{,\varphi\varphi} = \left(k_1 a_1 r_1 - k_2 a_2 r_2\right) \cos \varphi \tag{4.27}$$

This expression also equals zero, which was expected as its integral was zero too. Thus, it is proved that the rotation modification rule does not affect the neutral stability of the system.

The investigation of the DEF in the spring butterfly proceeds essentially as in the previous section, leading to the same conclusion that the force dynamically equivalent to the spring forces acts exactly at the pivot. When the graphical procedure for finding the DEP as proposed in section 3.4 is used,
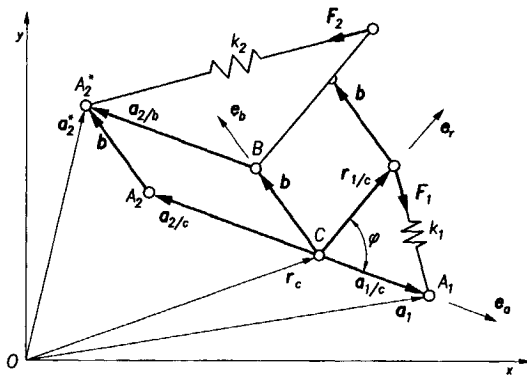
Figure 4.29   Investigation of the shifted configuration.

where a constant error term is expected (see equation 3.85), the following results are obtained. It is found that the DEP traces a circle of which the center does not coincide with the pivot (figure 4.28). Simultaneously, the resultant force is not constant either. It will be shown, however, that the error term is constant. Using the expressions from equation 4.23, the stability equation for constant forces (equation 3.39) yields the following:

$$F_r^T r_{r/c} = F_1^T r_{1/c} + F_2^T r_{2/c} \tag{4.28}$$

$$= k_1 \left(a_1 e_a - r_1 e_r \right)^T r_1 e_r + k_2 \left(-a_2 R(\beta) e_a - r_2 R(\beta) e_r \right)^T \left(r_2 R(\beta) e_r \right)$$

$$= k_1 a_1 r_1 e_a^T e_r - k_1 r_1^2 - k_2 a_2 r_2 e_a^T e_r - k_2 r_2^2 = -k_1 r_1^2 - k_2 r_2^2$$

This shows that the error introduced by applying the construction for constant forces to the situation of central linear forces introduces a constant error. It is interesting to note that applying the circle construction to the spring forces acting on the frame yields a similar result: $F_r^T r_{r/c} = -k_1 a_1^2 - k_2 a_2^2$, and that the addition of these products is equal to the opposite of twice the potential energy of the springs, which is found by substituting equation 4.7 into equation 4.5:

$$V = \tfrac{1}{2} k_1 \left(a_1^2 + r_1^2 \right) + \tfrac{1}{2} k_2 \left(a_2^2 + r_2^2 \right) \tag{4.29}$$

As may be gathered from figure 4.28, the construction of the DEPs of the forces on the moving lever and on the frame incorporates much geometric regularity [4.7], but this will not be pursued here.
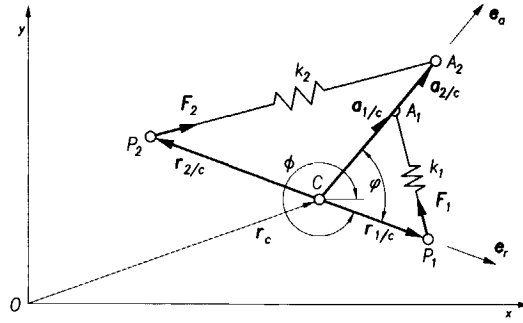
Figure 4.30 Dynamically equivalent force of the spring forces acting on the moving link of the kinematically inverted basic spring force balancer.

Shift

The shift modification is repeated in figure 4.29. The potential of the modified system yields:

$$V = \tfrac{1}{2}k_1\left(a_{1/c} - r_{1/c}\right)^T\left(a_{1/c} - r_{1/c}\right)$$

$$+ \tfrac{1}{2}k_2\left(\left(a_{2/c} + b\right) - \left(r_{2/c} + b\right)\right)^T\left(\left(a_{2/c} + b\right) - \left(r_{2/c} + b\right)\right)$$

$$= \tfrac{1}{2}k_1\left(a_{1/c} - r_{1/c}\right)^T\left(a_{1/c} - r_{1/c}\right) + \tfrac{1}{2}k_2\left(a_{2/c} - r_{2/c}\right)^T\left(a_{2/c} - r_{2/c}\right) \qquad (4.30)$$

As the shift vector b cancels, the potential of the modified configuration is equal to the potential of the standard configuration. Consequently, the resultant force and the conditions for static balance are the same. However, it should be noted that the springs do not act on the same rigid body. Therefore, it is not useful to determine the dynamically equivalent of the spring forces. Likewise, the Newtonian approach should consider the forces on the coupler bar, or consider the forces of the coupler bar acting on the cranks.

Kinematic inversion

For the kinematic inversion, figure 4.30, the equations remain essentially the same, apart from $a_{i/c}$ and $r_{i/c}$ changing places, which also implies that the spring force vectors reverse direction. Therefore, the expression for the potential is as follows:

$$V = \tfrac{1}{2}k_1\left(r_{1/c} - a_{1/c}\right)^T\left(r_{1/c} - a_{1/c}\right) + \tfrac{1}{2}k_2\left(r_{2/c} - a_{2/c}\right)^T\left(r_{2/c} - a_{2/c}\right)$$

$$= \tfrac{1}{2}k_1\left(a_{1/c} - r_{1/c}\right)^T\left(a_{1/c} - r_{1/c}\right) + \tfrac{1}{2}k_2\left(a_{2/c} - r_{2/c}\right)^T\left(a_{2/c} - r_{2/c}\right) \qquad (4.31)$$

85

Again, the potential is unaffected, and thus the dynamically equivalent force is found to attach at the pivot.

4.7   Summary

This chapter introduced ideal (zero-free-length) springs and the arrangement of two of these in a basic spring force balancer as the elementary ingredients of a framework for the design of statically balanced mechanisms.

The chapter aimed to illustrate how the basic spring force balancer can be modified without jeopardizing the neutral equilibrium. It proved to be very convenient to use the potential. Almost without computations, the basic spring force balancer can be modified in many ways. Each of these modifications is not spectacular in itself, but considerable transformations can be realized when a series of these modifications are carried out. The shift modification already shows that additional links can be introduced, whereas the resolution of springs gives a possibility to introduce additional springs. Smart use of the kinematic inversion rule can increase the number of degrees of freedom. Clearly, these modification rules can be employed as tools in the conception of statically balanced spring mechanisms. Due to the linearity of the equations of motion, order and grouping of a series of modifications is free, and superposition is allowed, provided that, in the case of more degrees of freedom, the parameters of the balancer for a specific degree of freedom are not affected by the other degrees of freedom. This independence of the balancers can be achieved by using the modification rules for conceiving the balancer for a specific degree of freedom in such a way that it works properly for any configuration of the other degrees of freedom. The modification rules, together with the superposition principle, constitute the framework for the conception of statically balanced spring mechanisms. The next chapter will show that the manipulation with the modification rules can result in many different energy-free systems, illustrating the usefulness of ideal springs and the framework presented in this chapter. It will also demonstrate that perfect static balance does not necessarily involve ideal springs, yet also these examples will be derived using the framework.

Figure 4.31 gives an overview of the modification rules. Seven modification rules were identified: (1) variation of parameters; (2) rotation of spring-lever elements; (3) shift of spring-lever elements; (4) kinematic inversion; (5) composition of ideal springs; (6) composition of spring-lever elements; (7) interchange of mass-lever and spring-lever element. It was noted that rules 2, 3,

and 4 can be effected in an energy-free manner, whereas using the others alters the potential.

The investigation of the dynamically equivalent resultant force of the two spring forces in the modified configurations still leaves some questions open. Apparently, substituting the two spring forces by a constant force yields satisfactory results with respect to dynamic equivalence.

Finally, this chapter showed that some remarkable geometric theorems, such as the intersection of a paraboloid and a cylinder with parallel lines of symmetry being an ellipse, can be proved by regarding the potential in zero-free-length-spring mechanisms.
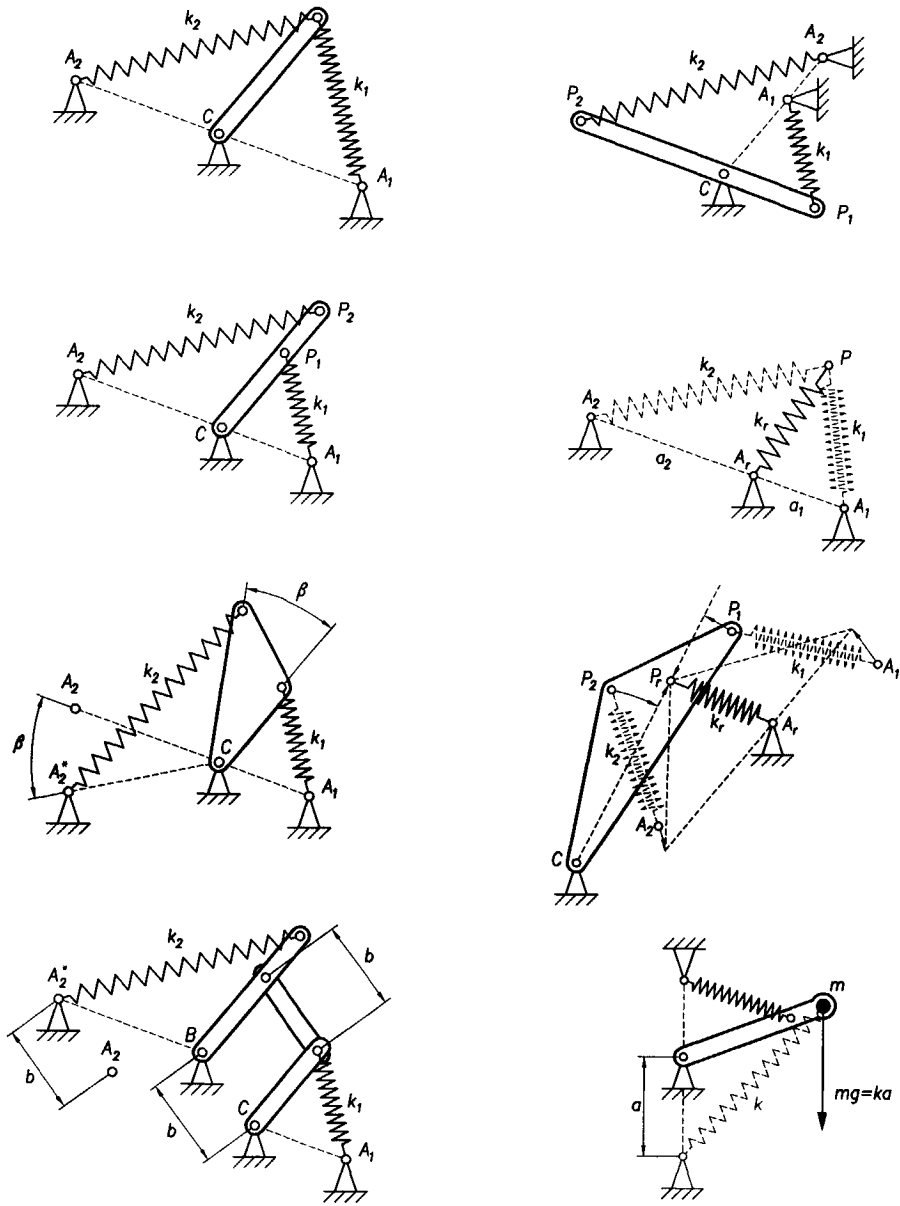
Figure 4.31 Overview of modification rules, based on a modified basic spring force balancer: (left column) basic spring force balancer, modified basic spring force balancer after changing parameters, modified basic spring force balancer after rotation, modified basic spring force balancer after shift, (right column) modified basic spring force balancer after inversion, resolution of springs, resolution of spring-lever elements, interchange of mass and spring.

88

5   Perfect balance

in which the use of the conception framework is demonstrated by the conception of a number of gravity equilibrators and spring force balancers with perfect static balance, aiming at a general understanding, and dexterity in the design of balanced spring mechanisms.

5.1   Introduction

Theoretically, all rigid body planar linkages having lower and/or higher order kinematic pairs can be perfectly equilibrated. Although proof of this claim is not complicated, this fact has not previously been recognized.

Donald A. Streit, Eungsoo Shin, 1993

With the aid of the framework presented in the previous chapter, many useful systems can be conceived. This chapter will present a variety of examples of *perfect* static balancing of mass (*equilibration*) and *perfect* spring force compensation. Most examples are planar mechanisms, but a number of spatial examples are included to show that not only all planar but also all spatial rigid body linkages having lower and/or higher order kinematic pairs can be perfectly equilibrated.

This chapter aims to increase general insight, to enhance dexterity in playing with arrangements of springs, rollers and links, to demonstrate the versatility of the approach, and to stimulate its creative use for other designs. It is intended to demonstrate that the framework allows stepwise conception of useful designs, without distracting computations. As not so much the resulting designs but the conception of these is the subject of this chapter, a lot of space is reserved for the figures showing the steps taken. Implicitly, a potential energy perspective is often assumed, yet a consideration of the forces is advantageous to arrive at a profitable practical embodiment. The forces acting on hinges can be reduced or even eliminated, as one example will show.

Theoretically, the proper use of the framework results in perfectly balanced systems. However, mechanical deficiencies in the actual realization of the mechanisms, and the errors due to the ideal spring simulation, will introduce some error. To confront the concepts with reality, prototypes were made of some of the examples in this chapter. The translation from a diagram into a working prototype is not at all trivial, let alone its development into a commercial product, as may be illustrated by the development of the elbow orthosis by Cool and his group (figure 2.6) from the diagram in figure 5.1b [5.1].
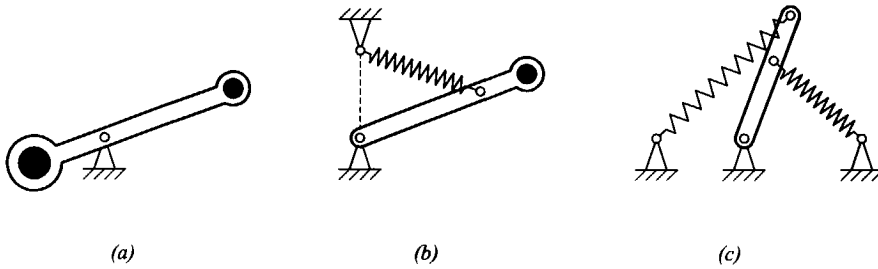
*Figure 5.1   Similar static balancing principles: (a) mass-to-mass, (b) spring-to-mass, and (c)
spring-to-spring balancing.*

This chapter will focus on the spring-to-mass and the spring-to-spring
balancers (figure 5.1). Although the previous chapters make clear that these
systems are strongly related, they have been assigned separate sections.
Section 5.2 will start with the conception of a number of gravity equilibrators,
followed by spring-to-spring balancers of different kinds in section 5.3. It is
shown that they can be conceived (and extended or simplified) in a precise and
logical, yet convenient and lucid way by using the proposed framework. Whilst
the previous sections are restricted to ideal springs, section 5.4 discusses special
solutions with normal springs and yet perfect static balance. Finally, section 5.5
demonstrates the surprisingly easy extendibility of the conception approach into
the third dimension.

5.2   Gravity equilibrators

> *Die Anordnung von zwei Federn ergibt im Allgemeinen einen
> resultierenden Drehmomentenverlauf mit der gleichen Charakteristik
> wie bei einer Feder. Man kann aber die Belastung des Lagers [-] durch
> die zweite Feder und deren Aufhängung beeinflussen.*
>
> The arrangement of two springs generally yields a torque similar to that
> of a single spring. However, the second spring and its attachement can
> affect the pivot load.
>
> Kurt Hain, 1952

Static balancing of the weight of mechanisms is a well-known field of
application of spring balancers. Many researchers have addressed the perfect
equilibration of weight by means of springs [1.5, 1.6], and an impressive body of
patent literature exists on this topic [1.6]. This section elucidates the conception
of a number of gravity equilibrators. In specific cases, such as in adjustable
desk lamps, a certain amount of friction may be desirable, but in many other
cases, friction will have a negative influence on the proper functioning of the
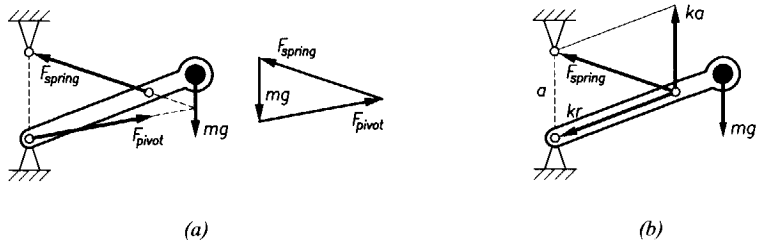
Figure 5.2 Forces in the basic gravity equilibrator: (a) determination of the pivot force, (b) skew resolution often enhances understanding.

device. Therefore, in several examples, the conventional pivots are replaced by rolling joints [1.14], resulting in low friction solutions that require few parts, little space and no lubrication. The value of a force analysis will be shown convincingly, especially in the example of the Floating Suspension, where the pivot load is eliminated by using a second spring in a profitable way, so that pivots are not required at all. For clarity of presentation, most of the examples consider only the payload. However, inclusion of link mass (and even spring mass [5.2]) still allows exact solutions, as will be illustrated in some of the examples.

Basic gravity equilibrator

Figure 5.1b presents the most elementary spring-to-mass balancer which will be called the *basic gravity equilibrator* (see also section 4.4). The forces present in the basic gravity equilibrator can be considered in two useful ways. Regarding the link as a system of three forces learns that the action lines must intersect, this quickly yields the pivot force (figure 5.2a). Skew resolution (into
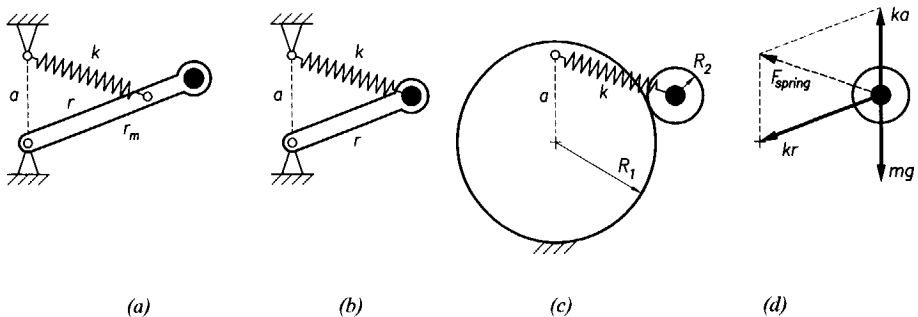

Figure 5.3 Rolling version of basic equilibrator with constant normal contact force: (a) basic equilibrator, (b) special version with $r=r_m$, (c) rolling version with $r=R_1+R_2$, (d) forces on the roller: as $mg=ka$, only kr remains as the resultant force.
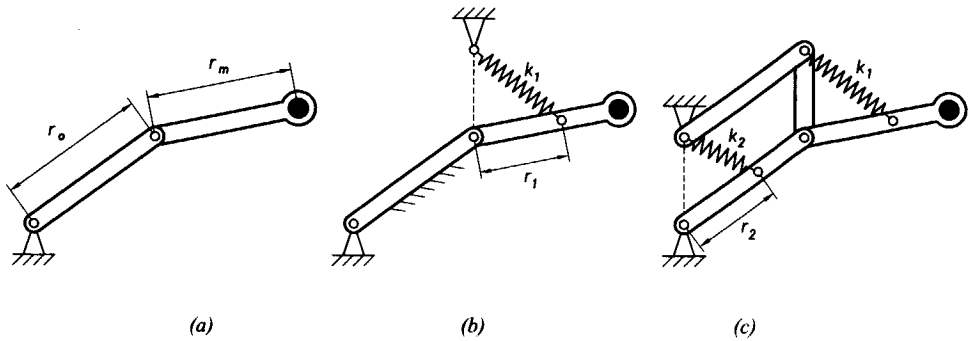
91

Figure 5.4   Two degrees-of-freedom: (a) statement of the problem, (b) equilibration of first element while second element remains fixed, (c) vertical yet mobile base for first element realized by parallelogram linkage, and balancer for second element.

components vertical and along lever, figure 5.2b) allows an easy proof of the perfect static balance, similar to the treatise in section 4.3 for the basic spring force balancer, since the vertical component of the spring force is constant. Using the components of the spring force, the moment equilibrium about the pivot yields the following condition:

$$mgr_m = rka \tag{5.1}$$

where k is the spring stiffness, r is the distance from the pivot to the attachment point of the spring on the link, and r_m is the distance from the pivot to the center of mass.

The magnitude of the spring force component along the link is constant as well, which can be useful as follows. Under the special condition that the spring attaches at the center of mass, the pivot force is always directed along the link. This allows a simple rolling version, where the link is replaced by two rollers (figure 5.3). An interesting feature of this configuration is that the contact force between the rollers is constant and purely normal, as is easily seen when the forces on the moving roller are resolved into vertical and radial components (figure 5.3d).

More degrees of freedom

There are several ways to design multiple-degree-of-freedom equilibrators. This section will present a first one, while others will follow later in this chapter. Figure 5.4a shows the principal problem of a two-link open-loop kinematic chain, loaded by a weight at its end. The distal element (far from the fixed pivot) can be equilibrated according to equation 5.1 when the proximal element (close to the pivot) is fixed (figure 5.4b). When this element is to move as well,
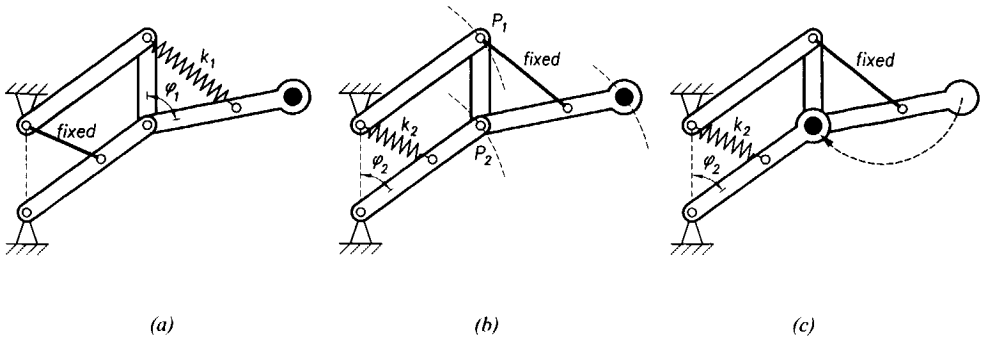
Figure 5.5   Derivation of balancing conditions using superposition: (a) spring k_2 fixed, yields the balancing system for angle φ_1, (b) spring k_1 fixed, yields the balancing system for angle φ_2, (c) with spring k_1 fixed, the mass may be moved along the translating link.

an auxiliary parallelogram can be constructed in order to keep the base of the distal spring-lever element vertical (figure 5.4c). One may now wonder how to balance the proximal element. The easiest solution is provided by using the potential energy perspective and the principle of superposition (figure 5.5). As the distal element is balanced, no energy needs to be taken or given by the spring of the proximal element when only the distal element moves (figure 5.5a). On the other hand, as the proximal element moves and the distal one is frozen, the mass traces a trajectory congruent with points P_1 and P_2 (figure 5.5b). Therefore, the balancer of the first element experiences the mass as if it were fixed anywhere on link P_1P_2 (figure 5.5c). Consequently, the balancer of the proximal element can be identical to the one of the distal element. This will be illustrated by writing down the potentials of the springs and the mass, respectively:

$$V = \tfrac{1}{2}k_1\left(a^2 + r_1^2\right) - r_1 k_1 a \cos\varphi_1 + \tfrac{1}{2}k_2\left(a^2 + r_2^2\right) - r_2 k_2 a \, \cos\varphi_2 \tag{5.2}$$

$$+ mg\left(r_m \cos\varphi_1 + r_o \cos\varphi_2\right)$$

$$= K + \left(mgr_m - r_1 k_1 a \right)\cos\varphi_1 + \left(mgr_o - r_2 k_2 a \right)\cos\varphi_2$$

where K is a constant value. It is seen that the balancers are independent, and that the balancing conditions are:

$$mgr_m = r_1 k_1 a \tag{5.3}$$

$$mgr_o = r_2 k_2 a \tag{5.4}$$

A force analysis gives the same result, and provides insight on how the system is loaded. It is especially interesting to see how this mechanism solves
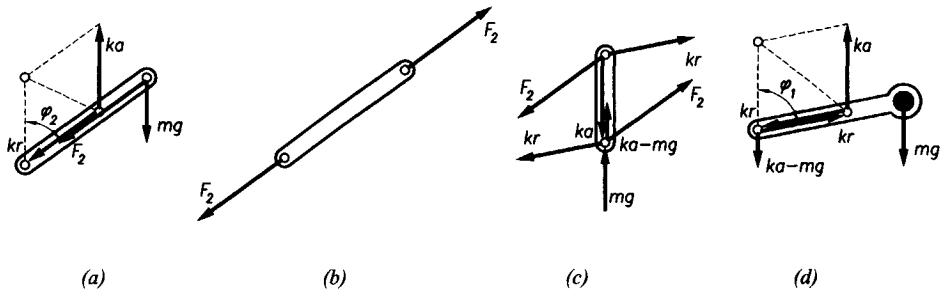
Figure 5.6   Forces in the two-degree-of-freedom equilibrator of figure 5.5: (a) lower proximal link, (b) upper proximal link, (c) vertical link, (d) distal link.

the question of how the variable moment of the mass (which is a function of φ_1) is taken up, without influencing the balancer for φ_2. It will prove to be convenient to resolve the forces in components along the links, and vertical components. First, the distal element is investigated (figure 5.6d). As the spring force is resolved in the components ka and kr, the components of the joint force are readily found to be kr along the link, and $ka - mg$ in the vertical direction. Next, the vertical link is investigated. The reactions of the spring force components and the joint force components from the distal element are applied, and equilibrium of the link is established as follows. The upper link of the parallelogram is a two-force system and can therefore transmit a force F_2 along its centerline only. From the equilibrium of moments of the vertical link about its lower joint, it follows that the upper link of the parallelogram is tensioned (figure 5.6b), and that $F_2 a \sin \varphi_2 = rka \sin \varphi_1$. For equilibrium, the lower link must exert the following forces on the vertical link: one component F_2 along its centerline, opposite to the direction of the component F_2 by the upper link of the parallelogram, and a component mg acting vertically upward. Consequently, the lower link of the parallelogram is loaded by F_2 along its centerline, and by the constant component mg at its end, acting vertically downward (figure 5.6a).

Although dependent on φ_1, the force F_2 has no moment contribution, so the balancer for φ_2 only needs to account for mg, which is equivalent to a mass fixed at its end. From this force analysis, it is seen that each element exerts a constant vertical force and a variable moment to its neighboring element. The variable moment $mgr_m \sin \varphi_1$ is taken up by the parallelogram mechanism (one link is tensioned, the other compressed), while the balancer equilibrates the moment due to the constant force mg. So as φ_1 varies, the tensile and compressive forces in the links change but the required spring force remains the same.

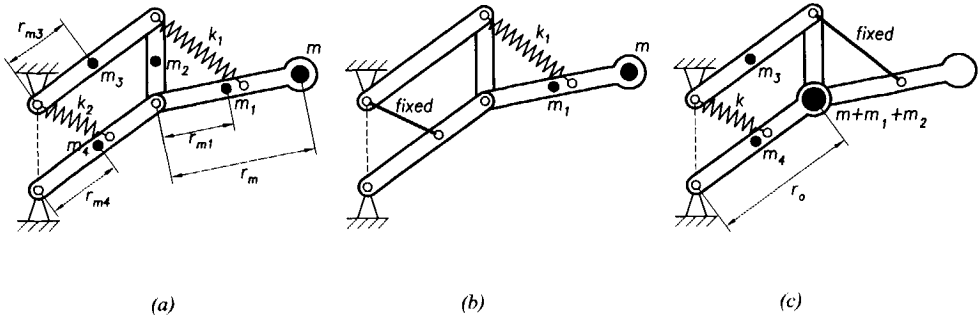(a)   (b)   (c)

Figure 5.7   Inclusion of link mass: (a) definition of masses and arm lengths, (b) spring k_2 fixed, only m_1 needs to be considered, (c) spring k_1 fixed, masses m, m_1, and m_2 reduced to the end point of the lower proximal link.

So far, link mass was neglected, but inclusion of link mass (and even spring mass can be accounted for [5.2]), need not introduce a balancing error. In figure 5.7, a solution is given using superposition. The balancer for φ_1 feels the mass m at a distance r_m and the mass m_1 at a distance r_{m1} (figure 5.7b). Similarly, when φ_1 is fixed, the balancer for φ_2 feels $m + m_1 + m_2$ at a distance r_o, and masses m_3 and m_4 at distances r_{m3} and r_{m4}, respectively (figure 5.7c). Therefore, the balancing conditions (equations 5.3 and 5.4) become:

$$mgr_m + m_1 gr_{m1} = r_1 k_1 a \tag{5.5}$$

$$(m + m_1 + m_2)gr_o + m_3 gr_{m3} + m_4 gr_{m4} = r_2 k_2 a \tag{5.6}$$

So one way to design multiple-degree-of-freedom gravity balancers is to stack a series of basic equilibrators on one another, where the base of each element is maintained vertical by the construction of a parallelogram linkage connected to the vertical base of the next proximal element [5.3]. Figure 5.8 shows an example having three degrees-of-freedom. Here, the mass is fixed to
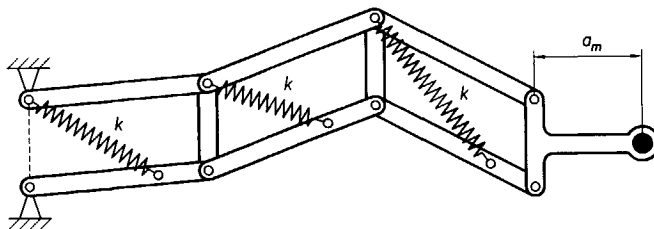

Figure 5.8   Series of basic equilibrators gives independent action of the degrees-of-freedom, regardless of the configuration and the distance a_m. When link mass is neglected, the successive spring-lever elements can be equal.
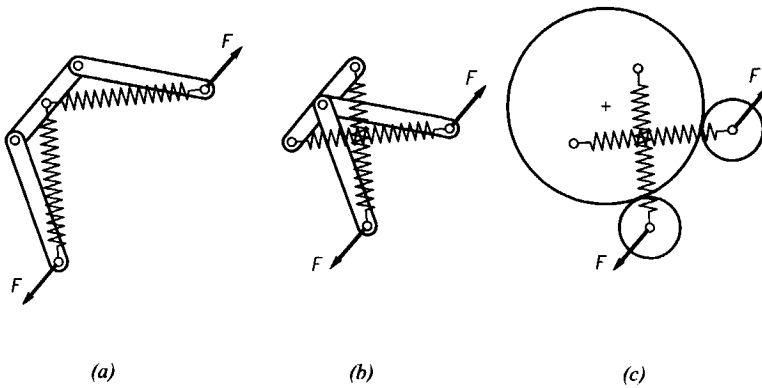
95

Figure 5.9   Constant force device: (a) two equilibrators without mass combined, (b) shifted, (c) rolling version. Stable action is to be ensured by constraining the rotation of the intermediate link or the roller, respectively.

the most distal vertical link, but the treatise of potential or forces essentially is the same. The distance a_m from the mass to the most distal vertical link does not affect the equilibrium and therefore the parameters of the balancer, and again, when link mass is neglected, the spring-lever elements in the subsequent units can be equal.

Constant force device
Gravity balancers can more generally be regarded as constant-force generators [5.4]. Constant force devices for more general use can be developed from the basic gravity balancer by connecting two equal gravity equilibrators to one another in such a way that the constant forces they generate act along the same line (figure 5.9). Neglecting link mass, a system with two forces results, which are constant, equal, and opposite. After shifting the two equilibrators towards each other until their joints coincide, the links can again be replaced by rollers. Note however, that in all of the systems in figure 5.9, an additional degree-of-freedom is introduced, which in this case is unstable. Therefore, care must be taken that the base does not get the opportunity to rotate. The rolling version can be stabilized by wrapping a flexible band between the rollers.

Rolling-link equilibrator
In the system in figure 5.3c, it is inconvenient that the spring must attach to the lever all the way up its end, at the location of the center of mass. In this section, an alternative configuration for a single degree-of-freedom rolling-link equilibrator will be derived. Figure 5.10a shows again the basic gravity equilibrator. To obtain a rolling version, the fixed pivot C is to be replaced by
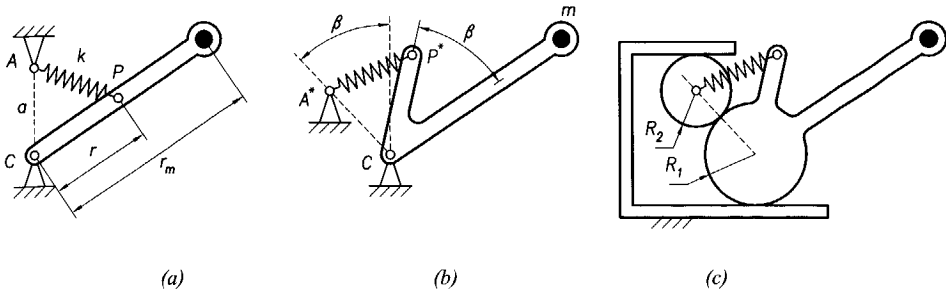
Figure 5.10 Rolling-link version of the basic equilibrator: (a) basic equilibrator, (b) rotated, (c) fixed points A and B replaced by two rollers in a Rolamite configuration, where the flexible bands can be omitted due to the presence of contact forces.

a rolling contact, such that the relative position of points A and C, and their vertical level are maintained. This is just what the Rolamite (figure 2.11b, Wilkes, 1967) does: the centers of the rollers move horizontally, but their distance remains constant. The orientation of the centers is constant too, be it not vertical. To match the standard equilibrator with the Rolamite configuration, the spring-lever element is rotated while keeping the mass-lever element as it is, according to figure 5.10b. Subsequently, two rollers are selected with the two fixed points A^* and C as their centers (figure 5.10c). Though no longer stationary, these points move perpendicular to the gravity field, and therefore do not affect the balance of potential energy. One is free to choose dimensions, as long as the angles β remain in correspondence with one another, and $mgr_m = rka$, where $a = R_1 + R_2$.
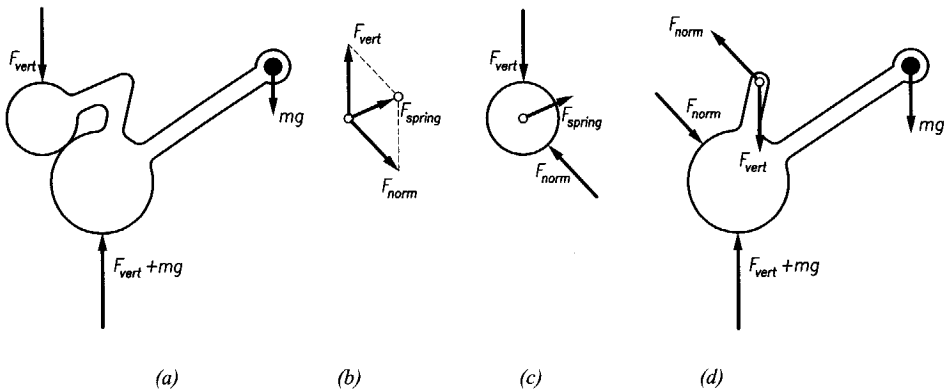

Figure 5.11 Forces in the rolling-link equilibrator: (a) rollers and spring as one system, (b) axis of upper roller, (c) upper roller, (d) lower roller with mass. Note that F_{norm} and F_{vert} are generally not of equal magnitude.
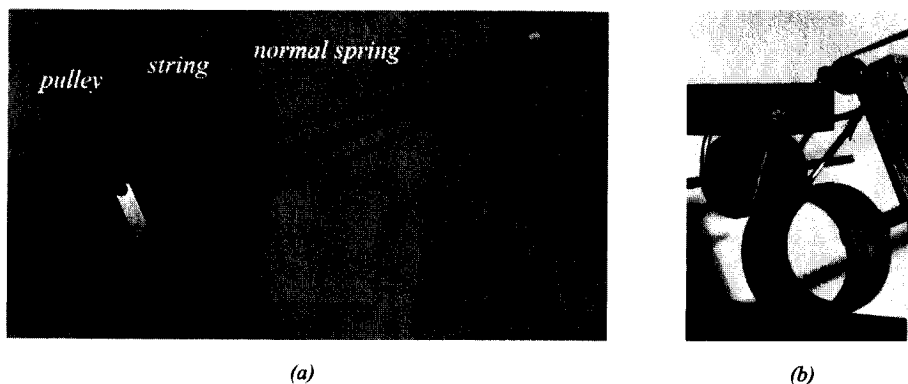
(a)   *(b)*

Figure 5.12   Photographs of demonstration model: (a) overview, (b) close-up of rollers.

In one respect, the arrangement of figure 5.10c is essentially different from the Rolamite configuration. The Rolamite consists of two rollers, a frame, and a flexible stabilization band. The rolling equilibrator, however, does not require a flexible band to keep the parts together. Due to the continuous presence of *forces*, the parts are kept in contact. Moreover, the configuration of figure 5.10c is a *true* rolling link mechanism, in the sense that there are no tangential forces present in the contact points, as is illustrated in figure 5.11.

A prototype was made out of available materials to verify this concept (figure 5.12). The ideal spring was realized by a pulley and string arrangement according to figure 4.5f, where the free length of the spring was stored on the moving link. An interesting feature is that the string is attached to the center of the smaller roller via an arc made out of welding wire to obtain a rolling connection. The main dimensions of the prototype are: $r_m \approx 400$ mm, $r_1 = 40$ mm, $r_2 = 25$ mm, and $r = 56$ mm.

Floating Suspension

The ultimate desire in conceiving a low-friction equilibrator is an arrangement with no pivot at all. Obviously, simply taking out the pivot from the basic gravity equilibrator (figure 5.1b) is not feasible: not so much because a pivot is needed for motion (motion directed design attitude) but because equilibrium requires a third force. Continuing on this force directed design attitude, one could argue that in order to maintain equilibrium during motion, the pivot can be omitted if another device, such as a second spring, were capable of supplying the correct force during motion.

In order to find an appropriate configuration for this spring, the sixth rule is applied to the basic equilibrator (figure 5.13a) as follows. First, the spring is
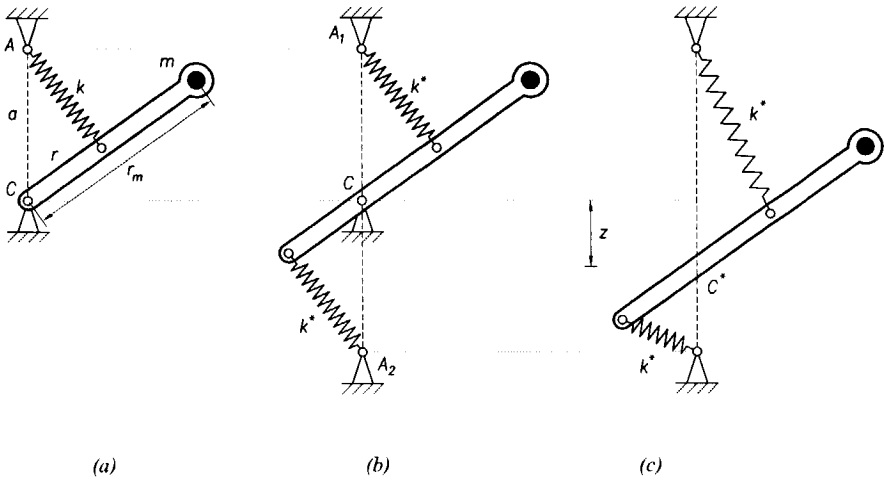
(a) (b) (c)

Figure 5.13 Floating Suspension, a perfectly balanced beam with a virtual pivot: (a) basic equilibrator, (b) spring replaced by two springs of halved stiffness, $k^*=k/2$, and one of these rotated by 180 degrees, (c) after removing the pivot, the link assumes a stationary, virtual pivot while maintaining its static balance.

replaced by two springs. Clearly, balance is preserved if the spring rate is halved: $k^* = \frac{1}{2}k$, where k is the stiffness of the original spring. Subsequently, one of the two spring-lever elements is rotated by 180 degrees, while the pivot remains present (figure 5.13b). When considering the forces acting on the beam, one finds that the spring forces are equal and opposite, regardless of the orientation of the beam. Hence, the pivot force on the lever is constant, directed vertically upward, equal and opposite to the weight of the mass. With the two equal spring-lever elements, the balancing condition is:

$$2rk^*a = rka = mgr_m \qquad (5.7)$$

If now the pivot is removed, the point of the beam where the pivot used to be, C, will come down. To investigate this phenomenon, several perspectives can be assumed. Perhaps the most convenient one is to regard the skew resolution of the spring forces (figure 5.14). The components of the spring forces along the link still need to cancel each other out, as there are no other forces present in this direction. Meanwhile, as point C is coming down, the vertical component of the upper spring increases and the vertical component of the lower spring decreases, both proportional with the vertical deflection, thanks to the ideal spring characteristics (see also figure 5.14). Thus, point C moves downward along a vertical line. New equilibrium is settled at C^*,
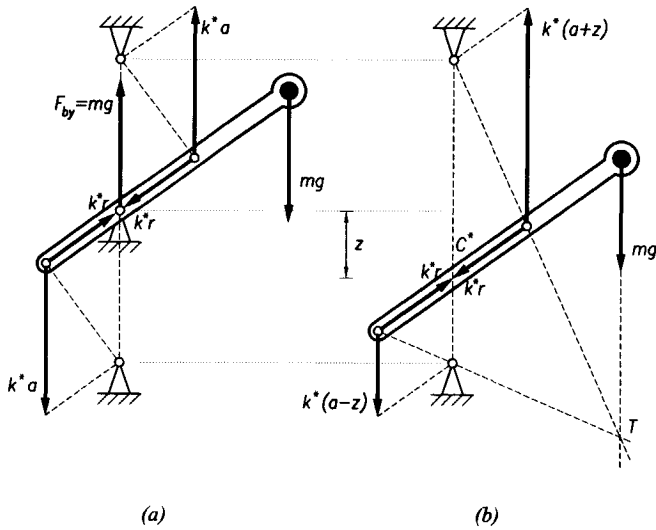
Figure 5.14 Forces in the Floating Suspension: (a) the pivot force after modification is directed vertically upward and equal to mg, (b) by moving down, the pivot force is taken over by the springs, so that $2k^*z=mg$ or $kz=mg$.

located at a distance z below C, where z follows from the vertical equilibrium:

$$k^*(a+z) - k^*(a-z) - mg = 0 \tag{5.8}$$

so

$$z = mg/2k^* = mg/k \tag{5.9}$$

regardless of the orientation of the beam: point C^* is stationary and has become a virtual pivot (figure 5.13c). Alternatively, the linkage with the pivot (figure 5.13b) can be regarded as the deflected configuration of figure 5.13c, where a force equal to the pivot force in figure 5.13b is applied to the virtual pivot. Since the pivot force is equal to mg and the spring system consists of two ideal springs k^*, the deflection becomes

$$z = mg/2k^* = mg/k \tag{5.10}$$

as was expected.

Thus, a statically balanced system is conceived which essentially consists of a single part and two springs. This part is suspended by the spring forces only, which has led to the designation *Floating Suspension* [5.5]. In addition to its remarkable principle, there are a number of practical advantages of a floating suspension. Firstly, an additional degree of freedom is obtained: without the

100
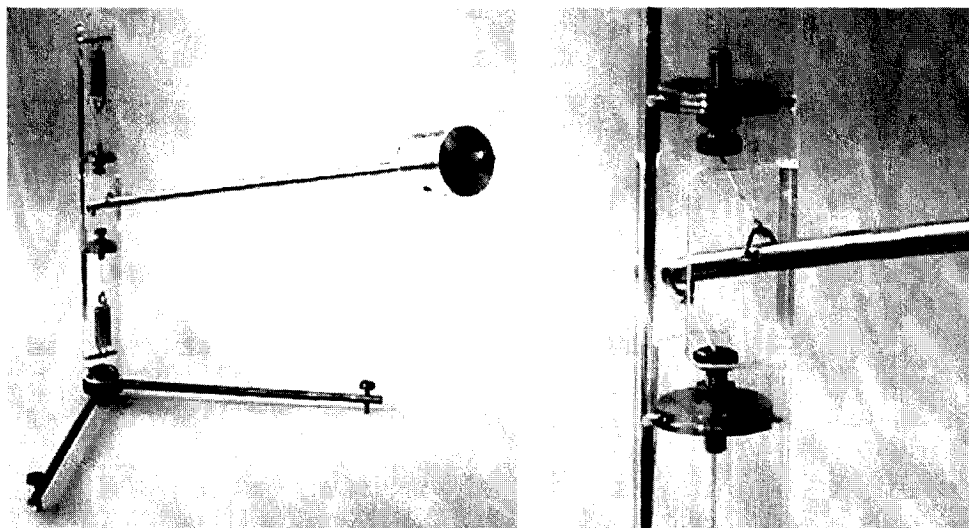
(a)   (b)

Figure 5.15 Photographs of the Floating Suspension [5.6]: *(a) overview of demonstration model, (b) close-up of spring system. The device has been patented* [5.5].

pivot, the beam is free to rotate about the vertical axis as well. Thus, the mass can be moved in an energy-free manner along the surface of a sphere. Secondly, the pivot can be omitted, which reduces friction, wear, cost, and space. When, sacrificing one degree of freedom, an axis is mounted at point C^* to drive the mechanism, it has the advantage of being unloaded (by static forces), thus preserving low friction. This can specifically be useful in direct-drive robots. Thirdly, the virtual pivot is self-adjusting. The beam settles itself at the position C^*, which reduces the need for accurate manufacturing.

A prototype was made demonstrating the proper functioning of this floating suspension (figure 5.15 [5.6]). Main dimensions are $r = 23$ mm, $a \approx 28$ mm (adjustable), $k = 0.83$ N/mm, while the mass, $m = 0.2$ kg, can be fixed anywhere along the link, presently set at $r_m \approx 550$ mm (adjustable). As the balancing condition is linear in all the parameters, one adjustment (*e.g.* r_m) is sufficient to accommodate for all imperfections, except for the free length: therefore also a was made adjustable. The link has been made out of thin-walled stainless steel tube. The free length of the springs was stored in a PMMA tube (40x30mm) of 360mm overall length. Waxed nylon strings were used which are led through hollow bolts. Noteworthy are the attachments of the string to the link. Holes were drilled through the center of the tube, and
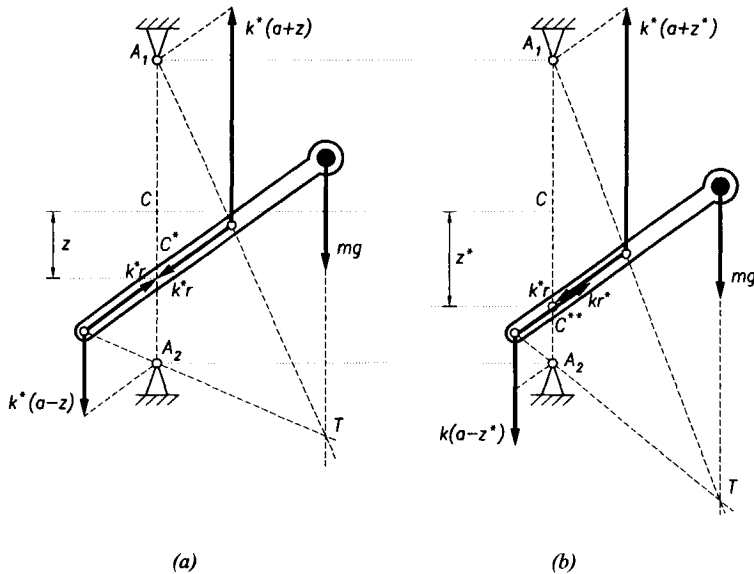
Figure 5.16 Modification of the Floating Suspension by variation of parameters: (a) equal springs as in figure 5.13c, (b) the lower spring rate is doubled while its lever arm on the link is halved. Static balance is preserved but the beam settles at a new stationary virtual pivot C^{**}.

triangular hooks were put through. Thus, the strings were attached to the center of the link while some stability was gained against rotation about the centerline of the tube.

Modifications

The floating suspension in figure 5.13c allows a number of modifications. Figure 5.16 shows a version with different springs. In this case, the stiffness of the lower spring was doubled, so $k^{**} = 2k^* = k$, while the arm length on the link was halved: $r^* = \frac{1}{2}r$ (rule 1). The fixed points of the springs were not changed. When the system of forces (figure 5.16b) is compared with the equal-springs case (figure 5.16a), it is observed that the forces along the link are still equal, so the virtual pivot has no tendency to move. However, the vertical equilibrium has changed since the vertical component has increased. Therefore, a new equilibrium will settle at a new point C^{**} on the vertical A_1A_2. From the equilibrium of vertical forces:

$$k^*(a+z^*) - k(a-z^*) - mg = 0 \qquad (5.11)$$

where $k^* = k/2$, the distance z^* is found to be:

$$z^* = a/3 - 2mg/3k \qquad (5.12)$$
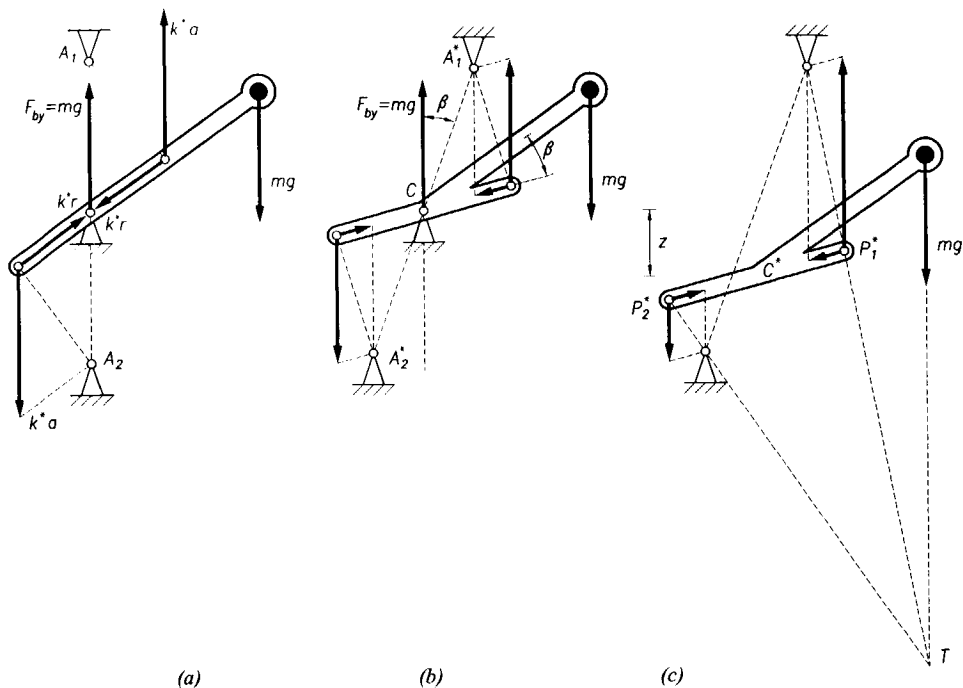
Figure 5.17 Modification of the Floating Suspension by rotating both spring-lever elements: (a) equal springs and pivot still present as in figure 5.8b, (b) spring-lever elements rotated by 20 degrees, (c) pivot removed. Since the springs have not changed, the virtual pivot settles at the same position as with non-rotated spring-lever elements. The three forces intersect at a different location due to the altered action lines of the spring forces.

Note that the deflection z^* is not equal to $mg/(k^* + k)$, as might have been expected when determining z^* according to the derivation of equation 5.10. This is due to the fact that the pivot force (not shown in figure 5.16) of the unequal-springs case is not equal to mg, as is seen when inspecting the equilibrium of forces:

$$F_r = k^* r - k r^* = 0 \tag{5.13}$$

$$F_v = mg + ka - k^* a = mg + k^* a \tag{5.14}$$

where F_r is the component of the pivot force in the direction of the link centerline, and F_v is the vertical component. This force divided by the summed spring stiffnesses yields the correct deflection:

$$z^* = \frac{F_v}{k^* + k} = \frac{mg + \frac{1}{2}ka}{\frac{3}{2}k} = a/3 - 2mg/3k \tag{5.15}$$

Figure 5.18   Definitions of vectors for the determination of the condition for static balance.

Another modification is achieved when the spring-lever elements are rotated by an angle β, as is suggested in figure 5.17. This has no effect on the moment contribution, but the system of forces changes considerably. Figure 5.17b gives the situation of rotated spring-lever elements while the pivot is still present. As the magnitude of the spring forces is not affected b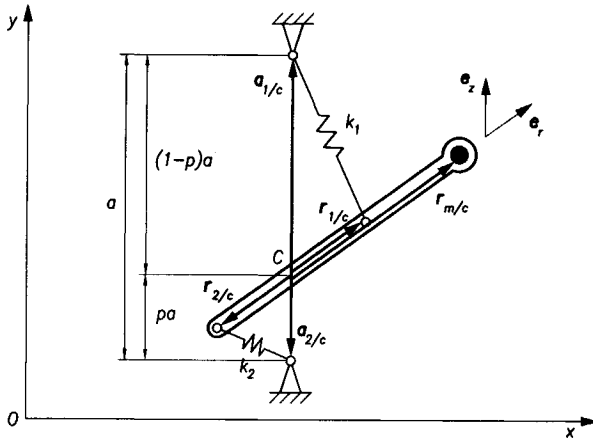y the rotation operation, the resultant force on the pivot remains mg upward. Furthermore, skew resolution in directions vertical and along the rotated spring lever-arms shows that the vertical components have changed with respect to the non-rotated configuration (figure 5.17a). However, since these components cancel in the equation of the vertical equilibrium, as the terms k^*a do in equation 5.8, removing the pivot results in the same position of the virtual pivot as in the non-rotated case, $z = mg / 2k^* = mg / k$, as is shown in figure 5.17c.

Although still balanced for rotation in the plane of drawing, the mechanism is not indifferent for rotation about the vertical axis or about $A_1^*A_2^*$. In fact, stability about $P_1^*P_2^*$ is threatened as well. In the figure, the mechanism has become stable about $A_1^*A_2^*$ and unstable about $P_1^*P_2^*$. Should the spring-lever element have been rotated in the other direction, it would have become unstable about $A_1^*A_2^*$ and stable about $P_1^*P_2^*$. Stability about $P_1^*P_2^*$ is regained by using two parallel springs for each of the springs in the diagram. One of each set in front of the plane of drawing, and one behind the plane of drawing.

In the above treatment, the balancing conditions were derived for some special cases. Slightly more general conditions will be derived for the unequal-springs case using the potential. The total potential is the summation of the potentials of the springs and of the mass (with respect to O, see figure 5.18):

(a)   (b)
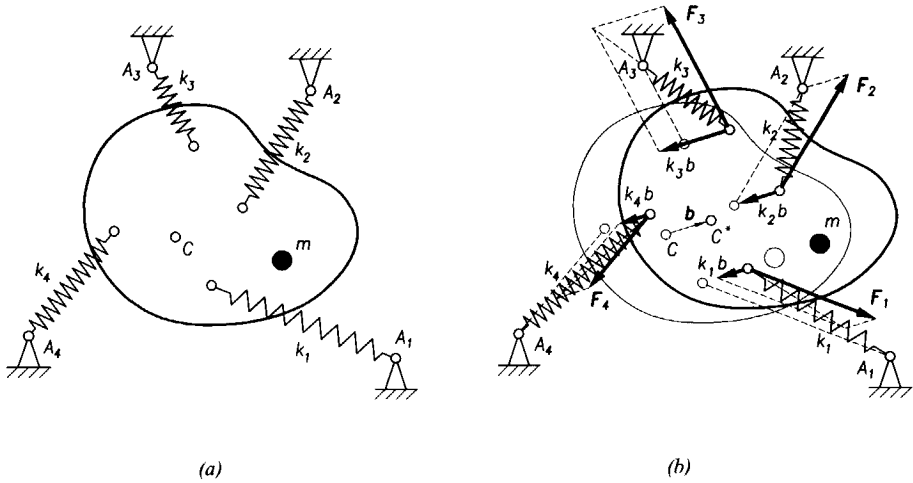
Figure 5.19 Generalized n-spring case, shown for n=4: (a) in arbitrary position, (b) deflected by translation, where skew resolution reveals the fact that the translational stiffness is equal to Σk_i.

$$V = \tfrac{1}{2} k_1 (a_1 - r_1 - r_{1/c})^T (a_1 - r_1 - r_{1/c}) + \tfrac{1}{2} k_2 (a_2 - r_2 - r_{2/c})^T (a_2 - r_2 - r_{2/c})$$
$$- mg(r_c + r_{m/c}) e_z \quad (5.16)$$

The equilibrium position can be found from the equilibrium of forces:

$$V_{,r_c} = -k_1 (a_{1/c} - r_{1/c}) - k_2 (a_{2/c} - r_{2/c}) + mg e_z = 0 \quad (5.17)$$

$$\Rightarrow -k_1 ((1-p)a^* e_z - r_1 e_r) - k_2 (-pa^* e_z + r_2 e_r) + mg e_z = 0 \quad (5.18)$$

where $a^* = |a_2 - a_1|$, which results in the following two conditions:

$$k_1 r_1 = k_2 r_2 \quad (5.19)$$

$$-k_1 (1-p)a^* + k_2 p a^* + mg = 0 \quad (5.20)$$

Selecting $k_1 = k_2 = k^*$ results in $p = \tfrac{1}{2} - mg / 2k^* a^*$ or $z = a/2 - pa^* = mg / 2k^*$. Setting $k_2 = 2k_1 = 2k^* = k$ gives $p = \tfrac{1}{3} - 2mg / 3ka^*$ or $z^* = a^* / 6 - 2mg / 3k$. These results are in agreement with the results found above for the configurations of figures 5.13c and 5.16b (note that $a^* = 2a$).

Generalized n-spring case

The Floating Suspension can be extended to incorporate more springs [5.7]. Figure 5.19a shows the planar case. Generally, this mechanism will not be statically balanced. This section will investigate the behavior of a rigid body

105

with mass m, suspended by n springs, and determine the conditions for static balance. For this purpose, the tangent stiffness matrix will be derived first.

The potential of a rigid body of mass m, on which n zero-free-length springs are attached, reads:

$$V = mg\left(r_c + Rr'_{m/c}\right)^T e_z + \sum \tfrac{1}{2}k_i\left(a_i - r_c - Rr'_{i/c}\right)^T\left(a_i - r_c - Rr'_{i/c}\right) \qquad (5.21)$$

where the potential of the mass is taken with respect to the fixed reference frame, and where the summation runs from 1 to n. Differentiating with respect to r_c and φ, respectively, gives:

$$V_{,r_c} = mge_z - \sum k_i\left(a_i - r_c - Rr'_{i/c}\right) = 0 \qquad (5.22)$$

$$V_{,\varphi} = mg\left(R_{,\varphi}r'_{m/c}\right)^T e_z - \sum k_i\left(R_{,\varphi}r'_{i/c}\right)^T\left(a_i - r_c - Rr'_{i/c}\right) \qquad (5.23)$$

Subsequent differentiation yields the elements of the tangent stiffness matrix:

$$V_{,r_c r_c} = \sum k_i I_2 \qquad (5.24)$$

$$V_{,r_c \varphi} = \sum k_i R_{,\varphi}r'_{i/c} = \sum k_i A R r'_{i/c} = \sum k_i A r_{i/c} \qquad (5.25)$$

$$V_{,\varphi r_c} = \sum k_i\left(R_{,\varphi}r'_{i/c}\right)^T = \sum k_i\left(A r_{i/c}\right)^T \qquad (5.26)$$

$$\begin{aligned}
V_{,\varphi\varphi} &= mg\left(R_{,\varphi\varphi}r'_{m/c}\right)^T e_z - \sum k_i\left(R_{,\varphi\varphi}r'_{i/c}\right)^T\left(a_i - r_c - Rr'_{i/c}\right) \\
&\qquad\qquad\qquad\qquad + \sum k_i\left(R_{,\varphi}r'_{i/c}\right)^T\left(R_{,\varphi}r'_{i/c}\right) \\
&= -mgr^T_{m/c}e_z + \sum k_i r^T_{i/c}\left(a_i - r_c - r_{i/c}\right) + \sum k_i r^T_{i/c}r_{i/c} \\
&= -mgr^T_{m/c}e_z + \sum k_i r^T_{i/c}\left(a_i - r_c\right) \qquad (5.27)
\end{aligned}$$

Equation 5.24 can be interpreted as follows. The equation shows that in all n-springs arrangements, statically balanced or not, the body while subjected to a pure translation, experiences a stiffness equal to the summation of the stiffnesses of the individual springs. This is verified graphically by skew resolution of the spring forces in the direction of the translation b, and the direction of the spring force in the original configuration (figure 5.19a). This way of resolution shows that the spring forces F_i in the original configuration have become components of the spring forces in the new configuration, while components $k_i b$ are added to each of the spring attachment points (see for instance spring k_2 in figure 5.19b). Consequently, the *change* in the total resultant force is equal to $\Sigma k_i b$. The configuration of figure 5.19a does not need to be an equilibrium position (in which case a force and a moment will generally be present at point C). When deflected from the *equilibrium* position, $\Sigma k_i b$ is the total resultant force at point C, while a moment may be
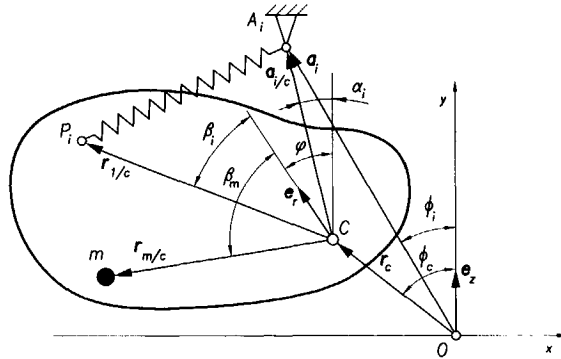
Figure 5.20 Definition of vectors and angles, illustrated for one spring and a mass relative to point C, where the angles α and φ are measured from the vertical, the angle β from the unit vector e_r which is defined relative to a local reference frame. To aid visualization small positive angles are drawn.

present. In either case, when differentiated with respect to b, the same result as in equation 5.24 is found. For the basic Floating Suspension (figure 5.13c), it means that a stiffness k is felt when one tries to move the virtual pivot.

The conditions for static balance with respect to rotation are found by setting equation 5.27 equal to zero. Using an arbitrary unit vector e_r relative to the local reference frame and the vertical unit vector relative to the fixed reference frame, the respective position vectors can be written as $r_{i/c} = r_i R(\beta_i)e_r$, $a_i = q_i R(\phi_i)e_z$, and $r_c = r_c R(\phi_c)e_z$. Using these expressions and the symbols according to figure 5.20, the expression becomes:

$$V_{,\varphi\varphi} = -mgr_m\left(R(\beta_m)e_r\right)^T e_z + \sum k_i r_i q_i \left(R(\beta_i)e_r\right)^T\left(R(\phi_i)e_z\right) \qquad (5.28)$$

$$+ \sum k_i r_i r_c \left(R(\beta_i)e_r\right)^T\left(R(\phi_c)e_z\right)$$

$$= -mgr_m \cos(\beta_m + \varphi) + \sum k_i r_i q_i \cos(\varphi + \beta_i - \phi_i) + \sum k_i r_i r_c \cos(\varphi + \beta_i - \phi_c)$$

These cosine functions can be combined into one cosine function. This will be pursued in order to be able to demand the amplitude of the combined cosine to be zero, thus satisfying the demand that $V_{,\varphi\varphi} = 0$. As a first step, the first summation term will be written in the form of a single cosine $K_s \cos(\varphi - \gamma_s)$, where K_s is the amplitude, and γ_s is the phase angle:

$$\sum k_i r_i q_i \cos(\varphi + \beta_i - \phi_i) =$$

$$\cos\varphi \sum k_i r_i q_i \cos(\beta_i - \phi_i) - \sin\varphi \sum k_i r_i q_i \sin(\beta_i - \phi_i) =$$

107

$$\frac{\sum K_i \cos\gamma_i}{\cos\gamma_s}\left(\cos\varphi\cos\gamma_s + \sin\varphi\cos\gamma_s\frac{\sum K_i \sin\gamma_i}{\sum K_i \cos\gamma_i}\right) \tag{5.29}$$

where $\gamma_i = (\beta_i - \phi_i)$, and $K_i = k_i r_i q_i$, and where the whole expression is multiplied by unity in the form $\cos\gamma_s / \cos\gamma_s$. Under the condition:

$$\cos\gamma_s \frac{\sum K_i \sin\gamma_i}{\sum K_i \cos\gamma_i} = \sin\gamma_s \tag{5.30}$$

expression 5.29 can be reduced to the single-cosine form $K_s \cos(\varphi + \gamma_s)$, where γ_s is found from equation 5.30 according to:

$$\tan\gamma_s = \frac{\sum k_i r_i q_i \sin(\beta_i - \phi_i)}{\sum k_i r_i q_i \cos(\beta_i - \phi_i)} \tag{5.31}$$

and where

$$K_s = \frac{\sum K_i \cos\gamma_i}{\cos\gamma_s} = \frac{\sum k_i r_i q_i \cos(\beta_i - \phi_i)}{\cos\gamma_s} \tag{5.32}$$

The same procedure is applied to the second summation term of equation 5.28, resulting in the single-cosine form $K_t \cos(\varphi + \gamma_t)$, where

$$\tan\gamma_t = \frac{\sum k_i r_i r_c \sin(\beta_i - \phi_c)}{\sum k_i r_i r_c \cos(\beta_i - \phi_c)} \tag{5.33}$$

and where

$$K_t = \frac{\sum k_i r_i r_c \cos(\beta_i - \phi_c)}{\cos\gamma_t} \tag{5.34}$$

These results are now substituted into equation 5.28, and the same strategy as above is followed to combine the resulting three cosine functions into a single cosine function $K_{tot} \cos(\varphi + \gamma_{tot})$, where:

$$\tan\gamma_{tot} = \frac{-mgr_m \sin\beta_m + K_s \sin\gamma_s + K_t \sin\gamma_t}{-mgr_m \cos\beta_m + K_s \cos\gamma_s + K_t \cos\gamma_t} \tag{5.35}$$

and where

$$K_{tot} = \frac{-mgr_m \cos\beta_m + K_s \cos\gamma_s + K_t \cos\gamma_t}{\cos\gamma_{tot}} \tag{5.36}$$

The amplitude K_{tot} of the combined cosine function is now demanded to be zero. Doing so, while using equations 5.32 and 5.34, the condition for static balance is found:

$$mgr_m \cos\beta_m = \sum k_i r_i q_i \cos(\beta_i - \phi_i) + \sum k_i r_i r_c \cos(\beta_i - \phi_c) \tag{5.37}$$
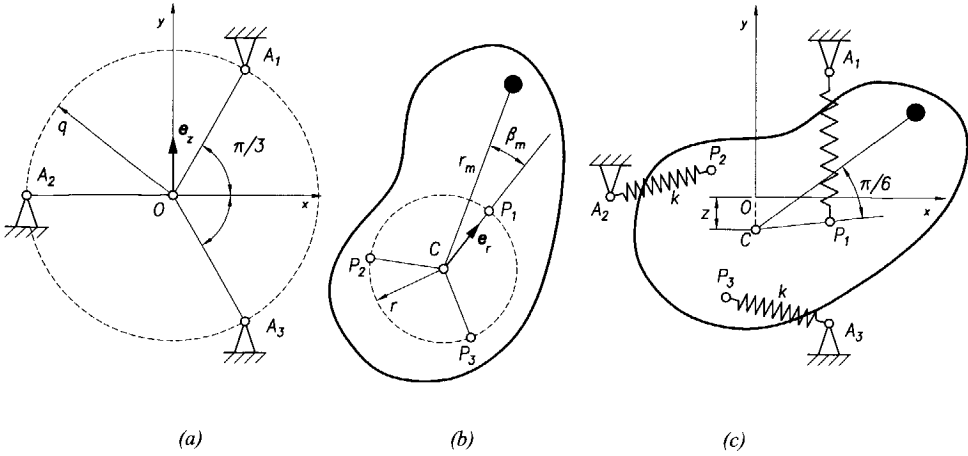
Figure 5.21 Example of a three-spring solution for the Floating Suspension: (a) selected fixed spring attachment points, (b) selected spring attachment points on the moving body, (c) resulting arrangement, solved for the parameters of the mass-lever element.

This expression can be simplified by selecting the virtual pivot for point C. For a virtual pivot to exist at all, it needs to be the stationary equilibrium position for point C when the beam rotates, and therefore independent of φ. Rearranging the equation of the equilibrium of forces, equation 5.22, gives:

$$r_c = \frac{-mg e_z + \sum k_i \left(a_i - R r'_{i/c}\right)}{\sum k_i} \tag{5.38}$$

Substituting $r_{i/c} = R(\varphi) r'_{i/c} = r_i R(\beta_i) R(\varphi) e'_r$ yields:

$$r_c = \frac{-mg e_z + \sum k_i a_i - \sum k_i r_i R(\beta_i) R(\varphi) e'_r}{\sum k_i} \tag{5.39}$$

For this expression to be constant, the term containing φ should cancel out:

$$\sum k_i r_i R(\beta_i) R(\varphi) e'_r = \sum k_i r_{i/c} = 0 \tag{5.40}$$

Under this condition the expression for r_c reduces to:

$$r_c = \frac{-mg e_z + \sum k_i a_i}{\sum k_i} \tag{5.41}$$

The condition $\sum k_i r_{i/c} = 0$ implies that the last term in equation 5.37 is zero. Therefore, the balancing condition is reduced to its final form:

$$mg r_m \cos \beta_m = \sum k_i r_i q_i \cos(\beta_i - \phi_i) \tag{5.42}$$

It is readily verified, for instance using figure 5.18, that the original two-spring Floating Suspension complies with this condition: when

selecting $k_1 = k_2 = k$, and placing the origin of the fixed reference frame at the midpoint of A_1A_2, equation 5.42 gives the condition $mgr_m = kra$, while equation 5.41 yields the location of the virtual pivot $r_c = -(mg/2k)e_z$. Other solutions for the two-spring case can be found according to equation 5.40 when $k_1r_1 = k_2r_2$ and $\beta_1 = \beta_2 + (2j-1)\pi$, where $j = 1,2,3,...$

Finally, one example for $n = 3$ will be given. Equal springs of stiffness k are used, while the spring attachment points are selected according to figure 5.21ab. This gives for the position vectors:

$$a_1 = qR(11\pi/6)e_z \ , \quad a_2 = qR(\pi/2)e_z \ , \quad a_3 = qR(7\pi/6)e_z \tag{5.43}$$

$$r_{1/c} = rR(0)e_r \ , \quad r_{2/c} = rR(2\pi/3)e_r \ , \quad r_{3/c} = rR(4\pi/3)e_r \tag{5.44}$$

Due to this selection, the condition in equation 5.40 is satisfied, so a virtual pivot is found:

$$r_c = \frac{-mge_z + \Sigma k_i a_i}{\Sigma k_i} = \frac{-mg}{3k}e_z \tag{5.45}$$

where it is noted that $\Sigma k_i a_i = 0$ because of the regular pattern selected for the fixed spring attachment points. The balancing condition (equation 5.42) can now be examined:

$$mgr_m \cos\beta_m = \sum k_i r_i q_i \cos(\beta_i - \phi_i) = 3krq\cos(\pi/6) \tag{5.46}$$

Thus a solution is found for $\beta_m = \pi/6$, $mgr_m = 3krq$, and $z = -mg/3k$ (figure 5.21c).

Stability

The Floating Suspension provides confirmation for the notion that a number of central linear forces can be substituted in a dynamically equivalent and unique way by a single constant force, as was suggested in section 3.3. For the case of $n = 2$, the following relation was formulated (equation 3.69):

$$F_r^T r_{r/c} = k_1 r_{1/c}^T r_{1/c} + F_1^T r_{1/c} + k_2 r_{2/c}^T r_{2/c} + F_2^T r_{2/c} \tag{5.47}$$

This relation is applied to the basic version of the Floating Suspension, taken with respect to the virtual pivot C (figure 5.18). Substituting the expression for the zero-free-length spring forces, $F_i = k_i(a_{i/c} - r_{i/c})$, gives:

$$F_r^T r_{r/c} = k_1 r_{1/c}^T r_{1/c} + k_1(a_{1/c} - r_{1/c})^T r_{1/c} + k_1 r_{1/c}^T r_{1/c} + k_2(a_{2/c} - r_{2/c})^T r_{2/c}$$

$$= k_1(a_1 - r_c)^T r_{1/c} + k_2(a_2 - r_c)^T r_{2/c} \tag{5.48}$$

The vector $(a_i - r_c) = a_{i/c}$ is the vector from the virtual pivot to the fixed spring attachment point A_i, while $r_{i/c}$ runs from the virtual pivot to the points where

the moving spring ends attach to the lever, so each set of $a_{i/c}$ and $r_{i/c}$ puts up a spring-lever element with spring k_i (figure 5.20). A solution to this equation is possible when it is assumed that F_r is parallel to the line connecting the fixed ends of the springs and its point of application is located on the line connecting the moving ends of the springs. Hence, $F_r = F_r e_a$ and $r_{r/c} = r_r e_r$. Under these conditions, the equation becomes:

$$F_r r_r e_a^T e_r = k_1 a_1 r_1 e_a^T e_r + k_2 a_2 r_2 e_a^T e_r \tag{5.49}$$

A solution is found for any angle φ when:

$$F_r r_r = k_1 a_1 r_1 + k_2 a_2 r_2 \tag{5.50}$$

Thus, the dynamically equivalent force of the two ideal spring forces is a constant force of magnitude F_r and directed along e_a, acting on the lever along the extension of $P_1 P_2$ at a distance r_r from point C. Consequently, a statically balanced system is created when an equal but opposite force is applied at the same position. Therefore, setting e_a vertical and taking $F_r = mg$ yields the same solution indeed. This solution is not unique. As the angle between F_r and $r_{r/c}$ is prescribed in relative terms by the scalar product $e_a^T e_r$, rather than relative to the vertical load mg, the spring system may be rotated using modification rule 2, as was already shown in figure 5.17. Note, however, that the original floating suspension, as a special case of a general concept, is particularly interesting as it is the only one that allows rotation about the vertical axis, without falling into instability. Furthermore, equation 5.50 allows the use of unequal springs. Figure 5.16 already showed one configuration with springs of different stiffness that is in agreement with the condition in equation 5.50.

Finally, it will be illustrated that application of the geometrical construction for the determination of the DEP (point of application of the dynamically equivalent resultant force, see section 3.4) indeed introduces an error which is a constant term, as was suggested in section 3.4. Figure 5.22 shows the Floating Suspension in three different configurations. In each of the configurations, the DEP is constructed as if the spring forces were constant forces. The diagram shows that the DEP is not located at the center of mass, where it should be for zero stability, but at a distance r_z right below the center of mass. This distance is equal in all configurations, so P_r traces a circle of radius r_m. Using the symbols from figure 5.18, and selecting the equal-springs case, the distance r_z is found as follows. First, the contribution of the spring forces is calculated as if they were constant forces to find P_r:

$$F_1^T r_{1/c} + F_2^T r_{2/c} = k^* (a_{1/c} - r_{1/c})^T r_{1/c} + k^* (a_{2/c} - r_{2/c})^T r_{2/c}$$
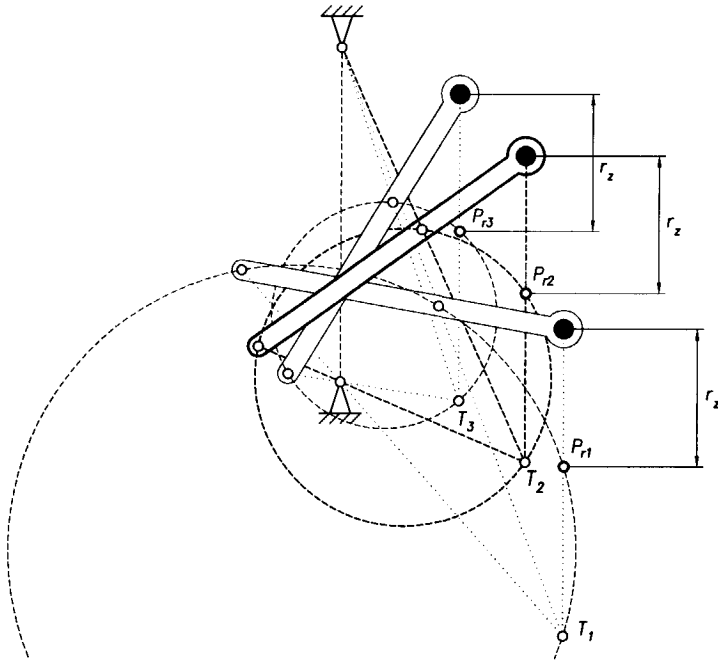
Figure 5.22 Illustration of the error introduced by applying the circle construction (for finding the dynamically equivalent resultant force, see section 3.4) to central linear forces: a constant distance is present between P_{ri} and the center of mass.

$$= k^*\left((1-p)a^*e_z - re_r\right)^T re_r - k^*\left((-p)a^*e_z + re_r\right)^T re_r$$

$$= k^* r a^* \cos\varphi - 2k^* r^2 \tag{5.51}$$

The resultant force is found as:

$$F_r = F_1 + F_2 = k^*\left((1-p)a^*e_z - re_r\right) + k^*\left((-p)a^*e_z + re_r\right) = k^*(1-2p)a^*e_z \tag{5.52}$$

The location $r_{r/c}$ of P_r will now be calculated using the stability equation for constant forces:

$$k^* r a^* \cos\varphi - 2k^* r^2 = k^*(1-2p)a^*e_z^T r_{r/c} = k^*(1-2p)a^*e_z^T\left(r_r e_r + r_z e_z\right)$$

$$= k^*(1-2p)a^* r_r \cos\varphi + k^*(1-2p)a^* r_z \tag{5.53}$$

Equation 5.53 is true if the cosine terms and the constant terms cancel each other out. This results in $r_r = r/(1-2p)$ and $r_z = -2r^2/(1-2p)a^*$. Using the result $p = \frac{1}{2} - mg/2k^*a^*$ from equation 5.20, it is found that $r_r = rk^*a^*/mg$ and $r_z = -2r^2 k^*/mg = -kr^2/mg$. This shows that P_r is located at a constant

112
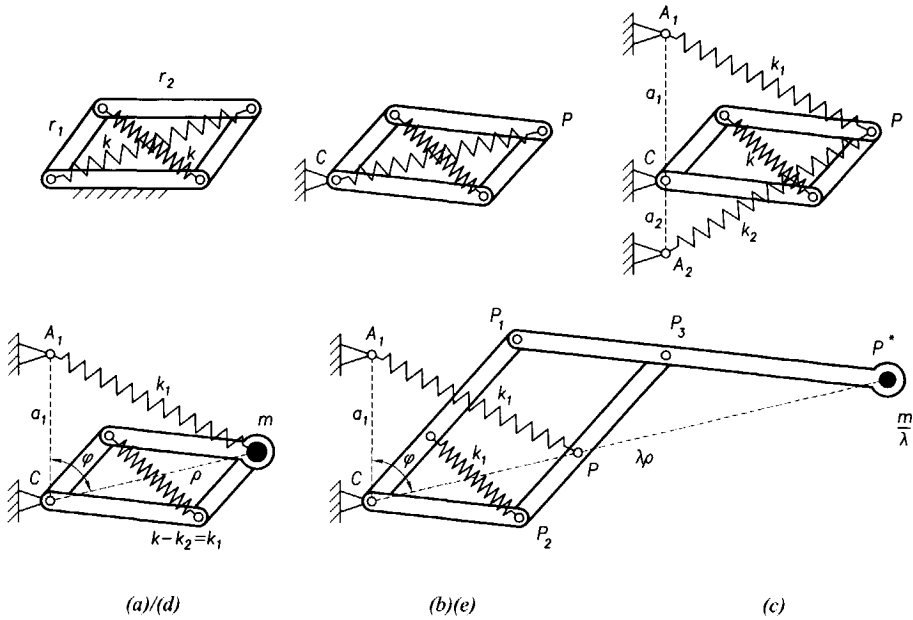
Figure 5.23 Conception of several two-degree-of-freedom equilibrators based on balanced parallelogram: (a) balanced parallelogram, (b) inverted in the sense that only C is fixed to ground, (c) resolution of one spring into two ones, (d) exchange of spring-lever element by mass-lever element and compensation for the collapse-effect, see text, (e) extension of parallelogram into pantograph.

distance r_z right below the location $r_r e_r$ of the mass. The result is in agreement with the expectation of a constant error term, given in equation 3.85. As the resultant of the spring forces is constant (equal to mg), a constant distance r_z is expected directed along the vertical.

Generalized lazy-tongs mechanisms

In this section, the transformation of the basic spring force balancer into several two-degree-of-freedom gravity equilibrators will be discussed. In order to obtain a second degree of freedom, the balanced parallelogram (figure 4.15b) is kinematically inverted in the sense that instead of a whole link, only one of the pivots is fixed to ground (figure 5.23b). Thus, an additional degree of freedom is obtained. Next, the spring connected to the fixed pivot is resolved into two springs k_1 and k_2, in such a way that their fixed points are on the vertical line through the fixed pivot (figure 5.23c). According to modification rule 5 this is allowed if both of the following equations are satisfied:

$$k_1 + k_2 = k \tag{5.54}$$

113
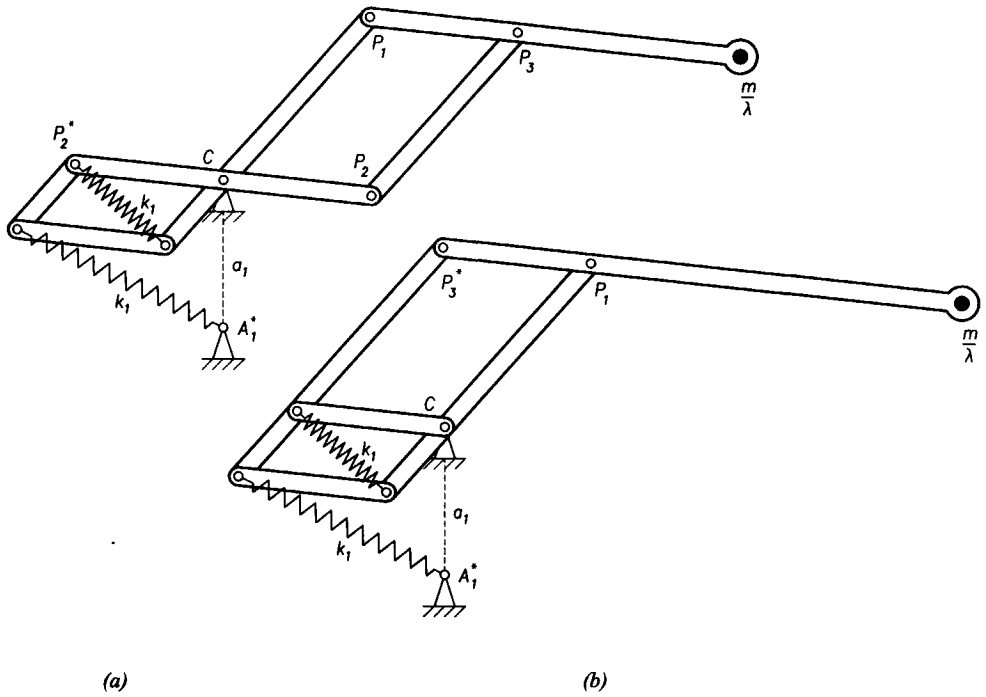
Figure 5.24 Modification of extended lazy-tongs equilibrator: (a) rotation of balancer unit by 180 degrees, (b) rearranging parallelogram $CP_2P_3P_1$ for improved mechanical performance.

$$k_1a_1 = k_2a_2 \tag{5.55}$$

The *imaginary* spring-lever element CPA_2 containing spring k_2 is now transformed into a mass-lever element with a variable link length ρ (figure 5.23d). It should be noted however, that in this case rule 7 does not apply in its simplest form. Acting on a solid lever, the force component of a spring-lever element along the link has no influence on the equilibrium: the link does not deform so only the equilibrium of *moments* needs to be taken into account. The imaginary lever CP in figure 5.23c however, is put up by a spring mechanism, and therefore the equilibrium of *forces* along the imaginary arm CP should be considered as well. Replacing the spring by a mass takes this force away, and therefore the action of spring k must be reduced by decreasing its spring rate to the value $k - k_2$. Equation 5.54 learns that $k - k_2 = k_1$, resulting in two equal springs in figure 5.23d. For the other parameters, the rule applies unchanged. Therefore:

$$mg = k_2a_2 \tag{5.56}$$

114

The result is a general form of the mechanism called an *equipoised lazy-tongs mechanism* by Carwardine (1938) and a *parallel-link equilibrator* by Streit and Shin (1993). Both the lazy-tongs mechanism and the parallel-link equilibrator were furnished with equal link lengths: $r_1 = r_2$. The above treatise shows that this limitation is not essential for proper functioning.

Extending the parallelogram into a pantograph linkage allows the gravity compensation mechanism to be more compact, relative to the whole mechanism. The pantograph assures that points C, P, and P^* are always collinear in such a way that $CP^*/CP = \lambda\rho/\rho = \lambda$, where λ is the magnification factor of the pantograph [5.8]. Figure 5.23e shows one of many possible arrangements. Static balance is proved by considering the potential:

$$V_1 = \tfrac{1}{2}k_1\left(a_1^2 + \rho^2\right) - \rho k_1 a_1 \cos\varphi \tag{5.57}$$

$$V_{diagonal} = \tfrac{1}{2}k_1\left(2(r_1 + r_2) - \rho^2\right) \tag{5.58}$$

$$V_m = (m/\lambda)g\lambda\rho\cos\varphi = mg\rho\cos\varphi \tag{5.59}$$

$$V = \tfrac{1}{2}k_1 a_1^2 + k_1(r_1 + r_2) + \tfrac{1}{2}k_1\rho^2 - \tfrac{1}{2}k_1\rho^2 + mg\rho\cos\varphi - \rho k_1 a_1 \cos\varphi \tag{5.60}$$

Demanding constant total potential V yields the balancing condition: $mg = k_1 a_1$, which is easily checked by inspection of equations 5.55 and 5.56. It is interesting to note that the energy functions are independent of λ, which is the magnification factor of the pantograph as well as the reduction factor of the supported mass.

Possible modifications include alteration of the points of attachment of the diagonal spring on links CP_1 and P_2P_3, respectively, according to rule 1 (parameters) or rule 3 (shift). For a more compact balancer unit, the whole spring system can be rotated about the pivot by 180 degrees (figure 5.24a), and the link P_2P_3 can be changed to the other side of CP_1 into $P_2^*P_3^*$ (figure 5.24b).

Five-bar parallelogram linkage

The equilibrators in the previous section were conceived based on the kinematically inverted balanced parallelogram. Another method for designing multiple-degrees-of-freedom mechanisms is to apply the principle of superposition. The example in section 4.5 (figure 4.25) already demonstrated this possibility, the result of which will be extended in this section towards a more useful gravity equilibrator.

Figures 5.25a shows the result of figure 4.25. For a more compact compensation unit relative to the workspace of the mechanism, the parallelogram can be extended into a pantograph linkage (figure 5.25b), so that $CP^*/CP = \lambda\rho/\rho = \lambda$, where λ is the magnification factor of the
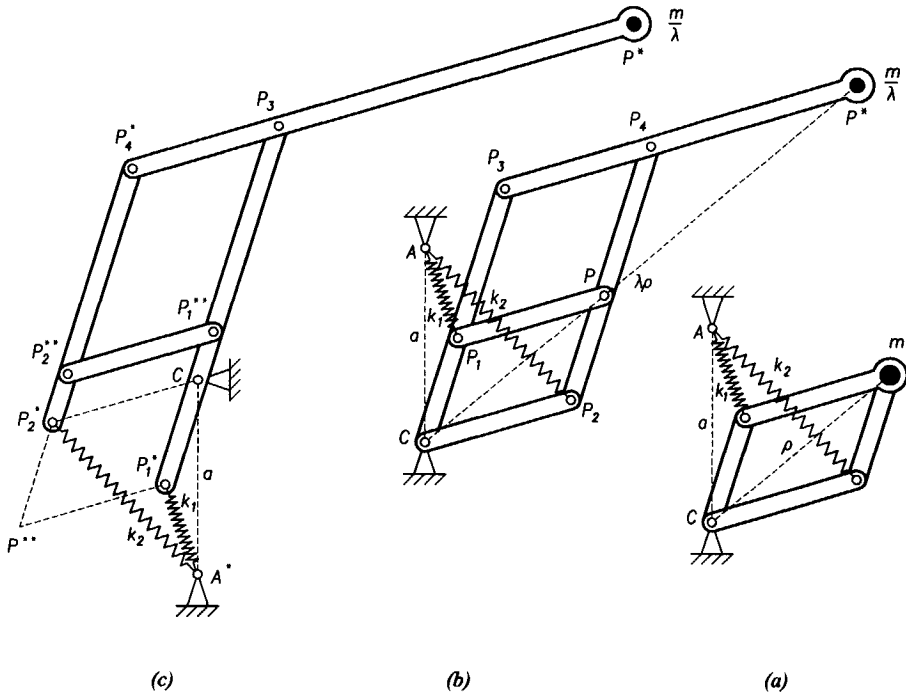
Figure 5.25 Conception of several two-degree-of-freedom equilibrators using the principle of superposition (from right to left): (a) combined balancing systems for two degrees-of-freedom according to figure 4.22, (b) extension using a pantograph linkage, (c) rotation of spring-lever elements.

pantograph. The governing equations do not change when the parallelogram is enlarged by a factor of λ and the mass is reduced by the same factor (according to modification rule 1). If desired, the compensation springs can be hinged below the fixed pivot by rotating the spring lever elements, including point A and parallelogram $CP_1P_3P_2$ by 180° about pivot C (modification rule 2). In figure 5.25c, point P^{**} has become a virtual point of the imaginary lever $P^{**}CP^*$. To avoid a double joint at point C, link CP_2 has been shifted to $P_1^{**}P_2^{**}$. Note that these modifications have no influence on the energy functions but considerably alter the force configuration. Specifically, the last modification turns link $P_2^*P_4^*$ into a three-force system. Consequently, link $P_1^{**}P_2^{**}$ should not be shifted up excessively.

The design parameters are easily derived from the potential functions. With $a_1=a_2=a$, the potentials of the springs (V_1 and V_2), the mass (V_m) and the total system (V) are given by, respectively:

116
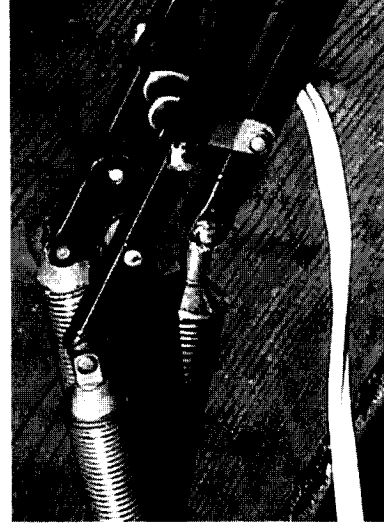
(a) *(b)*

Figure 5.26 Photographs of the Anglepoise desk lamp: (a) overview, (b) close-up of the balancing mechanism.

$$V_1 = \tfrac{1}{2} k_1 \left(a^2 + r_1^2 \right) - r_1 k_1 a \cos \varphi_1 \tag{5.61}$$

$$V_2 = \tfrac{1}{2} k_2 \left(a^2 + r_2^2 \right) - r_2 k_2 a \cos \varphi_2 \tag{5.62}$$

$$V_m = (m/\lambda) g h = (m/\lambda) g \left(\lambda r_1 \cos \varphi_1 + \lambda r_2 \cos \varphi_2 \right) = mg \left(r_1 \cos \varphi_1 + r_2 \cos \varphi_2 \right) \tag{5.63}$$

$$V = \tfrac{1}{2} k_1 \left(a_1^2 + r_1^2 \right) + \tfrac{1}{2} k \left(a_2^2 + r_2^2 \right) - r_1 k_1 a \cos \varphi_1 - r_2 k_2 a \cos \varphi_2 + \\ mgr_1 \cos \varphi_2 + mgr_2 \cos \varphi_2 \tag{5.64}$$

Thus in this example with $a_1 = a_2 = a$, the design parameters should relate according to the equation $mg = k_1 a = k_2 a$, so equal ideal springs are required of stiffness $k = mg / a$.

The linkage of figure 5.25c has been applied in the Anglepoise desk lamp, indeed "a lamp which was engineered rather than designed" [5.9], see also figure 2.7. Unlike most spring-balanced lamps, this design does not require friction to position the lamp in all positions. Figure 5.26 shows a close-up image of the spring mechanism. The linkage has also been applied in the model of the statically balanced parallel manipulator by Gosselin *et al.* in figure 2.8.

117

$\dfrac{m}{\lambda}$
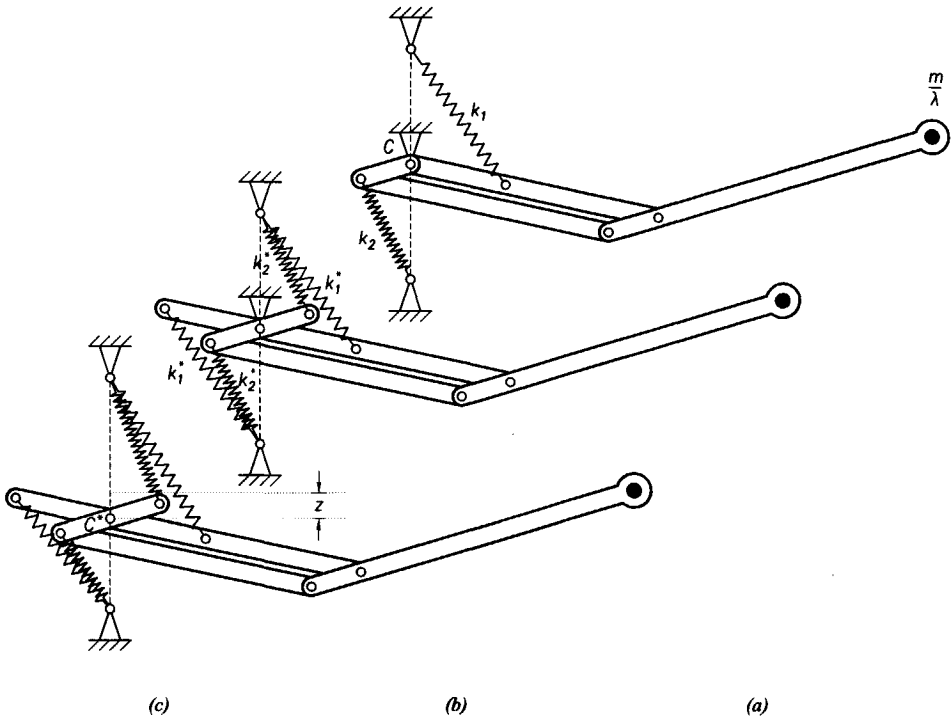
Figure 5.27   Floating version of the five-bar parallelogram equilibrator (patented [5.5]), (from upper right to lower left): (a) the mechanism of figure 5.25c in a different position, (b) each spring replaced by two springs of half the stiffness, and one of each set rotated by 180 degrees, (c) after removing the pivot.

Furthermore, the linkage is used as a leg in a walking robot, and in direct-drive robots [5.10].

Floating version

Above, a well-known equilibrator was discussed, which has been reported before, but its conception was not described earlier. Continuing using the framework of modification rules, a useful feature can be added to the mechanism: a floating suspension. The same approach will be used as was previously employed in figure 5.13. Figure 5.27a shows the same linkage as in figure 5.25c in a different configuration. As compared to figure 5.25c, spring k_1 has not been rotated by 180 degrees, while spring k_2 has. Furthermore, link CP^* has not been shifted to $P_1^{**}P_2^{**}$.

To obtain a floating version, springs k_1 and k_2 are replaced by two springs k_1^* and two springs k_2^*, respectively, where $k_i^* = \frac{1}{2}k_i$. Subsequently, one spring of each set is rotated about the pivot by 180 degrees (figure 5.27b). When the whole linkage is considered as one system, six external forces are

118

(a)   *(b)/(c)*   *(d)*
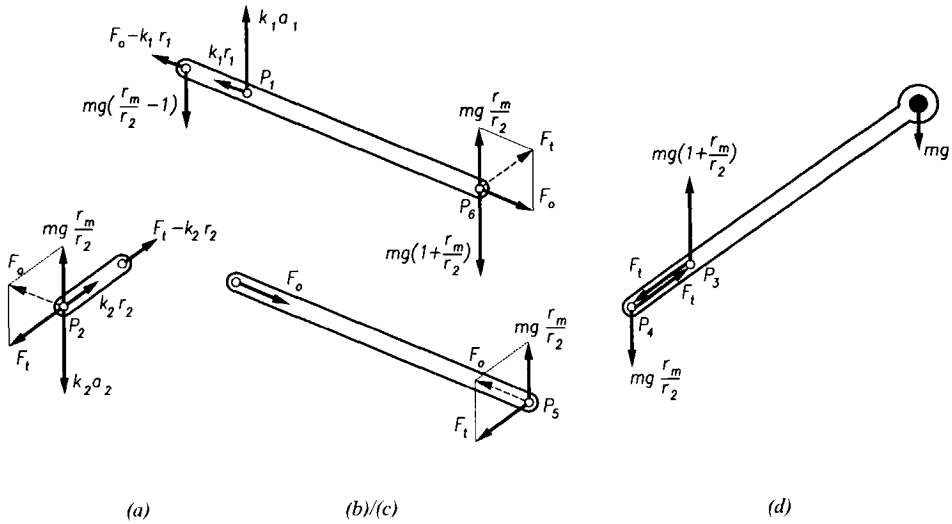
Figure 5.28 Forces in the separate links of the five-bar parallelogram equilibrator: (a) auxiliary distal link, (b) proximal link, (c) auxiliary proximal link, (d) distal link. Starting with the examination of the distal link and applying skew resolution, the balancing conditions can be derived.

present: the four spring forces, the weight, and the pivot force. Since the spring forces are in pairs equal and opposite, the pivot force is equal to the weight mg / λ and directed vertically upward. Therefore, when the pivot is removed, a virtual pivot will settle at C^*, a distance z below C, where $z = (mg / \lambda)/(2k_1^* + 2k_2^*) = (mg / \lambda)/2(k_1 + k_2)$ (figure 5.27c). Clearly, several kinds of modifications are possible, but they are not discussed here. One interesting extension is made in section 5.5.

Force analysis

The force analysis of this linkage is greatly facilitated by skew, rather than orthogonal, resolution of forces. It will be shown that the desired force configuration, resulting in independent balancers, is achieved. To illustrate this and to derive the balancing conditions in an additional manner, the free body diagrams of the separate links of the mechanism are considered (with slightly different symbols, figure 5.28). First, the distal link is examined. Vertical equilibrium requires the component mgr_m / r_2 to be present at P_4 and $mg(1 + r_m / r_2)$ at point P_3. This gives one component of the resultant force at point P_5. As the auxiliary proximal link is a two-force system, the resultant force F_o is directed along the line connecting its ends. Therefore, an additional component F_t is needed for equilibrium. This component also acts at the distal

119
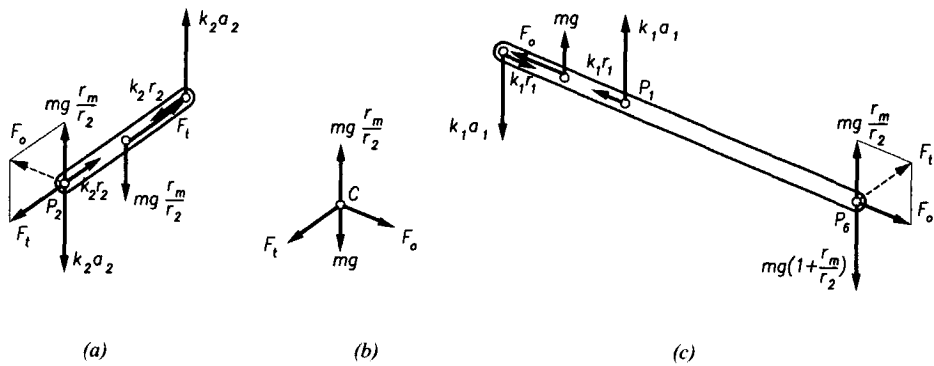
Figure 5.29 Forces in the modified version of the anthropomobile arm according to figure 5.27b, where the pivot is still present. Only the modified links are considered, and a constant pivot load of mg is found.

link at point P_4 and in opposite sense at point P_3. To appreciate the forces at point P_6, the component F_t is resolved into a vertical component mgr_m/r_2 and a component along the upper arm link F_o, as was done at point P_5. It is then seen that the total vertical component is directed downward, and equal to mg. Since the vertical component of the spring force at P_1 is k_1a_1, the balancing condition for spring k_1 is: $k_1a_1r_1 = mgr_o$. To find the balancing condition for spring k_2, the forces at point P_2 are investigated. The reaction of F_o is again resolved into a vertical component mgr_m/r_2 and a component F_t along the link P_2C. As the vertical component of the spring force at P_2 is k_2a_2, the balancing condition for spring k_2 is: $k_2a_2r_2 = mgr_m$.

For the investigation of the forces in the floating version, the version with the pivot still present is considered first (figure 5.29). The pivot forces required for equilibrium of the links are transferred (in opposite sense) to the pivot axis, resulting in components F_o, F_t, mg, and mgr_m/r_2 according to figure 5.29b. As F_o and F_t add up to mgr_m/r_2, a pivot load of mg vertically upward is found. This is in accordance with the result found previously.

120
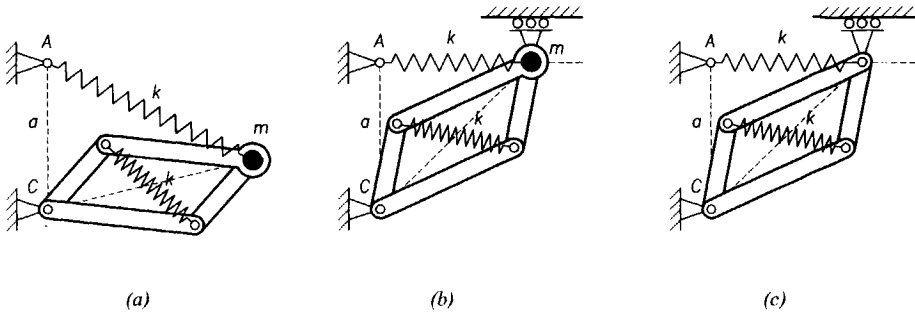
Figure 5.30 Design example of spring-to-spring balancers based on gravity equilibrators where mass travels horizontally: (a) parallelogram-based equilibrator, see figure 5.23d, (b) mass guided along horizontal path, in this case so that the spring acts along a stationary line, (c) elimination of mass.

5.3   Spring force balancers

So far as normal elastic material is used, the elastic element deforms according to Hooke's law. As a result, the compensation spring at the other end of the wire should have negative stiffness instead of the one following Hooke's law to cancel the tractive force [-].

S. Hirose, T. Kado, Y. Umetani, 1983

Of particular interest for this thesis is the question of spring-to-spring balancing. As was mentioned in chapter one, the compensation of the undesired spring action of the cosmetic covering in hand prostheses was one of the driving forces behind the present work. As compared to gravity equilibration, spring force compensation is much less described in literature [1.6, 5.11]. Nevertheless, many applications exist, not only to compensate flexible coverings but also in situations where forces need to be controlled, such as rolling-link mechanisms, or in situations where the system is to be preloaded in order to avoid backlash.

Apart from being useful in mechanisms, balanced spring mechanisms may also be present in biological systems. For instance, ligaments are ascribed a movement limiting function, but as ligaments are elastic (or at least visco-elastic) it might be nice to think of the ligaments as a biological balanced configuration. This would very elegantly explain the combination of firm contact and easy movement [5.12].

This section will again use the framework as an aid in the conception of spring force balancers. However, short cuts are possible, one of which will be

121
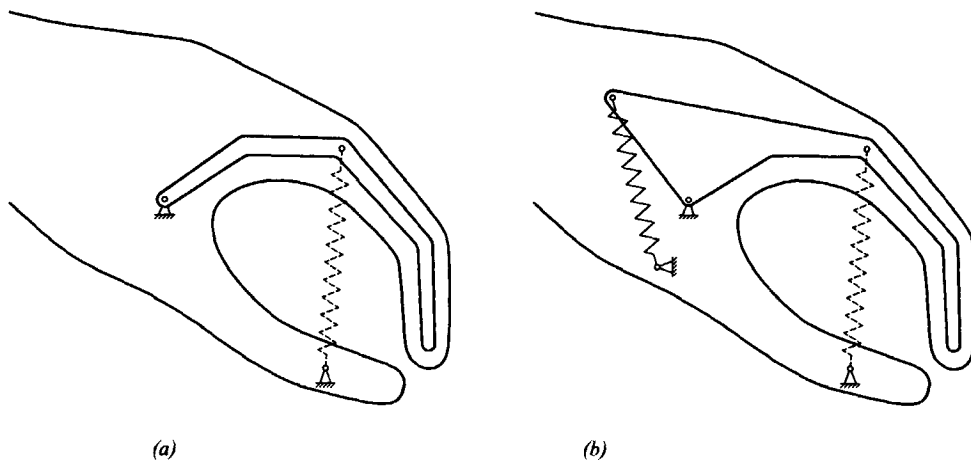
Figure 5.31 Compensation of cosmetic covering of a hand prosthesis: (a) moving finger hampered by cosmetic glove, represented by dashed spring, (b) compensation by means of spring butterfly.

given here. In gravity equilibrators where the mass moves along a horizontal path, the potential is constant also without the mass. Therefore, many of the systems in the previous section can be adapted. One example is given in figure 5.30. The mass of the generalized lazy-tongs mechanism of figure 5.23d is confined to move along the horizontal through the grounded spring attachment point A. When the mass is taken away, a spring-to-spring balancer remains, featuring one spring which moves along a stationary straight line. This feature makes the mechanism suitable for balancing a normal spring, which is the subject of section 5.4.

Basic spring force compensator
The first example of spring-to-spring arrangement is of course the basic spring force balancer, which has come across at various occasions in this thesis already. Over-simplified indeed, but illustrating the idea that initiated this dissertation project is the hand prosthesis sketched in figure 5.31. The finger mechanism essentially is a single link, which is hampered in its motion by the cosmetic covering, represented by an ideal spring. An appropriately shaped spring butterfly provides perfect balance. Unfortunately, the cosmetic covering does not at all behave like an ideal spring [1.4]. To a certain extent, the matter of balancing non-ideal springs is addressed in chapter six.

As was the case for the gravity equilibrators, there is also a floating version possible of the basic spring force balancer, which is in fact a special case of the n-spring mechanism in figure 5.19. In the case of zero mass, and four equal

(a)   (b)
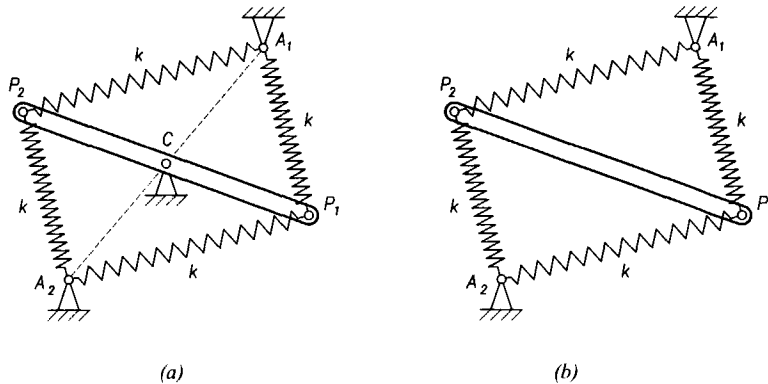
Figure 5.32 Floating version of the basic spring force balancer: (a) two basic spring force balancers arranged back-to-back, (b) floating version, elementary case, modifications are possible.

springs of stiffness k, the system can be arranged so that it can be regarded as an ensemble of two equal kinematically inverted basic spring force balancers in a back-to-back arrangement, according to figure 5.32 (see also figure 4.14). Clearly, the dynamically equivalent resultant forces of the elements are equal and opposite, and therefore the pivot can be removed. Modifications according to rule 1 are allowed to arrive at solutions with unequal springs. Alternatively, the system can be developed from the equations of the floating suspension by selecting equal springs and equal arm lengths, and substituting $m = 0$ into equations 5.41 and 5.42. This yields $r_c = \frac{1}{2}(a_1 + a_2)$ for any φ, and a confirmation of the balancing condition. Thus, a statically balanced lever is found with a stationary, unloaded virtual pivot.

One of the few spring-to-spring balancers reported in literature is the one based on the so-called *elliptic trammel* or *slipping ladder* [5.13]. This balanced spring mechanism can be derived as follows. A balanced rhombus (according to figure 4.17a) is considered with its joints sliding along the axes of a fixed orthogonal coordinate system (figure 5.33a). Arranged like this, the midpoints of the (ideal) springs are stationary at the origin. Each spring k might as well be seen as two springs of stiffness $k^* = 2k$ in series, and all of the resulting four springs may be thought fixed at the origin. If now the mechanism is divided into four equal parts, each comprising one link and two springs of stiffness $k^{**} = \frac{1}{2}k^* = k$, then each of these quarters becomes an independent balanced unit. Such a unit can be materialized by adding guiding elements that supply the support forces required, as is suggested in figure 5.33c.

The linkage of figure 5.33c is one of the embodiments of the elliptic trammel. The kinematic pole P is located on the path perpendiculars of
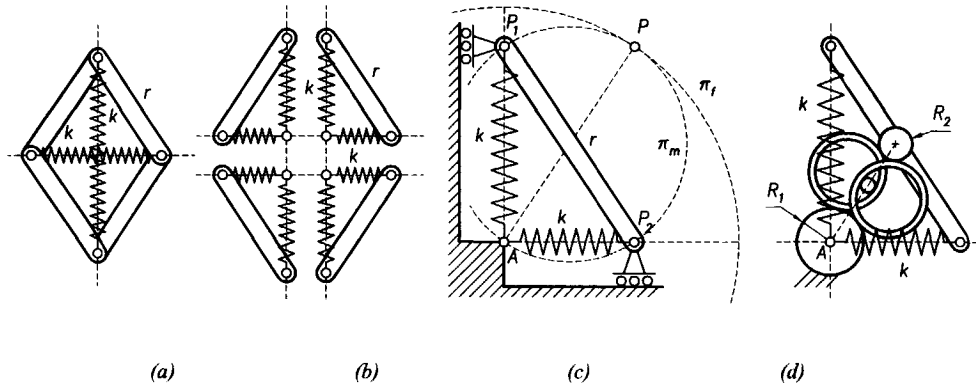
Figure 5.33 Conception of the slipping stepladder: (a) balanced rhombus, (b) division into four parts, (c) slipping ladder or elliptic trammel arrangement [5.13], (d) rolling version of the elliptic trammel [5.13].

points P_1 and P_2. As these path perpendiculars are mutually perpendicular, the pole is always on the circle through P_1, A, and P_2. In any position, AP is a diameter of this circle, so P traces a circle of radius r about the fixed point A. It is seen now that the moving polode π_m is a circle of diameter r, rolling inside a circle of radius r being the fixed polode π_f. All points of the link trace ellipses of which the ones by points P_1 and P_2 degenerate into straight lines, while the one by the midpoint of P_1P_2 is a circle. Consequently, kinematic inversion of the elliptic trammel by fixing link P_1P_2 and allowing point A to circle about its midpoint, yields the basic spring force balancer (see also figure 4.8).

A low friction version can now be obtained as follows. Unfortunately, materializing the polodes is not viable, as they are not pressed against each other by the spring forces. However, the kinematics of the moving polode can be realized in another way, by observing that rotation of the moving polode about its center is of doubled angular velocity and in opposite direction as compared to the rotation of its center about the fixed point A. Thus, three rollers, kept in line by two rings as in figure 5.33d, can accomplish the desired movement of the link. The only dimensional requirement is that the roller R_1 connected to the link be half the size of the fixed one R_2.

As the springs attach each with one end to the same body (the link), and with their other ends to the same point of another body (the frame), the configuration of springs can be modified (rule 5). Since the springs are equal, the resultant spring is found to attach at the midpoint of the link (figure 5.34b,

124
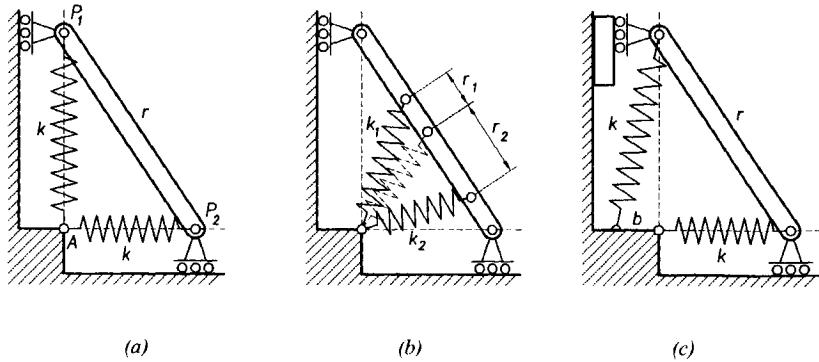
Figure 5.34 Modification of slipping ladder: (a) slipping ladder arrangement, (b) application of modification rule 5 to the springs (c) shift of spring attachment point by a distance b according to the diagram results in an additional clamping force of kb while the system still can be moved in an energy-free manner.

dashed spring). Subsequently, this spring can be resolved in many ways, as long as $k_1 r_1 = k_2 r_2$. The figure shows an example where $r_1 = r/6$ and $r_2 = r/3$.

If the springs are fixed at other points than the origin, constant force mechanisms of different kinds can be made. In the versions of figure 5.33, the springs act along stationary straight lines. If the grounded spring attachment points are shifted along the straight line guides, the spring force components in the direction of point A do not change. However, a component perpendicular to these lines is introduced (additional to the force in this direction already present), acting at the ends of the link. This force can be put to use for instance in a clamping device, but does not affect the state of static balance. Figure 5.34c shows an example where one spring attachment point is moved by a distance b, so the additional perpendicular component at point P_1 is equal to kb. This component can be controlled by adjusting b while the system can still be moved in an energy-free manner.

The fact that the grounded spring attachment points can be displaced arbitrarily in the direction perpendicular to the action lines of the springs allows the conception of a remarkable balanced system: two slipping ladders of arbitrary length, operating in opposite quadrants of an orthogonal system of sliders, sharing one set of two equal ideal springs (figure 5.35). Intertwined as the spring systems may seem, two independently balanced degrees of freedom are present. Proof is straightforward when considering the potential of the springs, and using Pythagoras' theorem:

$$V = \tfrac{1}{2}k\left(x_1^2 + y_2^2\right) + \tfrac{1}{2}k\left(x_2^2 + y_1^2\right) = \tfrac{1}{2}k\left(r_1^2 + r_2^2\right) \tag{5.65}$$

125
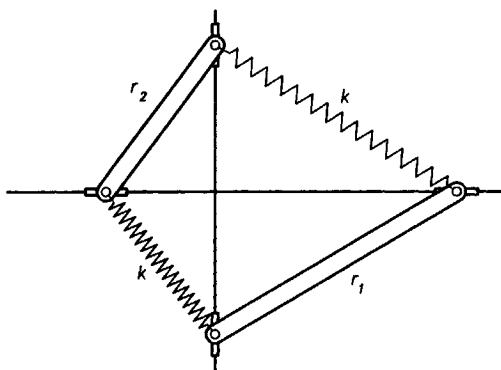
Figure 5.35   A system of two unequal slipping stepladders sharing one set of two equal ideal springs yields a statically balanced system with two independently balanced degrees of freedom.

where x_i is the x-coordinate of the horizontal slider of link r_i, and y_i is the y-coordinate of the vertical slider of link r_i. Clearly, the expression is constant.

A similar double ladder is hidden in the rotated basic spring force balancer. It will be unveiled to demonstrate that ideal spring systems provide a discovery paradise to suit all tastes. Under the condition of equal arm lengths r_1, r_2, a_1, and a_2, $A_1 P_1^* P_2^* A_2$ forms a cyclic quadrangle (figure 5.36a). As $P_1 P_1^* = P_2 P_2^*$, the angles ψ_1 and ψ_1 are subtended from equal cords of the circumscribed circle. Consequently, inclination angle γ remains constant as the system moves with the angle φ. Furthermore, points A_1 and A_2 subtend angles α_1 and α_2 from the cord $P_1^* P_2^*$. Therefore, $\alpha_1 = \alpha_2 = \frac{1}{2}\beta$, also independent of φ. It will now be shown that the quadrangle has perpendicular diagonals. In triangle $A_1 A_2 O$, the angles relate according to:

$$\phi_1 + \phi_2 + A_1 A_2 O = \pi \tag{5.66}$$

Using the fact that angle $A_1 C P_1^*$ is equal to $\frac{1}{2}\pi - \frac{1}{2}\varphi$, angle $C P_1^* A_1$ is found to be equal to $\frac{1}{4}\pi + \frac{1}{2}\varphi$. Around point A_1, the following equation is valid:

$$\phi_1 + \alpha_1 = \frac{1}{2}\beta + C A_1 P_1^* \tag{5.67}$$

Thus, $\phi_1 = \frac{1}{4}\pi + \frac{1}{2}\varphi$ is found. Similarly, it is seen that $\phi_1 = \frac{1}{4}\pi - \frac{1}{2}\varphi$. Substituting these results into equation 5.63 yields $A_1 A_2 O = \frac{1}{2}\pi$, irrespective of φ. This remarkable fact allows the symmetric spring butterfly to be regarded as a combination of two connected ladders moving in an orthogonal non-stationary frame (figure 5.36b). The links $A_1 A_2$ and $P_1^* P_2^*$ can be seen as ladders sliding on the diagonals of the quadrangle.

126

(a)   *(b)*
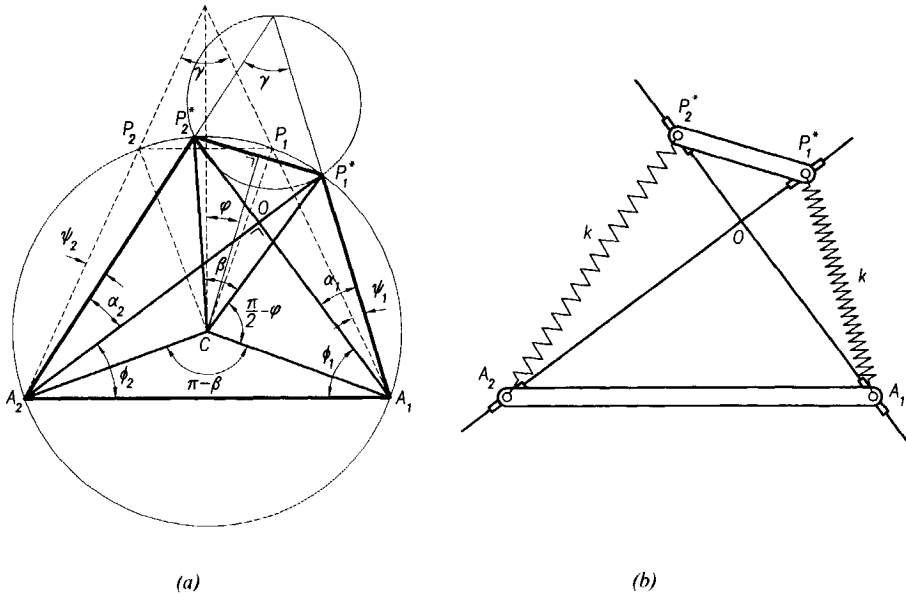
Figure 5.36 The symmetric spring butterfly seen as a system of two connected slipping ladders in a moving orthogonal frame: (a) cyclic quadrangle, (b) equivalent system of two slipping ladders.

Medical forceps

This section will present an example that is somewhat different from most of the preceding ones, where an undesired effect was statically balanced to eliminate its influence. Here, the principle of neutral equilibrium is utilized in the design itself to obtain a low friction mechanism of small dimensions, without backlash and need for lubrication.

The design concerns medical forceps for endoscopic surgery. In contrast with open surgery, where the surgeons manipulate tissue with their own hands, long and slender forceps are introduced through small incisions. Consequently, these instruments are the only source of tactile information for surgeons. Therefore, the force transmission characteristics of these instruments are important features: especially friction and backlash should be avoided, and a constant force transmission ratio is desirable [5.14].

A design, satisfying the demands mentioned, can be realized as follows. The inverted basic spring force balancer functions as point of departure. By giving this mechanism an additional degree of freedom ψ (figure 5.37a), an interesting practical version becomes possible: a simple rolling link mechanism (figure 5.37b). The rollers maintain a constant distance between their centers,

127

(a)/(d)   (b)/(e)   (c)/(f)
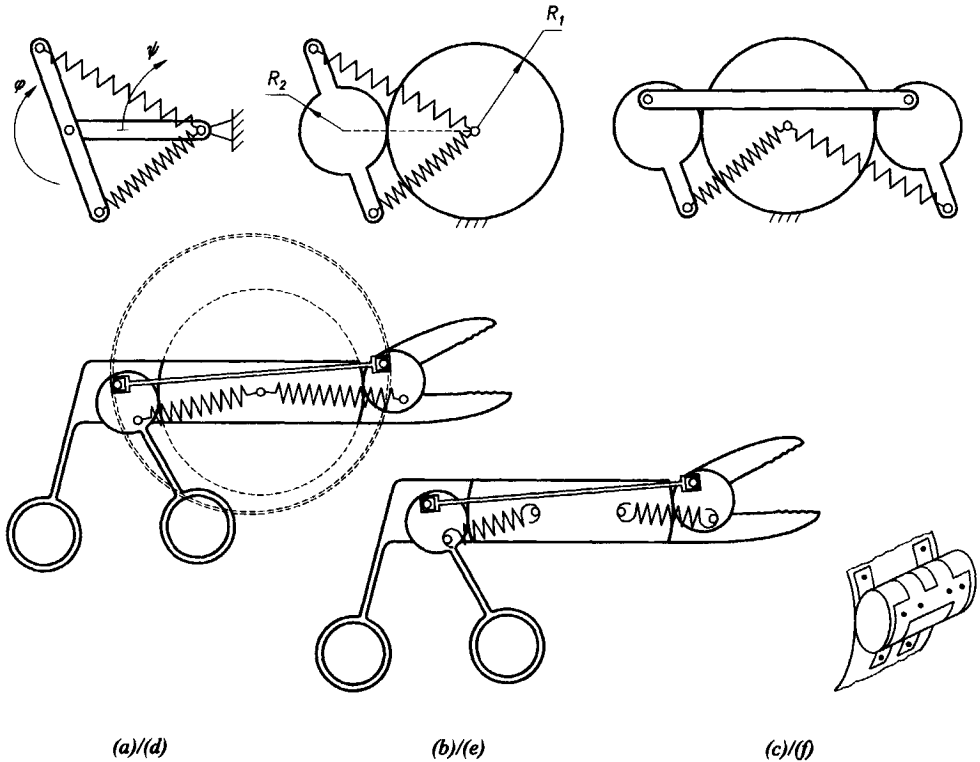
Figure 5.37 Medical forceps based on statically balanced springs: (a) inverted basic spring force balancer, (b) rolling version, (c) roller doubled and, together with one of the springs, rotated by 180 degrees about the center of the larger roller, (d) transformed into medical forceps, (e) schematically with normal springs, (f) flexible bands wrapped around the rollers to prevent them from slipping.

thus realizing a virtual link. Assuming no slip, mobility is reduced to one degree-of-freedom, according to $R_1\psi = R_2\varphi$. As a next step, the smaller roller is duplicated while the link attached to it is divided into two parts, each connected to one of the roller twins. Then the upper-half element is rotated by 180 degrees about the center of the larger roller. A connecting rod is added to synchronize the movement of the rollers (figure 5.37c).

From this configuration to a grasper mechanism is a small step: a jaw is fixed to one roller and a handgrip to the other (figure 5.37d). In order to keep friction low, the pivots of the connecting rod are also designed to roll: its contact areas are furnished such that the pins fixed to the rollers are rolling on the inside of an imaginary ring, which keeps these axes at constant distance [5.15]. Thus, the mechanism comprises four rolling pivots only (plus the rolling contacts of the spring loops), resulting in low friction. If the ideal

(a)/(c)   (b)/(d)
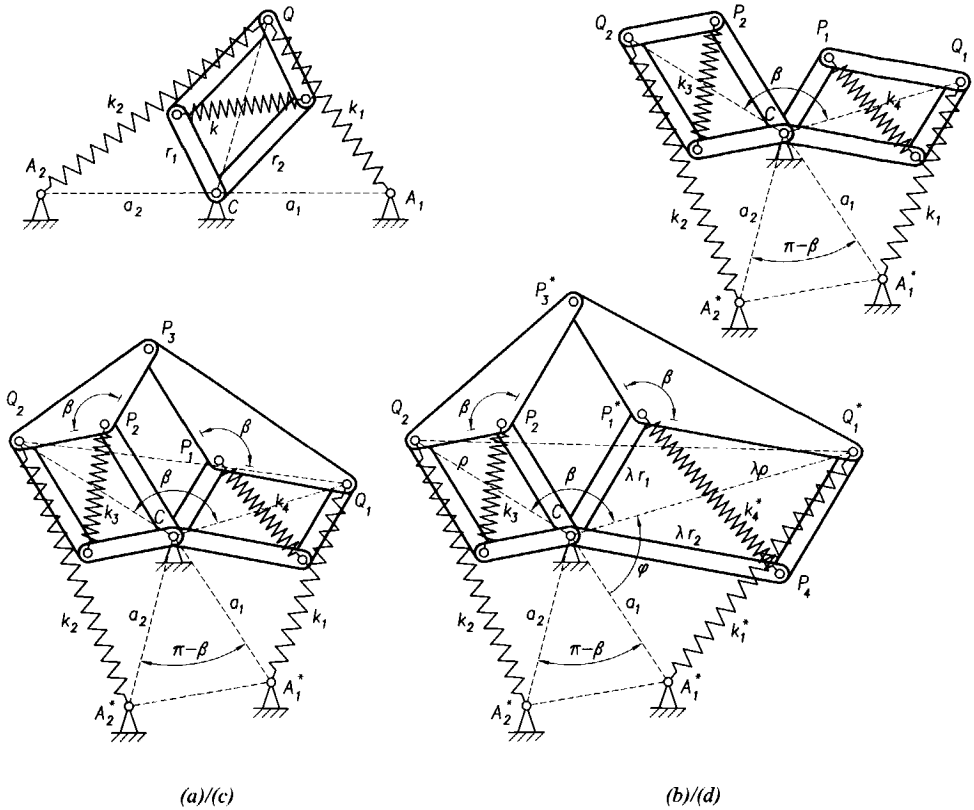
Figure 5.38 Synthesis of a two-degree-of-freedom spring force compensator, the Variable Spring Butterfly: (a) balanced parallelogram of which one spring k is resolved into k_1 and k_2, (b) the parallelograms doubled and rotated apart by an angle β, (c) kinematic coupling by means of a skew pantograph, (d) extension of one of the parallelograms and adaptation of the skew pantograph.

springs are to be replaced by normal springs, an approximation method needs to be used which will come up with altered fixation points of the springs, as is symbolically indicated in figure 5.37e. Approximation methods are included in chapter six.

Through all the steps, static balance is preserved, so it seems to the surgeon as if the springs are not present. Nevertheless, the springs prestress and stabilize the rolling link mechanism, thus eliminating backlash. Although the rollers are mainly kept in place by the forces in the springs and the connecting rod, flexible bands are to be wrapped around the rollers to prevent them from slipping (figure 5.37f).
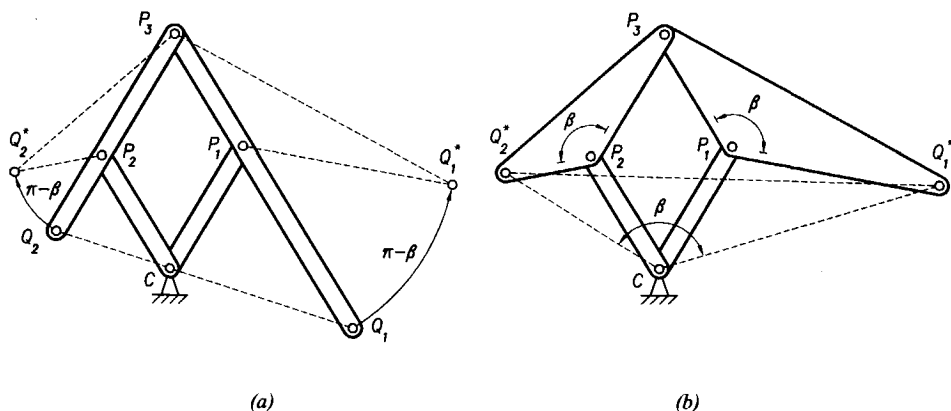
Figure 5.39 Pantograph linkages: (a) normal pantograph, (b) skew pantograph or plagiograph [5.8].

An interesting feature of this mechanism is the high quality force feedback. If an object is grasped with a certain grasp force, the reaction of this force acting on the movable jaw distorts the balance of forces. Balance is restored by applying an operating force onto the movable handgrip. Since the movement of the rollers is identical, input and output moments are equal, hence the force transmission function is constant. Thanks to the low-friction mechanism and the constant force transmission function, the operating force is an accurate measure for the grasping force [5.15]. Thus, the surgeons have a good feel of their grasp actions within the patient.

Another feature of this design is that the grasping force is limited by the spring connected to the jaw's roller. Maximum grasping force is reached when the connecting rod is forceless. If the construction of the rod prevents it from acting as a push rod, then a further increase of the operating force results in stretching of the other spring only. Thus, an inherent prevention against overload is present without additional parts. If this feature is not desired, mirroring the mechanism (exchanging the connecting rod with the springs) can be considered. In a practical version, the spring at the tip may be transferred to the hand grip [5.16].

Spring force compensation of four-bar linkage

Similar to the two-degrees-of-freedom gravity equilibrators in section 5.2, also two-degrees-of-freedom spring force compensators can be conceived using the framework proposed in this thesis. Figure 5.23c functions as a starting point (reprinted in figure 5.38a), where $k_1 + k_2 = k$ and $k_1 a_1 = k_2 a_2$. This is already a two-degree-of-freedom spring force compensator, but it can be extended into a

130
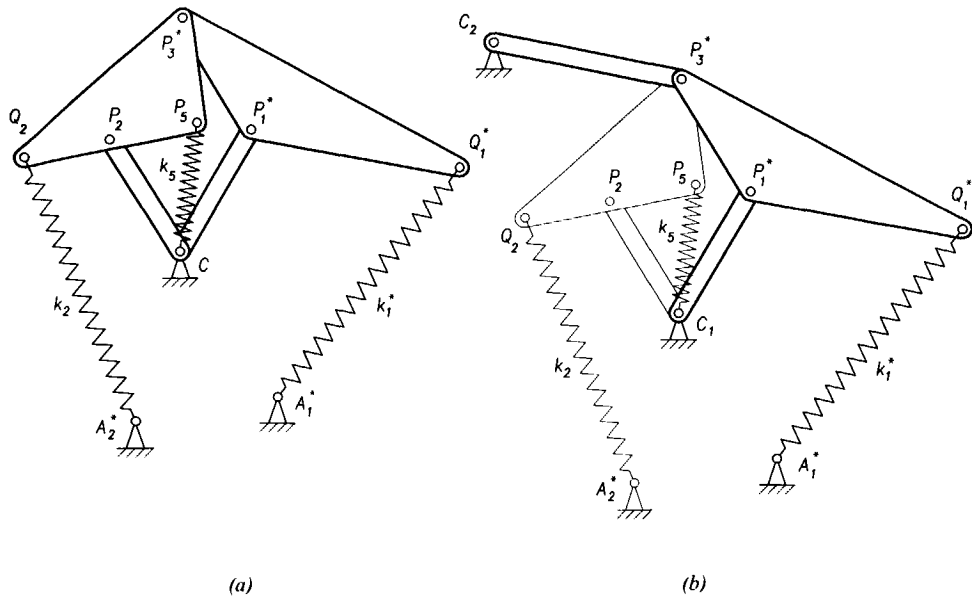
Figure 5.40 Modification of the variable spring butterfly: (a) simplification, (b) application as a balancer of a spring-loaded four-bar linkage.

form of more general interest. As a next step, it is desired to apply the rotation operation (rule 2) to the parallelogram (figure 5.38b). Because in this case no rigid links but compliant structures are rotated, the rotation rule is to be applied in a somewhat more complex way than the basic modification operation. In the basic operation (figure 4.13), the link is duplicated so that the two spring-lever elements can be rotated as units.

In this case, CQ can be regarded as an *imaginary* lever, put up by the parallelogram. This parallelogram is duplicated and the two imaginary spring-lever elements, each consisting of a parallelogram with a spring on one of its diagonals (k_3 and k_4, respectively, where $k_3 + k_4 = k$), and a spring connected to ground, are frozen and rotated about the fixed pivot. The amount of rotation determines the angle β between the two imaginary levers CQ_1 and CQ_2 (dashed lines in figure 5.38b). Rather than the simple rigid connection of the two levers as in figure 4.13, the parallelogram units are now to be connected such that the two-degrees-of-freedom mobility is maintained without influencing β and the imaginary arm length ratio $\lambda = CQ_1 / CQ_2$.

For the task of maintaining β and λ while allowing CQ_1 and CQ_2 to vary, a plagiograph or skew pantograph is perfectly suited (figure 5.39b, [5.8]). This mechanism is a general version of the normal pantograph (figure 5.39a). Both
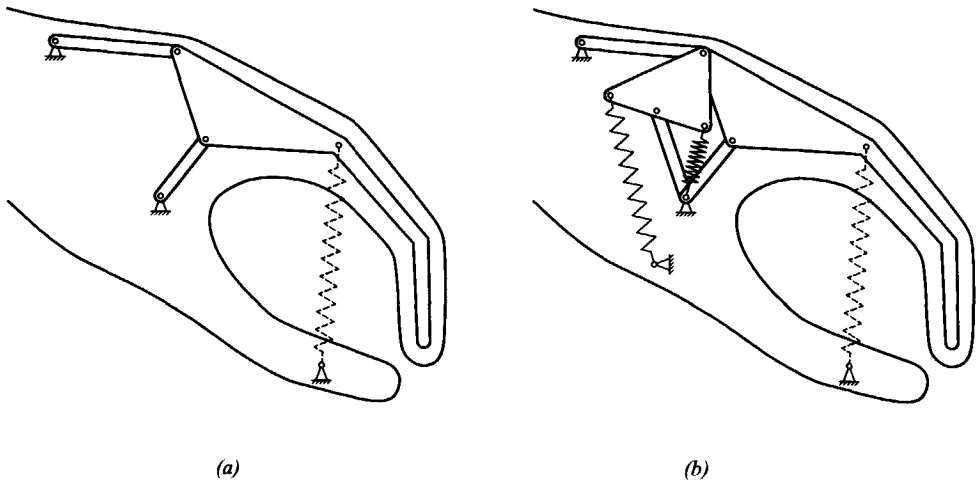
Figure 5.41   Application of the variable spring butterfly as a glove-force compensator: (a) four-bar linkage in hand prosthesis, hampered by cosmetic glove (represented by the dashed spring which is not actually present), (b) statically balanced by the four-bar spring force compensator.

linkages provide a constant transformation ratio $\lambda = CQ_1 / CQ_2$, but where the skew pantograph preserves a constant angle $\beta = Q_1CQ_2$, the normal pantograph keeps Q_1, C, and Q_2 collinear ($\beta = \pi$).

Thus, a modified spring force compensator results (figure 5.38c). It is interesting to note that the resulting mechanism can be seen as an imaginary skew lever Q_1CQ_2 with variable arm lengths (indicated with dashed lines), a *Variable Spring Butterfly*, so to speak. However, the skew angle β and the arm length ratio λ are constant, regardless of link orientations. As one compares the variable spring butterfly with the solid one, it occurs that springs k_1 and k_2 in figure 5.38c effect the equilibrium of *moments* about the pivot. For the variable spring butterfly, this is not sufficient, as the imaginary triangle Q_1CQ_2 will collapse under the influence of these springs alone: the equilibrium of *forces* is not satisfied. Springs k_3 and k_4 balance the collapse effect and realize constant potential energy. As the movement of springs k_3 and k_4 is synchronized by the pantograph linkage, the only demand for their spring rates is that $k_3 + k_4 = k$, so one of them may be eliminated, which also saves two links.

The general case of the variable spring butterfly can be obtained by applying rule 1 to one of the imaginary lever arms. This works most easily following the procedure indicated in figure 5.38d. One of the imaginary arms of the imaginary skew lever is extended, by enlarging the corresponding parallelogram. For example, the right-hand parallelogram is enlarged by a

132
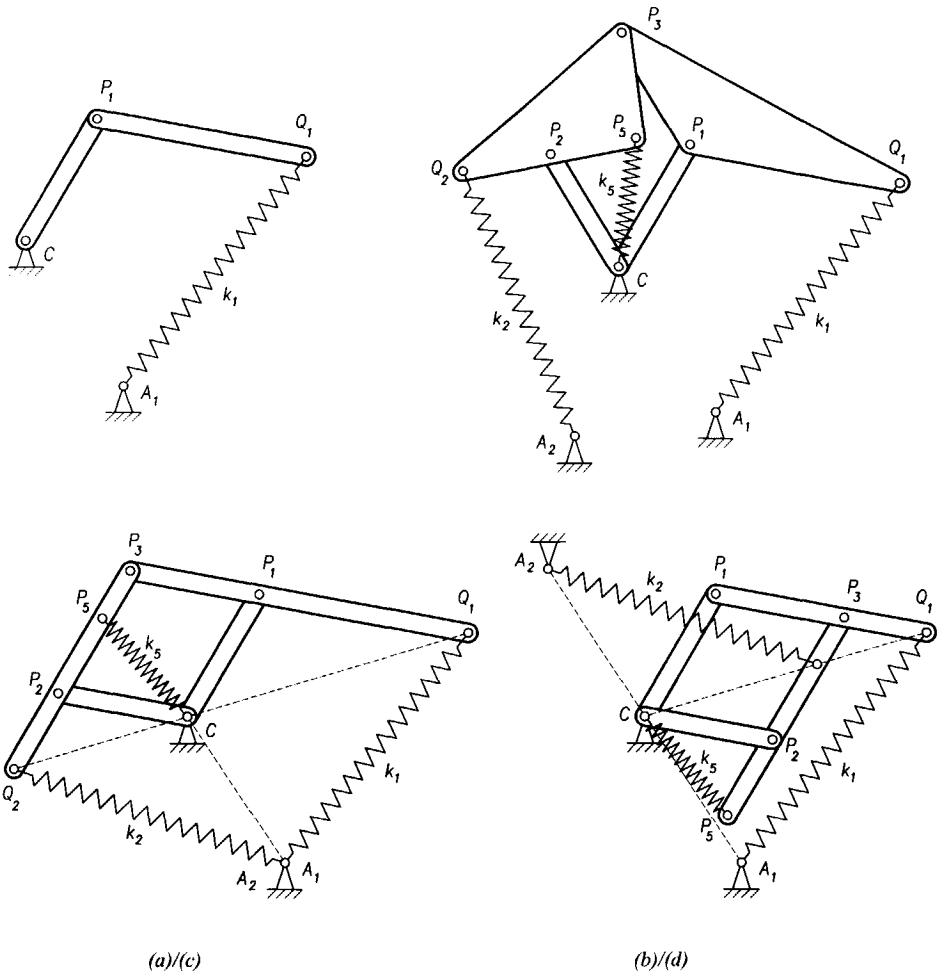
Figure 5.42 Static balance of a spring-loaded two-link open-loop chain: (a) unbalanced situation, (b) statically balanced by the four-bar spring force compensator with certain value for β, (c) the same for β=π, (d) the same for β=0.

factor λ in the direction of the line CQ_1, so that point Q_1 becomes Q_1^*. Balance is preserved if spring k_1 is replaced by k_1^*, such that $k_1^* = k_1 / \lambda$. Additionally, spring k_4 is to be replaced by k_4^*, where $k_4^* = k_4 / \lambda^2$. For the mechanism to remain a skew pantograph, link $P_2 P_3$ is extended to $P_2 P_3^*$. This whole procedure alters the arm length ratio λ but leaves the skew angle β unchanged. The parallelograms are no longer congruent but remain similar, the triangles of the pantograph lose their equilateral feature but also remain similar.

To check the static balance of this linkage the potential is used again. The potentials of the springs k_1^*, k_2, k_3, and k_4^*, and the total potential V, respectively, are:

$$V_1 = \tfrac{1}{2}k_1^*\left(a_1^2 + \lambda^2\rho^2\right) - \lambda\rho k_1^* a_1 \cos\varphi \tag{5.68}$$

$$V_2 = \tfrac{1}{2}k_2\left(a_2^2 + \rho^2\right) - \rho k_2 a_2 \cos(\pi - \varphi) \tag{5.69}$$

$$V_3 = \tfrac{1}{2}k_3\left(2\left(r_1^2 + r_2^2\right) - \rho^2\right) \tag{5.70}$$

$$V_4 = \tfrac{1}{2}k_4^*\left(2\left(\lambda^2 r_1^2 + \lambda^2 r_2^2\right) - \lambda^2\rho^2\right) \tag{5.71}$$

$$V = \tfrac{1}{2}k_1^* a_1^2 + \tfrac{1}{2}k_2 a_2^2 + k_4^*\lambda^2\left(r_1^2 + r_2^2\right) + k_3\left(r_1^2 + r_2^2\right) + \tag{5.72}$$

$$\tfrac{1}{2}k_1^*\lambda^2\rho^2 + \tfrac{1}{2}k_2\rho^2 - \tfrac{1}{2}k_3\rho^2 - \tfrac{1}{2}k_4^*\lambda^2\rho^2 + \lambda\rho k_1^* a_1 \cos\varphi - \rho k_2 a_2 \cos\varphi$$

From equation 5.72, it is seen that static balance is obtained if $\lambda k_1^* a_1 = k_2 a_2$, and $\lambda^2 k_1^* + k_2 = k_3 + \lambda^2 k_4^*$. Using $k_1 a_1 = k_2 a_2$, the first expression is satisfied if $\lambda k_1^* = k_1$, as was expected. For the second to be true for any value of λ, $k_1^* = k_4^*$ together with $k_2 = k_3$ is a solution, but as k_3 and k_4^* can take over each others function, there is more choice.

A considerable simplification can be realized by taking advantage of the similarity of the parallelograms and therewith the complementary functions of springs k_3 and k_4^*. For example, spring k_4^* can be omitted if spring k_3 is replaced by $k_5 = k_3 + \lambda^2 k_4^* = k_3 + k_4 = k$. If this is done, a simpler construction results, as links CP_4 and $P_4 Q_1^*$ can be omitted (figure 5.40a). A further simplification is reached if $Q_2 P_2$ is extended to $Q_2 P_5$ (in such a way that $Q_2 P_2 = P_2 P_5$) and spring k_5 is shifted to CP_5.

An application of this mechanism is the compensation of an ideal spring k_1^* acting on a coupler point Q_1^* of a four-bar linkage $C_2 P_3^* P_1^* C_1$, as shown in figure 5.40b. Link $C_2 P_3^*$ reduces the freedom of movement to one degree-of-freedom, but does not harm the balance. Thus, the influence of spring k_1^* can be fully eliminated by adding two links ($Q_2 P_5 P_3^*$ and $C_1 P_2$) and two springs (k_2 and k_5). Thus, any ideal spring acting on any coupler point of any four bar linkage can be perfectly compensated. As an example, figure 5.41 suggests the application in a hand prosthesis with a four-bar linkage finger mechanism. However, it should be remarked that the design in this specific application is impractical. Even if the cosmetic glove would be adequately represented by an ideal spring, the balancing quality will be disappointing due to excessive friction in all the joints, while the prosthesis will suffer from excessive weight.

Another general application of the variable spring butterfly is the static balancing of a spring-loaded two-link open-loop chain. In figure 5.42a, this

(a)   *(b)*   *(c)*
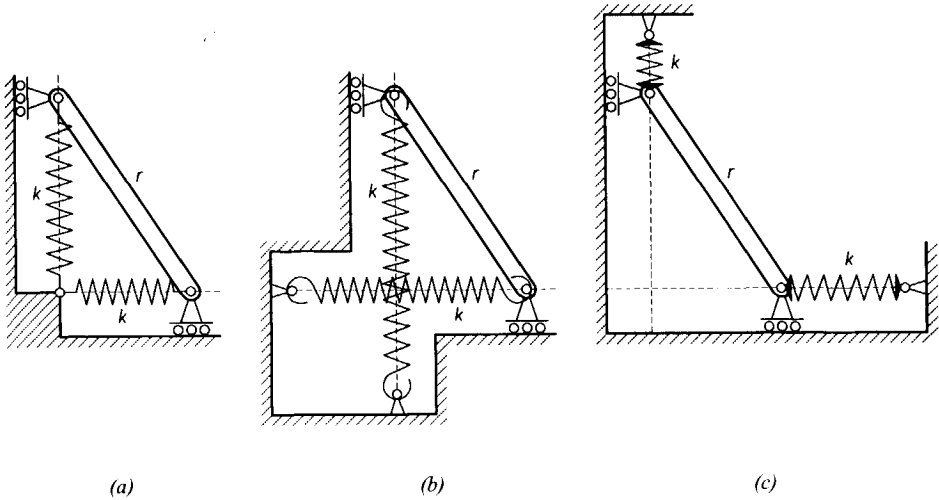
Figure 5.43 Elliptic trammel with various springs: (a) ideal springs, (b) normal extension springs, (c) compression springs.

problem is posed. Figures 5.42bcd suggest several solutions based on spring butterflies having an arbitrary angle of β, an angle $\beta = \pi$, and an angle of $\beta = 0$, respectively.

5.4   Special solutions with normal springs

[-] and the invention accordingly comprises a mechanism of the above kind, wherein the said points on a said movable member are constrained to move instantaneously in directions which are always mutually at right angles to one another.

George Carwardine, 1932

Since the free length problem does not occur when the springs are stretched along a stationary and straight line through their grounded attachment point, it is imaginable that perfectly balanced solutions exist in which the springs do not rotate. As a kinematic inversion can always be found to fix the stretching directions with respect to ground, the demand for the springs not to rotate can be relaxed. It is sufficient that the springs do not rotate with respect to one another. This section presents two configurations. Several other perfect balancers with normal springs have been reported. As these are of a more complex nature, unsuitable to this thesis' purposes, the reader is referred to literature [5.17]. Furthermore, wrapping cams have been used to match the characteristic of a normal spring to carrying a mass [5.18].

135
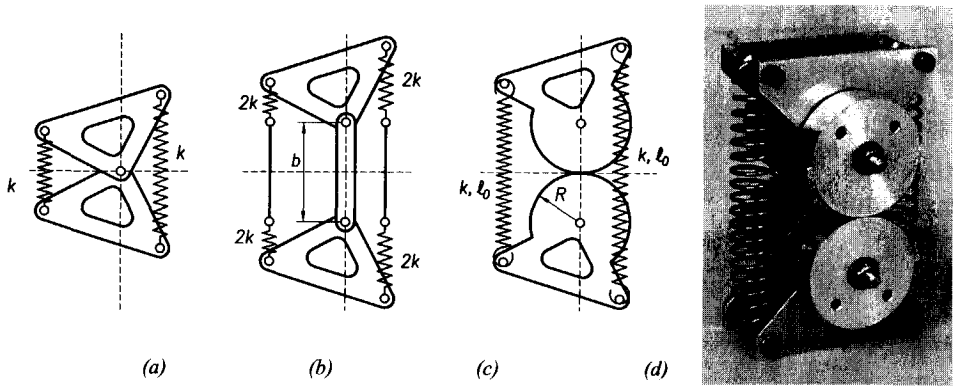
Figure 5.44   Conception of a perfect spring-to-spring balancer with normal springs and inherent low friction: (a) special version of the spring butterfly, (b) separated halves to include free length, (c) rolling version (see also Carwardine, 1932) [5.20], (d) photograph of prototype [5.21].

In principle, it is also possible to compensate for the positive free length of a normal spring by adding a spring with negative free length [5.19]. Springs with negative free length can be made according to the mechanism in figure 4.5a with altered dimensions. The normal spring and the negative free length spring together constitute an ideal spring, which can be statically balanced as any other ideal spring. This may be relevant for the perfect compensation of a pre-existing undesired non-ideal spring, but these solutions will not be considered in this section.

The elliptic trammel

The first configuration with non-rotating springs described is the elliptic trammel, which was presented in section 5.3 incorporating ideal springs [5.13]. Because the springs move along fixed straight lines through their fixed points, it is not necessary to use ideal springs. Two normal extension or even compression springs can be used, as long as they are equal and mounted such that they are just relaxed when their free ends pass through the origin. Figure 5.43 shows the elliptic trammel with ideal springs, normal extension springs, and with compression springs, respectively.

Figure-of-eight rolling link mechanism

A second configuration of a perfect spring balancer with normal springs and inherent low friction is presented next. This balancer is based on a special version of the spring butterfly: the one with $\alpha = \beta = \pi / 2$ and $r = a$. Since, in this case, the lengths of the lever arms all amount to a, two equal isosceles
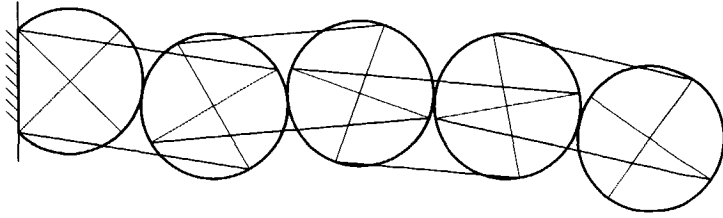
136

triangles result. The fact that in this arrangement the springs are always parallel is best observed if the horizontal line through the pivot is used as axis of symmetry (figure 5.44a). The midpoints of the springs move along the x-axis. With this observation, the upper and the lower part can be separated and offset by any vertical distance b. This is without consequences for the balancing quality if inactive elements of length b are inserted: one connecting the pivots and two between the spring halves (figure 5.44b). When the added link is fixed, clockwise rotation of one of the triangles by an angle φ has to induce a counterclockwise rotation of the other triangle by the same amount. Therefore, the triangles rotate by an angle of 2φ with respect to one another.

The fact that inactive elements of constant length can be inserted in series with the ideal springs offers the opportunity to use normal springs of which the free length ℓ_0 is equal to the offset distance b. The preferred embodiment of the design is the one where the triangles are fixed onto a set of two equal rollers having a radius R equal to half of the free length ℓ_0 of the springs, so that the constant distance between the centers of the rollers acts as the third inactive element (figure 5.44c). Thus, a perfect spring-to-spring balancer with low friction, normal springs, and essentially only two parts (excluding the flexible bands) has been conceived. Non-slipping rollers or gears guarantee correct motion, while the two members are being pressed together by the springs.

A prototype was made to evaluate its action (figure 5.44d), where flexible bands are wrapped between the rollers to prevent the rollers from slipping. Noteworthy is the fact that motion of the real system is restricted to $-45 < \varphi < 45$ degrees, because the helical tension springs used cannot effectively push when they are shorter than ℓ_0. Consequently, the mechanism would become unstable. Movement beyond the 45 degrees limits is restrained by axes through the centers of the rollers, preventing the springs from passing by. It was found that a slight unbalance was present, mainly due to minor
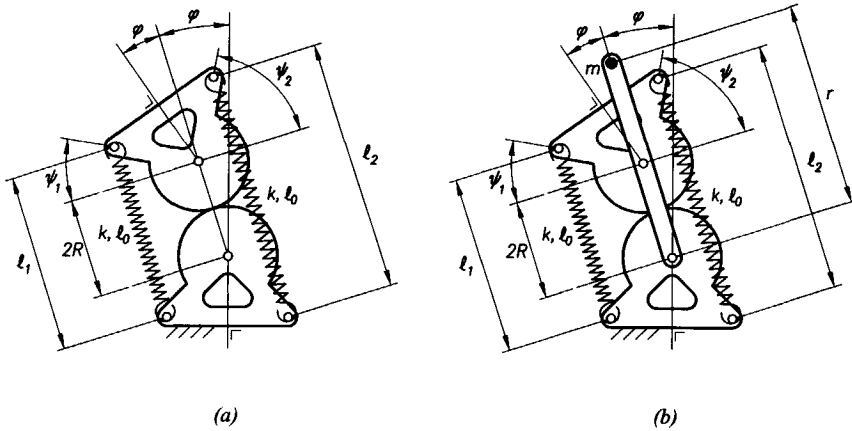
Figure 5.46   Perfect gravity equilibration with normal springs: (a) mechanism of figure 5.44c, now with normal springs, resulting in a residual moment which is a sine function of φ, (b) an additional link moving with φ and carrying a mass provides perfect static balance [5.22].

production errors, imperfections in the springs, and the travel of the spring attachment pins along the inside of the spring loops, thus moving the line of action of the spring force away from the centerline of the spring, and effectively decreasing the spring length.

Equal elements can be stacked on one another to form a balanced chain (figure 5.45). The springs provide a contact force, while the rollers can move in an energy-free way. Note that for simplicity, the figure presents a special case where the roller radius is equal to the spring arm lengths.

When the conditions for perfect balance are not satisfied, a residual moment will remain, which is a function of the angle φ, as will be demonstrated next. Using the symbols shown in figure 5.46a, where it is especially noted that the upper half of the mechanism is rotated by an angle of 2φ, the following geometrical relations can be identified:

$$\psi_1 = \tfrac{\pi}{4} - \varphi ; \quad \psi_2 = \tfrac{\pi}{4} + \varphi ; \quad \ell_1 = 2R + 2a\sin\psi_1 ; \quad \ell_2 = 2R + 2a\sin\psi_2 \qquad (5.73)$$

The total potential is written as:

$$V = \tfrac{1}{2}k\left(\ell_1 - \ell_0\right)^2 + \tfrac{1}{2}k\left(\ell_2 - \ell_0\right)^2 \qquad (5.74)$$

Substituting equations 5.73 into equation 5.74, using the geometric equality:

$$\sin\left(\tfrac{\pi}{4} - \varphi\right) + \sin\left(\tfrac{\pi}{4} + \varphi\right) = 2\sin\tfrac{\pi}{4}\cos\varphi = \sqrt{2}\cos\varphi \qquad (5.75)$$

and elaborating results in:

$$V = k\left(2a^2 + 4R^2 + \ell_0^2 - 8R\ell_0\right) + 2\sqrt{2}ka\left(2R - \ell_0\right)\cos\varphi \qquad (5.76)$$

138
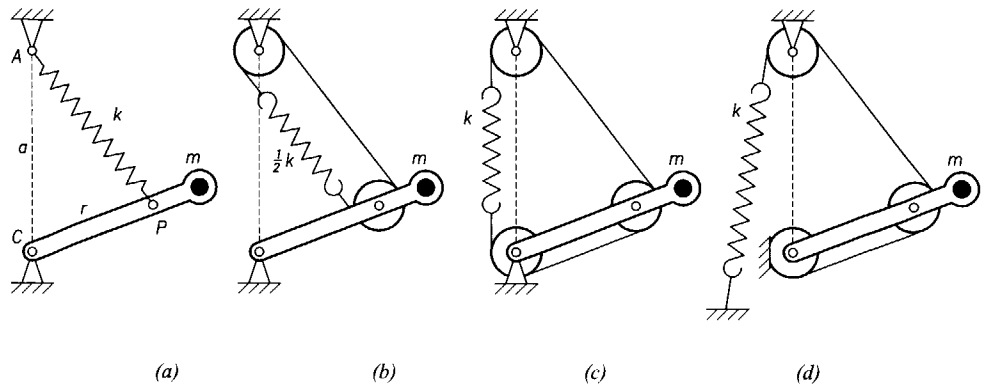
Figure 5.47 Pulleys-and-string arrangement providing perfect balance by a normal spring: (a) basic gravity equilibrator, (b) two-pulley system, (c) three-pulley system, (d) one pulley and the spring fixed to ground [5.23].

This expression is not constant, so the system is not statically balanced. The remnant moment is found as the derivative of the potential energy with respect to the rotation of the upper roller 2φ, according to:

$$M = V_{,2\varphi} = \tfrac{1}{2} V_{,\varphi} = \sqrt{2} ka\ell_0 \sin\varphi \qquad (5.77)$$

which is a function of φ, rather than of 2φ. Therefore, an opportunity to balance the system is to have a mass on the extension of the connecting line between the centers of the rollers, as is suggested in figure 5.46b [5.22]. The lower roller is fixed, the additional link moves as a function of φ, while the spring attachment points on the upper roller move as a function of 2φ. Considering the mass yields the following expression for the potential with respect to the center of the lower roller:

$$V = k\left(2a^2 + 4R^2 + \ell_0^2 - 8R\ell_0\right) + 2\sqrt{2} ka\left(2R - \ell_0\right)\cos\varphi + mgr\cos\varphi \qquad (5.78)$$

This expression becomes constant under the condition:

$$2\sqrt{2} ka\left(2R - \ell_0\right) + mgr = 0 \qquad (5.79)$$

This condition shows that the appropriate combination of mass, spring parameters, and geometry yield perfect static balance for infinite cases, as long as $\ell_0 > 2R$. In fact, any two equal springs (with $\ell_0 > 2R$) may be used since adjusting r can always restore perfect balance due to the linear nature of the expression. When $\ell_0 = 2R$, the only solution is the situation where $r = 0$.
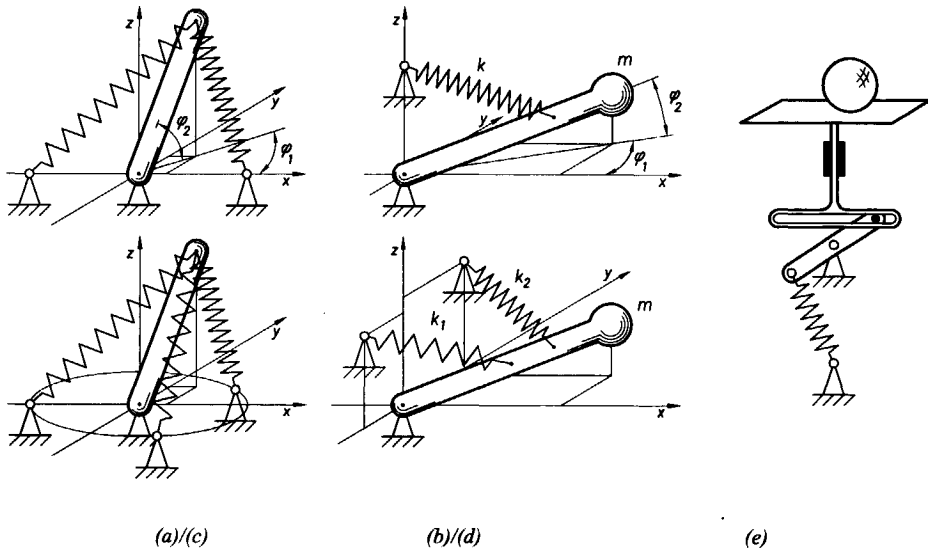
Figure 5.48   Spatial versions of several balancers: (a) basic spring force balancer, (b) basic gravity equilibrator, (c) spatial spring force balancer with three springs, (d) spatial equilibrator with two springs, (e) six-degree-of-freedom gravity equilibrator incorporating one ideal spring.

Pulleys and string arrangements

In figure 4.5a, a pulley-and-string arrangement was shown which provides approximate ideal-spring behavior. An error was introduced due to the wrapping of the string. This error can be avoided by using a pulley arrangement, which compensates the wrapping around one pulley by wrapping around another pulley [5.23]. Figure 5.47 shows a number of possible embodiments: an arrangement with two pulleys, an arrangement with three pulleys, and one with one pulley fixed to the frame and one end of the spring grounded at an almost arbitrary place on the frame.

The principle is based on the replacement of an ideal spring by a pulleys-and-string arrangement incorporating a normal spring, which is configured such that the string segments wrapped around the pulleys (of equal radius) add up to (a multiple of) one pulley circumference for any position of the link. Consequently, the amount of wrapped string is constant. The parts of the string running parallel to the arms a and r are constant as well, so the part of the string running parallel to AP is the only part which is variable. Therefore, the spring elongation is equal to the distance AP, which used to be the elongation

of the ideal spring, so perfect balance is obtained. Care must be taken to select the proper string length, which should be equal to:

$$L_s = a + r + 2\pi R - \ell_0 \qquad (5.80)$$

where L_s is the string length, R is the radius of the pulleys, and ℓ_0 is the non-zero free length of the normal spring. Depending on the desired range of motion, spring selection in the arrangement according to figure 5.47b can be difficult, while the arrangement according to figure 5.47d is most tolerant with respect to spring selection.

5.5   Spatial mechanisms

Robot designers, having a prevailing background in the design of machine-tool and material-handling equipment, often attempt to design robots with comparable rigidity or use worst-case loading conditions. To their chagrin, they have often realized that such animals could become grossly overweight and highly inept!

Hadi A. Akeel, In: Rivin, 1988, p ix

With the appropriate mindset, it is surprisingly easy to conceive spatial versions of balanced spring mechanisms. The spatial versions can often be regarded as chains of planar ones, so therefore the framework of chapter four, applied carefully, can be used. Since chapter three is strictly limited to the planar case, dynamically equivalent forces will not be considered in this section.

Starting with the basic spring force balancer, it is readily seen that it can be moved outside the plane of drawing without difficulty (figure 5.48a). Additionally, all gravity equilibrators obviously have a trivial degree of freedom: rotation about the vertical axis (figure 5.48b). Not only the movement of the mechanism may escape the two-dimensional plane, also the fixed points of the springs may be located spatially. As an example, figure 5.48c presents a symmetrical three-spring spatial spring force balancer, which can be derived from the two-spring version by using modification rule 5 (resolution of ideal springs). Naturally, the arrangement can be altered by employing the other modification rules from chapter two. An example of a spatial version of the single link equilibrator, comprising two ideal springs is given in figure 5.48d, but also more complicated degrees of freedom can be added [5.24].

This section will use the framework to derive a number of illustrative examples in the field of gravity compensation. Even though multiple degrees-of-freedom are involved, the vertical movement of the mass is the only degree-of-freedom that needs to be balanced. Therefore, one spring should be sufficient
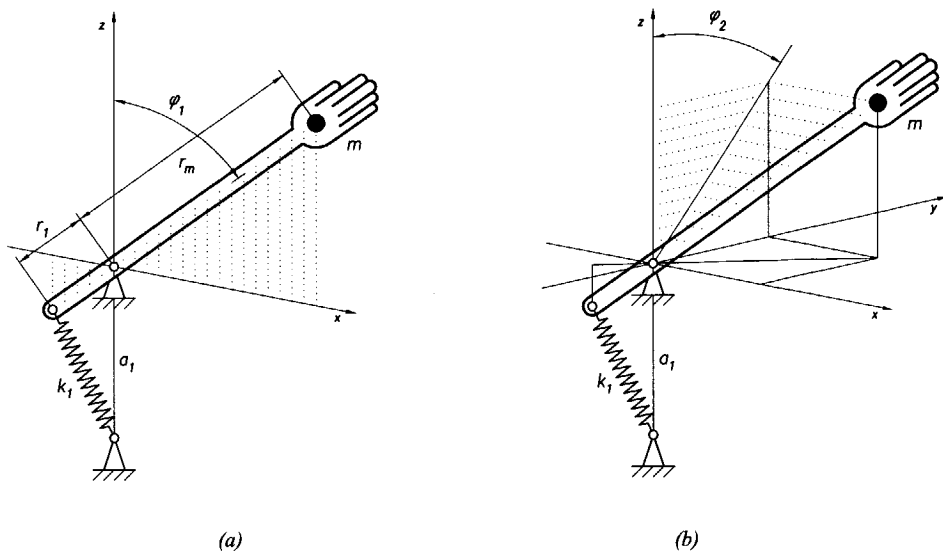
Figure 5.49 Conception of the anthropomobile arm: (a) basic spring force balancer of gravity equilibrator, (b) extended to three-dimensional operation (to be continued in figure 5.50).

for the static balancing of this mass. Figure 5.48e gives a solution for the static balancing of a mass with six degrees-of-freedom by a single spring. It consists of a ball that can slide and spin on a horizontal platform without friction. The platform can move up and down while suspended by a spring mechanism providing static balance for the vertical movement. Clearly, this is not a practical mechanism, but it raises the challenge of reducing the number of springs.

Anthropomobile arm

This section presents the design of an anthropomorphic robot arm with the same mobility as the human arm, including the out-of-plane motion of the forearm. Several gravity equilibrators exist capable of supporting a mass in the three-dimensional space. Section 5.2 presented a number of these planar mechanisms which can rotate about the vertical.

In spite of the fact that the supported mass can reach any position within the workspace, these designs are not satisfactory for some specific applications, such as an orthotic device for people with reduced muscular ability or paralysis of the arm [5.25]. In these cases, an anthropomorphic structure is desired which provides the same mobility as the human arm. This capacity will be called anthropomobility.
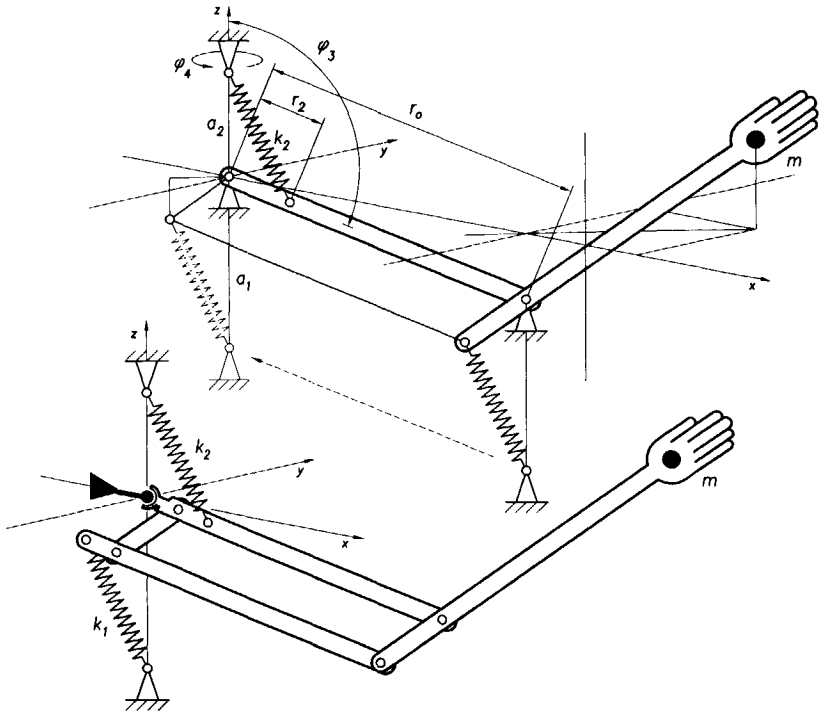
(a)/(b)

Figure 5.50 Conception of the anthropomobile arm (continued from figure 5.49): (a) addition of upper arm, shift of forearm compensation spring to the shoulder by means of parallelogram linkage, and inclusion of balancing spring for upper arm, (b) completed concept of anthropomobile balanced arm.

Conception

Figure 5.49 suggests the step-by-step conception of the anthropomobile arm, starting with the forearm. The elementary equilibrator shown in figure 5.49a functions as point of departure. This system can be seen as the basic gravity equilibrator of which the spring-lever element has been rotated by 180 degrees. The balancing condition is:

$$mgr_m = r_1 k_1 a_1 \tag{5.81}$$

When it is acknowledged that this configuration is valid for any vertical plane containing the pivot, an additional degree-of-freedom φ_2 can be obtained without the need to change parameters or add elements (figure 5.49b). The resulting structure is now regarded as the forearm, the pivot as the elbow joint.

As a next step, an upper arm is added (figure 5.50), connected between the elbow joint and a shoulder joint, fixed to the frame. At this stage, it is desired to release the elbow joint from the frame. In order to maintain static balance of the forearm, this needs to be done such that the configuration of spring k_1 becomes independent of the position of the upper arm. To this end, a construction similar to the one in the Anglepoise desk lamp is applied: a parallelogram of which the upper arm r_o and the hind part of the forearm r_i are two sides, and auxiliary links of length r_o and r_i respectively are the remaining sides. However, as opposed to the Anglepoise desk lamp, the parallelogram in this configuration can move spatially, *i.e.* rotate about the centerline of the upper arm (φ_2). Due to the parallelogram, spring k_1 can be moved to the new vertex and fixed to ground right under the shoulder joint while its potential energy function remains unaffected (figure 5.50a). Consequently, static balance of the forearm is assured, regardless of the position of the upper arm.

Finally, the upper arm is to be balanced. This becomes straightforward when it is recognized that the principle of superposition may be applied. When the free end of spring k_1 is fixed, two degrees of freedom remain: rotation about the vertical axis through the shoulder joint (φ_4), and elevation of the upper arm (φ_3). Clearly, only the latter needs attention. Since now the forearm can move parallel to itself only, the position of the mass along its centerline becomes arbitrary (this only affects the constant of the potential energy function). Locating the mass at the elbow joint reduces the equilibrator system to the basic gravity equilibrator. This is true for any angle φ_2. Therefore, the elementary configuration of spring k_2 as indicated in figure 5.50a suffices to fully equilibrate the upper arm, regardless of the position of the forearm. Consequently, the parameters of the upper arm equilibrator are to be selected such that the following condition is satisfied:

$$mgr_o = r_2 k_2 a_2 \tag{5.82}$$

where r_o is the length of the upper arm link.

Thus, an anthropomorphic gravity equilibrator is conceived having four degrees of freedom, and yet only two ideal springs for complete static balance. In addition to the three degrees of freedom found in the five-bar parallelogram linkage, the out-of-the-vertical-plane movement of the forearm is possible. The resulting *anthropomobile* arm is schematically depicted in figure 5.50b [5.26].

Link and spring masses will now be included without introducing errors in the equilibrator design [5.2]. This can be demonstrated by using the rules of the conception framework. This procedure is as follows. Figure 5.51a shows the linkage with all the masses. Using the principle of superposition, the degrees-

144

of-freedom are inspected sequentially. As noted previously, φ_4 needs no attention. The angles φ_1 and φ_2 can be regarded simultaneously while φ_3 remains fixed. This leads to the observation that the masses m, m_1, m_3, and m_4 trace similar trajectories through space. Consequently, their potential functions differ by a constant only, and the masses may be shifted as indicated without affecting the balancing parameters. For instance, when the masses are transferred to the forearm (figure 5.51b), it is readily seen that the parameters for spring k_1 are to be changed to include link mass according to:

$$mgr_m + m_1gr_{m1} - m_3gr_1 - m_4gr_{m41} = r_1k_1a_1 \tag{5.83}$$

Similarly, when φ_3 is considered while φ_1 and φ_2 are fixed, it is seen that the trajectory of m_1 is similar to the trajectory of mass m, while m_2, and m_3 can be transferred to the upper arm link (figure 5.51c). Therefore, the parameters of spring k_2 are to be changed according to:

$$mgr_o + m_1gr_o + m_2gr_{m2} + m_3gr_{m3} + m_4gr_{m42} = r_2k_2a_2 \tag{5.84}$$

In some applications, the link masses may be small as compared to the payload m, and equations 5.83 and 5.84 reduce to equations 5.81 and 5.82. However, in the application of a mobile arm support, mass m will be absent while masses m_1 and m_2, which now include the weight of the patients forearm and upper arm respectively, will be dominant. This consideration does not imply that the mechanism can directly be applied as an arm orthosis. Several difficult problems (notably the matter of the shoulder joint, and the fitting of the device to a person) need to be solved first [5.25].

Spring mass can easily be accounted for if one realizes that each end of the spring exerts, apart from the spring force, a constant vertical force of half the spring weight ($\frac{1}{2}m_sg$) on its support. Consequently, an additional term is introduced into the equations 5.83 and 5.84:

$$mgr_m + m_1gr_{m1} - m_3gr_1 - m_4gr_{m41} - \tfrac{1}{2}m_{s1}gr_1 = r_1k_1a_1 \tag{5.85}$$

$$mgr_o + m_1gr_o + m_2gr_{m2} + m_3gr_{m3} + m_4gr_{m42} + \tfrac{1}{2}m_{s2}gr_2 = r_2k_2a_2 \tag{5.86}$$

As can be seen from the equations, a practical convenience is that each of the masses has a linear influence on the balancing quality. Therefore, adjustable masses can be used to fine-tune the balancing mechanism.

Finally, it is noted that a floating version of the anthropomobile arm can be realized. In fact, nothing (in theory) restricts the mechanism shown in figure 5.27c from moving in other planes than the vertical only. However, in practice a number of challenging design questions need to be overcome, notably the connection of the moving spring ends to the spatial linkage.
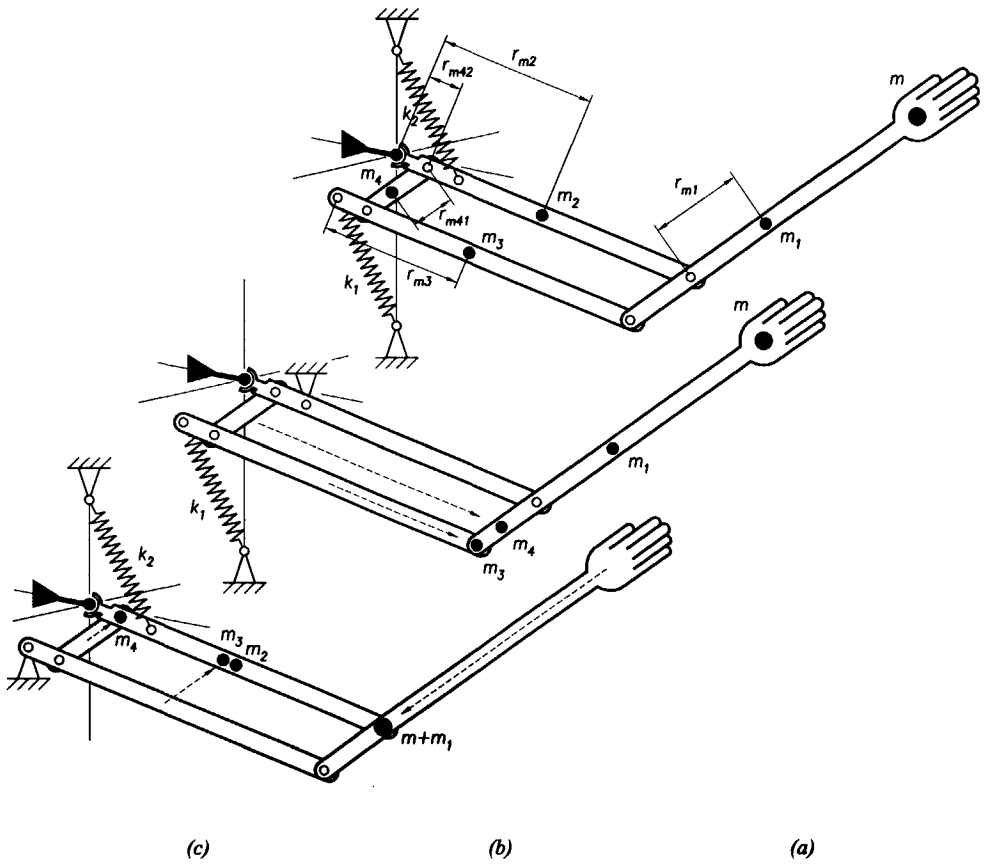
Figure 5.51 Inclusion of link mass in the anthropomobile arm design (from right to left): (a) link masses, (b) spring k_1 fixed, (c) spring k_2 fixed.

Design

To explore the functioning of the anthropomobile arm, a prototype was built [5.27]. Several practical problems needed to be overcome, such as the implementation of the ideal springs, and the attachment of the springs in a spatially moving structure. It was decided to use increased-preload ideal springs. The axial bearing to allow for rotation φ_2 at the distal end of the upper arm so that the spring attachment point of spring k_2 on the upper arm needs not to rotate, while the shoulder joint was furnished as a Hooke's joint. Due to the availability of only a limited number of sample springs, the practical embodiment of spring k_1 consists of two springs in parallel. Figure 5.52a shows a side view of the prototype. Figure 5.52b shows a close-up of the compensation springs in another position of the arm. Interesting details are the

146
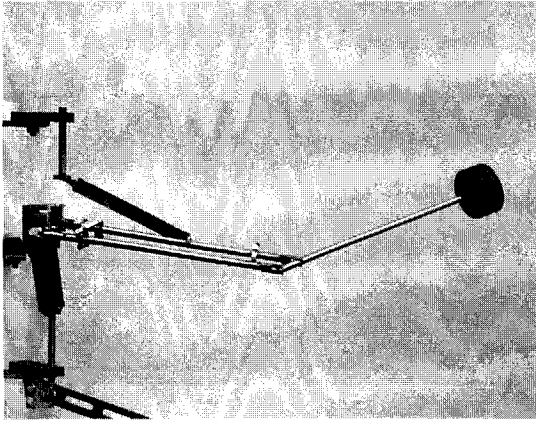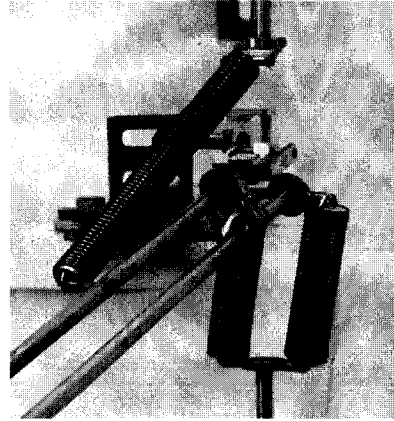
(a)   *(b)*

Figure 5.52 Photographs of the anthropomobile arm: (a) side view, (b) frontal view, close-up [5.27].

attachment of spring k_2 next to the upper arm (application of rotation modification rule) allowing a sufficiently long effective length of the spring, and the shorter supplementary link which is shifted aside to facilitate the attachment of spring k_1.

The prototype performs quite satisfactorily. The links are made of stainless steel thin-walled tube. Overall length is about 70cm, while a mass of 0.5kg is fixed to its end. From the initial position in which the upper arm is horizontal and the forearm points upwards, the allowable rotation according to each degree of freedom is at least 45° to each side. Due to several imperfections of the prototype, such as slightly irregularly coiled springs, friction, and deflection of the parallelogram, a maximum balancing error of 5% was found. However, in great parts of the workspace, the balancing inaccuracy is negligible and the load floats nicely.

General suspension unit

Many gravity equilibrators require that the load be suspended in its center of gravity, which is not always feasible. This section presents the extension of the anthropomobile equilibrator into an equilibrator configuration for six degrees of freedom, to be used in situations where the center of gravity of a body is not accessible, such as in a flight simulator or in certain medical diagnostic instruments. In case only the suspension of a point-load is concerned and the orientation of the center of gravity is therefore not relevant, one could say the

147
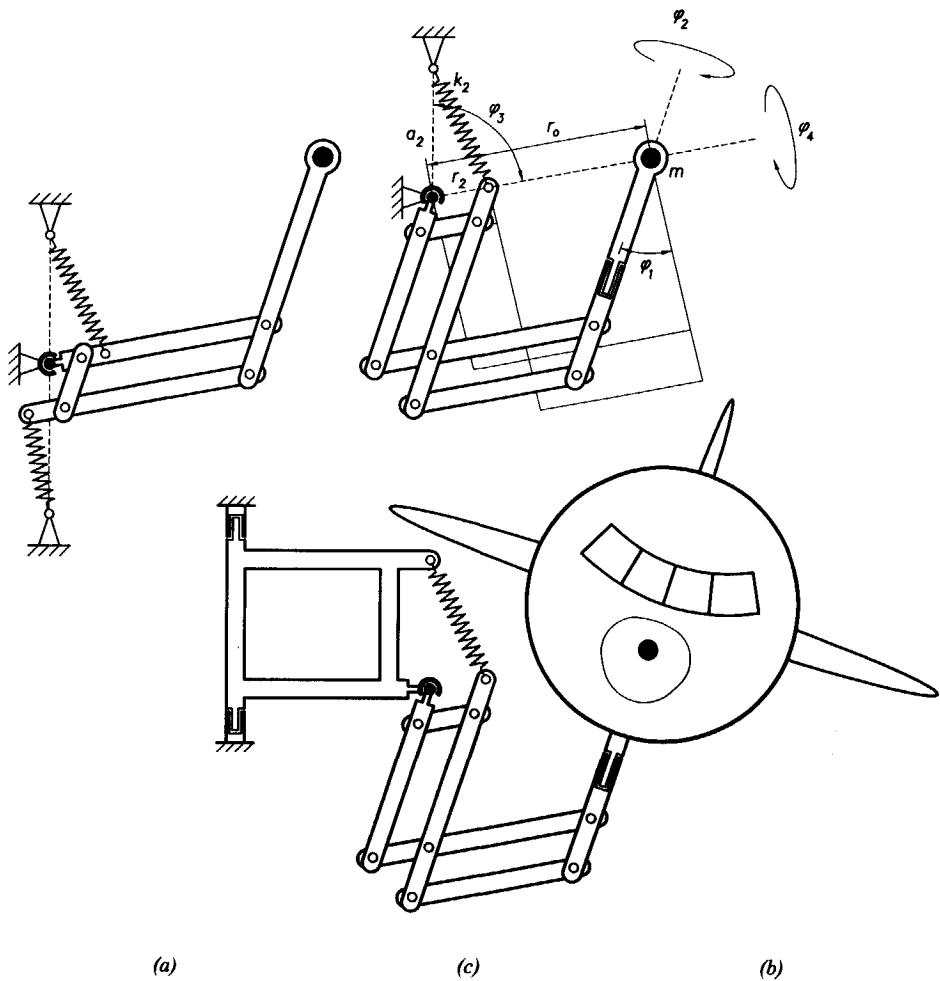
Figure 5.53   Conception of the general suspension unit: (a) the anthropomobile balanced arm as a starting point, (b) addition of a parallelogram segment to obtain three independent rotations, (c) addition of a rectangular segment to obtain three independent translations.

anthropomobile equilibrator has one degree of freedom too many. This changes when an object is to be supported of which the center of gravity is not accessible. Then the desire may arise to extend the mobility to six degrees of freedom.

A profitable way to add mobility to the balanced arm is suggested in figure 5.53b. The parallelogram configuration is extended by adding another segment, such that the resulting configuration constitutes a parallelogram of which two adjacent sides are formed by the forearm and the upper arm of the

148
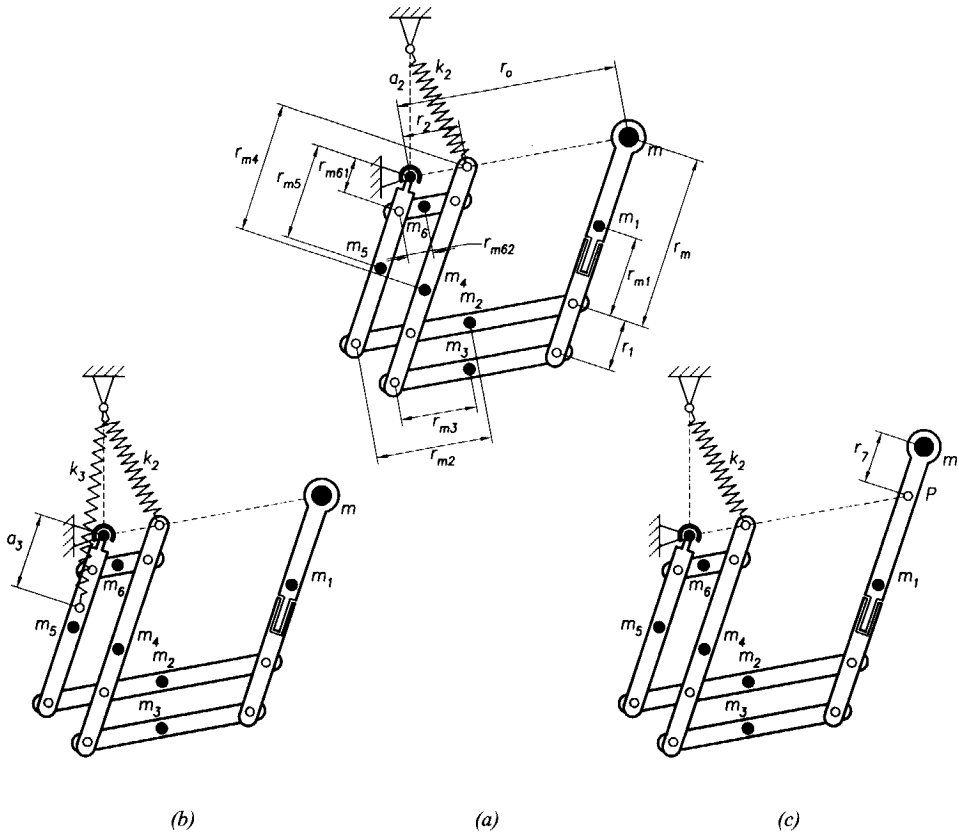
Figure 5.54 Inclusion of link mass in the general suspension unit design: (a) link masses, (b) additional spring, (c) rearrangement of payload.

original structure. As the ball joint is moved to the new vertex, the spatial mobility of the linkage is maintained. However, the distance between the ball joint and the center of gravity has become constant. Consequently, the movement of the supported mass is restrained to the surface of a sphere, and therefore the equilibrator system can be simplified to a single ideal spring as shown in figure 5.53b. This spring is to be fixed right above the ball joint and connected to the auxiliary link of the new parallelogram segment at the intersection of this link with the imaginary line between the ball joint and the mass. Thus, the movement of the mass over the sphere surface is equilibrated.

There is additional mobility of the mechanism according to the (instantaneous) rotations φ_1 and φ_4 as indicated in figure 5.53b. These movements do not influence the position of the mass but do change its orientation, which becomes interesting if the mass is a body rather than a point.

If an additional bearing is added allowing rotation about the centerline of the final link, indicated by φ_2 in figure 5.53b, three rotations of the supported body about independent axes through its center of gravity are available. As compared to the anthropomobile arm in figure 5.53a, the balancing conditions for the resulting configuration reduce to:

$$mgr_o = r_2 k_2 a_2 \tag{5.87}$$

As a final step, full mobility of the supported body is accomplished when the mechanism of figure 5.53b is mounted on a rectangle that is rotatable about a vertical axis. The plane of the rectangle is to make a considerable angle with the plane containing the rest of the structure to allow for sufficient x-, y-, and z-translation. Figure 5.53c gives a schematic representation of the result. However, for reasons of convenience, the rectangle is drawn in the same plane as the rest of the mechanism. This all results in a configuration with a single ideal spring, which in any position provides three independent translations and three independent rotations for the object supported. The object can therefore be connected to the equilibrator at any desired point, provided that the ball joint, the free end of the spring and the center of gravity of the supported body are collinear, and that the final link points at the center of gravity of the supported body.

When the link masses are not negligible, equilibrators for the rotations φ_1 and φ_4 are to be added. However, because these equilibrators support the same link system, similar to the situation in the anthropomobile arm, these equilibrators can be combined, so that only one additional spring is required. A suitable configuration for this spring is between the link connected to the ball joint and a point right above the ball joint (figure 5.54a). By reducing the link masses for φ_1 and φ_4 onto the link connected to the ball joint, the balancing conditions for this system are found:

$$mgr_o + m_1 gr_o + m_2 gr_{m2} + m_3 g(r_2 + r_{m3}) + m_4 gr_2 + m_6 gr_{m62} = r_2 k_2 a_2 \tag{5.88}$$

$$m_1 g(r_m - r_{m1}) + m_2 gr_m + m_3 g(r_m + r_1) + m_4 gr_{m4} + m_5 gr_{m5} + m_6 gr_{m61} = r_3 k_3 a_2 \tag{5.89}$$

Alternatively, the center of gravity of the load can be placed a little bit further up the final link (which therefore needs to be extended, see figure 5.54b), such that the combined center of gravity of the load and the linkage is located at point P. The balancing condition for this system is:

$$m_1 g(r_m - r_{m1}) + m_2 gr_m + m_3 g(r_m + r_1) + m_4 gr_{m4} + m_5 gr_{m5} + m_6 gr_{m61} = mgr_7 \tag{5.90}$$

(a)/(c)   *(b)*
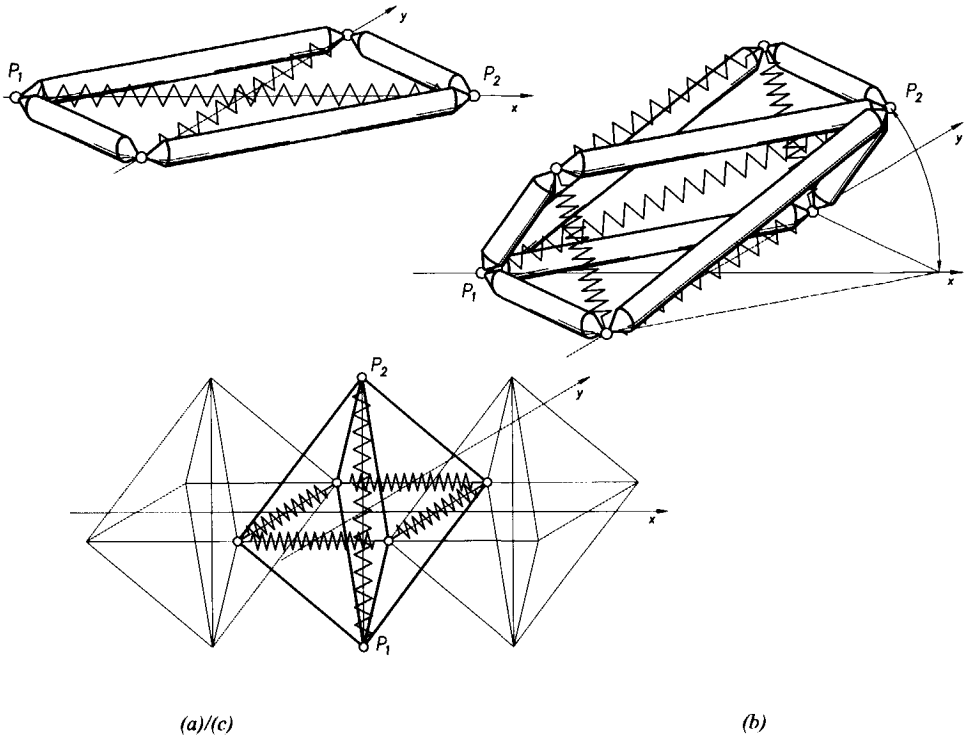
Figure 5.55 Conception of the Spring Diamond: (a) balanced rhombus, (b) duplicated and unfolded, (c) lattice.

The latter configuration is favorable in that no additional spring is required, but may in some applications be undesirable due to the more complex kinematics.

The spring diamond

An interesting structural element arises when a balanced rhombus is duplicated and unfolded into the third dimension as follows. Suppose a planar balanced rhombus with springs of stiffness k (as in figure 4.14a) is duplicated such that one is on top of the other and that they are jointed in two corresponding opposite vertices P_1 and P_2 (figure 5.55a). With a total of four springs of stiffness $\frac{1}{2}k$, balance is still complete in their initial plane of movement, but lifting one of the vertices, for instance P_2, results in a collapse because the moment about the y-axis by the spring between P_1 and P_2 can not be resisted.

This collapse is prevented from occurring if a spatial structure is put up of which the orthogonal projections are rhombi. To this end, the upper of the two rhombi is bent in the direction opposite to the lower one, as suggested in figure 5.55b. If the corresponding vertices that are now separated are connected

by a couple of additional ideal springs of stiffness $\frac{1}{2}k$, a symmetrical construction results, which is in perfect balance. Regarding P_1P_2 as axis of symmetry may enhance transparency. Effectively, a spring of stiffness k is present between vertices P_1 and P_2, whereas four springs of stiffness $\frac{1}{2}k$ are present between the other vertices.

Depending on the preferred perspective, this structure may be regarded as an unfolded double rhombus, a quadruple basic spring force balancer, or an octuple slipping ladder. The vertices P_1 and P_2 may be moved towards and from each other, and the two-link bridging structures may be rotated about the line connecting the joints P_1 and P_2. The structure is force-closed, so no stationary frame is needed. Interesting is that the forces in the links are constant. A lattice of these elements can be made (figure 5.55c). Since the elements share sides, all springs will be of equal stiffness if this lattice is extended indefinitely in x- and y-directions. If the spring between the vertices P_1 and P_2 of each element is offset, this network can obtain a distributed load carrying capacity with zero stiffness, or slightly deviant if desired.

5.6   Summary

This chapter presented the conception of a number of mechanisms with perfect static balance in theory. Using the framework presented in the previous chapter, energy-free systems of different kinds were conceived, representing useful working principles or interesting phenomena. For instance, the fact that a spatially moving mass can be equilibrated supports the statement that all spatial linkages (regarded as a related set of centers of mass) can be perfectly equilibrated.

In the course of the chapter, several conceptional techniques came across, some which will be briefly reviewed next: (1) It was found useful to build parallelograms around serial structures in order to be able to develop independent balancers for the sequential links. By using skew resolution of forces, it was shown that in multiple degree-of-freedom cases the parallelogram transmits the variable moment due to the more distal segments, while the constant shear force is directed to the springs. (2) Additional degrees-of-freedom were introduced by releasing structures from being fixed to ground. (3) Springs were multiplied to add springs or to replace spring-lever elements by mass-lever elements. (4) Links were replaced by arrangements of rollers to reduce friction and the number of parts. In performing these techniques, the modification rules of chapter four proved to be most useful. Remarkable is the

fact that similar designs, such as the two-degree-of-freedom gravity balancers (shown in figures 5.4, 5.23, and 5.25, respectively), can not be converted into each other.

However, especially in multi-degree-of-freedom cases, it was shown that the modification rules need to be applied with care. For instance, when the diagonal of a parallelogram linkage was regarded as an imaginary link (figures 5.23 and 5.38), it was found that using it as the arm for a spring force balancer resulted in a collapse of the linkage (as opposed to using such an imaginary link for a mass-to-mass balancer, as for instance in figure 2.3b). Another example is present in the system of figure 5.25, where it may be tempting to compose the springs into one spring, but this is not allowed as was explained at the end of section 4.5. This all demonstrates that the approach proposed in this thesis is not a recipe but requires the creative combination of the modification rules and other knowledge, especially kinematics (rolling link mechanisms, pantograph linkages). Nevertheless, when applied judiciously, the framework supports the conceptional design considerably.

Implicitly, a potential energy perspective was often assumed, yet a consideration of the forces often proved advantageous to arrive at a profitable practical embodiment. This was especially true in the Floating Suspension, where force directed design led to the elimination of the pivot, and to a general formulation of the behavior. In a way, this design has a central place in this thesis. It would not have been realized if only one perspective would have been adopted: at least the potential energy and the force directed design approach were essential in its conception. The Floating Suspension owes its central place also to the fact that several of the other balanced systems presented in this chapter can be derived from the generalized equations. For instance, setting the stiffness of one of the (ideal) springs at infinite results in a fixed pivot due to the zero free length. Selecting one infinitely stiff spring, two other ideal springs and zero mass, and demanding static balance, yields the basic spring force balancer (figure 3.6); one infinitely stiff spring, one other spring and one mass yields the basic gravity equilibrator (figure 5.1b); one infinitely stiff spring, two other ideal springs and a non-zero mass yields the example of combined mass and spring compensation (figure 4.24); four springs of finite stiffness and zero mass results in the floating version of the basic spring force balancer (figure 5.32b); while also rule 6 can be described (figure 4.20). Clearly, the description can be further generalized in order to accommodate for more masses, but this, together with the verification of the thoughts above, is left to the reader.

The investigation of the Floating Suspension revealed some other interesting features, for instance the fact that translation of a body with n ideal springs acting on it results in a translational stiffness of Σk_i, regardless of the configuration of the springs (figure 5.19a), and furthermore that rotation of such a body results in a sinusoidal moment. The Floating Suspension also provides confirmation of the observation in section 3.3 that two central linear forces are to be combined into a constant force for dynamic equivalence. Furthermore, the application of the geometric construction for the DEP of constant forces to the spring forces of the Floating Suspension results in a constant error, as was expected (figure 5.22).

In addition to the variety of ideal spring solutions, a class of energy-free mechanisms was found with perfect balance, yet incorporating normal (non-zero-free-length) springs. Advantages are that off-the-shelf springs can be used so that the special constructions (and the weight and friction associated with these) or special coiling techniques required to obtain zero-free-length behavior (or other special mechanisms such as wrapping cams), can be avoided. However, as opposed to the perfect equilibrators with ideal springs, the solutions in this class cannot turn a full 360 degrees.

The prototypes, which were made of some of the examples, demonstrated the proper functioning as well as the practical problems associated with the actual design. The attachment points of the springs, especially but not only in spatial linkages is a profound challenge, while spring selection is remarkably cumbersome, both in the case of springs with increased preload (difficult to manufacture accurately) and in the case of a pulley and string arrangement (sufficient strain). This is often overlooked, perhaps due to the easy calculation of the spring stiffness from the balancing conditions.

6   Approximate balance

in which balanced mechanisms with normal springs are developed, where optimization techniques are demonstrated using conceptional designs with ideal springs as initial estimates, and in which two practical designs are presented.

6.1   Introduction

Da in vielen Fällen noch die üblichen Federn am billigsten herzustellen sind, lohnt es sich, ihren Einbau in ein einfaches, ungleichformig übersetzendes Getriebe so vorzunehmen, daß die Federkräfte in gewünschter Weise umgewandelt werden.

As normal springs usually are cheapest to produce, it is worthwhile to consider their use in a simple non-linear linkage converting the spring forces as desired.

Kurt Hain, 1956

In the previous chapters, a framework for the conception of perfectly balanced spring mechanisms has been put up. Extensive use has been made of ideal springs (zero free length), although a number of arrangements were found where perfect balance was achieved using normal springs (non-zero free length). However, when a perfect solution with normal springs is not found and when the special spring constructions to obtain zero-free-length behavior (figure 4.5) are not feasible, for instance when cost, space or friction are critical, the design of approximate solutions with off-the-shelf springs may be considered. This chapter investigates methods for the design of balanced spring mechanisms using normal springs [6.1].

As was described in section 4.2, non-zero free length implies that the stiffness function does not intersect the force-length diagram in the origin. This results in increased complexity of the equations, since $F_i = k_i(l_i - \ell_{0i})$ instead of $F_i = k_i l_i$. Especially the roots emerging from the derivation of the potential equations are cumbersome. Graphically, the energy fields were found to be correspondingly complicated (figure 4.4cd). Figure 6.1 shows that the intersection of a normal spring's energy field and a cylinder with parallel lines of symmetry no longer is an ellipse. Indeed it is not a planar curve, and a non-sinusoidal potential energy function of the rotating link results.

This chapter will merge the conceptional design approach presented in the preceding chapters with optimization techniques. Some of the optimization techniques are adopted from literature [6.1], others are modifications of existing techniques, and some are specially developed. It will be shown that the ideal-

(a)   *(b)*
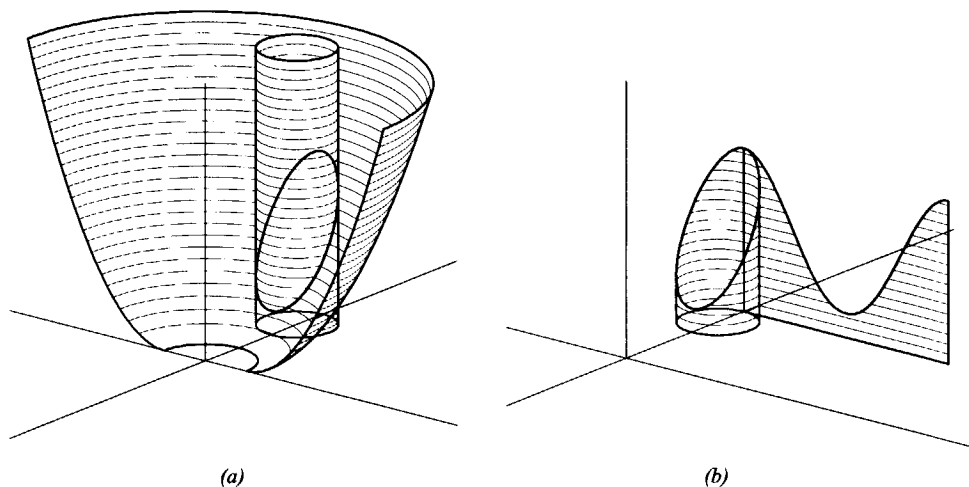
Figure 6.1   Graphical representation of energy function of a rotatable link and a normal spring: (a) the intersection of a cylinder and the normal spring energy field no longer is an ellipse, (b) the corresponding energy function of the rotatable link deviates from a sine, compare figure 4.10 [4.3].

spring designs according to the previous chapters can function as initial estimates needed for the optimization techniques. In section 6.2, several procedures based on graphical representations will be given. Section 6.3 provides an example pursuing the same goal employing a vector-based optimization technique. Subsequently, two examples of mechanisms with approximate static balance are presented in section 6.4.

6.2   Graphically inspired optimization

Mechanics is inherently a subject which depends on geometric and physical perception, and we should increase our efforts to develop this ability.

J.L. Meriam, L.G. Kraige, 1987, p. x

This section will explore optimization methods with a graphical background of different kinds. The first one (contour tracing) will use contour lines of the combined energy field of two springs, whereas the second one (field fitting) is based on shifting energy fields over the ground plane until a good fit with a desired potential energy curve is found. The approach for a third one (paraboloid placement) is illustrated using ideal springs, even though it also

(a)/(c)   (b)/(d)
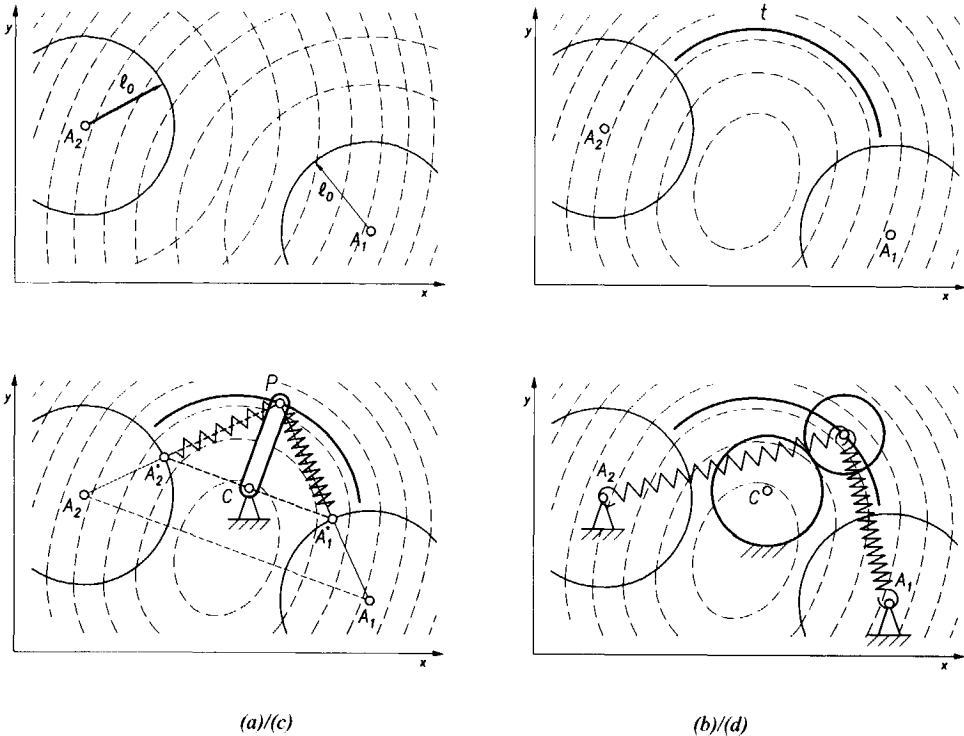
Figure 6.2   Illustration of the procedure of contour tracing: (a) the contour lines of the energy fields of two normal springs, (b) contour lines of the resultant energy field, (c) selected target path and initial estimate based on basic spring force balancer, (d) replacement of the ideal springs by normal springs, and the link by two rollers.

works for normal springs, to demonstrate the remarkable geometric theorem that the apex of the paraboloids containing two spatial points traces a circle. The final one presented in this section (overlay method) is based on a mechanism synthesis method using overlay sheets.

Contour tracing

The first optimization method proposed is based on the principle of following a contour line of the combined potential field of two or more potential energy storage devices, connected to the same point of the adjustment mechanism. This approach was also used as one way to conceive the basic spring force balancer (figure 4.9). The same line of thought is feasible when using normal springs. Leading a point, at which the free ends of two (or more) normal springs are attached, along a contour line of the resultant energy field of these springs results in a balanced spring mechanism. The only difference is that the energy
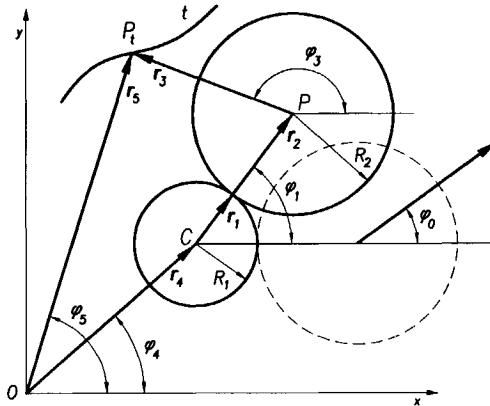
Figure 6.3   Definition of the vectors and the initial position of the two-roller layout used in the example. The springs need to be attached to the same point on the moving roller but this point is not confined to be the center of the moving roller.

fields are no longer paraboloids, hence the contour lines are no longer circles. Instead, they assume a non-circular shape, and a simple link (as in the basic spring force balancer) is not sufficient to provide adequate balance. In this strategy, called contour tracing, the design of balanced spring mechanisms has been reduced to the classical path generation problem [1.7]. One of the challenges remains finding simple solutions with low friction.

As an example, this section will describe the design of a spring mechanism consisting of two rollers and two equal normal springs. It is noted, however, that the procedure is not at all limited to equal springs. Indeed, any potential field qualifies for this procedure. The procedure followed is illustrated in figure 6.2. Figure 6.2a shows a number of contour lines of the given springs. The continuous circles indicate the free length of the springs. Figure 6.2b shows contour lines of the combined potential. Within each ℓ_0-circle, the potential of the corresponding spring is zero, so the contours inside each circle are sections of the circular contour lines of the opposite spring, as in figure 6.2a. Outside the ℓ_0-circles, the contour lines have smooth non-circular shapes. Far away from the fixed spring attachment points, unfortunately beyond the reach of the springs, the contour lines are almost circular. A section of one of the contour lines is selected as the target trajectory t for the spring mechanism. This trajectory is to be traced by the point of the mechanism where the springs attach.

Since the optimization procedure for force balancing problems has thus been reduced to a path generation problem, existing synthesis methods for the solution of this kind of problem can be applied, such as loop-closure [6.2].

158

Figure 6.3 illustrates the procedure using loop-closure for the example of two rollers. The demand for continuity is posed in vector form. A point of the moving roller is desired to follow the selected part of the contour line:

$$r_4 + r_1 + r_2 + r_3 = r_5 \qquad (6.1)$$

Using the definition of the initial position of the moving roller according to figure 6.3, and setting the orthogonal components in a Cartesian coordinate system to zero gives the following set of two continuity equations for the ith position (or *precision point*):

$$0 = r_4 \cos\varphi_4 + (r_1 + r_2)\cos\varphi_{1,i} + r_3 \cos\left(\varphi_0 + \left(1 + \frac{r_1}{r_2}\right)\varphi_{1,i}\right) - r_{5,i}\cos\varphi_{5,i} \qquad (4.2)$$

$$0 = r_4 \sin\varphi_4 + (r_1 + r_2)\sin\varphi_{1,i} + r_3 \sin\left(\varphi_0 + \left(1 + \frac{r_1}{r_2}\right)\varphi_{1,i}\right) - r_{5,i}\sin\varphi_{5,i} \qquad (4.3)$$

The variables governing the system are listed as C_x, C_y, r_1, r_2, r_3, φ_0, $\varphi_{1,i}$, $r_{5,i}$, and $\varphi_{5,i}$, where it should be noted that C_x, C_y, r_1, r_2, r_3, r_5 and φ_0 are unknown but remain fixed in number and do not vary with the number of precision points, whereas $\varphi_{1,i}$, $r_{5,i}$, and $\varphi_{5,i}$ are unknown variables with a different value for each precision point. As a distinguishing mark, the latter's index is expanded with the symbol i, where $1 \leq i \leq n$, and where n is the number of precision points in the target trajectory t.

The selection of free choices determines the number of precision points required to achieve a solution. Table 6.1 illustrates the relation between the number of precision points, equations, unknowns and free choices. In the example, the whole set of C_x, C_y, r_1, r_2, r_3, φ_0, and $\varphi_{1,1}$ through $\varphi_{1,6}$ is selected as unknowns, so no free choices were made. In total, there are $6 + n$

Number of Precision points	Number of scalar equations	Number of scalar unknowns (plus their symbols)		Number of free choices (plus suggested parameters)	
1	2	7	*(A_x, A_y, r_1, r_2, r_3, φ_0, φ_{1,1})*	5	*(A_x, r_1, r_2, r_3, φ_0)*
2	4	8	*(above + φ_{1,2})*	4	*(A_x, r_1, r_2, φ_0)*
3	6	9	*(above + φ_{1,3})*	3	*(A_x, r_1, φ_0)*
4	8	10	*(above + φ_{1,4})*	2	*(A_x, r_1)*
5	10	11	*(above + φ_{1,5})*	1	*(A_x)*
6	12	12	*(above + φ_{1,6})*	0	

Table 6.1   The relation between the number of precision points, equations, unknowns and free choices for the configuration of two rollers and given springs and spring attachment points.
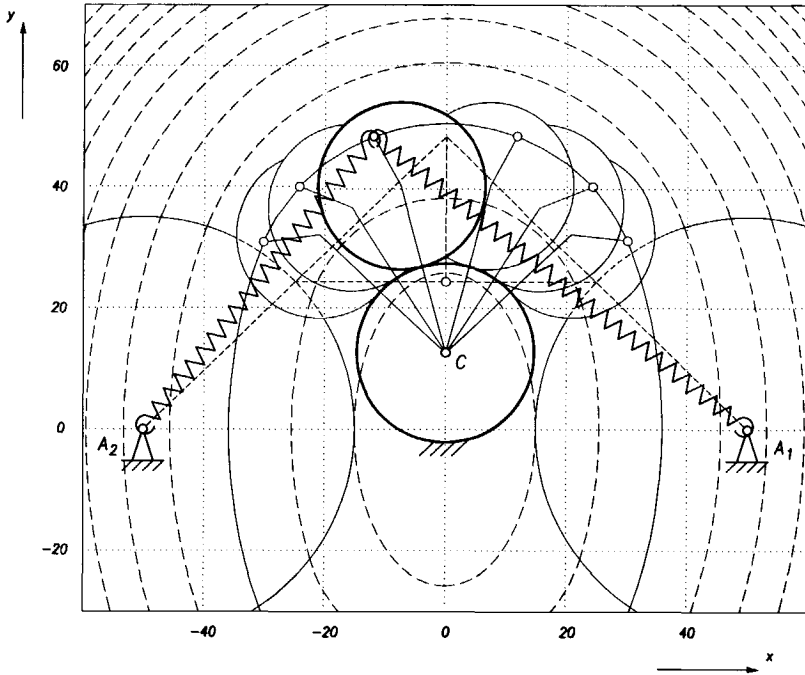
Figure 6.4   Optimization result, drawn in the six precision positions, while the error is calculated over the whole trajectory. This particular solution has a fixed roller radius of 16.8mm, moving roller radius of 14.1mm, and an arm length r_3=10.6mm. The spring parameters are k=0.85, ℓ_0=35mm, and K=1200Nmm. The initial estimate is shown in dotted lines. The error in this particular case amounts to 0.33%.

unknowns and $2n$ equations. Solving $6 + n = 2n$ yields six precision points for this case. The precision points are distributed along the target trajectory using Chebychev spacing [6.3]. The resulting set of twelve nonlinear equations is solved using the Gauss-Newton optimization routine in the MATLAB package, while the required initial estimate is based on a basic spring force balancer.

Figure 6.2c shows how the initial estimate for the optimization is selected. A basic spring force balancer is placed in one position, in this case the symmetric central position, while the fixed spring attachment points are placed at the ℓ_0-circles, so that at least for small rotations of the link, the mechanism is statically balanced also when the ideal springs PA_1^* and PA_2^* are replaced by normal springs PA_1 and PA_2 having free length ℓ_0.

As the number of precision points increases, finding solutions depends more on the accuracy of the initial estimates. With six precision points, the initial estimate based on the basic spring force balancer still suffices. Each choice of

160
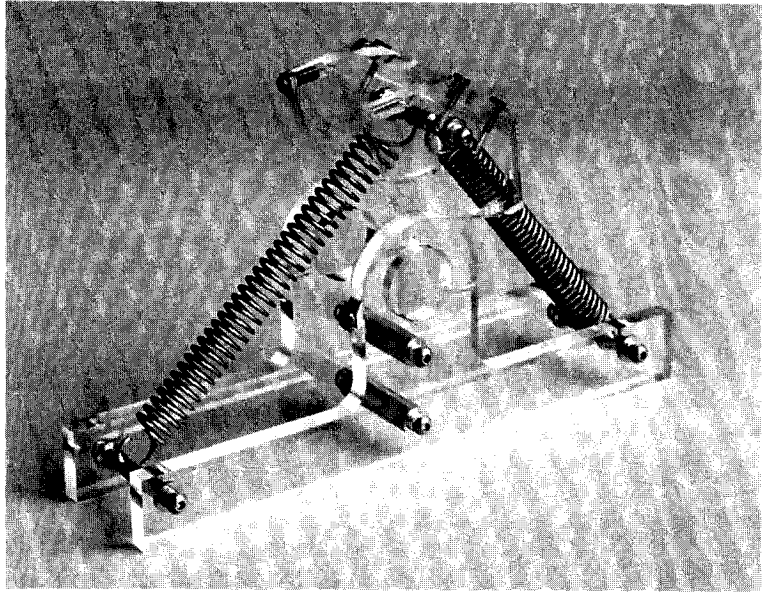
Figure 6.5   Demonstration model based on the contour tracing procedure [6.5].

the target trajectory yields a different solution. Figure 6.4 shows one of the solutions. The balance error was calculated as the maximum deviation from the constant potential K of the target trajectory, divided by K.

Sometimes internally rolling arrangements are found. This is undesirable since then the resultant spring force will separate the rollers rather than press them together. Fortunately, a useful solution exists in many cases because identical cycloids can be generated by two different rolling mechanisms [6.4].

Based on one of the solutions with an error of 0.07%, a working model was manufactured (figure 6.5). Contrary to the solution in figure 6.4, the spring attachment point on the moving roller is in between the centers of the rollers (figure 6.5). The model consists of a frame part incorporating the fixed roller, and a moving part being a section of the moving roller. The springs operate in parallel planes. Consequently, a moment is introduced which tends to rotate the moving part relative to the frame. Furthermore, the contact force between the rollers is not normal to the contact surface. This is readily seen, as the moving part is in fact a two-force system, and the spring attachment point is not in the center of the moving roller (as opposed to the systems in figures 5.3c and 5.37b). Due to the moment and the non-normal contact force, the moving roller needs to be prevented from slipping. Flexible bands were wrapped
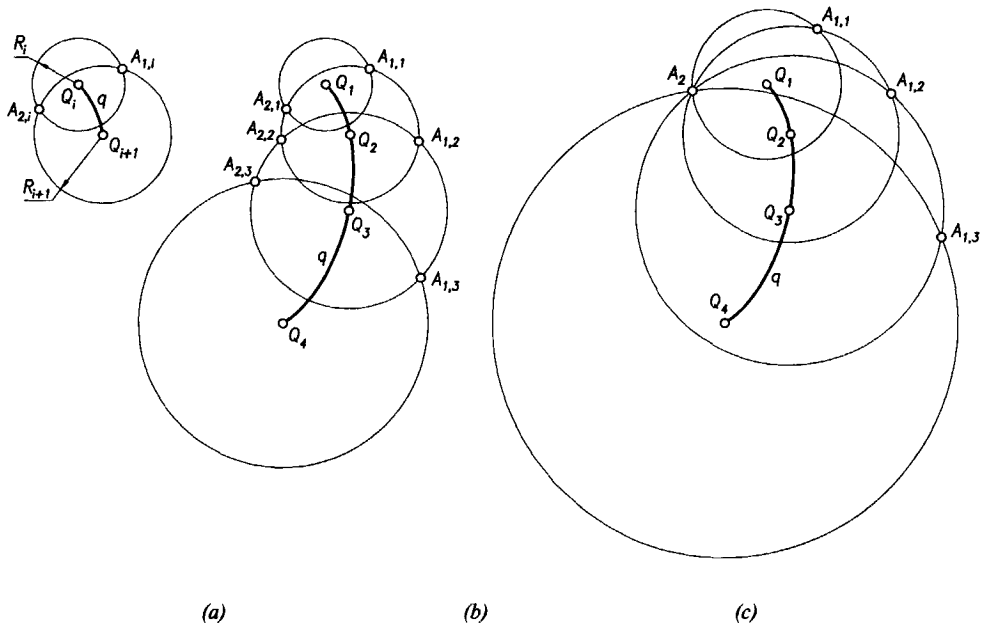
Figure 6.6   Energy-distance circles: (a) the potential energy demand of each point Q_i corresponds with a spring elongation R_i so two possible spring attachment points A_i result, (b) situation for more points, (c) optimized situation.

between the rollers. Only two bands were required (recognizable by the screws: the one on the front plane from left below to right above, the other in the hind plane from left above to right below), because the moment pulls the rollers into the bands. The mechanism performs well, it actually has a range of equilibrium positions throughout its range of motion.

Field fitting

The contour tracing method works well if the potential energy storage elements attach to the same point of the mechanism to be designed. For cases where this condition does not apply, the following method, called *field fitting*, was developed. The case of the static balancing of a pre-existing planar mechanism is addressed. One point Q of the mechanism is selected for the attachment of a compensation spring. Over the path q traced in the ground plane by this point, the potential energy curve p required to balance the original mechanism is plotted. Note that the shape of this curve is determined by the potential energy characteristic of the original mechanism, but that an arbitrary constant value may be added, resulting in different elevations over the plane of motion. Since $V_p + V_c = K$, where V_p is the pre-existing potential, and V_c is the potential of

162
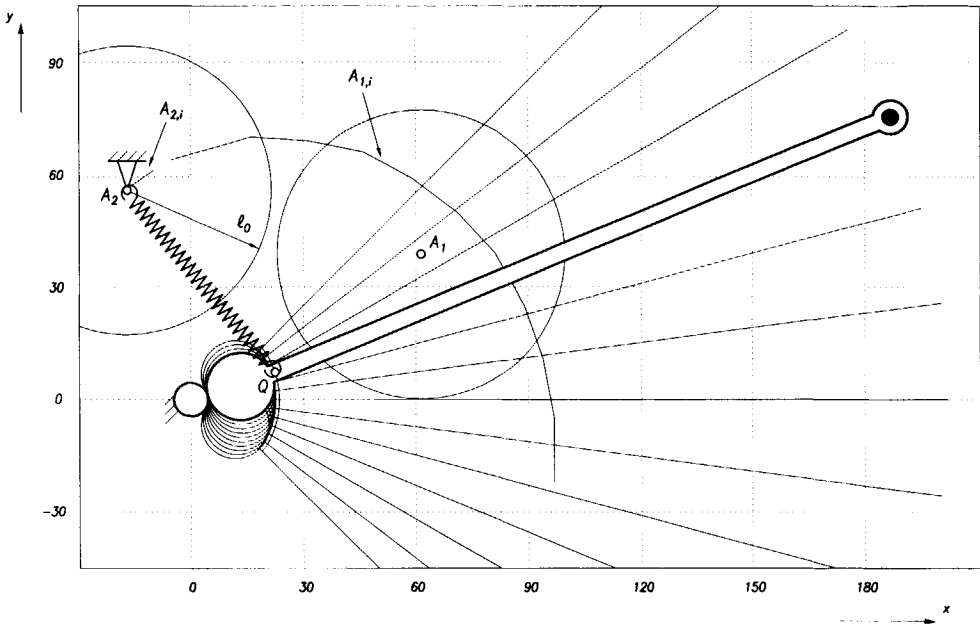
Figure 6.7   Rolling link equilibrator: optimization output showing the pre-existing rolling link mechanism with one fixed roller and one moving roller with a lever and mass attached to it. The point Q was selected just in front of the moving roller. With the proper choice of the spring parameters and the value for K, a satisfactory fixed spring attachment point A_2 is found.

the compensation spring, the lowest possible value for K is the maximum value of V_p. Next, the energy surface of a preselected compensation device, which can be moved in the plane of motion of the mechanism, is fitted optimally against the spatial curve p. A perfect fit would result in perfect balance. The location of the compensation energy surface determines the attachment point A of the compensatory element. There are many ways to find an optimal configuration, including multiparameter gradient-based methods [6.1]. However, this section will be restricted to the description of a straightforward procedure, which has the advantage of being very simple.

When the trajectory q is subdivided into n points, and a value for the constant K is selected, then the required potential energy of each position is known. When a preselected spring is to be used, the elongation of this spring required to meet the energy demand at each point Q_i can easily be calculated. Circles with the required spring lengths as their radius (*energy-distance circles*) can now be drawn, having the corresponding points Q_i and Q_{i+1} on the trajectory q as their center, as is indicated in figure 6.6a. If two successive

163
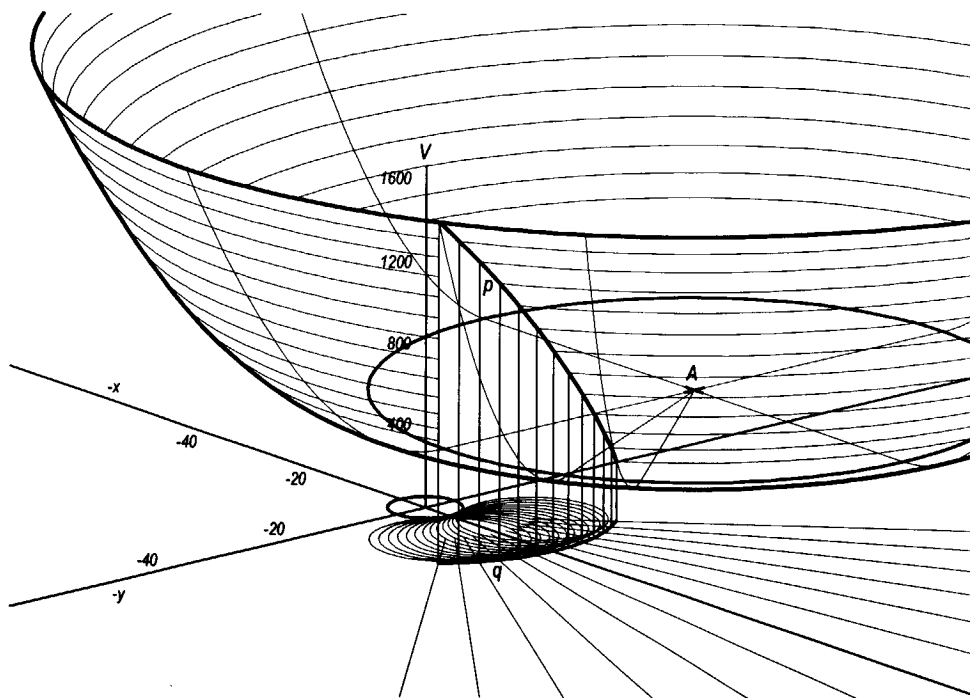
Figure 6.8   Rolling link equilibrator: optimization output giving a graphical impression of the fitting of the required potential curve p and the compensation spring potential field [4.3].

positions Q_i and Q_{i+1} are regarded, a maximum of two suitable positions, $A_{1,i}$ and $A_{2,i}$ for the attachment of the compensation spring are found at the intersections of the corresponding circles. A spring attached at either of these points will satisfy the potential energy demands for the points Q_i and Q_{i+1}.

When more than two points are considered, a series of spring attachment points will be found (figure 6.6b). In general, the attachment points $A_{1,i}$ and $A_{2,i}$, respectively, will not coincide. However, in case of an arc-like trajectory q without inflection points, an acceptable solution is often found by selecting an appropriate value for K, as is suggested in figure 6.6c. Under these circumstances, one spring attachment point approximately satisfies the potential energy demands of all points Q_i. It is wise to start with low K-values in order to avoid high total potential energy. For a satisfactory solution it may be necessary to repeat the procedure with different parameters: another point Q of the mechanism to be balanced may be selected for the attachment of the compensation spring, or a different spring may be used.

164
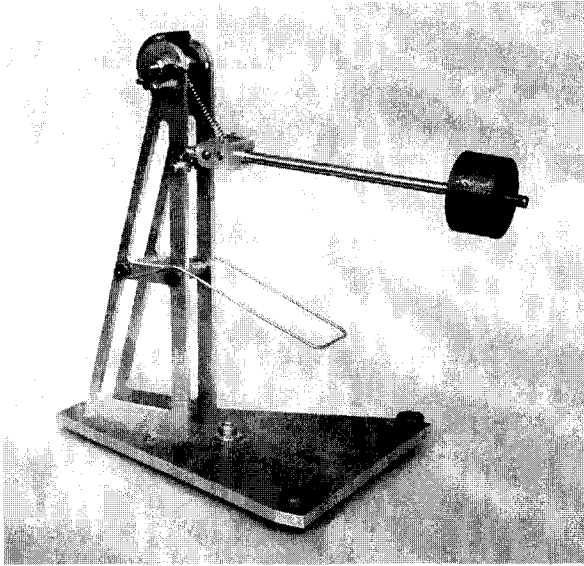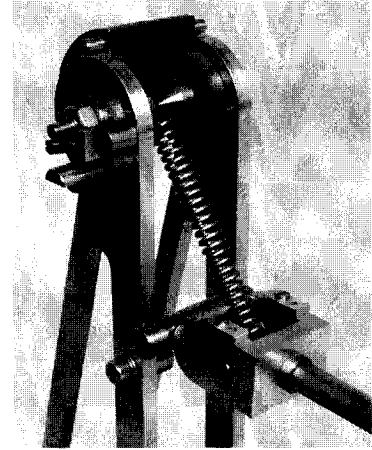
(a)   (b)/(c)

Figure 6.9   Demonstration model of rolling link equilibrator, designed using field fitting: (a) overview, (b) close-up of rollers and spring, (c) drawing, showing the flexible band, the spring, and the adjustment mechanism for the fixed spring attachment point [6.5].
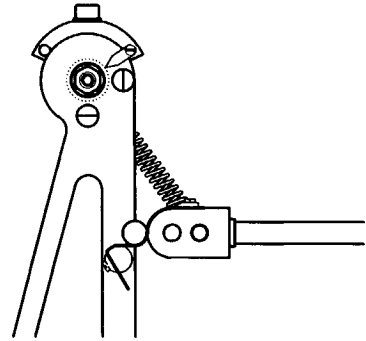
Figure 6.7 shows the optimization result for a one-degree-of-freedom gravity equilibrator with a rolling joint. One roller of diameter 9mm was fixed, while the other one, having a diameter of 18 mm, was to move between plus and minus 30 degrees with respect to the horizontal. Due to the rolling process, the lever attached to the moving roller, being 188 mm long, assumes angles from -45 to 45 degrees. The mass at the end of the lever was 0.5 kg. An available spring was used having a stiffness of 2.09 N/mm and a free length of 38.5 mm, indicated by a circle in the diagram. The value of K was increased, starting from the lowest possible value, to find an optimal balance. The result is shown in figure 6.7. The trajectory of the points A_{2i} is very compact. Their average value, A_2, was taken as the fixed spring attachment point, resulting in a balancing error (maximum relative deviation of potential energy) of 0.4 %. Figure 6.8 gives an impression of the fit between the required potential energy curve p and the energy field of the selected normal spring.
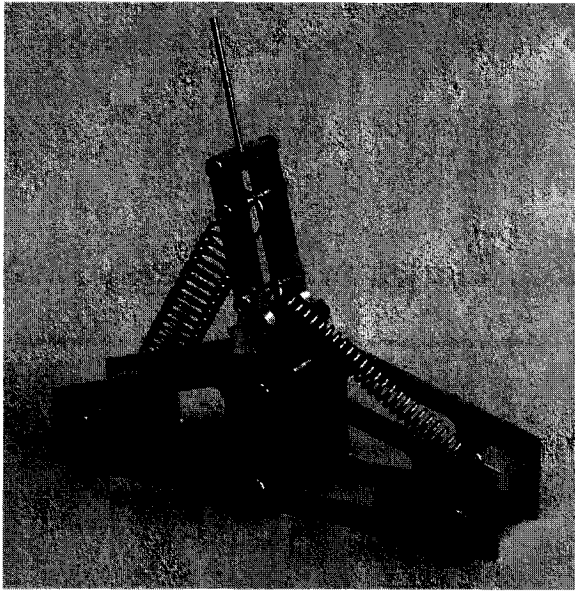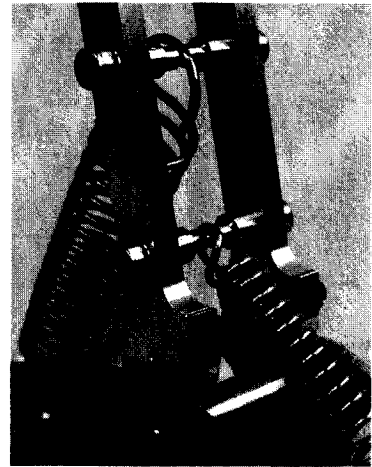
(a)   (b)/(c)
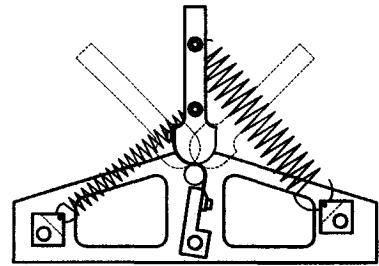
Figure 6.10   Demonstration model of rolling link spring force balancer: (a) overview, (b) close-up of rollers, spring attachment points, and flexible bands, (c) drawing showing the flexible band mounting [6.6].

A demonstration model was made (figure 6.9 [6.5]), which performs well. Its potential energy function is not perfectly constant, rendering a stable and an unstable equilibrium position for the rolling lever. In the stable equilibrium position the oscillation period is several seconds, and, in spite of the low error, it is very difficult to keep the mechanism in its unstable equilibrium position, due to the very low friction in the rolling joint. A spring-to-spring balancer was made using the same approach (figure 6.10 [6.6]). In both cases the flexible bands are single sided. The forces present make sure that the roller will be pressed into the bands.

Paraboloid placement

Another approach is also based on the parameterized trajectory q of a specified point Q of the mechanism to be balanced. This time, not the positions Q_i and Q_{i+1} are used, but their corresponding points P_i and P_{i+1} on the energy curve p. The question now becomes to find the potential energy surfaces that contain both points P_i and P_{i+1}. In the case of ideal springs, the surfaces are
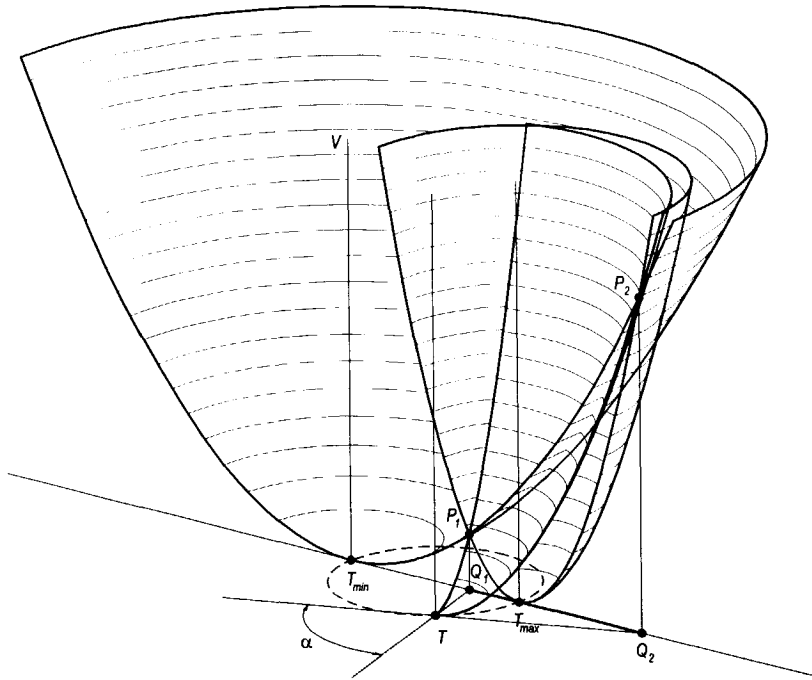
Figure 6.11 Possible paraboloids through two points P_1 and P_2[4.3]. Two generating parabolas of the paraboloid through point T are drawn. As the angle α between the vertical planes containing the generating parabolas is changed, other solutions are found. Two extremes are drawn: the one with $\alpha=0$ (through point T_{min}), and the one with $\alpha=\pi$ (through point T_{max}). The locus of point T is a circle.

paraboloids and a nice solution exists. For this reason, the ideal spring case is described here, but the same procedure can be applied to the case of normal springs.

A variety of paraboloids exist containing two given points P_1 and P_2. Two extremes are sketched in figure 6.11: the ones with their axis of symmetry on the straight line containing points Q_1 and Q_2. Clearly, these are not the only solutions. Another arbitrary solution is also indicated: the paraboloid with its axis of symmetry passing through T. Two of its generating parabolas are drawn, the ones through points P_1 and P_2, lying in vertical planes at a relative angle α. For the distances TQ_1 and TQ_2 the following expressions hold:

$$TQ_1 = \sqrt{\frac{2V_1}{k}} \qquad\qquad (6.4)$$

167

$$TQ_2 = \sqrt{\frac{2V_2}{k}} \tag{6.5}$$

where V_i is the required potential energy in point Q_i. So it is observed that the ratio of TQ_1 and TQ_2 is constant as k is varied, and therefore the locus of points T is a circle of Appolonius [3.6]. The spring stiffness k varies along this circle. The spring of minimum required stiffness is located at T_{min}, whereas the spring of maximum stiffness is located at T_{max}.

A locus of points T, which is a circle in the case of ideal springs, can be found for each pair (Q_i, Q_{i+1}). The points $T_{k,j}$ of these loci that correspond to the same spring rate can now be connected. For a specified range of spring rates, a family of curves is formed. The shortest of these is likely to serve best as a basis for determining the optimal point of attachment. A spring of the spring rate k_j belonging to this curve is attached to the point (x_{tkj}, y_{tkj}), where x_{tkj} is the mean of the x-components of the points $T_{k,j}$ used, and y_{tkj} is the mean of the y-components. Again, it may be necessary to add a different constant K to the energy curve p to obtain a good solution. If normal springs are to be used, the loci t will assume a shape different from a circle, and the free length will be an additional parameter.

Overlay methods

A graphical procedure of a different kind than the ones in the previous section is found when overlays are used. This method using overlays is also applied in mechanism synthesis. For instance, when designing a four-bar linkage as a function generator, several positions of the input crank are specified, a connecting rod length is selected and an overlay of the output crank featuring the desired output angles is fitted to this picture [6.7]. By adding an overlay containing a spring's potential energy contour lines, the procedure can easily be extended to solve counterbalancing problems of many kinds.

As a first example, figure 6.12 suggests the static balancing of a spring-lever element with normal springs. A point Q on the link is selected, and several configurations of the link are drawn. Each configuration is labeled with the amount of required potential energy for static balance (figure 6.12a). Since $V_1 + V_2 = K$, the required potential at each point Q_i is equal to $V_{2,i} = K - V_{1,i}$, where $V_{1,i}$ is the potential of spring k_1 at point Q_i, and where $V_{2,i}$ is the potential of spring k_2 at point Q_i. Any value greater than the maximum of the values of $V_{1,i}$ may be selected for the constant K. Next, an overlay of the contour lines of the compensation spring (figure 6.12b) is placed onto the drawing, such that the required potential energy at each point Q_i corresponds to the potential energy contour of the compensation spring.

168
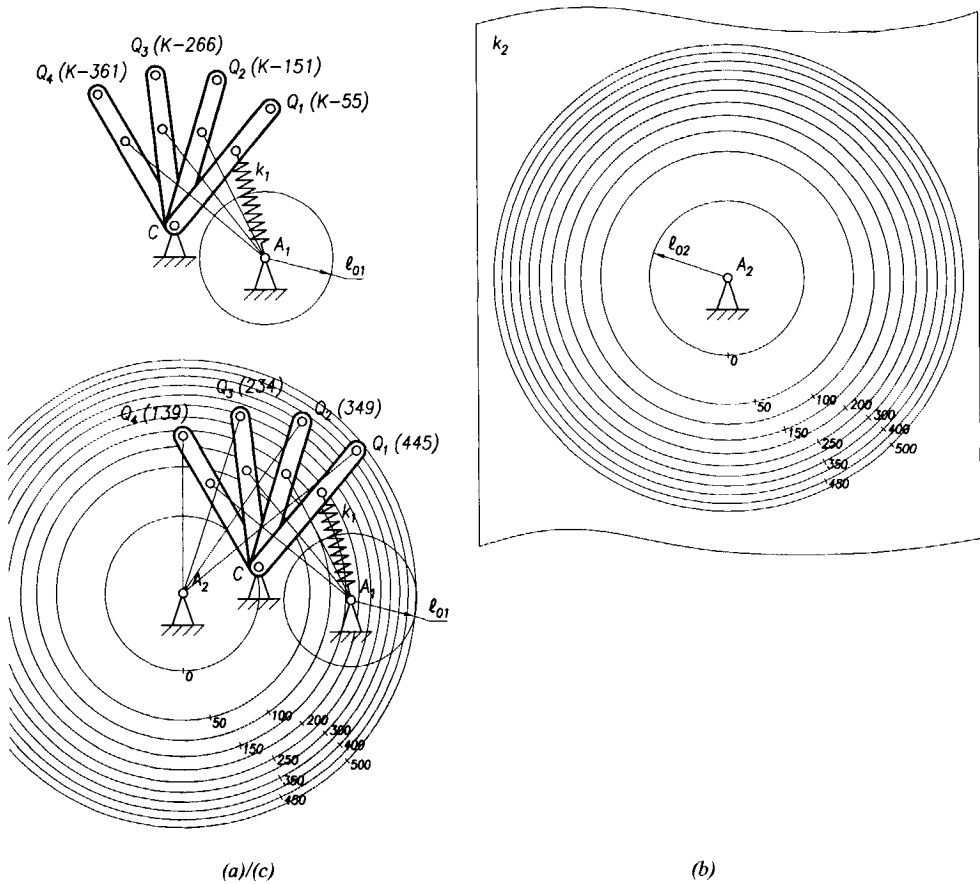
Figure 6.12 Conception of a simple balancer incorporating normal springs using an overlay: (a) rotatable link with normal spring, while a compensation spring is to be attached at point Q, (b) overlay of compensation energy field contour lines, (c) after selecting K, in this case a value of 500 is chosen, the overlay is matched with points Q_i, and a location for A_2 is found.

In the example in figure 6.12, the following parameters were used. The spring parameters are $k_1 = 2$, $\ell_{01} = 11$, $k_2 = 1.5$, and $\ell_{02} = 12.7$, while the arm lengths are $r_1 = 16$, and $r_2 = 25$. The selected value for K was 500. An approximate position for the fixed point A_2 of the compensation spring was readily found.

A second example will demonstrate the procedure for a four-bar linkage. The rotatable link r_1 hinged at C_1 is hampered by a parasitic potential energy function V_1 as a result of the action of a mass (figure 6.13a). The compensation is designed as follows. Successive positions $P_{1,i}$ of a selected point of the link are specified, and a family of circles is drawn with these points as their centers

169
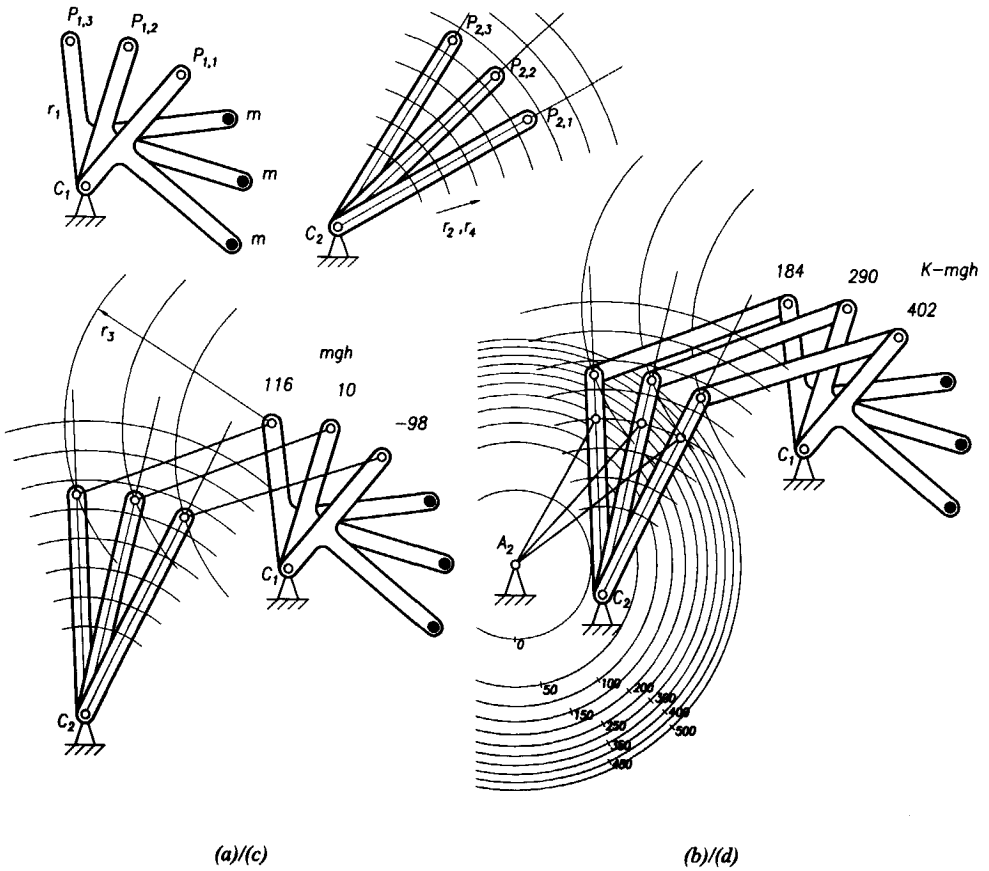
Figure 6.13 Conception of a four-bar gravity balancer incorporating a normal spring using an overlay: (a) rotatable link hampered by mass, (b) prespecified output crank parameters, (c) overlay of output crank to match the coupler bar circles, (d) overlay of compensation energy field contour lines.

and with a radius r_3 equal to the assumed length of the coupler link (figure 6.13c). A desired energy value $V_{2,i} = K - V_{1,i}$ is assigned to each of the positions [6.8].

Now a first overlay is made, including concentric circles, representing possible lengths of the output crank r_4, and of the arm length r_2 of the compensation spring. This overlay can also include desired angles of the output crank in the respective configurations (figure 6.13b shows such an overlay with a fixed arm length r_4 and concentric circles for r_2). This overlay is fitted to the original layout in such a way that the links form a four-bar arrangement in every configuration, while simultaneously a second overlay containing the contour

170
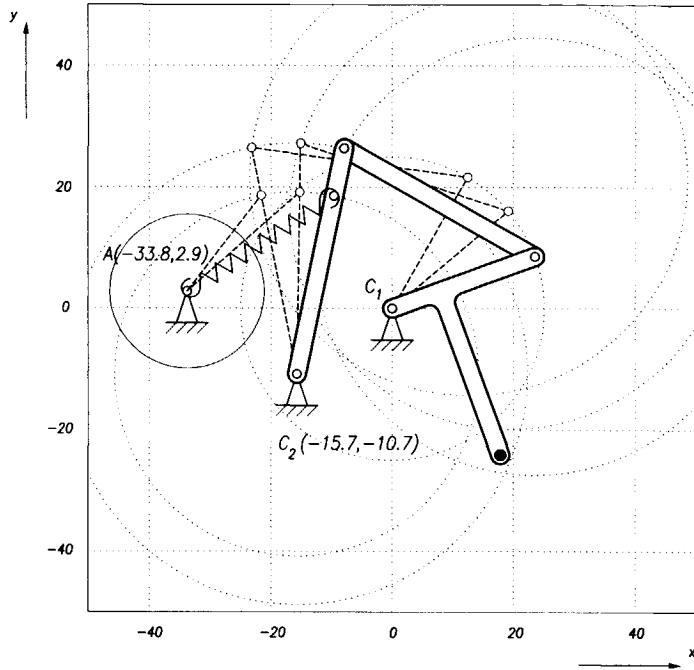
Figure 6.14 Optimization output of the four-bar balancer procedure: the input crank is hinged at point C_1, connected by the coupler to the output link hinged at point C_2, while the fixed spring attachment point is found at point A_2. The compensation error amounts to less than 0.002%.

lines of the compensatory spring's energy field is fitted to points Q_i of the output crank, to be determined by sliding the spring potential overlay until a satisfactory match is found (figure 6.13d). Several scale divisions on the spring potential overlay may be applied to be able to quickly check for different spring rates.

The two overlays are fitted to the original drawing, while trying to match the desired energy value for each configuration of the linkage with the energy values of the compensation spring. It may be necessary to try other connecting rod lengths, output crank lengths, compensation spring arms, or compensation spring parameters, before a satisfactory match is obtained or it is concluded that no solution exists. With some exercise, this method works surprisingly well, and is more intuitive than one might expect.

To a certain extent, the computer can facilitate finding a solution. Rather than a completely automated procedure, a computer assisted manual procedure will be given, as this provides more control over the arrangement obtained. The

171

variables which are manually adjusted are the configurations of the rotatable link to be balanced ($\varphi_{1,i}$), the value for the total potential energy (K), the compensation spring parameters (k_2 and ℓ_{02}), and the lengths of the input crank (r_1), connecting rod (r_3), output crank (r_4), and the arm length (r_2) of the compensation spring on the output crank. In each fitting attempt, a position of the second fixed pivot is selected with the mouse. The kinematics is completed by a MATLAB-routine, and the spring attachment point is calculated by the surface fitting technique, presented in the previous section.

Figure 6.14 gives the optimization result of the same arrangement as in figure 6.13, where a mass attached to a rotatable link is to be balanced. The mass parameters are $m = 1$, $r_m = 30$, the link lengths are $r_1 = 25$, $r_2 = 30$, $r_3 = 36$, $r_4 = 38$, while the spring parameters are $k_2 = 1.5$ and $\ell_{02} = 12.7$, and the selected value for K was 300. The balancing error was found to be below 0.002%, while this solution was easily found.

6.3   Extended vector-loop closure

> In optimal design [-], existence of even a nominal design satisfying constraints is not assured, much less existence of an optimum design. Even when an optimum design exists, numerical methods for its solution are often quite sensitive to initial estimates and require considerable computational art for iterative convergence.
>
> Edward J. Haug, Jasbir S. Arora, 1980, p7

The contour tracing procedure described in section 6.2 only works well if the springs to be balanced against each other are attached to the same point of the moving link. The loop closure method, however, as applied in the contour tracing procedure, can be extended to directly incorporate desired energy characteristics [6.9]. To this end, an energy equation is added to the set of loop equations, so that the demand for the springs to be attached to the same point is canceled. Two examples will be given next. In the first example the springs are attached to the same point of the mechanism, as previously. The second example is a generalized version where the springs are attached to different points.

Roller on surface

Figure 6.15 suggests the layout of the first example: a lever is attached to a roller which can roll over a flat surface. Two springs are attached to point P of the link attached to the roller in a symmetrical arrangement. For this case, two loops can be identified. The loop equations and the energy equation yield:

(a)/(c)   *(b)*
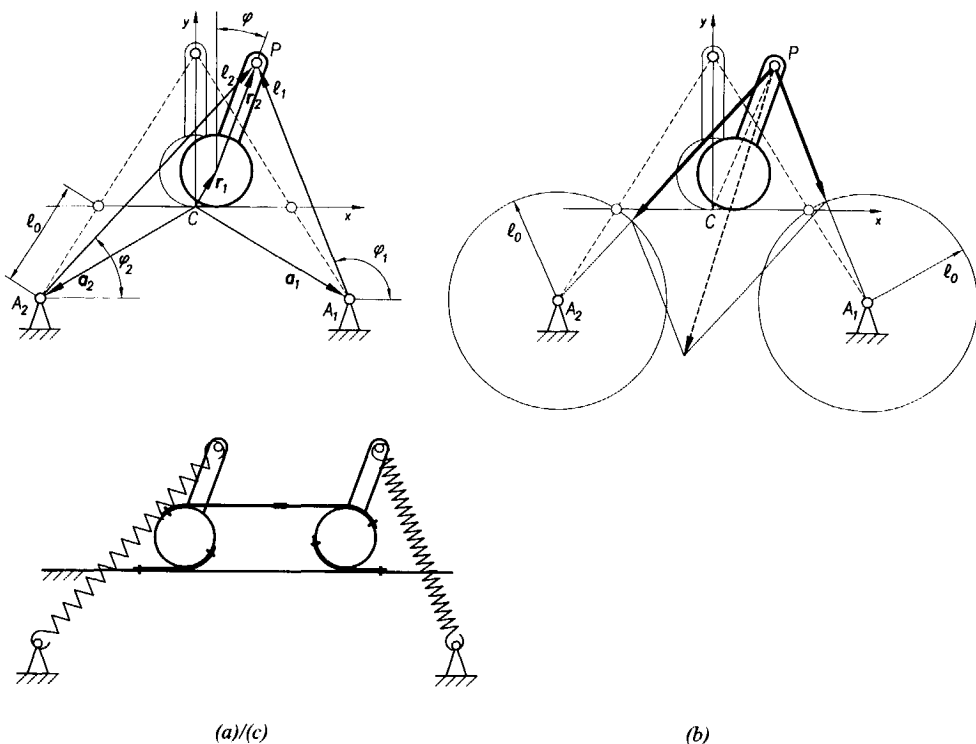
Figure 6.15 Roller on flat surface balancing two normal springs: (a) definition of vectors, (b) determination of initial guess, (c) application as a low-friction, backlash-free straight-line guidance.

$$\boldsymbol{a}_1 + \boldsymbol{l}_1 = \boldsymbol{r}_1 + \boldsymbol{r}_2 \tag{6.6}$$

$$\boldsymbol{a}_2 + \boldsymbol{l}_2 = \boldsymbol{r}_1 + \boldsymbol{r}_2 \tag{6.7}$$

$$V_1 + V_2 = K \tag{6.8}$$

where $\boldsymbol{a}_1$ is the vector from the origin to the right fixed spring attachment point, $\boldsymbol{a}_2$ to the left one, l_1 and l_2 the lengths of the right and left spring, respectively, $\boldsymbol{r}_1$ the vector from the origin to the center of the roller, and $\boldsymbol{r}_2$ the vector along the link. V_1 and V_2 represent the potential energy in the springs, whereas K is a constant energy value, which can be regarded as a variable to be determined or as a given constant. Expressing the vector terms in Cartesian coordinates and rearranging gives the following set of five equations for each of n positions:

$$0 = A_x + R\varphi_i + r_2 \sin\varphi_i + \ell_{1,i} \cos\varphi_{1,i} \tag{6.9}$$

173
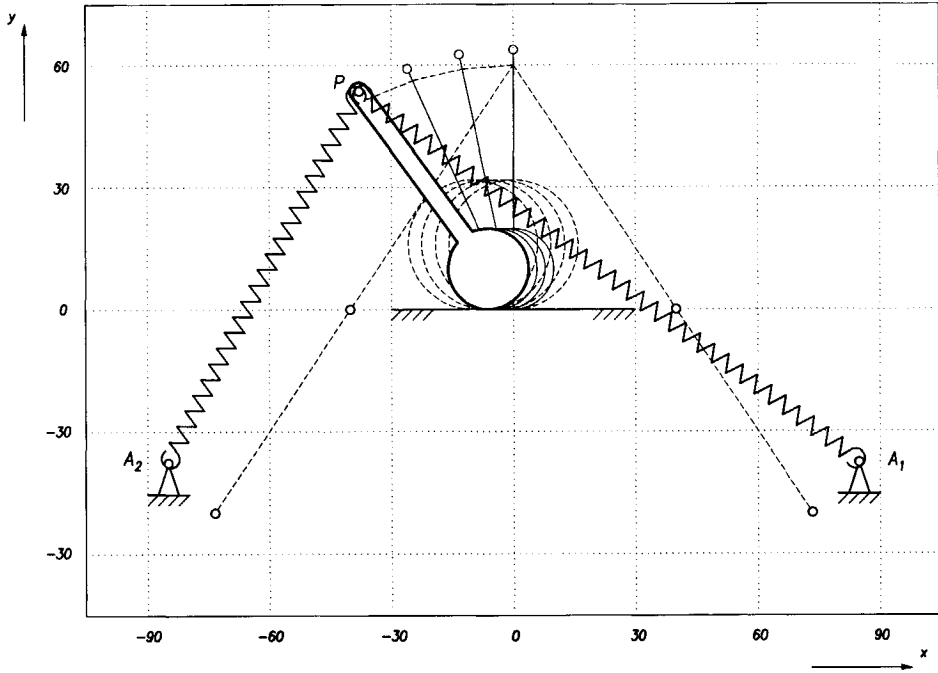
Figure 6.16 Optimization output of the roller on the flat surface: The initial estimate is shown in dotted lines, while the optimized arrangement is drawn in continuous lines, where A_1 and A_2 are the optimized positions of the fixed spring attachment points. The balancing error amounts to 3e-6%.

$$0 = A_y + R + r_2 \cos\varphi_i - \ell_{1,i} \sin\varphi_{1,i} \qquad (6.10)$$

$$0 = -A_x - R\varphi_i - r_2 \sin\varphi_i + \ell_{2,i} \cos\varphi_{2,i} \qquad (6.11)$$

$$0 = A_y + R + r_2 \cos\varphi_i - \ell_{2,i} \sin\varphi_{2,i} \qquad (6.12)$$

$$0 = \tfrac{1}{2}k\left(\ell_{1,i} - \ell_{01}\right)^2 + \tfrac{1}{2}k\left(\ell_{2,i} - \ell_{02}\right)^2 - K \qquad (6.13)$$

where R is the radius of the roller, where $1 \le i \le n$, and where the coordinates of the fixed spring attachment points are $A_1 = (A_x, A_y)$ and $A_2 = (A_x, -A_y)$. When φ_i are given, a value for K is agreed upon, and the springs are preselected, then a maximum of $4 + 4n$ unknowns are to be solved using the above $5n$ equations.

The initial estimate is based on the basic configuration, as shown in figure 6.15b. The initial lengths of the springs are appended in the central position of the lever, which gives the initial estimate for the fixed spring

174
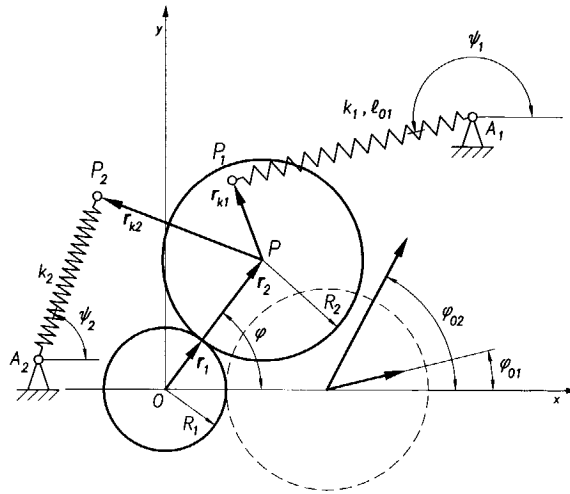
Figure 6.17 Definition of vectors for the general two-roller layout.

attachment points. In the deflected position, the resultant of the spring forces does not pass the pivot, due to the free length of the springs. Using a rolling link instead of the fixed pivot moves the contact point in the desired direction, thereby reducing the balance error. The optimization result for a configuration with equal springs is shown in figure 6.16. The balancing accuracy of the initial estimate is about 5% over the range of motion shown in the diagram, whereas this value has been decreased to practically zero after optimization. A possible application is suggested in figure 6.15c: a low-friction, backlash-free straight-line guidance.

General two-spring two-roller balancer

The two-roller layout of figure 6.3 can be generalized into the configuration of figure 6.17 in order to eliminate the constraint of the two springs attaching to the roller at the same point. Two loops are present, resulting in two continuity equations in vector form. Together with the potential energy equation, the following set of governing equations results:

$$a_1 + l_1 = r_1 + r_2 + r_{k1} \tag{6.14}$$

$$a_2 + l_2 = r_1 + r_2 + r_{k2} \tag{6.15}$$

$$V_1 + V_2 = V \tag{6.16}$$

where r_{ki} is the vector from the center of the roller P to the attachment point P_i of spring k_i. In principle, any energy function can be assigned to V,

175

but the discussion here is limited to constant energy: $V = K$. The constant energy value K, however, can be regarded as a variable to be determined. Expressing the vector terms in Cartesian coordinates and rearranging gives the following set of five equations for each of n positions:

$$0 = (r_1 + r_2)\cos\varphi_i + r_{k1}\cos\left(\left(1 + \frac{r_1}{r_2}\right)\varphi_i + \varphi_{01}\right) - A_{1x} - \ell_{1,i}\cos\psi_{1,i} \qquad (6.17)$$

$$0 = (r_1 + r_2)\sin\varphi_i + r_{k1}\sin\left(\left(1 + \frac{r_1}{r_2}\right)\varphi_i + \varphi_{01}\right) - A_{1y} - \ell_{1,i}\sin\psi_{1,i} \qquad (6.18)$$

$$0 = (r_1 + r_2)\cos\varphi_i + r_{k2}\cos\left(\left(1 + \frac{r_1}{r_2}\right)\varphi_i + \varphi_{02}\right) - A_{2x} - \ell_{2,n}\cos\psi_{2,i} \qquad (6.19)$$

$$0 = (r_1 + r_2)\sin\varphi_i + r_{k2}\sin\left(\left(1 + \frac{r_1}{r_2}\right)\varphi_i + \varphi_{02}\right) - A_{2y} - \ell_{2,i}\sin\psi_{2,i} \qquad (6.20)$$

$$0 = \tfrac{1}{2}k_1(\ell_{1,i} - \ell_{01})^2 + \tfrac{1}{2}k_2(\ell_{2,i} - \ell_{02})^2 - K \qquad (6.21)$$

Based on the above expressions, a maximum of $15 + 4n$ unknowns and $5n$ equations arise, when φ_i is given. Setting $15 + 4n = 5n$ yields a maximum of $n = 15$ precision points. In common cases, the characteristics of the springs will be given, and K will be preset. This results in a total of $10 + 4n$ unknowns and ten precision points. This case is given in table 6.2.

Nr of pos. (n)	Nr of scal. eqs. (5n)	Number of scalar unknowns (plus symbols) (10+4n)	Number of free choices (plus suggested symbols) (10-n)
1	5	14 ($\ell_{1,1}$, $\ell_{2,1}$, $\psi_{1,1}$, $\psi_{2,1}$, r_1, r_2, r_{k1}, r_{k2}, φ_{01}, φ_{02}, A_{1x}, A_{1y}, A_{2x}, A_{2y})	9 (r_1, r_{k1}, r_{k2}, φ_{01}, φ_{02}, A_{1x}, A_{1y}, A_{2x}, A_{2y})
2	10	18 (above + $\ell_{1,2}$, $\ell_{2,2}$, $\psi_{1,2}$, $\psi_{2,2}$)	8 (r_{k1}, r_{k2}, φ_{01}, φ_{02}, A_{1x}, A_{1y}, A_{2x}, A_{2y})
3	15	22 (above + $\ell_{1,3}$, $\ell_{2,3}$, $\psi_{1,3}$, $\psi_{2,3}$)	7 (r_{k2}, φ_{01}, φ_{02}, A_{1x}, A_{1y}, A_{2x}, A_{2y})
4	20	26 (above + $\ell_{1,4}$, $\ell_{2,4}$, $\psi_{1,4}$, $\psi_{2,4}$)	6 (φ_{01}, φ_{02}, A_{1x}, A_{1y}, A_{2x}, A_{2y})
5	25	30 (above + $\ell_{1,5}$, $\ell_{2,5}$, $\psi_{1,5}$, $\psi_{2,5}$)	5 (φ_{02}, A_{1x}, A_{1y}, A_{2x}, A_{2y})
6	30	34 (above + $\ell_{1,6}$, $\ell_{2,6}$, $\psi_{1,6}$, $\psi_{2,6}$)	4 (A_{1x}, A_{1y}, A_{2x}, A_{2y})
7	35	38 (above + $\ell_{1,7}$, $\ell_{2,7}$, $\psi_{1,7}$, $\psi_{2,7}$)	3 (A_{1y}, A_{2x}, A_{2y})
8	40	42 (above + $\ell_{1,8}$, $\ell_{2,8}$, $\psi_{1,8}$, $\psi_{2,8}$)	2 (A_{2x}, A_{2y})
9	45	46 (above + $\ell_{1,9}$, $\ell_{2,9}$, $\psi_{1,9}$, $\psi_{2,9}$)	1 (A_{2y})
10	50	50 (above + $\ell_{1,10}$, $\ell_{2,10}$, $\psi_{1,10}$, $\psi_{2,10}$)	0

Table 6.2   The relation between the number of precision points, equations, unknowns and free choices for the generalized configuration of two rollers, with given springs and spring attachment points.

(a)   *(b)*
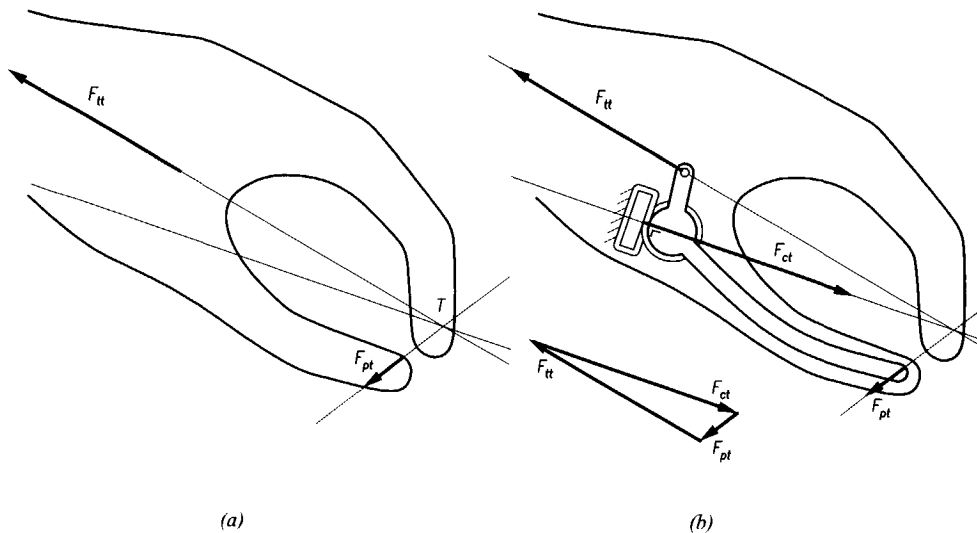
Figure 6.18 Force directed design of a thumb mechanism in a hand prosthesis: (a) two forces are roughly known, (b) the third force required for equilibrium applies at a roller, which is supported by a plane perpendicular to the action line of the third force. An O-ring is wrapped around the roller and the frame in a figure-of-eight arrangement.

6.4   Practical examples

> *In order to provide a functional artificial finger motion, it may be necessary to use rolling joints.*
>
> N. Newman, 1973

This section will present two prototypes incorporating approximate spring force balancers with great practical value: a prosthetic hand, and surgical forceps for use in minimally invasive surgery.

Force directed design of a voluntary closing hand prosthesis

The design of a body powered voluntary closing prosthetic hand [6.10] stems from a long-term project on the design of rehabilitation aids [1.2]. Prior to the design, several workshops and interviews with the members of two Dutch rehabilitation teams were organized [6.11], where early ideas were discussed. It was found that an elbow-controlled design, without direct grasp [6.12] would fulfill many basic needs [6.13]. As force feedback was a primary goal, a research project on the perception of forces by humans was initiated [6.14], in order to be able to design an optimal human-machine interface. Preliminary results are that
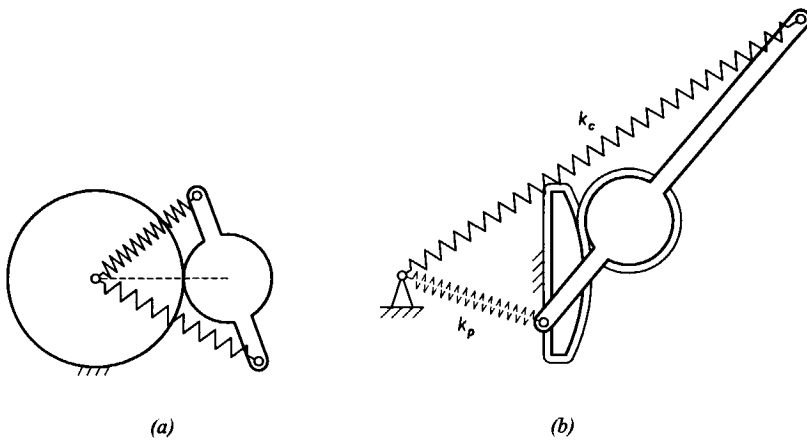
Figure 6.19 Compensation of glove force based on perfectly balanced rolling link: (a) repetition of figure 5.37b, (b) one of the springs, k_p, can be regarded as the parasitic glove stiffness, the other as the compensation spring.

the sensitivity of the human arm with respect to elbow-control is best when the operating forces are not below 9N [6.15].

The design presented here is inspired by the idea that the motion of the fingers before establishing a grip is much less relevant for good control of the object held than the distribution of forces once the object has been contacted. Based on this notion (force directed design, [1.8; 1.9]), the configurations of forces on the fingers and the force transmission through the whole mechanism were taken as point of departure for the design, rather than motion characteristics [6.16]. Furthermore, for a good distribution of pinching forces on the object and a natural behavior, it was intended to make the prosthesis adaptive and flexible. Other basic principles were the use of rolling links to minimize friction, and to reduce the disturbing influences of the cosmetic glove by a compensation mechanism, in order to obtain good force feedback.

The course of the design is first illustrated in figure 6.18 for the thumb. In a given position, two forces are roughly known: the pinch force F_{pt} and the operating force F_{tt}, which is transmitted by a tendon from the forearm section. The points of application of these forces are connected by a link. On this link, a third force needs to act for equilibrium, while its line of action must pass through point T. Of many possibilities, a convenient one is selected (figure 6.18b), and a roller is placed at the intersection of this action line and the link. The preferred position of the roller is such that changes in the assumptions for F_{pt} and F_{tt} affect the action line of F_{ct} as little as possible. The most profitable way to support the roller is perpendicular to the action line of the

(a)   *(b)/(c)*
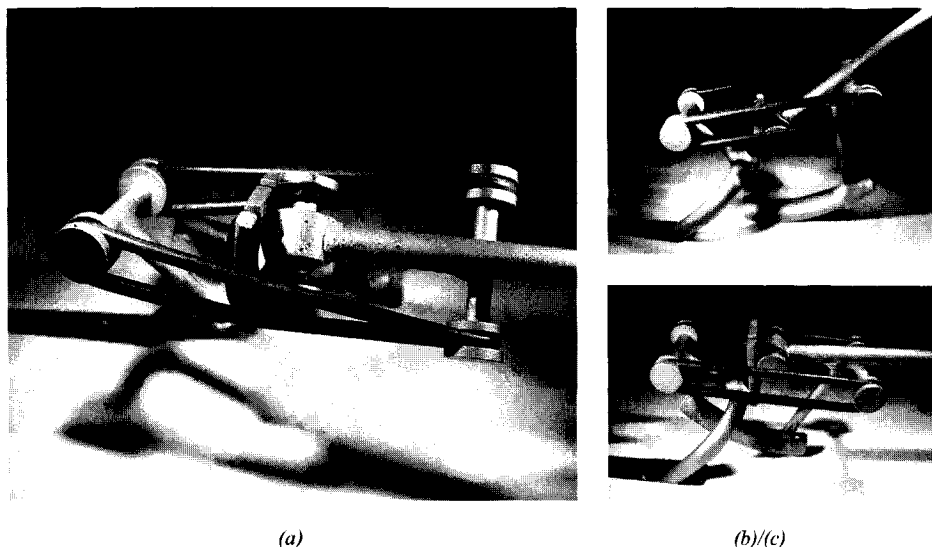
Figure 6.20 Photographs of the thumb joint of the second prototype: (a) in twisted position, showing the flexibility of the O-rings, (b) in opened position, (c) in closed position (operating tendon not shown) [6.17].

third force. This way, the force component tangential to the roller is minimal, so the flexible bands wrapped around the roller are not loaded much. Indeed, rubber O-rings wrapped in a figure-of-eight layout can be used rather than metal foils. Thus, an arrangement has been obtained which is very flexible when unloaded, very much like a relaxed human hand, while the mechanism stiffens itself considerably when the forces are present.

The compensation of the glove force was inspired by the rolling joint in figure 5.37b (reprinted in figure 6.19a). One of the springs, k_p, can be regarded to represent the counteraction of the cosmetic glove. Therefore, the other spring, k_c, would balance the cosmetic glove if it would behave as an ideal spring. Unfortunately, due to the non-linear behavior of the glove [1.4], perfect compensation is not attained, yet a significant reduction of the glove counteraction was achieved [6.18]. Figure 6.20 shows photographs of the thumb joint, showing the figure-of-eight O-ring which prevents the roller from slipping, and keeps the parts together when the mechanism is not operated, as well as the O-rings which serve as glove compensation springs [6.17].

The design of the fingers proceeds in a similar manner as the thumb, the main difference being that the fingers consist of two digits each (the proximal phalanx near the frame, and the distal phalanx at the end), to allow greater adaptivity. The pinch forces F_1 and F_2 were assumed to be equal in magnitude

179
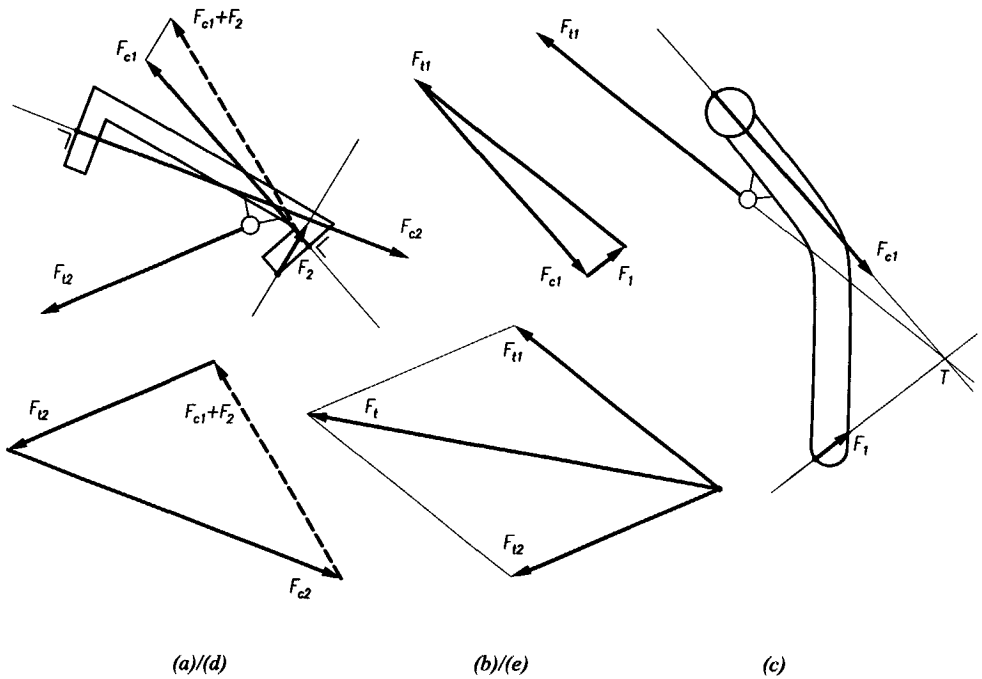
Figure 6.21 Force directed design of a finger mechanism: (a) proximal phalanx, (b) triangle of forces of distal phalanx, (c) distal phalanx, (d) force triangle of proximal phalanx, (e) composition of tendon forces.

(uniform force distribution), to act perpendicular to the glove contour, and to apply at the most distal point of the respective phalanges. As was the case with the thumb, the shapes of the parts followed from the configuration of forces. When the free-body diagram of the distal phalanx is drawn (figure 6.21bc), F_{c1} follows from static equilibrium with given estimates for F_1 and F_{t1}. This defines the orientation of the contact surface between the two phalanges (figure 6.21a). Together with estimates for F_2 and F_{t2}, F_{c2} is now determined from the free-body diagram of the proximal phalanx. To this end, the forces F_{c1} and F_2 are first composed to obtain a three-force system. F_{c2} follows from equilibrium (figure 6.21d), and therewith the orientation of the contact surface between the proximal phalanx and the frame. In the resulting configuration, the shear components of the contact forces F_{c1} and F_{c2} are zero in the neutral position, and, depending on the specific dimensions, small in the remainder of the range of motion. What remains of the shear forces is absorbed by the O-rings.

The driving tendon, which splits into a branch to the proximal phalanx and a branch to the distal phalanx, distributes the operating force among the two
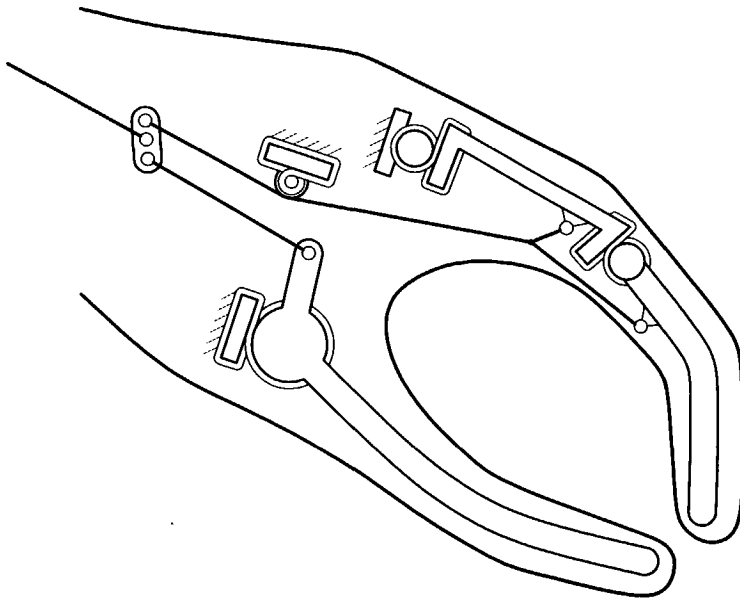
Figure 6.22 Schematic representation of complete hand prosthesis design.

phalanges. It is led around a cylinder which rolls over a small plane which is fixed to the frame. This prevents the tendon from sliding across the inside of the glove, which would ruin both good force feedback and low operating force. Furthermore, it prescribes the direction of the cable. When the direction of the cable is equal to the direction of the resultant force of the two tendon forces F_{t1} and F_{t2} (figure 6.21e), the assumption of equal pinch forces F_1 and F_2 is realized. Due to the assumptions about the use of the prosthesis (indirect grasping only), no tendons are provided to open the hand.

A diagram of the complete design is given in figure 6.22. The tendons of the thumb and the fingers (only one finger shown) are connected to a force leveling floating link, to ensure a desired force distribution ratio, regardless of the configuration of the fingers.

Two prototypes of the proposed concept were built (figure 6.23, [6.17, 6.18]). Measurements showed that the force distribution was indeed approximately constant throughout the range of motion. The operating effort was reduced by the compensation mechanism by more than 80% [6.18]. Furthermore, even though force rather than motion characteristics were used as design objectives, the hand moved very naturally, due to the fact that the objective of uniform pinch forces result in uniform accelerations when no object is present. The
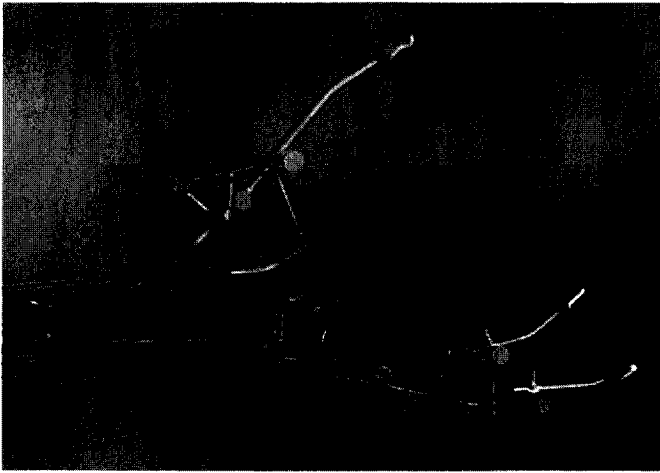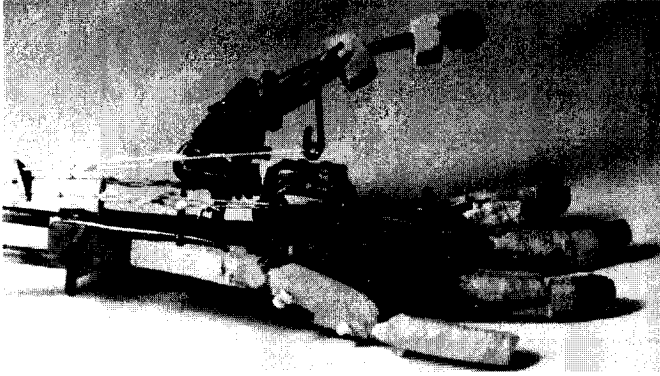
(a)/(b)

Figure 6.23 Prototype of hand prosthesis: (a) photograph of first prototype [6.18], *(b) photograph of second prototype* [6.17]. *In both cases the cosmetic glove is removed.*

prototypes are not yet applicable in clinical practice. However, they showed that the concept works, and that it has potential. Also the fact that the second prototype weighs only 47 grams adds to the high expectations.

Statically balanced compliant forceps

A compliant mechanism is a mechanism that gains some or all of its motion from the relative flexibility of its members rather than from rigid-body joints only [1.13, 6.19]. In some applications of compliant mechanisms, the fact that energy is stored in the elastic members presents a problem. For instance, in manually operated instruments, such as surgical forceps, the forces introduced
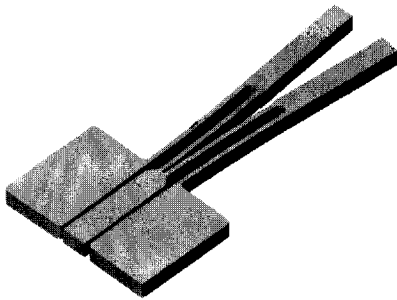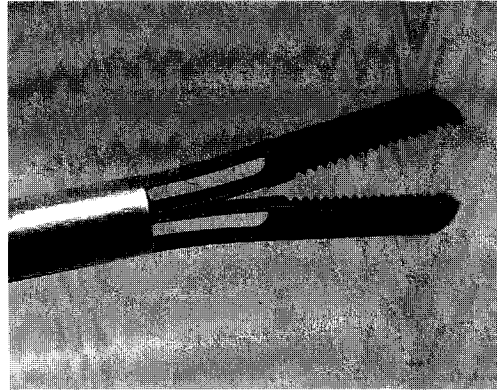
(a)   *(b)*

Figure 6.24 Compliant gripper [6.21]*: (a) working principle showing the four compliant sections and part of the central pull-pushrod, (b) photograph of the compliant gripper.*

by the bending of elastic elements would disturb the force transmission. To restore the force transmission quality, compliant mechanisms may be statically balanced. This section presents an example of a compliant surgical forceps mechanism, which is statically balanced by a rolling-link compensation mechanism.

The conceptual design was divided into two parts: the gripper and the compensation device. For the gripper, a configuration of parallel plate springs was chosen (figure 6.24) [6.20]. The initial (unstrained) position of the compliant gripper is half-opened. Therefore, a pull force in the pull-pushrod is required to close the gripper, whereas a push force is needed to further open the gripper. The dimensions of the compliant gripper mechanism were selected to attain sufficient lateral stiffness. There was no need to minimize the stiffness of the open-and-close movement, as this stiffness would be neutralized by the compensation device. Due to the relatively simple configuration and the moderate strains, the stiffness of the gripper (force versus translation in the pull-pushrod with unloaded gripper) are almost linear for a wide range of plate spring dimensions. The selected dimensions render the stiffness of the gripper, reduced to the translational stiffness of the pull-pushrod to be 43 N/mm.

For the compensation device, a rolling-link mechanism was selected. Due to the linear stiffness characteristic of the gripper, a lever attached to a roller between the pull-pushrod and a parallel frame suffices (figure 6.25). Flexible bands are provided in an opposite U-configuration. A spring is hinged between a fixed point on the frame and the free end of a lever that is attached to the

183
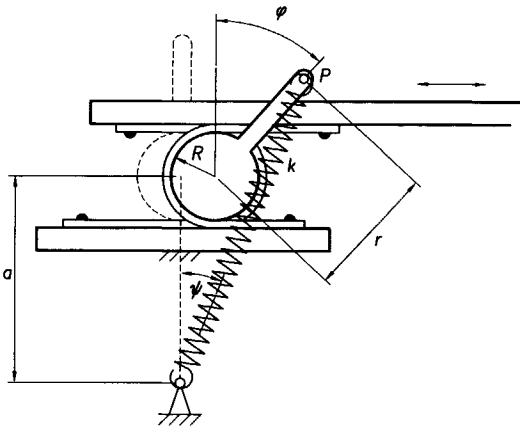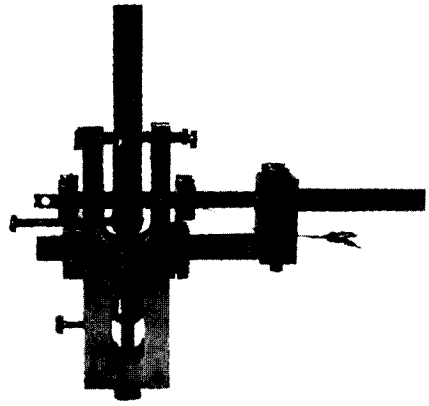
(a)   (b)

*Figure 6.25   Compensation mechanism for compliant surgical forceps: (a) working principle,
(b) photograph of prototype, where the spring is removed to provide a view on the roller [6.21].*

roller. The compensation mechanism was optimized for minimum
compensation error using the extended loop closure procedure (see section 6.3).
To this end, a potential equation is added to the loop equation. Together the
equations are:

$$r_1 + r_2 = r_3 \tag{6.21}$$

$$V_p + V_c = K \tag{6.22}$$

where V_p is the parasitic elastic energy in the compliant gripper mechanism,
which was measured, V_c is the elastic energy in the compensation mechanism,
and K is a constant energy value, which was regarded as a given constant.
Expressing equation 6.21 in Cartesian coordinates and rearranging gives the
following set of three equations for each of n positions:

$$0 = R\varphi_i + r\cos\varphi_i - \ell_i\cos\psi_i \tag{6.23}$$

$$0 = a + r\sin\varphi_i - \ell_i\sin\psi_i \tag{6.24}$$

$$0 = V_{p,i} + \tfrac{1}{2}k\left(\ell_i - \ell_0\right)^2 - K \tag{6.25}$$

where φ is the rotation of the roller from the neutral position, ψ is the angle
between the spring and the vertical, R is the roller radius, r is the length of the
lever, a is the distance from the fixed spring attachment point to the center or
the roller in the neutral position, ℓ is the length of the spring, k is the stiffness
of the spring, and ℓ_0 is the free length of the spring. It should be noted that $V_{p,i}$
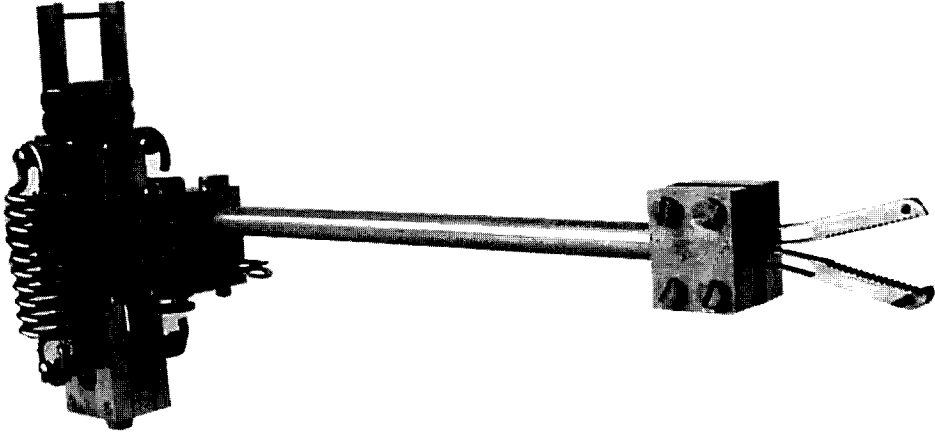
Figure 6.26 Photograph of the first prototype, where the block at the tip is for easy assembly and disassembly, and is omitted in the second prototype as shown in figure 6.24b [6.21].

are given, that k and ℓ_0 are prespecified, and that R, r, and a are unknown but remain fixed, whereas φ_i, ψ_i, and ℓ_i are unknown variables for each position, as represented by the additional index i. When values for φ_i are given, and a value for K is agreed upon, then $3 + 2n$ unknowns and $3n$ equations result, where n is the number of precision points. Using three precision points, several solutions were found, of which one with convenient dimensions was selected. The rounded-off values are: roller radius $R = 3$ mm, lever length $r = 17$ mm, distance $a = 24$ mm. The preselected spring parameters are: stiffness $\frac{1}{2}k = 8.7$ N/mm, initial length $\ell_0 = 33$ mm. Note that for reasons of convenience two springs of stiffness $\frac{1}{2}k$ are used in the prototype.

Figure 6.26 shows a photograph of the first prototype [6.21] (the block around the shaft near the gripper is only for easy assembly and disassembly in the prototype phase, it was eliminated in the second prototype, shown in figure 6.24). This prototype is not yet applicable in clinical practice, mainly because a handgrip was not yet included. It was used to evaluate the mechanism, to assess the force transmission characteristic, and for performing some explorative experiments. When the gripper is unloaded, the maximum operating force (maximum compensation error) on the experimental handgrip amounts to 0.05N. Without the compensation mechanism, a force of approximately 12.9N would have been felt. Additionally, a preliminary sensitivity test was performed. An artery was simulated by a silicon hose, filled with water, in which a pulse was generated by using a syringe. The pulse was

clearly perceivable with the prototype, whereas this sensation was absent when using conventional forceps.

6.5   Summary

This chapter presented several procedures for the design of approximate balancers. It was argued that the conception with ideal springs, as described in the preceding chapters, is very useful even when normal springs are to be applied, because the idealized concepts can function as accurate enough initial estimates in the numerical methods which are required for some of the optimization procedures. Furthermore, it was demonstrated that balancing quality benefits from the application of rolling links, not only due to their low friction, but also because the non-linearity of the normal springs can be partly compensated by the complex kinematics of the rolling links.

Some of the methods explicitly use an initial estimate, which in each case was derived using the approach presented in the previous chapters. In other methods, this happens more implicitly. For instance, in the first example using the overlay method, knowledge on a profitable position of the attachment of the compensation spring on the lever facilitates finding a solution, as does the expectation based on the basic spring force compensator concerning the fixed spring attachment point.

Several modifications or mixes of the methods are possible. Contour tracing for instance is also possible in a mass-spring arrangement. This is even so when the mass is not located at the spring attachment point under the condition that the gravity energy field is reduced onto the new location.

A number of demonstration models were made according to solutions obtained using various optimization procedures. Rolling links were used to reduce friction so that the balancing quality could be judged better. The models function fine. Some unbalance is present, which, given the low friction, results in a preferred position in all models except the one in figure 6.5, which has a range of equilibrium configurations.

The last section presented two applications of compensation mechanisms in medical technology. Especially in this kind of applications low friction and high quality force feedback make the difference of a cumbersome tool or an extension of the human body. Even though the examples given are still in the prototype phase, they demonstrate important virtues.

7   Conclusion

in which the preceding chapters are overlooked, the approach proposed in the introduction is evaluated, the results are discussed and suggestions for improvement and further research are given.

7.1   Accomplishments

They were well-balanced and they could be operated, with some exaggeration perhaps, by the finger of the engineer.

Andrew D. Dimarogonas, 1992

Work in the field of rehabilitation engineering has initiated the aspiration to design mechanical systems with high energy-efficiency and good force transmission quality. Statically balanced systems were found particularly suited to meet the demands of low operating effort in the presence of (undesired) forces, especially when springs are used to avoid the weight and inertia associated with counterweights.

A design approach was proposed in which different methods and perspectives would alternate. This applies firstly to the alternation of bottom-up and top-down approaches. The conceptual design was performed in a bottom-up fashion (chapter five), based on a framework of modification operations, which were in turn (partially) derived from existing designs (chapter four). Closer examination of the resulting designs inspired the top-down development of the theory presented in chapter three.

Another alternation was performed between the three perspectives of force, potential, and stability. Theoretically equivalent, their difference is one of emphasis. Switching from one to the other enriches the conceptual design of mechanical systems. Even though many examples were provided, no directives on when to use each of the perspectives were given. It was not intended to develop an automated design method. Instead, it was foreseen that a fair amount of creativity, knowledge of mechanics and kinematics, as well as the flexibility of mind to switch between different perspectives would be required to realize the designs in view.

The approach has resulted in a diversity of statically balanced spring mechanisms, both gravity equilibrators and spring force balancers; not only designs where a pre-existing undesired force was compensated, but also designs where the principle of static balance was included from the start. Prototypes

187

were made of several conceptional designs, both according to working principles derived in the chapter on perfect balance, and according to those derived in the chapter on approximate balance. They demonstrated good operation and provided feeling for the challenges involved in the elaboration of a diagram into a working model. As static balance eliminates the major operation forces, small errors easily result in a reduced range of equilibrium positions.

In addition to the designs themselves, the work has yielded two concomitant developments: a framework for the conceptional design of statically balanced spring mechanisms, and a general treatise on the stability of forces acting on a rigid body. These issues will be discussed successively.

Development of conception framework

One of the main accomplishments of the approach is the insight it provides in subsequent steps taken during the conceptional design phase, which may benefit the future design of mechanisms. This is in contrast with most literature (the patents by Carwardine amongst the exceptions), where conceptional designs appear as by miracle. Partly derived from existing systems, partly introduced by the author, a set of modification operations was proposed, namely the variation of parameters, rotation, shift, kinematic inversion, composition of springs, composition of spring-lever elements, and the exchange of spring-lever and mass-lever elements. Together with an elementary statically balanced mechanism (figure 3.6), they constitute a logical framework for the design of statically balanced systems. Its versatility was shown in chapter five, where also guidelines for the correct application were found. The most important ones are that the introduction of auxiliary parallelograms is useful, additional degrees-of-freedom can be introduced by kinematic inversion, and that rollers can often substitute links. Care was needed when imaginary links (put up by a parallelogram, see for instance figure 5.23) were considered, as they may collapse when changing the arrangement of masses and springs associated with them. Examples were given to illustrate the procedure. It was also shown that extension into the third dimension is possible. The whole procedure confirms the usefulness of the step-by-step bottom-up design approach. Successive extensions of a particular, elementary system have led to a general framework for the design of statically balanced mechanisms incorporating ideal springs. It was further shown that when the use of normal springs is required, the ideal-spring designs can function as initial estimates in optimization procedures. Rolling joints were shown to improve the resulting mechanisms, not only due to their low friction, but also because the non-linearity of their kinematics

facilitates matching of the normal springs' elastic potential functions. In many cases where strongly non-linear transfer functions are needed, complex linkages like four-bars can be avoided by using the hypocycloidal motion of two rollers.

Development of theory

The alternation of perspectives is prominently present in the relation between the systems designed and the theory developed. Close inspection of especially the spring butterfly (figure 4.23) led to a procedure for the composition of two forces in such a way that a point of application could be assigned to the resultant force [7.1]. It was found that the point of application of the resultant force of two arbitrary constant forces, which ensures dynamic equivalence (rather than instantaneous equivalence) is located on the circle circumscribing the points of application of the original forces and the intersection of their action lines. Subsequent investigation of the fundamentals from the perspective of stability has resulted in the theory presented in chapter three. Consideration of the contribution of two forces to the stability of a rigid body yielded an equation in addition to the resultant force and the resultant moment equations. This equation, called the stability equation, determined the location of the point of application on the line of action of the resultant force for dynamic equivalence. For constant forces, this point was the same as the one found using the circle. In the case of central linear forces, a different stability equation was found, and an additional translation along the resultant line of action was found to be required. The procedure was illustrated by the Floating Suspension, where the dynamically equivalent resultant of the spring forces was found to apply at the center of mass, according to the equations. The graphical procedure, assuming constant forces rather than ideal spring forces, yielded an application point right below the center of mass, at a distance according to the correction term.

Potential and force perspectives

The Floating Suspension is also a fine example of the profit alternating perspectives can give, namely the alternation of the potential energy perspective and the force directed design approach. The Floating Suspension would not have come to being had the forces not been considered. The wish to eliminate the pivot in the basic equilibrator led to the introduction of an additional spring force without losing static balance by applying the modification rule of the resolution of ideal springs, and the rotation rule. Investigation of the resulting configuration of forces (by skew resolution) paved the way to the elimination of the pivot. This example demonstrated the usefulness of the force directed design

approach. The force directed design approach is perhaps even stronger present in the design of the hand prosthesis in chapter six. Starting with the formulation of the design objective in terms of desired force distribution on the object held, the use of rolling links to avoid the introduction of undesired friction forces, and the application of a balanced system to (partly) compensate for the elastic glove forces, a conceptional design was developed which is light-weight, soft when relaxed, and which moves naturally. It once again demonstrates the value of a different vision on mechanical design, especially in rehabilitation technology.

7.2 Challenges

Certain – few – memories from the past have strong steel springs, and if we, in the present, touch these springs, they suddenly stretch, and shoot us into the future.

<div align="right">Yukio Mishima, 1956</div>

Besides the accomplishments, some loose ends remain. Chapter three, for instance, is limited to the two-dimensional case. In three-dimensional space, the action lines of two forces do not generally intersect. Clearly this obstructs the procedure of the circle construction (section 3.4). The moment introduced by the composition of forces in three-dimensional space also influences the mathematical treatise. No attempts have been made yet to account for this. Another unanswered question is what to do with the observed phenomenon that the dynamically equivalent of two central linear forces is a constant force. This statement was confirmed by the analysis of the Floating Suspension, yet not physically explained. The development of full understanding and the application to any other kind of system are logical lines of further investigation.

Another challenge is the simplification of the designs. Some of the examples presented are too complex for their intended use. For instance the spring force compensation of the four-bar linkage (figure 5.40b) yields a degree of complexity which is prohibitive in the application as a prosthetic hand mechanism (figure 5.41b). Indeed, the four-bar finger linkage is too complex to begin with, and the glove is far from a central linear force, yet the example is included to demonstrate the versatility of the conception framework, as well as to make the general statement that not only any mass, but also any ideal spring acting on any coupler point of a four-bar linkage can be compensated. Practical application may be less obvious, which may place the four-bar finger linkage in a category between fundamental research and applied technology called fundamental technology.

190

Notes

Notes to chapter one

[1.1]   *Energy efficiency.* Many authors mention the inefficient energy expenditure of current robots, and report improvements due to static balancing of the gravity forces. Asada and Youcef-Toumi (1984) designed a parallel drive mechanism for a robot in which power dissipation was reduced by about 70 percent, mostly due to static balancing using counterweights. Chung *et al.* (1986) report that in their balanced manipulator design the total variations of input torques were about three times smaller than those of the unbalanced one. Lim *et al.* (1990) found that payload capacity can be improved by about nine times through the introduction of a balancing mechanism. All of these balancing mechanisms are based on counterweighting. This requires the addition of masses. Therefore they are not appropriate in prosthesis design. Furthermore, due to the additional weight and inertia of the counterweights, mass-to-mass balancing is especially useful at low operating speeds. To reduce these drawbacks, several authors suggest static balancing with springs. Gopalswamy *et al.* (1992) suggest static balancing with a torsional spring, which may not be exact but yields a simple solution with great improvement of system behavior. Mahalingam and Sharan (1986) compare counterweight with spring balancing and conclude that spring balancing is superior. Ulrich and Kumar (1991) state that robots commonly exert as much as two-thirds of available joint torque to counteract gravity at full extension. They illustrate the power of static balancing by designing a prototype that consumes less than ten percent of the conventional arm. Rivin (1988) reports significant peak-torque reduction together with a more uniform loading leading to better performance and better energy efficiency.

[1.2]   *Design criteria prosthetics.* The Wilmer group at Delft University of Technology has been involved in the design of hand and arm prosthetics for several decades. In close collaboration with two specialized rehabilitation teams, general criteria for arm prosthetics have been derived that may be summarized as the triple-C demands: cosmetics, comfort, and control (Cool, 1981, 1991; Cool and Plettenburg, 1992). For most users an inconspicuous appearance is the primary goal of using a prosthesis. Furthermore, as the motoric function of the prosthesis is used only a few times per day (van Lunteren *et al.*, 1983), the burdens of wearing should be minimal. Weight and discomfort due to the fitting and possible harnesses should be as low as possible. Finally, the prosthesis should be easy to operate, in terms of operating effort as well as intuitive use. So, although it may be tempting to aim at increasing the motoric functionality, the main design efforts are to be directed at reducing the burdens. Further information on the Wilmer group is available from the Internet address http://www.wbmt.tudelft.nl/~wilmer and http://mms.tudelft.nl

[1.3]   *Feedback in hand prosthetics.* In body powered devices, feedback is intrinsically present. The central nervous system directs muscle action through alpha and gamma signals and reads the current status of the motoric system from sensors within muscles, tendons, around joints, and in tissue (Kandel and Schwartz, 1991). When there is a clear relationship between the state of limbs, tissue and musculature

that operate the prosthesis, and the state of the prosthesis, the proprioceptive information is useful for the control of prosthesis operation. This has been called extended physiological proprioception by Simpson (1974). To achieve this clear relationship in hand prosthetics, firstly operating force should correspond to pinching, and secondly the force transmission between operating site and pinching site should not be disturbed. The first demand is satisfied by the concept of voluntary closing control (Klopsteg and Wilson, 1964; Radocy, 1986). For the second demand, low friction and the elimination of other disturbing forces are required.

[1.4]   *Cosmetic glove.* The cosmetic glove covering the hand-like types of hand prosthetics (as opposed to the hook types) usually is made of PVC or silicone (Clarke *et al.*, 1947, Clarke and Weinberg, 1949; Dembo and Tane-Baskin, 1955; Carnelli *et al.*, 1955; Klopsteg and Wilson, 1968; Klasson and Winderlich 1969; Kenworthy and Small, 1974; Davies et al., 1977; Fillauer and Quingly 1979; Bilotto, 1986; Robert, 1989; Erb, 1989; Lee *et al.*, 1991; Arkles, 1983; Bruckner, 1992; Pereira *et al.*, 1992). As these materials are viscoelastic, some of the energy input is stored and recovered (elasticity), and some is dissipated (viscosity) during deformation (Ferry, 1970; Treloar, 1975; Bueche, 1979; Fung, 1981; Rosen, 1982). A study was carried out to asses some of the glove parameters, and to reduce both elastic and viscous forces (Kruit, 1987; Blom, 1990; Herder *et al.*, 1998). It was found that the stiffness of a specific glove-prosthesis combination was highly non-linear, the ultimate slope being about five times steeper than the initial slope. In rectangular specimens of a PVC glove, this factor was found equal to 3, approximately. Glove modification (melting grooves on the inside of the glove) reduced the elastic and viscous forces by 50% approximately. Optimizing finger motion resulted in an even greater positive effect in the particular case studied (Herder *et al.*, 1998).

[1.5]   *Static balancing using counterweights.* The addition or redistribution of mass can lead to significant improvements in system behavior, both by static and dynamic balancing. For a static consideration the reader is referred to Hilpert (1968), Skorecki (1971), Chung *et al.* (1984), Asada *et al.* (1985), Lim *et al.* (1990), Huissoon and Wang (1991). Specifically interesting is the work by Kreutzinger (1942), who constructs the center of mass of a four-bar linkage, an approach used to statically balance this type and the open chain type of linkage by Agrawal and Gökce (1998), Gökce and Agrawal (1999), and Agrawal *et al.* (2000). Rivin (1988) points out that mass balancing assures compliance with most requirements (including dynamic phenomena) to counterbalancing. References to the use of counterweights for dynamic balancing are included in [1.11].

[1.6]   *Static balancing using springs.* As opposed to counterweights (see [1.5]), springs do not add weight or inertia. Several authors worked on the design of spring mechanisms providing perfect balance in theory. Hain (1952, 1955, 1961) used special characteristics of zero-free-length springs (see chapter four) to balance the weight of hefty agricultural machinery, an approach that was generalized for several springs by Haupt and Grewolls (1963) and further by Streit and Gilmore (1989), and extended to three dimensions by Walsh, Streit and Gilmore (1991). Hilpert (1968), Shin and Streit (1991), and Pracht *et al.* (1987) expanded the theory to include additional links, for both open and closed loops, prismatic and revolute joints. Rivin (1988) describes a socalled sine mechanism incorporating a zero-free-length spring to compensate gravity induced actuator torques in various manipulator structures. Several authors apply static balance in the design of rehabilitation aids (Skorecky, 1971; Cool, 1976; Nathan, 1985; Rahman *et al.*, 1995). Gosselin (1999), and Gosselin and Wang (2000) present several

192

statically balanced multi-degree-of-freedom parallel manipulators. Several applications of static balance are found in Hoek (1986), later issued by Koster (1996).

The literature on balancing undesired effects other than gravity, such as unwanted elasticity, is limited. Mechanisms with elastic elements or plate springs may possess undesired stiffness. Van Eijk (1985) has designed a zero translational stiffness system by the smart use of buckled plate springs. Some reports are known on balancing parasitic spring forces generated in the cosmetic covering of hand prostheses (Hekman, 1979; Kruit and Cool, 1989), compensating for the finite stiffness of prosthesis fingers in grasping an infinitely stiff object (Eibergen Santhagens, 1985), the buckling of compression springs (Hirose, 1993), and magnetic force (Hirose *et al.*, 1986). Several other applications are included in Carwardine (1932a, 1932b, 1938), and in Hoek (1986).

A substantial body of patent literature is available on static balancing systems incorporating springs. Especially noteworthy are the patents by George Carwardine (1932-1938), including the Anglepoise desk lamp (figure 2.7). Many patents are special versions these, see for example Vertut (1981), who describes version of Anglepoise principle, as do Guilbaud and Vertut (1971), Mosher and Kugath (1971), and Tuda *et al.* (1986). An application of Carwardine's vertical-base parallelogram equilibrator is described in Brown and DiGuilio (1980). There is also a large number of patents describing modifications of the basic gravity equilibrator (figure 5.1b), including Neumann *et al.* (1993), Tsuda (1980); Gerlach (1993); Spronck (1984); Hahn *et al.* (1987); Goro *et al.* (1983). An extension with a spatial version and a floating suspension is patented by Herder and Tuijthof (1998), see also sections 5.2 and 5.5 of this thesis.

[1.7]   *Mechanism design.* There is a vast literature on mechanism design (*e.g.* Reuleaux, 1876; Hall, 1961; Hirschhorn, 1962; Hartenberg and Denavit, 1964; Hain, 1967; Suh and Radcliffe, 1978; Hunt, 1978; Erdman and Sandor, 1997). The design of mechanisms is often divided in two phases: type synthesis and dimension synthesis. The design starts with the specification of desired motion characteristics, in which three categories are usually distinguished: path generation, body guidance and function generation. In the first phase (type synthesis) a suitable mechanism type is selected, such as a four-bar linkage, a slider-crank or a cam system. In the second phase (dimension synthesis) the dimensions are determined, classically based on graphical methods, such as geometry (*e.g.* Ruzinov, 1968), kinematics (*e.g.* Bottema and Roth, 1990) or Burmester theory (*e.g.* Beyer, 1963). Fast computers have stimulated the use of sophisticated optimization methods in the design of mechanisms based on vector algebra (*e.g.* Haug and Arora, 1979; Erdman and Sandor, 1997), finite elements (van der Werff, 1977; Klein Breteler, 1987), and even randomized design methods (*e.g.* Camuto and Kinzel, 1998).

[1.8]   *Force directed design.* The ideas on force directed design are still maturing. The essence, in a narrative style included in professor Cool's valedictory address (1995) and more technically in Cool (1997), is that when forces are applied in a correct manner, the desired motion will follow as a matter of course (Verdult, 1998). Echos of Cool's work can be found in the references under [1.9]. Other literature related to force directed design includes the following. First and foremost, the laws of statics can be used, preferably in their graphical form with free-body diagrams, extendible to more than three forces by using the Pole Force Method (Hain, 1967). Especially at contact points, such as between rollers in Rolling Link Mechanisms (Kuntz, 1995), acting lines of forces prescribe preferable configurations. The procedure used in this thesis is similar to the construction of Force-Closure Grasps for manipulative grippers by

Nguyen (1988) in the sense that desirable configurations of action lines determine the force attachment points and thus the geometry of the design. Secondly, methodologies have been developed which include the specification of force transmission characteristics in dimension synthesis. A first group can be identified that concerns instantaneous input-output relationships, for instance the Instant-Center Approach for mechanical advantage determination (Erdman and Sandor, 1997), a second group that handles continuous forms of force transmission functions, such as the Mechanical Advantage Method (Bagci, 1987a and 1987b), and a third group that includes load bearing capacity during motion, for instance Force Synthesis (Roth, 1989; Huang and Roth, 1993, 1994), where movement and enforcement are considered simultaneously. In addition to these 'force methods', several methods have been developed that include force considerations through energy specifications. These include the Integration of Power Equilibrium Method (Bagci, 1987a and 1987b), and the Synthesis for Specified Energy Absorption (Jenuwine and Midha, 1992). Unlike the present thesis, these works are mainly concerned with dimensional synthesis, rather than with conceptional design.

[1.9]   *Applications of force directed design.* Projects in rehabilitation technology where a force directed design approach has proved to be very useful include the Wilmer elbow orthosis (Cool, 1976). This device statically balances the weight of the forearm (which allows the control of a paralyzed elbow by the shoulder muscles, see the description of figure 2.5 in chapter two), and is designed such that only normal stress is exerted to the patient's skin, in any position of the arm. Furthermore, all fitting forces are in a single plane, which allows a single-sided pivot without torsional moments. Another example is the Wilmer open socket, a socket with just enough contact areas to be able to generate the required support forces, thus leaving 75% of the skin free (Walta *et al.*, 1989). Other examples are a knee-ankle-foot-orthosis for persons with instability of the knee (van Leerdam, 1993), and the design of a scoliosis orthosis for persons with severe thorax deformation (Nijenbanning, 1998). Kuntz (1995) describes the design of a high efficiency hook prosthesis for children based on rolling links. Another noteworthy development is the design of an adaptive hand prosthesis by De Visser (1998) and Herder and De Visser(2000) in which the force transmission function of the mechanism and the shapes of the elements are optimized simultaneously. A different application is the force directed design of a directional drilling device that creates a U-shaped tunnel inside a human vertebra (Verdult, 1998). For use in minimal access therapy, low friction forceps were developed based on force directed design (Herder and Horward, 1998; Herder, 1998b, see also [5.16]).

[1.10]   *The need for simple mechanisms.* Already since the time of the mechanical analogue computing machines, which were highly complex, efforts have been undertaken to set up design methods to realize mechanisms with a specified transfer function. Klein Breteler (1987, 1990) describes a procedure for the synthesis of linkages based on the Fourier-coefficients of the desired transfer function. However, this procedure and some of the procedures listed under [1.7] tend to result in fairly complex mechanisms, usually comprising at least a four-bar linkage and a number of gears or cams. From an efficiency perspective, every hinge is one too many and a four-bar linkage must already be considered troublesome (see also [1.14]). For the same reason, spring actuated cam-followers (*e.g.* Klein Breteler, 1990) are not present in this thesis.

[1.11]   *Dynamic balancing.* Dynamic balancing or force balancing has been studied extensively in literature, for instance in Berkof and Lowen (1969), Stevenson (1973), Oldham and Walker (1978), Bagci (1992), Ricard and Gosselin (2000), and in the extensive literature cited by Lowen *et al.* (1983), and by Yao and Smith (1993).

Mechanisms are said to be force-balanced when the total force applied by the mechanism on the fixed base is constant for any motion of the mechanism. Mechanisms are said to be statically balanced, when the weight of the links does not produce any torque (or force) at the actuators under static conditions, for any configuration of the mechanism. This condition is also referred to as gravity compensation (Wang and Gosselin, 1998).

[1.12] *Specified dynamics.* In the dynamic domain, the equivalent of static balancing is the design of oscillating systems, where mechanisms are furnished with appropriate combinations of masses and springs in order to perform desired motion in their natural frequency (*e.g.* Van der Linde, 1999). In these cases, potential and kinetic energy are exchanged during movement, again in such a way that the total energy of the system is constant, thus eliminating the need for external energy. Note that this kind of dynamic balancing is different from the shaking force kind of dynamic balancing. Another dynamic approach could be to include kinetic energy specifications to satisfy acceleration requirements over some range of motion (*e.g.* Idlani *et al.*, 1993). These issues may comprise challenging extensions, but they are beyond the scope of this thesis.

[1.13] *Compliant mechanisms.* Compliant mechanisms gain some or all of their mobility from the flexibility of their members rather than from rigid-body joints only (Howell and Midha, 1995). They have many potential advantages, such as the reduction of the number of parts, reduced weight, wear, backlash, noise, need for lubrication, and reduction of manufacturing and assembly cost and time. Reported disadvantages are the complexity of their design, the nonlinearities introduced due to the large deformations, and the energy storage in the flexible members (*e.g.* Sevak and McLaranan, 1974; Salamon, 1989; Burns and Crossley, 1968; Ananthasuresh and Kota, 1995; Howell, 1993; Howell, Midha and Murphy, 1994; Howell and Midha, 1995; Howell, Midha and Norton, 1996). Examples of statically balanced compliant mechanisms are very rare. Van Eijk (1985) has studied zero-stiffness straight-line guidance by using buckled plate springs, while Van den Berg (1999) and Herder and Van den Berg (2000) report on a compliant forceps design incorporating a separate rolling-link compensation mechanism. When the segments of the flexible robot arm Elastor are considered compliant members, this is another example (see figure 2.9; Hirose, 1993).

[1.14] *Rolling-link mechanisms.* Rolling-link mechanisms are mechanisms consisting of links that are shaped such that they roll directly on one another, so that no specific bearing elements are needed. Thus avoiding sliding friction, they possess a high mechanical efficiency, comparable to ball bearings. However, as compared to ball bearings, rolling-link mechanisms consist of fewer parts, take up less space, possess higher load bearing capacity, are virtually insensitive to pollution, have no backlash, and require no lubrication. Another advantage is that rollers allow straightforward transfer of forces, as opposed to the situation with ball bearings, where the forces are guided through fork constructions. Disadvantages are that the elements require special shaping for each application (no off-the-shelf parts) and the care that must be taken to assure contact between the elements. A spring hinged on a pin such that the inside of the loop is rolling on the pin, in the plane of motion, constitutes a special rolling joint (Hoek, 1986). Literature on these mechanisms includes Whitehead (1954); Sieker (1956); Godden (1968); Newman (1973); NASA (1985); Rivin (1988); Kuntz (1995); Herder *et al.* (1997). The Rolamite is described in Wilkes (1967); Brickman (1967); Cadman (1969); Wise (1967); Betts (1979), and Lushbough (2000). Patent literature

includes the following: Carwardine (1931a, 1931b), Hillberry and Hall (1976), Bora Jr. (1981), Ruoff (1985), and Herder and Horward (1998).

[1.15]   *Sparse application*. Baudisch (1985) and Papadopoulos (1997) point out that non-perfect balancing or the additional parts and cost involved in balancing devices prohibit their use in some cases. Rivin (1988) and Baudisch (1985) note that friction in some cases accounts for a force balancing error of 20%.

[1.16]   *System, shape, material*. Distinguished by Cool (1990) as the three principal influence factors in mechanical design.

[1.17]   *Desired balancing quality*. Citation from Hall (1961).

Notes to chapter two

[2.1]   *Kinetic Art*. Several similar works of art designed by George Rickey (1993). The one in the picture is in permanent outdoor action in the heart of Rotterdam, the Netherlands. Three of these Breaking columns, two hanging, one standing in the center, are mounted on the front of the theater.

[2.2]   *Dionysos*. Reconstruction of the mechane by Dimarogonas (1992).

[2.3]   *Drawing board*. See for instance Hilpert (1968).

[2.4]   *Arm support*. This linkage was designed in the course of the development of a mobile arm support for people with reduced muscular ability by Skorecki (1971). See also [5.25].

[2.5]   *Floating bodies*. Mauldin, cited in Wells (1995).

[2.6]   *Internally-balanced magnet*. Hirose et al. (1986).

[2.7]   *Wilmer*. This orthosis was designed by Cool and other members of the Wilmer group (Cool, 1976). The picture was taken from the Internet address of the Wilmer research group at Delft University of Technology: http://mms.tudelft.nl or http://www.wbmt.tudelft.nl/~wilmer, displaying a number of orthotic and prosthetic products.

[2.8]   *Anglepoise*. The Anglepoise desk lamp is still available in different versions. Information on these products can be found at the Internet address of Anglepoise Ltd.: http://www.anglepoise.com. Information on the inventor and designer George Carwardine, his patents, and related work (including parts of this thesis) are available from www.carwardine.org.

[2.9]   *Laval University Robotics Laboratory*. The picture can be found on the Internet address http://wwwrobot.gmc.ulaval.ca/recherche/theme05_a.html of the Laval University Robotics Laboratory, headed by Prof. dr C.M. Gosselin. The site also shows two working models of statically balanced three-degree-of-freedom parallel mechanisms.

[2.10]   *Glove compensation*. Kruit and Cool (1989).

[2.11]   *Hirose and Yoneda Laboratory*. The Elastor was designed by Hirose (1993). The picture is available from the Internet address of the Hirose and Yoneda Lab: http://mozu.mes.titech.ac.jp.

[2.12]   *Loop in hose*. This phenomenon was suggested by Van Dieten (1997-1998).

[2.13]   *Rolamite*. Designed by Wilkes (1967).

[2.14]   *Knife edge pivot*. Wolf, cited in Van der Hoek (1986).

[2.15]   *Balanced plate springs*. Van Eijk (1985) presents straight-line guides based on buckled plate springs so as to provide zero translational stiffness along the guide path.

[2.16]   *Contact pressure*. A nice example is present in Van der Hoek (1986), p148.

[2.17]   *Vibration isolation*. See for instance Chironis (1961), p252, Haringx (1948), and Alabuzhev *et al.* (1989), who suggest stiffness correctors to arrive at vibration isolation systems with quasi-zero stiffness.

[2.18]   *Ballistic systems*. See for instance Van der Linde, 1999.

[2.19]   *Zero gravity simulation*. Several techniques are applied to attain zero gravity, mainly in space research: horizontal centrifugation, inclined plane technique, suspension systems, parabolic flight, and neutral buoyancy (Luna *et al.*, 1993). An overview of the suspension systems for the purpose of metabolism research is given by Davis and Cavanagh (1993). Some counterweight-based compensation mechanisms are presented by Brown and Dolan (1994), while constant-tension springs are used by Sato and Ejiri, 1991.

[2.20]   *Reduced loading characteristics*. Matthew and Tesar (1976), Rivin (1988).

[2.21]   *Improved performance*. See for instance Ulrich and Kumar (1991) and Rivin (1988).

Notes to chapter three

[3.1]   *Acknowledgment*. This chapter has been developed in the course of numerous discussions with a number of people in various circumstances. In the first place regular meetings with my supervisor, Prof. ir J.C. Cool. A presentation at a colloquium of the Section of Technical Mechanics at Delft University of Technology elicited ten pages of handwritten comments from Prof. dr ir J.F. Besseling, stressing the possibility of a more formal derivation. His encouragements led to the involvement of Dr ir A.L. Schwab, who suggested much of the structure of chapter three, and close-edited parts of it, thus lending great support.

[3.2]   *Composition of forces*. Many textbooks on mechanics describe the procedure of the composition of forces, *e.g.* Beer and Johnston Jr. (1997), Meriam and Kraige (1987a and 1987b). A treatise on dynamic equivalence was not found in literature.

[3.3]   *Equivalence*. The term dynamically equivalent force should be well distinguished from the term equivalent force, which is used for instance in Beer and Johnston Jr. (1997), which denotes instantaneous equivalence only: "The *principle of transmissibility* states that the conditions of equilibrium or motion of a rigid body will remain unchanged if a force *F* acting at a given point of the rigid body is replaced by a force *F'* of the same magnitude and same direction, but acting at a different point, *provided that the two forces have the same line of action*. The two forces *F* and *F'* have the same effect on the rigid body and are said to be *equivalent*" (Beer and Johnston Jr., 1997, p73).

[3.4]   *Mechanics.* Many references are available on the equations of motion, the principle of virtual work, and the energy potential. To a great extent, they have their origins in the work by Lagrange (1997). Other references include Beer and Johnston (1997), Meriam and Kraige (1987), Bottema (1987), Roest (1990), and Alonso and Finn (1971).

[3.5]   *Circle construction.* Prof. ir J.C. Cool was the first to discover this circle-construction (see also [7.1]).

[3.6]   *Geometry.* Much has been taken from Introduction to Geometry by H.S.M. Coxeter (1989): the circle of Apollonius (p88) which is found as the locus of a point whose distances from two fixed points are in a constant ratio; pencils of circles (p85); and orthogonal circles (p79). Other notable works are by Coxeter and Greitzler (1967), Bottema (1987), and Bottema and Roth (1990).

Notes to chapter four

[4.1]   *Mechanism synthesis.* Of the classical tasks of mechanisms, i.e. path following, rigid body guidance, and function generation, the design of an adjustment mechanism is closest to the latter, since not the absolute movement but the relative movement of the energy storage elements is of importance. Classically, to support mechanism design, the process is often divided into two phases: type synthesis and dimension synthesis (*e.g.* Hall, 1961), also called conceptual design and optimal design (*e.g.* Haug and Arora, 1979). Once the desired function of a system has been defined, an appropriate mechanism topology (type) is selected first, and then the geometry is optimized. When the body of literature on mechanism synthesis is overlooked, it is clear that great efforts have been directed towards the dimensional synthesis, especially of four-bar linkages. Known methods range from kinematic synthesis (*e.g.* Hain, 1961; Hartenberg and Denavit, 1964; Dijksman, 1976; Hunt, 1978), via loop closure (*e.g.* Erdman and Sandor, 1997; Midha and Zhao, 1985), finite element methods (Van der Werff, 1976; Klein Breteler, 1987), to random walk algorithms (Camuto and Kinzel, 1998). Type synthesis is performed by way of classification (Grashof, 1883), supplying an atlas of examples (Hrones and Nelson, 1951) or by permutational or number techniques (*e.g.* Hain, 1961; Johnson and Towfigh, 1971; Freudenstein and Maki, 1980; Erdman *et al.,* 1980).

[4.2]   *Zero-free-length springs.* Many authors who are concerned with static balancing use zero-free-length springs, often without too much concern on how these springs are to be realized. Carwardine was probably the first to introduce the concept of zero free length, as he mentions their characteristic explicitly in one of his patents (1932), proposes a mechanism to simulate zero free length behavior (1932), and describes in great detail how to manufacture these springs by increasing the preload (1934). Other useful publications on the theory and manufacturing of springs with initial tension includes Andreeva (1966), who distinguishes three coiling schemes for springs with initial tension (twisting, partial-overlap, and pins method) and alerts to possible loss of stability in springs with initial tension. Carlson (1961) provides a diagram on attainable initial tension.

   The compression spring and brackets are described in Hoek (1986) and Koster (1996), as well as by Küspert *et al.* (1998). Another kind of ideal spring arrangements stores the initial length behind a pivot and aligns the spring using some guiding device. Many versions are described, including those by Carwardine (1932), Haupt and

198

Grewolls (1963), Streit and Gilmore (1989). Apart from aligning solutions, another group is formed by arrangements of a string attached to a normal spring guided by some element, such as an eye (*e.g.* Walsh *et al.,* 1991) or a pulley (e.g. Hain, 1952; Pracht *et al.,* 1987; Soper *et al.,* 1997). Usually the spring is stored on the fixed body or frame, but sometimes on the moving link (Nathan, 1985; Rahman *et al.,* 1995).

Most zero-free-length springs are not described separately but in connection with the application of mass balancer, as is also the case for most ideal spring arrangements. A few special mechanisms were found in which normal springs are arranged so that they exhibit ideal spring behavior. These mechanisms will be described in section 5.4. In addition to these, Hilpert (1968) describes a mechanism incorporating a slider and a 2:1 gear train, which perfectly adjusts a normal spring to a mass. Hervé (1983, 1986a, 1986b) was granted a patent on a similar mechanism using a chain instead of gears. As these mechanisms are too complex for the goals in this thesis, they will not be discussed further. Some additional remarks are provided in appendix 4.1.

[4.3]   *Paraboloids.* These figures were drawn by Marc L. Brinkman, who at the time of this writing is doing a MSc-project on statically balanced laparoscopic forceps, see figure 5.37 and [5.16].

[4.4]   *Modification rules.* Several authors have reported one or several of the modification rules presented in this chapter. Hain (1952, 1961), Halter and Carson (1975a and 1975b), Carson (1976a, 1976b), Matthew and Tesar (1976), Oostvogels (cited in Hoek, 1986), Rivin (1988), and Kochev (1991) make remarks about the variation of parameters and the rotation rule, while Haupt and Grewolls (1963) describe the composition of ideal springs.

[4.5]   *Carwardine.* This geometric insight may very well have put George Carwardine on the track of the invention of a number of statically balanced spring mechanisms: "Referring to Figure 1, a member b o c has pivoted at its middle a lever arm o a of length A which is the radius of the circle of which b c is a diameter. It follows from the 31st proposition in the third book of Euclid that since the path of point a is a circle then angle b a c is always a right angle and angle b a o is always the trigonometric complement of the angle o a c. An elastic member such as a helical extension spring is stretched between the points a and d on line a c produced and is considered to be strained by an amount equal to the length a c. It can be shown that if another spring of the same stiffness were stretched between points a and e on line a b produced, then the moments exerted about o by the spring between a and d would be exactly balanced for any position of the lever arm o a provided that this latter spring be arranged so that its strain is represented by the length a b " (Carwardine, 1932).

[4.6]   *Adjustable stiffness.* This solution for an adjustable spring has been applied in an office chair with a static balancer. The idea behind this chair was to carry the person (constant force) through a limited range of motion, in order to stimulate mobility of the spine and to reduce low back pain. A patent has been applied for (Vrijland and Herder, 2001). Akeel (1987) describes another mechanism featuring a variable counterbalance force.

[4.7]   *Geometry of faulty DEPs.* A lot of geometric regularity is associated with the construction of the DEPs of the spring butterfly. Note that the construction is only valid for constant forces so that an error is introduced. The fact that this error is constant accounts to a great extent for the geometric phenomena. Some of these will be mentioned here. The faulty DEP of the spring forces associated with the moving triangle (DEP_{mov}) and the faulty DEP of the spring forces associated with the fixed triangle (DEP_{fix}) trace circles as the moving triangle rotates about the pivot. Both DEPs

and the pivot are collinear in such a way that the pivot is the (internal) center of similitude of the two circles (for more on the center of similitude of two circles see Coxeter, 1969).

Notes to chapter five

[5.1] *Wilmer elbow orthosis*. The development of this orthosis illustrates that a considerable amount of creativity and smart engineering are required for a diagram (figure 5.1b) to evolve into a commercially available product (figure 2.6 and corresponding explanation in text; Cool, 1976). Notable features are the single-sided hinge and the low weight. The use of a single-sided hinge is possible due to the fact that the main forces are in one plane. As a result, the hinge is not loaded by torsional moments. The omission of a second hinge contributes to low weight, as does the stainless steel tubing of oval cross-section, and the rubber spring (high energy-storage to weight ratio).

[5.2] *Spring mass*. Inclusion of spring mass need not introduce a balancing error. This can be demonstrated using potential energy calculus such as in Streit and Shin (1993), or the approach used here, where the forces exerted by the spring are resolved into components along the centerline of the spring (equal and opposite spring forces) and vertical components. As the weight of the spring is independent of its excursion, the vertical components at the spring ends are always vertical and half the magnitude of the spring weight. Therefore, the weight of the spring can be modeled as two masses at the spring ends, each equal to half the spring mass.

[5.3] *Parallelogram linkage*. The peculiar features of the parallelogram linkage in its use in (mass-to-mass) balancers is attributed to Robertval by N. Treitz, who gives examples at http://ubntint.uni-duisburg.de/hands-on/files/autoren/treitz/treitz.htm). The linkage was also applied in balancers by Carwardine (1932), and by Streit and Shin (1993), who call it "vertical-link system".

[5.4] *Constant force generators*. This term was introduced by Nathan (1985), who describes a mechanism to adjust the spring-lever element to a varying load. To this end, a pulley and string system connects the mass and the attachment point of the spring on the link. Under special conditions, including a horizontal position of the link, the attachment point is automatically positioned into the correct position by the load. Other constant force mechanisms can be found in Boerner (1954); Pich and Wiemer (1955); Gärtner (1957); Groesberg (1960); Chironis (1961); Jenuwine and Midha (1989).

[5.5] *Patent*. The Floating Suspension has been patented in its simple one-degree-of-freedom form (figure 5.13), and in the form of the spatial floating anthropomobile arm (shown in planar form in figure 5.27), together with the pivoted anthropomobile arm (figure 5.50) (Herder and Tuijthof, 2000).

[5.6] *Demonstration model*. This demonstration model was skillfully manufactured by Ing J. Verbeek in 1996. Since then it has traveled the world, and has been played with by numerous students and a considerable number of professors. Yet the strings have not been replaced to date. At the time of writing this, the model never even had to be readjusted.

[5.7]   *General form of floating suspension.* The existence of a general form of the floating suspension was suggested by Prof. Andy Ruina during a visit to our group at Delft University of Technology. On this occasion, a broom was balanced according to the floating suspension configuration, using latex covers for medical instruments as ideal springs. Unfortunately, no photographs of this event are available (Ruina, 1997-1998; see also http://www.tam.cornell.edu/~ruina/ under random mechanics).

[5.8]   *Pantograph linkages.* A treatise on pantograph linkages, including the skew pantograph or plagiograph is found in Dijksman (1976), and in Tao (1964).

[5.9]   *Anglepoise.* Citation from the Anglepoise website [2.2], see also the photograph in figure 2.7 and a close-up in figure 5.26 (Anglepoise is a registered trademark, see also [2.8]). French (2000) published a paper on the Anglepoise lamp.

[5.10]   *Balanced five-bar parallelogram linkage.* Many multilegged robots have legs with two segments, extended to the configuration of a five-bar parallelogram linkage in order to be able to mount the motors on the frame. Example of statically balanced versions of these legs found in Shin and Streit (1991) and Shieh *et al.* (1996). Some direct-drive robots have a similar structure including one of several kinds of static balancer (*e.g.* Asada and Youcef-Toumi, 1984; Gopalswamy *et al.*, 1992; Huissoon and Wang, 1991; Ulrich and Kumar, 1991a and 1991b; Shieh *et al.*, 1996).

[5.11]   *Published previously.* Parts of this section were published previously (Herder, 1998a and 1998c).

[5.12]   *Ligaments as balanced springs.* Not so much a design example but all the more a balanced-springs configuration might very well be the configuration of ligaments in some biological joints. Generally, ligaments are ascribed a movement-limiting function. Although it is beyond doubt that there are ligaments with this function, this does not explain why the two bone parts of a joint are in firm contact throughout the range of motion, even when all muscles are fully relaxed. However, it is known that ligaments are elastic to a high degree. Ker (1981) showed that 93% of the work done stretching ligaments is returned during recoil (cited in Alexander, 1990). It might be nice to think of the ligaments as a biological balanced configuration. This would very elegantly explain the combination of firm contact and easy movement. The forces present keep the joint firmly together, yet the force generators, i.e. the springs, balance each other so that they generate zero joint moment. Thus, it is imaginable that a primary function of the ligaments is to ensure firm contact between bones throughout their range of motion, without undesired side effects such as elastic counteraction of movement. (Alexander, 1990)

[5.13]   *Elliptic trammel.* The statically balanced ladder was previously described in Carwardine (1932), Van der Hoek (1986), and Koster (1996). The elliptic trammel or Cardan mechanism is a well known mechanism (*e.g.* Hunt, 1978). The rolling version was discovered and actually made by Cool (1994).

[5.14]   *Laparoscopy.* Laparoscopic surgery is an operating technique based on several small incisions in the abdominal wall instead of a single large one. In spite of limited accessibility, it is still possible to perform operations of considerable importance (*e.g.* Cuschieri, 1995; Dallemagne *et al.*, 1991; Jansen, 1994; Wilson *et al.*, 1995). Hospitalization time is significantly reduced, and the advantages for the patients have led to widespread acceptance of this technique for several treatments. In comparison with conventional operating techniques, however, the fact that in laparoscopic surgery the surgeon is deprived of a direct view and touch, presents a serious impairment. Instead of direct vision, a 2D-image must be obtained from a

monitor, and contrary to conventional surgery in which the surgeon can manually manipulate and palpate tissue, all manipulations must be carried out using laparoscopic instruments. Thus, only severely limited tactile information is available for the surgeon, since mechanical feedback is obtained solely through these instruments.

It is therefore important that laparoscopic instruments possess good mechanical qualities. According to the concept of *extended physiological proprioception* (Simpson, 1974), originally derived for hand prostheses, good feedback of motion and force variables enhances the perception of an instrument to be an extension of the human body. With regard to both force and movement feedback, laparoscopic graspers preferably have a constant force transmission characteristic throughout its range of motion. This implies the absence of friction or other energy dissipating phenomena, and backlash (Sjoerdsma *et al.*, 1997).

Laparoscopic grasping instruments currently available allow only minor perception due to several mechanical deficiencies. Most current forceps contain slide bearings. The better forceps are furnished with pin-in-hole journal bearings, whereas others possess pen-in-slot joints (Melzer *et al.*, 1992). Since normal lubrication is not feasible for mechanisms entering the human body, overall friction is considerable, especially under loaded conditions. The mechanical efficiency of the best of these graspers is only about 33%. In addition, the force transmission ratio varies up to a factor of 6 over the working range (Sjoerdsma *et al.*, 1997).

In principle, it is possible to circumvent the problems of a non-linear force transmission characteristic and the presence of friction by measuring the grasping force with a sensor, and reproducing this force on the operating handle by using a servo system (*e.g.* Hill *et al.*, 1994; Howe *et al.*, 1995; Green *et al.*, 1995; Lazeroms *et al.*, 1997; Majima and Matsushima, 1991). This tele-operation approach should allow easy adjustment of the transfer function, which may be advantageous for example in situations where operating forces are below the human sensory threshold, such as in microsurgery, and tremor can be filtered out before the master's movement is transmitted to the slave unit. However, master-slave systems are complex, sensitive to disturbances, may suffer from contact instability (Sheridan, 1996; Lazeroms *et al.*, 1997), and may be unreliable in comparison with non-active systems. Besides, an electric feed wire would present a serious practical inconvenience.

[5.15]   *Rolling-link medical forceps.* To overcome the problems mentioned in [5.14], a simple mechanical solution, which inherently possesses both a constant force transmission characteristic (maximum deviation about 3%), low friction (mechanical efficiency about 96%) and no backlash was developed (Horward, 1995; Herder *et al.*, 1997; Herder and Horward, 1998). A brief discussion on this mechanism is given in appendix 5.1.

[5.16]   *Balanced medical forceps.* The development of the spring-balanced forceps is pursued by graduate students M.L. Brinkman and J. Drenth. Due to the fact that the use of normal springs requires optimization, several constructive simplifications were considered. The large-radius support planes were approximated by flat surfaces, and the closing spring was moved to the handgrip, where much more space is available. The other spring was made adjustable to provide slight voluntary opening or voluntary closing behavior (see also [6.10]). Due to the similar construction as compared to the version with two connecting rods (see [5.15]), it is expected that the spring-balanced version will perform comparably.

[5.17]   *Complex solutions.* Hervé (1986) and Hilpert (1968) independently present a highly similar perfect gravity balancer, incorporating gears and a linear guidance. Due

to its complexity and the slider, the design is not practical for the purposes in view of this thesis.

[5.18]   *Wrapping cams.* Several authors propose the use of flexible bands, cables, or chains, wrapping on irregularly shaped cams (Hain, 1953; Baudisch, 1985; Okada, 1986; Ulrich and Kumar, 1991a and 1991b; Fidweel *et al.*, 1992).

[5.19]   *Positive and negative free length cancel.* Streit and Gilmore (1989) demonstrate that a normal (positive free length) and a negative free-length spring arrangement together can be designed to act as an ideal spring, even though the conditions for achieving this are rather strict. Consequently, a pre-existing normal spring can be perfectly balanced by adding a negative free-length spring arrangement and compensate using an ideal spring. However, in other cases this approach is not attractive since realizing a negative free length involves the same additional constructions as does a zero-free-length spring. It will therefore remain unattended to in the remainder of this thesis.

[5.20]   *Figure-of-eight mechanism.* A similar mechanism appears in a patent by Carwardine (1932). Evidently, geometric insight triggered the invention. Independently, and ignorant of Carwardine's patent, the same working principle (with flexible bands instead of a connecting rod) was found by employing the approach presented here.

[5.21]   *Prototype.* The prototype of the spring-to-spring version of the figure-of-eight mechanism was manufactured by Ing J. Verbeek. Bloem *et al.* (2000) optimized its performance. The balancing error is well below 1%.

[5.22]   *Equilibrator version of figure-of-eight.* The perfect gravity equilibrator was developed by Te Riele (Te Riele, 2000; Te Riele and Herder, 2001). Previously, Te Riele (1997) presented an approximate version of the mechanism presented here.

[5.23]   *Wrapping compensation.* At the occasion of a visit to his lab, Prof. dr S. Hirose suggested that the error of a string wrapping on one pulley could possibly be compensated by wrapping the other end of the string on another pulley. In several projects, the perfect solution presented here as well as others were found by Soethoudt, 1998; Brinkman, 1998; and Cardoso and Tomázio (2001). The last mentioned found a solution including multiple degrees of freedom.

[5.24]   *Spatial balancers.* Walsh *et al.* (1991) investigated spatial gravity equilibrators comprising *n* springs acting on a single link pivoted by a Hooke's joint. Gosselin and his group designed a number of statically balanced parallel manipulators, ranging from three to six degrees-of-freedom; with revolute as well as with prismatic actuators (Leblond and Gosselin, 1998; Ebert-Uphoff, Gosselin *et al.*, 1998; Wang and Gosselin, 1999; Wang and Gosselin, 2000; Gosselin, 1999; Gosselin and Wang, 2000). Several legs work together in a complementary way to perfectly balance the moving platform. One example is given in figure 2.8. This system stimulated the development of the General Suspension Unit in figure 5.53.

[5.25]   *Mobile arm supports.* Other research in this field includes the works by Pritchard and Windsor (1965), Skorecki (1967 and 1971), Fielding *et al.* (1971), Cowan *et al.* (1975), and Rahman *et al.* (1995), Chyatte and Vignos (1965), Harwin (1997), Homma and Arai (1995), Landsberger *et al.* (1998), Rahman *et al.* (2000), Stern and Lauko (1975). Patents include Gammer and Broekl (1996), and Brown and DiGuilio (1980).

In spite of substantial research, not many arm support systems are commercially available. Among the major design challenges yet to be solved are the shoulder joint, the fitting of an arm support to the human body, and (due to the fact that most arm supports take the place of the conventional arm rest) the issue that one is not capable of finding support against trunk unbalance on a statically balanced arm rest. The shoulder joint should ideally be located at the location of the human shoulder joint. Apart from the fact that it is not fixed but highly mobile, it is not accessible. One solution is the one applied in the MULOS project: a three-dimensional cardanic joint (three intersection axes of rotation; Johnson and Buckley, 1997).

A project on the design of a statically balanced arm support in which the problems mentioned above are solved is currently in progress at Delft University of Technology (Cardoso and Tomázio, 2001).

[5.26]   *Anthropomobile arm*. The device has been patented (Herder and Tuijthof, 2000), together with the Floating Suspension and the floating version of the anthropomobile arm. A formal proof of the correctness of the equilibrator design in the pivoted arm, based on potential energy, is included in Tuijthof and Herder (2000).

[5.27]   *Prototype of anthropomobile arm*. Original prototype developed by Tuijthof during her MSc-project (1998). Subsequent improvements by Ros and Scholten (1999) and Van Weverwijk and Fokkert (2000). Contributions were made by Surentu and Van der Linde (personal communication). Most of the mechanical details are described in Tuijthof (1998), Tuijthof and Herder (2000), and Herder and Tuijthof (2000). Some aspects are repeated here. For the ideal spring embodiment a choice was made between the helical extension spring with increased initial tension, and the approximate solution of the pulley and string arrangement (see section 4.2). Due to the spatial movement, a simple pulley would not suffice: it should be rotatable about the vertical axis through the shoulder joint. This can be realized but the singularity associated with this construction would present a serious problem for spring k_1. To eliminate this problem, the string can be guided through a smoothened hole. However, to avoid friction and wear in the string, the springs with increased preload were selected. A spring manufacturer (Roveron BV; Van Rhee, 1996-2000) was found willing to devise these special springs. It proved to be difficult to accurately predict the amount of initial tension. Springs with an unusually high spring index (ratio of coil diameter to wire diameter) performed best. Screw-in spring ends were made and adjusted to obtain the desired zero-free-length behavior. Note that the stiffness of the spring is much less critical than the free length: the balancing characteristics depend on the product *rka*, and can therefore be tuned by adjusting *r* or *a*. For reasons of convenience, the fixed points of the springs were made adjustable. The attachment of the moving spring ends required special attention due to the spatial mobility. Low friction and low wear at the spring ends are favored by rolling suspension. In a planar mechanism, this is achieved when the spring loops are in the plane of movement and the insides of the preferable large spring loops roll on thin suspension axes perpendicular to the plane of movement. Unfortunately, this solution is not sufficient when spatial movement occurs. For spring k_2 this problem was circumvented by placing the bearings for the out-of-the-vertical-plane movement of the forearm at the distal end of the upper arm, just before the elbow joint, while furnishing the shoulder with a Hooke's joint. The free end of the spring combination k_1 was connected to the auxiliary link via a bearing that allows rotation about the axis of the longer supplementary link.

Notes to chapter six

[6.1]   *Literature approximate balancing.* Literature related to approximate spring balancer design includes the following. Hain (1952) employs a graphical method for both a given spring and a spring that is still to be selected, to assess the fixed point in case the point of attachment at the lever is given, or the determination of the shape of a wrapping cam in case the fixed point of the spring and the pivot of the cam are given. Harmening (1974) uses a torsion spring in combination with a four-bar linkage to achieve approximate balance of a rotatable mass in a range of 120° with 0.2% error), or 180° with 2% error, respectively, by way of a simplified analytic complex number linkage synthesis technique (Sieker, 1955). Matthew and Tesar (1976a and 1976b) present an analytical formulation for a finitely separated position synthesis of an ideal spring on planar linkages to balance specified energy requirements. Mahalingam and Sharan (1986) use the Hooke and Jeeves direct-search technique to find a suitable location for the fixed point of a tension spring. Bagci (1987a and 1987b) balances a rotatable mass with his Integration of Power Equilibrium Method by way of a four-bar linkage and a spring. Klein Breteler (1990) reduces the question of the design of a compensation cam mechanism to a kinematic problem. Baudisch (1985), and Ulrich and Kumar (1991) design wrapping cams to match a spring characteristic with the mass of a robotic arm. Jenuwine and Midha (1992) extend the vector loop approach (Erdman and Sandor, 1997; Midha and Zhao, 1985) to include arbitrary energy demands. Huang and Roth (1993 and 1994) apply the principle of virtual work to attach a spring to a pre-existing mechanism at an appropriate position. Idlani *et al.* (1993) follow a similar approach, resulting in approximate solutions, provided a sufficiently accurate initial estimate is available. Pons *et al.* (1998) use two normal springs with opposite lever angles to proved quasi-exactly balance. Least squares optimization reduced the remaining torque to less than 1% of the initial gravity torque. Segla *et al.* (1998) use Monte Carlo methods and genetic algorithms to optimize a balancer for a six-degree-of-freedom industrial robot. Literature on numerical solution methods includes Beveridge and Schechter (1970), and Haug and Arora (1979). Patents on approximate balancing systems include Gammer and Broekl (1996), Green (1995), Nakashima *et al.* (1988), Christiansen and Weiss (1992), Mosher and Kugath (1971), and Flach and Montcuquet (1981).

[6.2]   *Loop closure.* Planar linkages can be seen as combinations of vectors. Demanding the vectors to constitute a closed loop provides the continuity equations (*e.g.* Erdman and Sandor, 1997; Idlani *et al.*, 1993).

[6.3]   *Chebychev spacing.* In this procedure the distances between the points of a trajectory are found as follows. The trajectory is straightened and used as the diameter of a circle. A polygon of the desired number of edges in inscribed in the circle, and the orthogonal projections of the edges are indicated on the diameter. Finally, the distances between the projected points are transferred to the trajectory (Hartenberg and Denavit, 1964).

[6.4]   *Cycloid-cognates.* "Thus, a hypocycloid is the curve generated by a point lying on the rolling circle that performs the hypocycloid motion. If, in addition, the tracing point lies inside the rolling circle, we say that the curve generated by that point, is a contracted hypocycloid. For an outside point, it is a protracted hypocycloid. (...) Now, we want to draw attention to the fact that a protracted hypocycloid is identical to a contracted hypocycloid. This statement means that such curves may be generated by

different hypocycloid motions Therefore we are dealing with curve-cognates for these motions" (Dijksman, 1976, p194/7).

[6.5] *Demonstration model*. The demonstration models in figures 6.5 and 6.9ab were manufactured by Ing J. Verbeek (1995-1997).

[6.6] *Demonstration model*. This demonstration model was developed by Van Passel (1995) during his BSc-project.

[6.7] *Overlay method*. In his classic work "Kinematics and Linkage Design", Hall (1961) presents a graphical method, called the overlay method, for the design of a four-bar linkage, to synthesize a function generator. A number of positions of the input crank are specified, a connecting rod length is selected and an overlay of the output crank is fitted to this picture. "This is a good, practical procedure that will yield satisfactory results for many problems, especially those for which tolerance on position of the output crank is of the order of 0.5 deg. or more" (*op. cit.*, p46).

[6.8] *Dynamics in overlay method*. Note that kinetic energy could very well be included, but this is omitted as it would go beyond the scope of this thesis.

[6.9] *Extended loop closure*. Jenuwine and Midha (1992) proposed to extend the loop-closure method (see [6.2]) with an additional energy equation. Using this procedure, a constant force mechanism was designed which has a working principle similar to the balanced elliptic trammel (figure 5.33). See also: Erdman and Sandor (1997), Midha and Zhao (1985), Idlani *et al.* (1993).

[6.10] *Voluntary closing*. Hand prostheses can be body powered (operating force and excursion generated by the user, see [1.3] and for instance Carlson, 1990, 1992), or externally powered (external energy sources) (Schlesinger, 1919; Fletcher and Leonard, 1955; Binder, 1957; Childress, 1977; Becker, 1979; Boldingh, 1982, Weaver and Lange, 1985; Shaperman *et al.*, 1995). Body powered devices are preferred from a control point of view [1.2]. Within the class of body powered hand prostheses, a distinction can be made between voluntary opening and voluntary closing (Böhm, 1926; Püschel, 1955; Klopsteg and Wilson, 1964; Baumgartner, 1977; Kristen and Weteschnik 1981; Löffler, 1984; Radocy and Ronald, 1981; Radocy, 1986; Carlson and Heim, 1989; Kaniewski, 1989; Frey and Carlson, 1994). In voluntary opening devices, a spring provides the pinch force while increasing operating force reduces the pinch force, and eventually opens the hand against the action of the closing spring and the cosmetic covering [1.4]. This is counterintuitive, as we are used to exert greater pinch force when we tense our muscles. Voluntary closing devices function according to the same operating principle: a pliant spring provides a weak opening action, whereas the force generated by the user is transferred into pinch force. Several comparative studies have been performed, the results of which are dependent on the specific types of prostheses involved, and which are all dependent on the mechanical imperfectness of the current designs (Groth and Lyman, 1957; Angliss, 1992; Shapiro and Locast (1989). Another distinction is between hooks (two fingers) and hands (five fingers), the latter having the advantage of better cosmetics, but the disadvantage of reduced view of the object held, and counteraction of mechanism motion (Blaschke and Santschi, 1949; Sears, 1983; Burrough and Brook, 1985; Gilad, 1985; Murphy, 1986; Billock, 1986; Meeks and LeBlanc, 1988; Crandall and Hansen, 1989). Previous works by the Wilmer group on the development of voluntary closing prostheses include Cool and Van Hooreweder (1971), Thomassen (1991).

[6.11] *Collaboration with rehabilitation teams*. Two Dutch rehabilitation teams were actively involved: De Hoogstraat at Utrecht, and Maartenskliniek at Nijmegen. The input provided by this cooperation is invaluable and therefore highly appreciated.

[6.12] *Direct and indirect grasp*. The functionality of hand prostheses is limited. They do not replace all the functions of a sound hand. Consequently, the use of prostheses differs from the use of the sound hand. Unilaterals perform most activities single-handed, while the prosthesis is used to support certain tasks. Grasping something with the prosthesis only, without using the sound hand, is very rare (Van Lunteren *et al.*, 1983). Indirect grasping (*i.e.* putting something in the prosthesis with the sound hand, or pushing the prosthesis around the object, or using the environment) is much more frequent.

[6.13] *Results of interviews*. Results of the interviews are included in Herder *et al.* (1994), and Herder and De Visser (1998).

[6.14] *Psychophysics*. The subjective perception of physical stimuli is studied in the science of psychophysics (Gescheider, 1976); Stevens, 1975; Kandell and Schwartz, 1991; Norwich, 1993; Woodword and Schlossberg, 1966; Dixon and Massey, 1969). Essentially, psychophysical experiments are based on the comparison of two stimuli (either simultaneously using different receptors, or successively, using the same receptor). The report by Munneke (1994) contains an overview of measurement methods available. Several studies have followed (see [6.15]) and continue to be pursued.

[6.15] *Sensitivity*. As it was intended to design an elbow controlled prosthesis, where an operating lever on the upper arm supplies the operating force, perception measurements were carried out to asses the sensitivity of the human upper arm (Munneke, 1994; Herder and Munneke, 1995; Magermans and Van der Tol, 1999; Pieterse, 2000; Bakker, 2001). Even though different measurement methods and different test set-ups were used, the results were consistent. It was found that forces below 9N were perceived less accurately than higher forces. Furthermore, it was found that the size of the contact area had little influence on the sensitivity.

[6.16] *Motion directed design*. By far most existing hand prostheses are designed with desired motion characteristics in mind, see for instance Kato and Sadamoto (1985); Guo *et al.,* (1992), Figliolini and Ceccarelli (1998); Kyberd and Chappell (1994). Nguyen (1988) considers force closure grasps, which can be seen as form of force directed design (see also [1.8, 1.9]), while Laliberté and Gosselin (1998) discuss the principle of underactuation to control multiple degrees of freedom with one control signal.

[6.17] *Second prototype hand prosthesis*. This prototype was manufactured by Van de Burgt (2000).

[6.18] *First prototype of hand prosthesis*. This prototype was the result of the MSc-Thesis project by De Visser (1998). This design was awarded the ASME GM/Freudenstein Young Investigator Award at the 26th Mechanisms and Robotics Conference ASME DETC 2000, Baltimore, MA (Herder and De Visser, 2000).

The specifications of the performance are summarized as follows. For the finger, a uniform distribution of the operating force to the pinch forces was aimed at. For the most common finger movements ($\alpha=\beta$), both pinch forces vary only slightly. Within the range of 40 to 80 degrees, the deviation from the constant ratio is less than 5%. In the extreme cases where either α or β is zero, greater deviations occur, especially for larger angles. The compensation device reduces the maximum operating force required

to bend the finger from well over 10N to approximately 1.5N. This would translate into an additional operating force at the upper arm site of about 1N, as compared to the situation of ideal glove compensation.

[6.19]   *Compliant mechanisms.* A compliant mechanism is a mechanism that gains some or all of its motion from the relative flexibility of its members rather than from rigid-body joints only (*e.g.* Howell, Midha and Norton, 1996). Among the advantages of compliant mechanisms are the single-piece production, absence of coulomb friction, no need for lubrication, and compactness, however at the cost of increased complexity of their design, non-linearities introduced due to the large deformations, and energy storage in the flexible members distorting the input-output relationship (references included in [1.13]). Due to the energy storage in the elastic members of the mechanism, energy is not conserved between input and output ports, which is a serious drawback in some cases (Salamon and Midha, 1992). For instance, in manually operated instruments, such as surgical forceps, operating effort is required even when no external work is done, and, more importantly, the force feedback quality is reduced. The elastic forces introduced by the bending of the compliant members disturb the force transmission from the gripper to the hand grip, thus reducing the feel one has for the object or tissue in the gripper (Sjoerdsma *et al.*, 1997).

[6.20]   *Compliant gripper.* For the gripper, a compliant configuration was chosen comparable to the ones used by Ananthasuresh and Kota (1995), Balázs (1998) and Canfield *et al.* (1999). For reasons of convenience, the design is simplified to a configuration of parallel plate springs. A detailed description is contained in Van den Berg (1999), and Herder and van den Berg (2000).

[6.21]   *Prototype surgical forceps.* The prototype in figure 6.26 was the result of the MSc-Thesis project by Van den Berg (1999). The mechanical performance can be summarized as follows. The calculated unbalance results in a maximum remnant force on the pull-pushrod amounts to 0,022N. The hysteresis of one operating cycle of the unloaded gripper was found to be 0.20mJ. The measured value of the unbalance in this case was 0.05N. When loaded by 0.8N at the tip, the hysteresis increased to 2.33mJ. In terms of energy, this results in an efficiency of approximately 80%. A second prototype (shown in figure 6.24) is under construction by Van der Pijl (2000-2001).

Notes to chapter seven

[7.1]   *Origin of theory.* Initially, these results were found as follows (see also [3.1]). When composing two forces into a resultant force, the common procedure is to shift the forces to the intersection of the lines of action and then find the resultant using the parallelogram construction. However, in systems where constant potential energy is essential, shifting forces along their line of action may have the adverse effect of changing the system potential. Therefore it seemed wise to shift the resultant force back in such a way that the original potential level was restored. Thus it was found by Prof. ir J.C. Cool that the resultant force applies at the intersection of its line of action and the circle put up by the points of application of the original forces and the intersection of their lines of action. Application of the procedure to the spring butterfly (figure 4.28), the elliptic trammel (figure 5.33c), and the Floating Suspension (figure 5.22) revealed that the product of the magnitude of the resultant force and the distance from its supposed point of application was constant, even though in the spring butterfly ($\beta\neq0$) the magnitude of the resultant force and the distance between the points

of application both were variable (see figure 4.28). The remarkable fact that the product mentioned, having the unit of energy or work, was equal to twice the elastic potential in the springs, gave rise to a number of theories, similar to the ideas of pertinacity by French (1992). What initially was regarded to be in some way associated with the potential energy, turned out to be equal to the correction term for the location of the dynamically equivalent resultant force which is required when not constant but central linear forces are considered (see the discussion at the end of section 3.4).

Bibliography

A

Abe K (1924) *The woman in the dunes* (Suna no onna, 1924), ISBN 0-679-73378-7, transl. A. Knopf 1964, Vintage International NY, 1991, p17/8

Agrawal SK, Hirzinger G, Landzettel, Schwertassek R (1996) A new laboratory simulator for study of motion of free-floating robots relative to space targets, *IEEE Transactions ofn Robotics and Automation*, 12(4)627/33.

Agrawal SK, Gökce A (1998) Mass center of planar mechanisms using auxiliary parallelograms, *Proceedings of ASME Design Engineering Technical Conference*, Atlanta, GA, Paper number DETC2000/MECH-5938.

Agrawal SK, Gardner G, Pledgie S (2000) Design and fabrication of a gravity balanced planar mechanism using auxiliary parallelograms, *Proceedings of ASME Design Engineering Technical Conference*, Baltimore, MA, Paper number DETC2000/MECH-14073.

Akeel HA (1987) *Robot with balancing mechanism having a variable counterbalance force*, US Patent 4,659,280.

Alabuzhev P, Gritchin A, Kim L, Migirenko G, Chon V, Stepanov P (1989) *Vibration protecting and measuring systems with quasi-zero stiffness*, English edition editor E. Rivin, ISBN 0-89116-811-7.

Alexander R McN (1990) Three uses for springs in legged locomotion, *The International Journal of Robotics*, 9(2)53/61.

Alonso M, Finn EJ (1971) *Fundamental university physics*, Addison-Wesley, Reading MA, USA.

Ananthasuresh GK, Kota S (1995) Designing compliant mechanisms, *Mechanical Engineering*, 117(11)93/6.

Andreeva LE (1966) *Elastic elements of instruments*, Israel Program for Scientific Translations, Jerusalem.

Arkles B (1983) Look what you can make out of silicones, *Chemteck*, 13(9)542/55.

Asada H, Youcef-Toumi K (1984) Analysis and design of a direct-drive arm with a five-bar-link parallel drive mechanism, *Journal of dynamic systems, Measurements, and Control*, 106(3)225/30.

Asada H, Youcef-Toumi K, Ramirez R (1985) Design of MIT direct-drive arm, In: Yoshikawa H, Design and Synthesis, Elsevier Science Publishers B.V. (North Holland), p325/32.

B

Bagci C (1987a) Synthesis of linkages to generate specified histories of forces and torques, the planar 4R four-bar mechanism, *ASME Design and Automation Conference*, 10(2)227/36.

Bagci C (1987b) Synthesis of linkages to generate specified histories of forces and torques, the planar slider-crank mechanism, *ASME Design and Automation Conference*, 10(2)237/44.

Bagci C (1992) Complete balancing of linkages using complete dynamical equivalents of floating links: CDEL method, *Proceedings 22nd Biennial Mechanisms Conference, Flexible Mechanisms, Dynamics, and Analysis*, DE-Vol. 47, ASME, p477/88.

Bakker (2001) *Development of measurement system for sensitivity of the upper arm*, BSc-Thesis HHS-BT The Hague.

Balázs M, Feussner H, Hirzinger G, Omote K, Ungeheuer A (1998) A new tool for minor-acces surgery, *IEEE Engineering in Medicine and Biology*, 17(3)45/8.

Baudisch R (1985) Statischer Ausgleich bei Gelenkrobotern (static balancing in articulated robots), *Feingerätetechnik* 34(4)160/2.

Baumgartner, RF (1977) *Amputation und Prothesenversorgung beim Kind*, Ferdinand Enke Verlag, Stuttgart.

Becker FF (1979) Untersuchungen über den Gebrauchswert von eigen Kraftbetätigten und fremd-kraftangetriebenen Handpassteilen, *Orthopädie Technik*, 10/79, 157-159.

Beer FP, Johnston ER jr (1997) *Vector Mechanics for Engineers: Statics and Dynamics*, McGraw-Hill, ISBN 0-07-005365-0.

Berg, FPA van den (1999) *Design of low-friction laparoscopic forceps in 5mm version* (in Dutch), MSc-Thesis, A-864, OCP-MMS, Delft University of Technology.

Berkof RS, Lowen GG (1969) A new method for completely force balancing simple linkages, *Transactions of ASME, Journal of Engineering for Industry (B)*, 91(1)21/26.

Betts J (1993) *John Harrison,* Old Royal Observatory, Greenwich.

Beveridge SG, Schechter RS (1970) *Optimization, Theory and Practice*, McGraw-Hill Book Co, NY.

Beyer R (1963) *The kinematic synthesis of mechanisms,* Chapman and Hall, London.

Billock JN (1986) Upper limb prosthetic terminal devices: hands versus hooks, Clinic. Prosthet. Orthot. 10(2)57/65.

Bilotto S, Upper extremity cosmetic gloves, Clinical Prosthetics and Orthotics, 10(2)87/9, *The American Academy of Orthotists and Prosthetists*, 1986.

Binder, U (1957) *Die fremdenergetisch angetriebene handprothese*, ihre möglichen Antrieb-systeme und Steuerungen, sowie ihre Brauchbarkeit im Vergleich zur eigenenergetisch betriebenen Prothese (the externally powered hand prosthesis).

Blaschke AC Santschi WR (1949) *Studies to determine functional requirements affecting hook fingers design*, Special Report No 12, University of California at Los Angeles.

Bloem M, Langeveld T, Dekker D (2000) Losses in statically balanced spring mechanisms (In Dutch), *Bachelor's Mechanical Engineering Congress*, 6 July, Delft University of Technology.

Blom TTJ (1990) *Measurement of Otto Bock glove size 12*, (In Dutch) Internal report, TU Delft, WMR.

Boer KT den, Herder JL, Sjoerdsma W, Meijer DW, Gouma DJ, Stassen HG (1999) Sensitivity of laparoscopic dissectors, what can you feel? *Surgical Endoscopy*, Vol. 13, pp. 869/73.

Boerner EH (1954) Constant force compression springs, *Product Engineering*, p129/35.

Böhm (1926) Die lehre von den Ersatzgliedern. Von Reg.-Med.-Rat Dr.M.Böhm, Berlin In: Bauer *et al.*, *Die Chirurgie*, Urban & Schwarzenberg, Berlin.

Boldingh EJK (1982) Prothesiology, upper extremities (In Dutch), *Ned. T. Geneesk.*, Vol. 126, nr. 40.

Bora FW jr (1981) *Prosthetic joint*, US Patent 4,267,608.

Bottema O (1987) *Chapters from elementary geometry*, (In Dutch), Epsilon Uitgaven, ISBN 90-5041-013-8, Utrecht.

Bottema O, Roth, B (1990) *Theoretical kinematics,* Dover, New York.

Bowles P (1967) *Up above the world*, Peter Owen Publishers, London.

Brickman AD (1967) Rolamite, what makes it tick? *Machine Design,* december 1967, p111/3.

Brinkman ML (1998) Personal communication.

Brown T, DiGuilio AO (1980) *Support apparatus*, US Patent 4,208,028.

Brown HB, Dolan JM (1993) A novel gravity compensation system for space robots, *ASCE Specialty Conference on Robotics for Challenging Environments,* p250/8

Buckner H (1992) Functional, cosmetic silicone prostheses & orthoses, *Proceedings 7th world congress of ISPO*, Chicago USA, p64.

Bueche F (1979) Physical properties of polymers, ISBN 0-88275-833-0, RE Krieger Publishing Co. Inc., New York.

Burgt E van de (2000) *Voluntary closing hand prosthesis*, (In Dutch) BSc-Thesis, HHS-BT, The Hague.

Burrough SF, Brook JA (1985) Patterns of acceptance and rejection of upper limb prostheses, *Orthotics and Prosthetics*, 39(2)40/7.

Burns RH, Crossley FRE (1968) Kinetostatic synthesis of flexible link mechanisms, *ASME paper 68-MECH-36.*

C

Cadman RV (1969) Rolamite-geometry and force analysis, *Transactions of ASME, Journal of Engineering for Industry (B)*, 91(1)186/92.

Camuto M, Kinzel GL (1998) Path Generation Using a Random Walk Algorithm, *Proceedings of the 25th Biennial Mechanisms Conference*, ASME-DETC98, Atlanta, GA.

Canfield S, Edinger B, Frecker M, and Koopman G (1999) Design of Piezoelectric Inchworm Actuator and Compliant End-Effector for Minimally Invasive Surgery, *Proceedings SPIE Smart Strucutres and Materials*, March, 1999, Newport Beach, CA, Paper 3668-77.

Cardoso L, Tomázio S (2001) *Task analysis and range of motion for an arm orthosis*, Internal Report S-963, OCP-MMS, Delft University of Technology.

Carlson H, Deflection of coiled springs wound with initial tension, In: Chironis NP ed. (1961) *Spring design and application*, McGraw-Hill, New York.

Carlson LE (1990) Improved actuation of body powered prostheses, In: *Rehabilitation R&D Reports*.

Carlson LE (1992) Synergetic Prehension, *Proceedings 7th world congress of ISPO*, Chicago USA, p61.

Carlson LE, Heim R (1989) Holding assist for a voluntary closing prosthetic prehensor, *ASME Dyn Syst Control Div Publ* (17)79/87

Carnelli WA, Defries MG, Leonard F (1955) Color realism in the cosmetic glove, *Artificial Limbs*, Vol. 2, May, p57/65.

Carson WL (1976a) Design of alternate force systems for producing the same mechanism motion-time response and/or input/output forces, *Linkage Design Monographs*, Ed. A. H. Soni, Final Report NSF Gk-36624, p72.1-72.7.

Carson WL (1976b) Example applications illustrating the breath of mechanism-force system synthesis for a desred motion-time and/or input-output forces, and a survey of design techniques, *Linkage Design Monographs*, Ed. A. H. Soni, Final Report NSF Gk-36624, p71.1-71.7.

Carson WL, Lee CSI (1983) A force system synthesis algorithm for use as a companion to mechanis dynamic analysis programs, *Journal of Mechanisms, Transmissions, and Automation in Design*, 105(2)273/7.

Carwardine G (1931a) Improvements in drafting machines and the like, UK Patent 345.015, *Specifications of Inventions*, Patent Office Sale Branch, London.

Carwardine G (1931b) Improvements in suspensions fo automobiles and the like, UK Patent 349.582, *Specifications of Inventions*, Patent Office Sale Branch, London.

Carwardine G (1932a) Improvements in elastic force mechanisms, UK Patent 377.251, *Specifications of Inventions*, Vol. 2773, Patent Office Sale Branch, London.

Carwardine G (1932b) Improvements in elastic force mechanisms, UK Patent 379.680, *Specifications of Inventions*, Vol. 2729, Patent Office Sale Branch, London.

Carwardine G (1934a) Improvements in elastic equipoising mechanisms, UK Patent 404.615, *Specifications of Inventions*, Vol. 3047, Patent Office Sale Branch, London.

Carwardine G (1934b) Improvements in equipoising mechanism, UK Patent 417.970, *Specifications of Inventions*, Vol. 3180, Patent Office Sale Branch, London.

Carwardine G (1935) Improvements in equipoising mechanism, UK Patent 433.617, *Specifications of Inventions*, Vol. 3337, Patent Office Sale Branch, London.

Carwardine G (1938a) Improvements in equipoising mechanism, UK Patent 481.198, *Specifications of Inventions*, Vol. 3812, Patent Office Sale Branch, London.

Carwardine G (1938b) Improvements in or relating to spring controlled mechanism, UK Patent 484.108, *Specifications of Inventions*, Patent Office Sale Branch, London.

Carwardine G (1938c) Improvements in and relating to elastic force and equipoising mechanisms, UK Patent 484.108, *Specifications of Inventions*, Vol. 3896, Patent Office Sale Branch, London.

Cathcart A (1983) *Ducati Motorcycles*, Osprey Publishing Limited, London.

Childress DS (1977) Report: panel on upper-limb prosthetics, *Orthotics and Prosthetics*, Vol. 31, No. 4.

Chironis NP (1961) *Mechanisms & mechanical devices sourcebook*, McGraw-Hill, ISBN 0-07-010918-4.

Chironis NP (1961) *Spring design and application*, McGraw-Hill, New York.

Christiansen H, Weiss J (1992) *Vorrichtung zum statischen Ausgleich eines Drehmoments*, (device for static balancing of torque), Patent application DE 40,23,841,A1.

Chung WK, Cho HS, Chung MJ, Kang YK (1986) On the dynamic characteristics of balanced robotic manipulators, *Proc. of Japan-USA Symposium on Flexible Automation*, Osaka, July 14-18, 1986, p119/26.

Chung WK, Cho HS, Lee CW, Warnecke HJ (1984) Performance of robotic manipulators with an automatic balancing mechanism, In: *Computer-Integrated Manufacturing and Robotics*, ASME PED-13, p111/21.

Chyatte SB, Vignos PJ (1965) The Balanced Forearm Orthosis in Muscular Dystrophy, *Archives of Physical Medicine & Rehabilitation*, pp633/6.

Clarke CD, Weinberg FB, Blevins GC (1947) Seamless prosthetic hands, *Arch. Surg.* 54, pp. 491/516.

Clarke CD, Weinberg FB (1949) New advances in seamless prosthetic hands, *Arch Surg.* 59 p355/72

Cool JC (1976) An elbow orthosis, *Biomedical Engineering*, 11(10)344/7.

Cool JC (1990) System, shape and material (In Dutch), *Mikroniek*, 30(3)77/84.

Cool JC (1981) *WILMER assistive devices, design philosophy and working principle* (In Dutch), Congresverslag Boerhaave cursus over revalidatieve geneeskunde, Leiden, RUL, 1981.

Cool JC (1987) Prothesiology, principles, new developments (In Dutch), *Basiscursus amputatie en prothesiologie van de bovenste extremiteit*, PAOG, Katholieke Universiteit Nijmegen.

Cool JC (1991) *Uit drie delen (Out of three parts)*, Uitgangspunten, uitwerkingen en uitkomsten, Lezing bij aanvaarding Peter Prakke-prijs, Boerhaave instituut voor post-academisch onderwijs, Noordwijkerhout, i.s.m. Academisch ziekenhuis Leiden en het ISPO.

Cool JC (1991-2001) Personal communication.

Cool JC (1997) Design of anthropomorphic appliances, In: Sheridan TB, Lunteren T van (eds.) *Perspectives on the human controller: essays in honor of Henk G. Stassen*, ISBN 0-8058-2190-2, pp 110/19.

Cool JC, Hooreweder GJO van (1971) Hand prosthesis with adaptive internally powered fingers, *Med. And Biol. Engineering*, Vol. 9, p33/6.

Cool JC (1995) *Artis* (in Dutch), Valedictory address, Delft University of Technology, Delft.

Cowan P, Dennison K, Nathan RH, Skorecki J (1975) Floating arm supports: Preliminary trails and further developement, *Proceedings of the fourth World Congress on the Theory of Machines and Mechanisms*, Newcastle-Upon-Tyne, England, p815/20.

Coxeter HMS (1989) *Introduction to Geometry*, Second Edition, John Wiley & Sons.

Coxeter HMS, Greitzer SL (1967) *Geometry Revisited*, Random House, The L. W. Singer Company.

Crandall RC, Hansen D (1989) Clinical evaluation of a voluntary-closing terminal device, *Journal of the Association of Children's Prosthetic-Orthotic Clinics*, 24(2/3)36.

Cuschieri A (1995) Whither Minimal Access Surgery: Tribulations and Expectations, *The American Journal of Surgery*, Vol. 169, pp. 9/19.

D

Dallemagne B, Weerts JM, Jehaes C, Markiewicz S, Lombard R (1991) Laparoscopic Nissen Fundoplication: preliminary report, *Surg Laparosc Endosc*, pp.138/43.

Davies EW, Douglas WB, Small AD (1977) A cosmetic funtional hand incorporating a silicone rubber cosmetic glove, *Prosthetics and Orthotics International*, (1)89/93.

Davis BL, Cavanagh PR (1993) Simulating reduced gravity: a review of biomechanical issues pertaining to human locomotion, *Aviat. Space Environ. Med.* (64)557/66.

Dieten J van (1997-1998) Personal communication.

Dijksman EA (1976) *Motion geometry of mechanisms*, Cambridge University Press, ISBN 0-521-20841-6.

Dimarogonas AD (1992) Mechanisms of the ancient greek theater, *Proceedings 22nd Biennial Mechanisms Conference, Robotics, Spatial Mechanisms and Mechanical Systems*, DE-Vol. 45, ASME, p229/34.

Dixon WJ, Massey FJ (1969) *Introduction to statistical analysis*, Chapter 19: Sensitivity experiments, McGraw-Hill Book Company.

E

Ebert-Uphoff I, Gosselin CM (1998) Kinematic study of a new type of spatial parallel platform mechanism, *Proceedings ASME DETC 25th Biennial Mechanisms Conference*, Sept 13-16, Atlanta, Georgia, paper number DETC98/MECH-5962.

Eibergen-Santhagens RA van (1985) *De ellebooggestuurde kinderhandprothese*, Report N252, Delft University of Technology, Delft.

Eijk J van (1985) *On the design of plate-spring mechanisms*, PhD-Thesis, Delft University of Technology, Delft.

Erb RA (1989) Cosmetic covers for upper and lower extremity prostheses, *Rehabilitation R&D Progress Reports*, pp. 3/4.

Erdman AG, Nelson E, Peterson J, Bowen J (1980) Type and dimensional synthesis of casement window mechanisms, *ASME paper No. 80-DET-78*.

Erdman AG, Sandor GN (1984) *Mechanism design: analysis and synthesis*, Vol 1, Prentice-Hall, Englewood Cliffs, New Yersey, p472/7.

F

Ferry JD (1970) *Viscoelastic properties of polymers*, Second edition, ISBN 471-25774-5, John Wiley & Sons, Inc, New York.

Fidweel PH, Bandukwala N, Dhande SG, Rheinholz CF, Webb G (1992) Synthesis of wrapping cams, *Proceedings of 22nd Biennial Mechanisms Conference ASME, Robotics, Spatial Mechanisms and Mechanical Systems*, ASME Design Engineering Division DE v 45 p337/43.

Fielding B, Nathan R, Skorecki J (1971) Design of an unenergized aid to rising and sitting down for the partially disabled, *Medical and Biological Engineering*, Vol 9, p523/39.

Figliolini G, Ceccarelli M (1998) A motion analysis for one d.o.f. anthropomorphic finger mechanism, *Proceedings of ASME Design Engineering Technical Conferences '98*, Atlanta.

Fillauer C, Quingly M (1979) Clinical evaluation of an acrylic latex material used as a prosthetic skin on limb prostheses, 33(4)30/8

Flach O, Montcuquet P (1981) Manipulateur industriel perfectionné, *Demande de brevet d'invention* 80.12348.

Fletcher M, Leonard F (1955) Principles of artificial hand design, *Artificial Limbs*, Vol. 2, May, pp. 78/94.

French MJ (1985) *Conceptual design for engineers*, 2nd edition, p127/31.

French MJ (1988) *Invention and evolution: design in nature*, Cambridge University Press, ISBN 0-521-30759-7, p158.

French MJ (1992) *Form, structure and mechanism*, Macmillan, ISBN 0-333-51885-6.

French MJ (2000) The spring-and-lever balancing mechanism, George Carwardine and the Anglepoise lamp, *Proc Instn Mech Engrs*, Vol. 214, part C, p501/8.

Freudenstein F, Maki ER (1980) The creation of mechanisms accoding to kinematic sturcture and function, General Motors Research Publications, GMR-3073, September 1979, *International Journal for the Science of Architecture and Design*.

Frey DD, Carlson LE (1994) A body powered prehensor with variable mechanical advantage, *Prosthetics and Orthotics International*, (18)118/23.

Fung YC (1981) Biomechanics, Mechanical properties of living tissues, ISBN 0-387-90472-7, Springer Verlag, New York.

G

Gammer P, Broekl H (1996) *Forearm lifter*, US Patent 5,549,712.

Gärtner R (1957) Konstante Kraft mit Hilfe gewöhnlicher Schraubenfedern (constant force using normal helical springs), *Konstruktion*, 9(4)157/9.

Gescheider GA (1976) *Psychophysics, method and theory*, John Wiley and Sons, New York.

Gilad I (1985) Motion pattern analysis for evaluation and design of a prosthetic hook, *Arch. Phys. Med. Rehabil.*, Vol. 66, p399/402

Godden AK (1968) Some factors in the design of an adaptive artificial hand, *Symposium on the basic problems of prehension, movement and control of artificial limbs*, The Institution of Mechanical Engineers, London, 30th October and 1st November.

Gökce A, Agrawal SK (1999) Mass center of planar mechanisms using auxiliary parallelograms, *Journal of Mechanical Design*, Vol. 121, p166/8.

Gopalswamy A, Gupta P, Vidyasagar M (1992) A new parallelogram linkage configuration for gravity compensation using torsional springs, *Proceedings of the 1992 IEEE International Conference on Robotics and Automation*, Nice, France, May 1992, p664/9.

Gosselin CM, Wang J (2000) Static balancing of spatial six-degree-of-freedom parallel mechanisms with revolute actuators, *Journal of Robotic Systems* 17(3)159/70.

Gosselin CM (1999) Static balancing of spherical 3-dof parallel mechanisms and manipulators, *The International Journal of Robotics Research* 18(8)819/29.

Grashof F (1883) *Theoretische Maschinenlehre*, Vol. 2, Voss, Leipzig.

Green PS, Hill JW, Jensen JF, Shah A (1995) Telepresence Surgery, *IEEE Engineering in Medicine and Biology*, pp. 324/9.

Greene HP (1995) *Load compensator for spring counter-weighting mechanism*, US Patent 5,400,721.

Groesberg SW (1960) Designing a zero-gradient spring system for constant-tension service, *Machine Design*, January, p143/7.

Groth H, Lyman J (1957) An experimental assessment of amputee performance with voluntary opening and voluntary closing terminal devices, *Special technical report No 23*, University of California at Los Angeles.

Guilbaud J-P, Vertut J (1971) *Dispositif d'équilibrage indifférent*, Brevet d'Invention, Institut National de la Propriété Industrielle, No de publication: 2086976, No dénregistrement national: 70.13606.

Guo G, Qian X, Gruver WA (1992) Single degree of freedom multi-function prosthetic hand mechanism with an automatically variable speed transmission. *22nd Biennial Mechanisms Conference ASME 1992, Robotics, Spatial Mechanisms and Mechanical Systems* ASME Design Engineering Division DE v 45 p149/54.

H

Hain K (1952) Der Federausgleich von Lasten (spring-balancing of loads), *Grundlagen der Landtechnik*, (3)38/50.

Hain K (1953) Gelenkarme Bandgetriebe für den Kraftausbleich durch Federn , *Grundlagen der Landtechnik*, (4)100/9.

Hain K (1955) Feder-Getriebe un Band-Getriebe für den Kraftausgleich, *VDI-Z* 97(9)278

Hain K (1955) Federeinbau für gegebene praktische Bedingungen, *Konstruktion* 7(9)343/8.

Hain K (1961) Spring mechanisms, In Chironis, *Spring Design and Application*, 268/75.

Hain K (1967) *Applied Kinematics*, second edition, McGraw-Hill, New York.

Hall AS Jr (1961) *Kinematics and linkage design*, Prentice-Hall Inc, Englewood Cliffs, N.J.

Halter JM, Carson WL (1975a) Mechanism-force system synthesis to obtain a desired motion-time response, *Proceedings Fourth World Congress on the Theory of Machines and Mechanisms*, Newcastle upon Tyne, 8-12 September, Mechanical Engineering Publications Limited, London, p399/404.

Halter JM, Carson WL (1975b) A technique to design physically realistic alternate force systems for producing the exact same mechanism motion-time response, *Proceedings Fourth World Congress on the Theory of Machines and Mechanisms*, Newcastle upon Tyne, 8-12 September, Mechanical Engineering Publications Limited, London, p477/82.

Haringx JA (1948) On highly compressible helical springs and rubber rods, and their application for vibration-free mountings, *Philips Res. Rep.*, 3, 401.

Harmening WA (1974) Static mass balancing with a torsion spring and four-bar linkage, *ASME-paper* 74-DET-29.

Hartenberg RS, Denavit J (1964) *Kinematic synthesis of linkages*, McGraw-Hill, New York.

Harwin WS (1997) Design and Control of a Compliant Mobile Arm Support for Assisting Arm Movements, In: Anoianakis G *et al.*, *Advancement of Assistive Technology*, IOS Press, pp320/5.

Haug EJ, Arora JS (1979) *Applied optimal design, mechanical and structural systems*, John Wiley & Sons, NY.

Haupt G, Grewolls J (1963) Über das Gleichgewicht zwischen Federkräften und konstanten Kräften, *Maschinenbautechnik* 8(12)423/8.

Herder JL, Cool JC, Plettenburg DH (1994) The WILMER voluntary closing hand prosthesis, a multidisciplinary design approach, *Congress Summaries 11th International Congress of the World Federation of Occupational Therapists*, London, p1046/8

Herder JL, Munneke M (1995) Improving feedback in body powered prostheses, In: Stassen HG, Wieringa PA (eds), *Proceedings of the XIV European annual conference on human decision making and manual control*, Delft University of Technology, The Netherlands, June 14-16, p7.4-1/5.

Herder JL, Horward MJ, Sjoerdsma W (1997) A laparoscopic grasper with force perception, *Minimally Invasive Therapy and Allied Technologies*, 6(4)279/86.

Herder JL, Cool JC, Plettenburg DH (1998) Methods for reducing energy dissipation in cosmetic gloves, *Journal of Rehabilitation Research and Development*, 35(2)201/9.

Herder JL (1998a) Conception of balanced spring mechanisms, *Proceedings ASME DETC 25th Biennial Mechanisms Conference*, Sept 13-16, Atlanta, Georgia, paper number DETC98/MECH-5934.

Herder JL (1998b) Force directed design of laparoscopic forceps, *Proceedings ASME DETC 25th Biennial Mechanisms Conference*, Sept 13-16, Atlanta, Georgia, paper number DETC98/MECH-5978.

Herder JL (1998c) Design of spring force compensation systems, *Mechanism and Machine Theory*, 33(1-2)151/61.

Herder JL, Horward MJ (1998) *Manipulating pliers*, patent NL 1004056, PCT/NL97/00521.

Herder JL, Tuijthof GJM (2000) *Balancing mechanism*, patent NL 1009886.

Herder JL, Visser H de (2000) Force directed design of a voluntary closing hand prosthesis, *Proceedings ASME DETC 26th Biennial Mechanisms and Robotics Conference*, Sept 10-13, Baltimore, Maryland, paper number DETC2000/MECH-14149.

Herder JL, Berg FPA van den (2000) Statically balanced compliant mechanisms (SBCM's), an example and prospects, *Proceedings ASME DETC 26th Biennial Mechanisms and Robotics Conference*, Sept 10-13, Baltimore, Maryland, paper number DETC2000/MECH-14144.

Herder JL, Tuijthof GJM (2000) Two spatial gravity equilibrators, *Proceedings ASME DETC 26th Biennial Mechanisms and Robotics Conference*, Sept 10-13, Baltimore, Maryland, paper number DETC2000/MECH-14120.

Hervé JM (1983) Brevet Européen, no 85 400938.8, Ecole Centrale, France.

Hervé JM (1986a) Design of spring mechanisms for balancing the weight of robots, *Proceedings of the sixth CISM-IFToMM Symposium on Theory and Practice of Robots and Manipulators*, RoManSy 6, Cracow, Poland, Morecky A, Bianchi G, Kedzior K (eds.) p564/7.

Hervé JM (1986b) *Device for counterbalancing the forces due to gravity in a robot arm*, US Patent 4,620,829.

Hill JW, Green PS, Jensen JF, Gorfu Y, Shah AS (1994) Telepresence Surgery Demonstration System, *Proc 1994 IEEE Int. Conf. On Robotics & Automation*, San Diego, CA, pp. 2302/7.

Hillberry BM, Hall AS jr (1976) *Rolling contact prosthetic knee joint*, US Patent 3,945,053.

Hilpert H (1968) Weight balancing of precision mechanical instruments, *Jnl Mechanisms*, (3)289/302.

Hirose S (1993) *Biologically inpired robots*, Oxford University Press.

Hirose S (1997) Personal communication.

Hirose S, Imazato M, Kudo Y, Umetani Y (1986) Internally-balanced magnet unit, *Advanced Robotics*, 1(3)225/42.

Hirose S, Kado T, Umetani Y (1983) Tensor actuated elastic manipulator, *Proceedings of the sixth World Congress on Theory of Machines and Mechanisms*, Vol. 2, p978/81.

Hirschhorn J (1962) *Kinematics and dynamics of plane mechanisms*, McGraw-Hill.

Hoek, W van der (1986) *A mechanical designer's case book: DDP*, Philips CFT Report 59/85, Compiled by the Mechanical Engineering Dept of the Eindhoven University of Technology.

Hoek, W van der (1996) Personal communication.

Homma K, Arai T (1995) Design of an Upper Limb Motion Assist System with Parallel Mechanism, *Proceedings of the IEEE International Conference on Robotics and Automation*, pp1302/7.

Horward MJ (1995) *Design of a low-friction mechanism for laparoscopic forceps* (In Dutch), MSc-Thesis, Delft University of Technology, OCP-MMS.

Howe RD, Peine WJ, Kontarinis DA, Son JS (1995) Remote palpation technology, *IEEE Engineering in Medicine and Biology*, pp. 318/23.

Howell LL (1993) *A generalized loop-closure theory for the analysis and synthesis of compliant mechanisms*, PhD-dissertation, Purdue University.

Howell LL, Midha A (1995) Parametric deflextion approximations for end loaded, large deflection beams in compliant mechanisms, Journal of Mechanical Design, 117(1)156/65.

Howell LL, Midha A, Norton TW (1996) Evaluation of equivalent spring stiffness for use in a pseudo-rigid-body model of large deflection compliant mechanisms, Journal of Mechanical Design, 118(1)126/31.

Howell LL, Midha A, Murphy MD (1994) Dimensional synthesis of compliant constant-force slider mechanisms, *Machine Elements and Machine Dynamics*, DE-Vol. 71, 23rd ASME Biennial Mechanism Conference, pp. 509/15.

Hrones JA, Nelson (1951) *Analysis of the four-bar linkage*, John Wiley and Sons, New York.

Huang C, Roth B, (1993) Dimensional Synthesis of Closed-Loop Linkages to Match Force and Position Specifications, *ASME Journal of Mechanical Design,* 115(2)194/8.

Huang C, Roth B, (1994) Position-Force Synthesis of Closed-Loop Linkages, *ASME Journal of Mechanical Design*, 116(1)155/62.

Huissoon JP, Wang D (1991) On the design of a direct drive 5-bar-linkage manipulator, *Robotica*, Vol. 9, p441/6.

Hunt KH (1978) *Kinematic geometry of mechanisms*, Oxford University Press, Oxford.

Hunt KH (1986) The particular or the general? Some examples from robot kinematics, *Mechanism and Machine Theory*, 21(6)481/7.

I

Idlani S, Streit DA, Gilmore BJ (1993) Elastic Potential Synthesis, A generalized procedure for dynamic synthesis of machine and mechanism systems, *Journal of Mechanical Design*, sep 115(3)568/75.

IFToMM (1996) International Federation for the Theory of Machines and Mechanisms, IFToMM Commision A Standards for Terminology, Abbreviation/Symbols for Terms in TMM, *Mechanism and Machine Theory*, 32(6)641/66.

J

Jansen A (1994) Laparoscopic-assisted colon resection, *Annales Chirurgiae et Gynaecologiae*, Vol. 83, p86/91.

Jean M, Gosselin CM (1996) Static balancing of planar parallel manipulators, *Proceedings of the IEEE International Conference on Robotics and Automation*, Minneapolis, Minnesota, USA, p3732/7.

Jenuwine JG, Midha A (1989) Design of an exact constant force generating mechanism, *Proceedings of the 1st National Applied Mechanisms & Robotics Conference*, Vol 2, p10B-4-1/5.

Jenuwine JG, Midha A (1992) Synthesis of single-input and multiple output port mechanisms with springs for specified energy absorption, 22nd Biennial Mechanisms conference, DE-Vol 46, *Mechanical Design and Synthesis*, ASME 1992.

Johnson GR, Buckley MA (1997) Development of a new motorised upper limb orthotic system (MULOS), *Resna 1997*.

Johnson RC, Towfigh K (1971) Application of number synthesis to practical problems in creative design, In: Johnson RC (ed.), *Mechanical design synthesis with optimization applications*, Van Nostrand Reinhold Company, New York.

K

Kandel ER, Schwartz JH (1991) *Principles of neural sciences*, third edition, Elsevier, NY.

Kaniewski B (1989) Voluntary-closing terminal device, *Journal of the Association of Children's Prosthetic-Orthotic Clinics*, 24(2/3)35.

Kato I, Sadamoto K (1985) *Mechanical hands illustrated*, revised edition, Hemisphere Publisching Corporation, ISBN 0-89116-374-3

Kenworthy G, Small ADS (1974) New techniques used in the production of cosmetic gloves, *Medical and Biological Engineering*, January.

Klasson B, Winderlich H (1969) *Rapport über einleitende Entwicklungsarbeit für einen dünnen kosmetischen Prothesenhandschuh aus PVC*, (Report on exploratory research on a thin cosmetic prothesis glove out of PVC), (In German), Sven rapport 110 D, Norrbackinstitutet, Stockholm, Sweden.

Klein Breteler AJ (1987) *Kinematic optimization of mechanisms, a finite element approach*, PhD Thesis, Delft University of Technology, Delft.

Klein Breteler AJ (1990) *Mechanism design* (in Dutch), Report w76, Delft University of Technology, Delft.

Klopsteg PE, Wilson P (1964) *Human limbs and their substitutes*, Hafner Publishing Company, New York. Reprint of 1954 edition by McGraw Hill Company.

Kochev IS (1991) Optimum balancing of a class of multiloop linkages by function cognate transformations, *Mech. Mach. Theory*, 26(3)285/97.

Koster MP (1996) *Constructionprinciples for accurate motion and positioning*, (In Dutch), Uitgeverij Universiteit Twente, Enschede, ISBN 9036508320.

Kreutzinger R (1942) Über die Bewegung des Schwerpunktes beim Kurbelgetriebe, (On the motion of the center of mass in a four-bar linkage), (In German), *Maschinenbau, Betrieb*, p397/8.

Kristen H, Weteschnik V (1981) Die aktieve Pro- und Supination als ein zu gering genütztes Prinzip zur Steuerung von Unterarm-Prothesen? (Active pro- and supination as undervalued principle for forearm prosthesis control?), (In German) *Med. Orthop. Techn.* (3)73/6.

Kruit J (1987) *Otto Bock gloves size 42 en 43, measurement thumb pivot, glove modification*, (In Dutch), WMR, Delft university of Technology, Delft.

Kruit J (1990) *Elbow controlled hand prosthesis for children II, final report,* (In Dutch), Report WMR-N336, Delft University of Technology, Delft.

Kruit J, Cool JC (1989) Body powered hand prosthesis with low operating power for children, *Journal of Medical Engineering and Technology,* Vol. 13, No. 1/2, p129/33.

Kumar V, Waldron KJ (1988) Force Distribution in Closed Kinematic Chains, *IEEE Trans. on Rob. and Aut.,* 4(6)657/64.

Kuntz JP (1995) *Rolling Link Mechanisms*, PhD Thesis, Delft University of Technology, Delft, The Netherlands.

Küspert M, Heinke J, Heinl T (1998) *Hood lifting device with spring support*, PCT/DE97/02367.

Kyberd PJ, Chappell PH (1994) The Southampton Hand, An Intelligent Myoelectric Prosthesis, *Journal of Rehabilitation Research and Development*, 31(4)326/34.

Kyberd PJ, Evans M, Winkel S te (1998) An intelligent anthropomorphic hand, with automatic grasp, *Robotica* (16)531/6.

L

Lachmann K (1929) Mechanics, statics of rigid bodies (In German), In: Dubbel H (1929) *Taschenbuch für den Maschinenbau*, Springer, Berlin, Vol. 1.

Lagrange JL (1997) *Analytical Mechanics*, Translated from the French and edited by A Boisonnade and VN Vagliente, first published (1788) Méchanique analitique, Desaint, Paris, second edition published as Méchanique analitique, Courcier, Paris (1811).

Laliberté T, Gosselin CM (1998) Simulation and design of underactuated mechanical hands, *Mechanism and Machine Theory*, 3(1/2)39/57.

Lamb H (1916) *Statics, including hydrostatics and the elements of the theory of elasticity*, 2nd edition, Cambridge University Press, Cambridge.

Landsberger S, Shaperman J, Vargas V, Meadows E, Mitani M, McNeal DR, Doing Less For More: A New Mobile Arm Support, *BED-Vol.39, Advances in Bioengineering, ASME 1998*, pp389/90

Lazeroms M, Jongkind W, Honderd G (1997) Telemanipulator Design for Minimally Invasive Surgery, Proceedings of the American Control Conference, Albuquerque, New Mexico, p2982/6.

Leblond M, Gosselin CM (1998) Static balancing of spatial and parallel manipulators with prismatic actuators, *Proceedings ASME DETC 25th Biennial Mechanisms Conference*, Sept 13-16, Atlanta, Georgia, paper number DETC98/MECH-5963.

Lee JM, Burchett D, Ryan S, Evaluation of the material properties of cosmetic gloves for upper extremity prosthetic use, Rehabilitation R&D Reports, 1991.

Leerdam NGA van (1993) *The swinging UTX orthosis, biomechanical fundamentals and conceptual design,* PhD-Thesis, University of Twente, Enschede, The Netherlands.

Lewis PE, Ward JP (1989) *Vector analysis for engineers and scientists,* Addison-Wesley Publishers Ltd.

Lim TG, Cho HS, Chung WK (1990) Payload capacity of balanced robotic manipulators, *Robotica,* Vol 8, p117/23.

Linde RQ van der (1999) Design, analysis and control of a low power joint for walking robots, by phasic activation of McKibben muscles, *IEEE Trans. Robotics and Automation,* 15(4)599/604.

Löffler L (1984) *Der Ersatz für die obere Extremität,* Die entwicklung von den ersten Zeugnissen bis heute, (The replacement for the upper extremity, development from the first evidence till today), (In German), Ferdinand Enke Verlag, Stuttgart.

Lowen GG, Tepper FR, Berkof RS (1983) Balancing of linkages – an update, *Mechanism and Machine Theory,* 18(3)213/20.

Luna B, Lomax CW, Smith DD (1993) Space simulation in the neutral buoyancy test facility, *In Aerospace Proceedings of the Aeroteck Conference,* Sep 27-30.

Lunteren A van, GHM Van Lunteren-Gerritsen, HG Stassen, MJ Zuithof (1983) A field evaluation of arm prostheses for unilateral amputees, *Prosthetics and Orthotics International,* 7(3)141/51.

Lushbough C (2000) Rolamite postal scale, *Equilibrium, Quarterly Magazine of the International Society of Antique Scale Collectors,* 2499/504.

M

Maase S (1996) *A manipulator for minimally invasive surgery* (in Dutch), MSc-Thesis, Delft University of Technology, Delft.

Magermans DJ, Tol PPJ van der (1999) *Feedback concerning pinch forces of a voluntary closing elbow controlled hand prosthesis,* MSc-Thesis Free University of Amsterdam.

Mahalingam S, Sharan AM (1986) The optimal balancing of the robotic manipulators, *IEEE international conference on robotics and automation,* p828/35

Majima S, Matsushima K (1991) On a micro-manipulator for medical application, stability consideration of its bilateral controller, *Mechatronics,* Vol. 1, pp. 293/309.

Matthew GK, Tesar D (1976a) Synthesis of spring parameters to balance general forcing functions in planar mechanisms, *ASME-paper* 76-DET-45.

Matthew GK, Tesar D (1976b) Synthesis of spring parameters to satisfy specified energy levels in planar mechanisms, *ASME-paper* 76-DET-44.

Meeks D, LeBlanc M (1988) Preliminary assessment of three new designs of prehensors for upper limb amputees, *Prosthetics and orthotics International,* Vol. 12, 41/5.

Melzer A, Buess G, Cuschieri A (1992) Instruments for endoscopic surgery, In: *Operative Manual of Endoscopic Surgery,* Cuschieri A, Buess G, Périssat J (Eds) Springer Verlag, Berlin.

Meriam JL, Kraige LG (1987) *Engineering mechanics,* Vol. 1, Statics, 2nd edition, John Wiley and Sons, New York.

Meriam JL, Kraige LG (1987) *Engineering mechanics,* Vol. 2, Dynamics, 2nd edition, John Wiley and Sons, New York.

Midha A, Zhen-Lu Zhao (1985) Synthesis of planar linkage via loop closure and nonlinear equations solution, *Mechanism and Machine theory,* 20(6)491/501.

Minotti P, Dahan M (1985) Application of mechanisms on design of robots, In: Yoshikawa H (ed) Design and Synthesis, Elsevier Science Publishers B.V. (North Holland), p347/52.

Mishima Y (1956) *Kinkakuji,* Het Gouden Paviljoen, Meulenhoff, 1986.

Mosher RS, Kugath DA (1971) *Material handling apparatus,* US Patent 3,608,743.

Munneke M (1994) *Optimising feedback in voluntary closing hand prostheses* (In Dutch), MScThesis, Free University, Amsterdam, published at Delft University of Technology, WBMT-MR.

Murphy GM (1986) In support of the hook, *Clin. Prosthet. Orthot.* 10(2)78/81.

Musil R (1921) *Die Schwärmer*, (In German), Rowohlt Taschenbuch Verlag, Reinbek bei Hamburg, 1982.

Musil R (1930) *Der Mann ohne Eigenschaften*, (In German), Adolf Frisé, 1952.

N

Nathan RH (1985) A constant force generating mechanism, *Journal of Mechanisms, Transmissions, and Automation in Design*, 107(12)508/12.

Nakashima S, Toyoda K, Torii N, Mizuno H (1988) *Industrial robot*, US Patent 4,728,247.

NASA (1985) Low friction joint for robot fingers, *NASA Tech Briefs*, p140.

Neumann K-H, Hase W, Gerlach R, Schellbach D, Gärtner P (1993) Raumbegrenzte Anordnung zum statischen Ausgleichs konstanter Kräfte, *Offenlegungsschrift* DE 41.40.476.A1.

Newman N (1973) Mechanical relationships of a rolling joint with offset insertion, *Medical and Biological Engineering*. September, p645/7.

Nguyen V-D (1988) Constructing Force-Closure Grasps, *The International Journal of Robotics Research*, MIT, Vol. 7, No. 3, p3/16.

Nijenbanning G (1998) *Scoliosis redress, design of a force controlled orthosis*, PhD-Thesis, University of Twente, Enschede, The Netherlands.

Norwich HN (1993) *Information, sensation and perception*, Academic Press Inc, San Diego.

O

Okada T (1986) Optimization of mechanisms for force generation by using pulleys and springs, *The International Journal of Robotics Research*, 5(1)77/89.

Oldham K, Walker MJ (1978) A procedure for force-balancing planar linkages using counterweights, *Journal of Mechanical Engineering Science*, 20(4)177/82.

P

Papadopoulos J (1997) Personal communication.

Passel V van (1995) *A low friction mechanism for spring force compensation*, BSc-Thesis, OCP-MMS, Delft University of Technology.

Pereira BP, Leow EL, Kour AK, Pho RWH (1992) Reinforced silicone rubber cosmetic prostheses: clinical trails, *Proceedings 7th world congress of ISPO*, Chicago USA, p386.

Pich R, Wiemer A (1955) Zum Thema: Hebel, der einen gleichmäbigen Mebdruck gewährt, *Feingerätetechnik* 4(8)348/51.

Pieterse M (2000) *Sensitivity of the upper arm for the operating force of a hand prosthesis*, BSc-Thesis, HHS The Hague.

Pijl AJ van der (2000-2001) Personal communication.

Pijl AJ van der, Herder JL (2001) Development of 5mm-trocar laparosopic forceps with force feedback, *Proceedings ASME Design Engineering Technical Conferences*, Sept 9-12, Pittsburg, Pennsylvania, paper number DETC2001/DAC-21070.

Plettenburg DH, Cool JC (1992) Upper extremity prostheses, the WILMER approach, *Proceedings of the 7th ISPO World Congress*, June 28 - July 3, Chicago, p311.

Plettenburg DH, Cool JC (1994) Basic requirements for hand prosthesis and orthoses, *Congress Summaries 11th International Congress of the World Federation of Occupational Therapists*, London, p781/3.

Pons JL, Ceres R, Jiménez AR (1998) Quasi-exact linear spring countergravity system for robotic manipulators, *Mechanism and Machine Theory*, 3(1/2)59/70.

Pracht P, Minotti P, Dahan M (1987) Synthesis and balancing of cam-modulated linkages, *ASME Design and Automation Conference*, 10(2)221/6.

Pritchard JG, Windsor J (1965) Hemiplegic arm rest, *Lancet*, Vol. 1, p1199/200.

Püschel F (1955) *Künstliche Hände, Künstliche Ärme*, (Artificial hands, artificial arms), (In German), Technischer Verlag Herbert Cram, Berlin

R

Radocy B (1986) Voluntary closing control: a succesful new design approach to an old concept, *Clinical Prosthetics and Orthotics*, 10(2)82/6.

Radocy B, *Product Catalog TRS*, Boulder, Colorado.

Radocy B, Ronald ED (1981) A terminal question, *Orthotics and Prosthetics*, 35(1)1/6.

Rahman T, Ramanathan R, Seliktar R, Harwin W (1995) A simple technique to passively gravity-balance articulated mechanisms, *Journal of Mechanical Design*, 117(4)655/8.

Rahman T, Sample W, Seliktar R, Alexander M, Scavina M (2000) A Body-Powered Functional Upper Limb Orthosis, *Journal of Rehabilitation Research and Development*, 37(6).

Reuleaux F (1876, 1963) *The kinematics of machinery,* McMillan, 1876, Dover, New York, 1963.

Rhee van (1996-2000) Personal communication.

Ricard R, Gosselin CM (2000) On the development of reactionless parallel manipulators, Proceedings of ASME Design Engineering Technical Conferences, Baltimore, Maryland, sept 10-13, paper number DETC2000/MECH-14098.

Rickey G (1993) A technology of kinetic art, *Scientific American,* February, p50/5.

Riele FLS te (1997) The design of a system that attaines neutral equilibrium for rotation about a moving pivot (in Dutch), Masters thesis, Report BW-94, Twente University, Enschede, The Netherlands.

Riele FLS te (2000) The development of a highly efficient energetic locomotion foot, In: Bante I, Feijen J (eds) *Proceedings of the Dutch Annual Conference on BioMedical Engineering*, Oct 9-10, Papendal, The Netherlands, p112/3.

Riele FLS te, Herder JL (2001) Perfect static balance with normal springs, *Proceedings ASME Design Engineering Technical Conferences*, Sept 9-12, Pittsburg, Pennsylvania, paper number DETC2001/DAC21096.

Rivin EI (1988) *Mechanical design of robots*, McGraw-Hill, ISBN 0-07-052992-2.

Robert AE (1989) Cosmetic covers for upper and lower extremity prostheses, *Rehabilitation R&D Progress Reports*.

Roest R (1990) *Inleiding mechanica,* (Introduction mechanics), (In Dutch), DUM Delft, 3rd ed., in Dutch, ISBN 90-6562-127-X.

Ros S, Scholten S (1998) *Development of robot arm with McKibben muscles*, BSc-Thesis, HS Utrecht.

Rosen SL (1982) Fundamental principles of polymeric materials, ISBN 0-471-08704-1, John Wiley & Sons, New York.

Roth B, (1989) Design and Kinematics for Force and Velocity Control of Manipulators and End-Effectors, *Robotics Science,* Brady, M., ed., MIT-Press.

Ruina A (1997-1998) Personal communication.

Ruoff CF (1985) *Rolling contact robot joint*, US Patent 4,558,911.

S

Salamon BA (1989) *Mechanical advantage aspects in compliant mechanism design*, MSc-Thesis, Purdue University.

Salamon BA, Midha A (1992) An Introduction to Mechanical Advantage in Compliant Mechanisms, *DE-Vol. 44-2, Advances in Design Automation*, Vol. 2, pp. 47/51.

Sato Y, Ejiri A (1991) Micro-g emulation system using constant tension suspension for a space manipulator, *Proceedings of the 1991 IEEE International Conference on Robotics and Automation,* Sacramento, CA.

Schlesinger G (1919) *Ersatzglieder und Arbeitshilfen für Kriegsbeschädigte und Unfallverletzte* (Replacement members and labour aids for war casualties and accident victims), (In German), Verlag von Julius Springer, Berlin.

Sears H (1983) *Evaluation and developement of a new hook type terminal device*, PhD-Thesis, University of Utah, Departement of Bioengineering.

Sefrioui J, Gosselin CM (1995) On the quadratic nature of the singularity curves of planar three-degree-of-freedom parallel manipulators, *Mechanism and Machine Theory,* 30(4)533/51.

Segla S, Kalker-Kalkman CM, Schwab AL (1998) Statical balancing of a robot mechanism with the aid of a genetic algorithm, *Mechanism and Machine Theory,* 3(1/2)163/74.

Sevak NM, McLarnan CW (1974) Optimal synthesis of flexible link mechanisms with large static deflexions, ASME paper 74-DET-83.

Seydel R (1947) *From equilibrium to chaos: practical bifurcation and stability analysis*, Elsevier Science Publishing Co Inc, New York, ISBN 0-444-01250-8.

Shaperman J, LeBlanc M, Setogutchi Y, McNeal DR (1995) Is body powered operation of upper limb prostheses feasible for young limb deficient children?, *Prosthetics and Orthotics International*, Vol. 19, p165/75.

Shapiro S, Locast M (1989) Comparison of ADEPT terminal device to hook terminal device for children with below-elbow amputations, *Journal of the Association of Children's Prosthetic-Orthotic Clinics*, 24(2/3)36.

Sheridan TB (1996) Human Factors in Telesurgery, In: *Computer Integrated Surgery, Technology and Clinical* Applications, Taylor RH, Lavallée S, Burdea GC, Mösges R (Eds), MIT Press, Cambridge, Mass., p223/9.

Shieh W-B, Tsai L-W, Azarm S, Tits AL (1996) Multiobjective optimization of a leg mechanism with various spring configurations for force reduction, *Journal of Mechanical Design*, 118(2)179/85.

Shin E, Streit DA (1991) Spring equilibrator theory for static balancing of planar pantograph linkages, *Mechanisms and Machine Theory*, 26(7)645/57.

Shin E, Streit DA (1993) An energy efficient quadruped with two-stage equilibrator, *Journal of Mechanical Design*, 115(3)156/63.

Sieker KH (1953) Federgelenke und federnde Getriebe, (Spring pivots and elastic linkages), *VDI-Tagungsheft 1*, p141/8.

Sieker KH (1956) *Einfache Getriebe*, 2. Auflage, (Eementary linkages), (In German) C.F. Winter'sche Verlagshandlung, Füssen.

Simpson DC (1974) The choice of control system for the multimovement prosthesis: extended physiological proprioception (e.p.p.), In: Herberts P *et al.*, *The control of upper extremity prostheses and orthoses*, Thomas, Springfield, Vol. III, p146/50.

Sjoerdsma W, Herder JL, Horward MJ, Jansen A, Bannenberg J, Grimbergen CA (1997) Force transmission of laparoscopic grasping instruments, *Minimally Invasive Therapy and Allied Technologies*, 6(4)274/8.

Skorecki J (1967) A Floating Arm Support for wheelchairs, *Annals of Physical Medicine*, Vol IX, No. 2.

Skorecki J (1971) Biomechanical applications of the synthesis of mechanisms, *Proceedings of the third world congress for the theory of machines and mechanisms*, Kupari, Yugoslavia, Sept 13-20, Vol. E, Paper E-24, p311/22.

Soethoudt B (1998) *A new ideal spring arrangement* (in Dutch), internal report, Delft University of Technology, OCP-MMS.

Soper R, Mook D, Reinholtz C (1997) Vibration of nearly perfect spring equilibrators, *Proceedings of the 1997 ASME Design Engineering Technical Conference*, Paper number DAC-3768.

Sprague CW (1971) *Weighing scales of force-balancing type*, US Patent 3,621,928

Spronck ESM (1984) *Balancing device*, European Patent Specification EP 0 007 680 B1, European Patent Office.

Stern PH, Lauko T (1975) Modular designed, wheelchair based orthotic system for upper extremities, *Paraplegia*, Vol. 12, p299/304.

Stevens SS (1975) *Psychophysics, introduction to its perceptual, neural, and social prospects*, John Wiley and Sons, NY.

Stevenson EN Jr (1973) Balancing of machines, *ASME Journal of Engineering for Industry*, 95(2)650/6.

Streit DA, Chung H, Gilmore BJ (1991) Perfect equilibrators for rigid body spatial rotations about a Hooke's joint, *Journal of Mechanical Design*, 113(4)500/7.

Streit DA, Gilmore BJ (1989) 'Perfect' spring equilibrators for rotatable bodies, *Journal of Mechanisms, Transmissions and Automation in Design*, 111(12)451/8.

Streit DA, Shin E (1993) Equilibrators for planar linkages, *Journal of Mechanical Design*, sep 115(3)604/11.

Suh CH, Radcliffe CW (1978) *Kinematics and Mechanisms Design*, John Wiley and Sons Inc, ISBN 0-471-01461-3, p141/6, 312/26.

T

Tao DC (1964) *Applied linkage synthesis*, Addison-Wesley Publishing Company Inc, Reading MA.

Thomassen EW (1991) Design of a below elbow arm prosthesis with open frame socket and elbow controlled voluntary closing hand, *Annual Scientific Meeting ISPO* UK and The Netherlands National Member Society, Norwich, April 10-12.

Treloar LRG (1975) *The physics of rubber elasticity*, 3rd edition, Clarendon Press, Oxford.

Tsuda F, Mizuguchi O (1980) Arm with gravity-balancing function, *European Patent Application* EP 0.024.433.A1.

Tuda G, Kada H, Sekino T, Nagahama Y (1986) Gravity balancing device for rocking arm, *US Patent* 4.592.697.

Tuijthof GJM, Herder JL (2000) Design, actuation and control of an anthropomorphic robot arm, *Mechanism and Machine Theory* 35(7)945/62.

Tuijthof GJM (1998) *Design, actuation and control of an anthropomorphic robot arm*, MSc-Thesis, OCP-MMS A867, Delft University of Technology.

U

Ulrich N, Kumar V (1991) Passive mechanical gravity compensation for robot manipulators, *Proceedings of the 1991 IEEE International Conference on Robotics and Automation*, Sacramento, California, April 1991, p1536/41.

Ulrich N, Kumar V (1991) Design methods of improving robot manipulator performance, *ASME DTC 17th Design Automation Conference, September 22-25, Miami FL*, DE-Vol. 32-2, p545/50.

V

Verbeek J (1995-1997) Personal communication.

Verdult E (1998) *Drilling back*, PhD-Thesis, Delft University of Technology, Delft.

Vertut J (1981) Motorized manipulator of the cable transmission type having an increased field of action, *US Patent* 4,283,165.

Visser H de (1998) Force directed design of a voluntary closing hand prosthesis, MSc-Thesis A840, OCP-MMS, Delft University of Technology.

Visser H de, Herder JL (2000) Force directed design of a voluntary closing hand prosthesis, *Journal of Rehabilitation Research and Development*, 37(3)261/71.

Vrijland N, Herder JL (2001) *Chair*, Patent application.

W

Wahl AM (1963) *Mechanical springs*, McGraw-Hill Book Company Inc, New York.

Walsh GJ, Streit DA, Gilmore BJ (1991) Spatial spring equilibrator theory, *Mech. Mach. Theory* 26(2)155/70.

Walta JH, P Ariese, JC Cool (1989) Ergonomic socket design for congenital below elbow amputated children, *Journal of rehabilitation sciences*, 2(1)19/24.

Wang J, Gosselin CM (1998) Static balancing of spatial six-degree-of-freedom parallel mechanisms with revolute joints, *Proceedings ASME DETC 25th Biennial Mechanisms Conference*, Sept 13-16, Atlanta, Georgia, paper number DETC98/MECH-5961.

Wang J, Gosselin CM (1999) Static balancing of spatial three-degree-of-freedom parallel mechanisms, *Mechanism and Machine Theory*, Vol. 34, p437/52.

Wang J, Gosselin CM (2000) Static balancing of spatial four-degree-of-freedom parallel mechanisms, *Mechanism and Machine Theory*, Vol. 35, p563/92.

Weaver SA, Lange LR (1985) Myoelectric prostheses versus body powered prostheses with unilateral, congenital, adolescent below-elbow amputees, American Orthotic and Prosthetic Association National Assembly Scientific Presentation on October 16.

Wells D (1995), *Mysterieuze en fascinerende raadsels*, Translated (Jos den Bekker) from the English: *You are a mathematician*, Bert Bakker.

Werff, K van der (1976) A finite element approach to kinematics and dynamics of mechanisms, *Proceedings of the Fifth world Congress on the Theory of Machines and Mechanisms,* Montreal, Canada, Vol. 1, p587/90.

Werff, K van der (1977) *Kinematic and dynamic analysis of mechanisms, a finite element approach*, PhD Thesis, Delft University of Technology, Delft.

Weverwijk R van, Fokkert J (1999) *Anthropomorphic robot arm*, BSc-Thesis, HS Utrecht.

Whitehead TN (1954) *The design and use of instruments and accurate mechanism, underlying principles*, 2nd edition, Dover Publications Inc., New York.

Wilkes DF (1967) *Rolamite: a new mechanical design concept*, Report SC-RR-67-656A, Sandia Laboratory, Albuquerque.

Wilkes DF (1969) *Roller band device*, US Patent 3,452,175.

Wilson MS, Deans GT, Brough WA (1995) Prospective trial comparing Lichtenstein with laparoscopic tension-free mesh repair of inguinal hernia, *British Journal of Surgery,* pp. 274/7.

Wise CE (1967) Rolamite, *Machine Design,* november 1967, p44/8.

Woodworth RS, Schlosberg H (1966) *Experimental psychology*, Chapter 8: Psychophysics, determination of thresholds, 3rd edition, John Duckens & Co. Ltd, Northampton.

Y

Yao J, Smith MR (1993) Force-balancing of linkages, *Mechanism and Machine Theory*, 28(4)583/91.

Ye Z, Smith MR (1994) Complete balancing of planar linkages by an equivalence method, *Mechanism and Machine Theory*, 29(5)701/12.

A   Appendix

A1.1   Definitions   (see also IFToMM, 1996)

Compensate	Add a force in order to eliminate the influence on the operating characteristic of another force, in such a way that a statically balanced system results.
Distal	Far from fixed point.
Dynamic equivalence	Equivalent with respect to variations about the nominal state of motion.
Energy-free	Can be moved without operating effort.
Equilibrate	Compensate for gravity forces.
Force origin	Intersection of (the extension of) the force-length characteristic with length-axis.
Free length	The (virtual) distance between the attachment points of a spring when the external force is zero, or graphically, the distance from the origin to the *force origin* in the force-length diagram.
Free length circle	Locus of the *force origin* of a spring.
Ideal spring	Tension spring with zero *free length*, constant spring rate, limitless strain, and forces acting along their centerline.
Indifferent	State of equilibrium between stable equilibrium and unstable equilibrium.
Initial tension	Force which presses the coils of a helical extension spring together when no external load is present. The initial

227

	tension is equal to the force needed to separate the coils at all.
Instantaneous equivalence	Equivalent with respect to the nominal state of motion.
Neutral equilibrium	State of equilibrium between stable equilibrium and unstable equilibrium.
Proximal	Close to fixed point.
Rolling-link mechanism	Mechanism in which the links roll directly on one another without special bearing elements.
Static balance	State of equilibrium throughout the range of motion.
Stability equation	The equation which determines the location of the resultant of two forces on its line of action using the criterion of dynamic equivalence.

A3.1   Proof of circle-constructions

In this section, additional proof will be supplied for the theorem that locates the potential-equivalent point of attachment of the resultant of two forces on the circle through the original points of attachment and the intersection point of their lines of action. If this is to be true, then figure A3.1 must be valid. By inspection, the following relations are identified:

$$\angle QM_\gamma P_1 = 2\varepsilon - \gamma \tag{A3.1}$$

$$\angle QM_\gamma P_2 = 2\varepsilon + \gamma \tag{A3.2}$$

$$\angle QM_\gamma P_r = 2\varepsilon + 2\delta \tag{A3.3}$$

Validity is now inspected of the relation:

$$F_r r_r = F_1 r_1 + F_2 r_2 \tag{A3.4}$$

From the triangles in figure A3.1 the following equations are derived:

$$\Delta TM_\gamma D_1 \quad d_1 = 2R\sin\tfrac{1}{2}(\pi - \gamma + 2\varepsilon) = 2R\cos\left(\tfrac{1}{2}\gamma - \varepsilon\right) \tag{A3.5}$$

$$\Delta TM_\gamma D_2 \quad d_2 = 2R\sin\tfrac{1}{2}(\pi - \gamma - 2\varepsilon) = 2R\cos\left(\tfrac{1}{2}\gamma + \varepsilon\right) \tag{A3.6}$$

$$\Delta TM_\gamma D_r \quad d_r = 2R\sin\tfrac{1}{2}(\pi - 2\delta - 2\varepsilon) = 2R\cos(\delta + \varepsilon) \tag{A3.7}$$

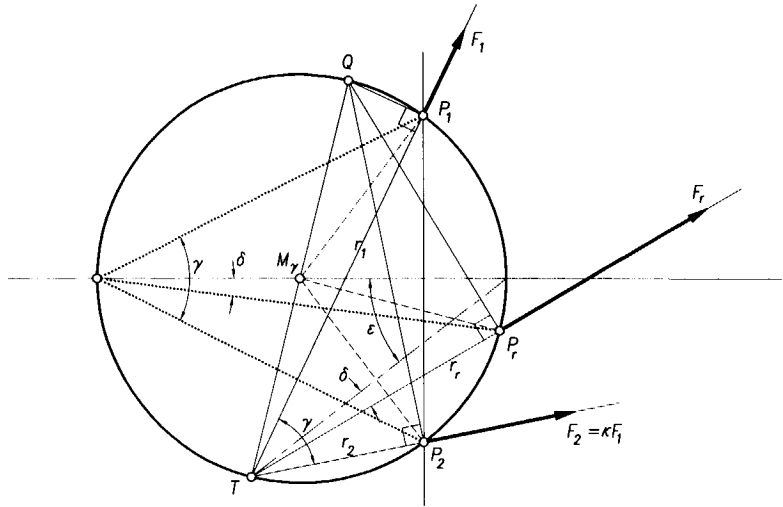From the force triangle in figure A3.2, one reads:

Figure A3.1 Proof of circle-construction.

$$F_r = F_1 \cos\left(\tfrac{1}{2}\gamma + \delta\right) + \kappa F_1 \cos\left(\tfrac{1}{2}\gamma - \delta\right) \tag{A3.8}$$

$$\kappa = \frac{\sin\left(\tfrac{1}{2}\gamma + \delta\right)}{\sin\left(\tfrac{1}{2}\gamma + \delta\right)} \tag{A3.9}$$

Substituting equations A3.5 through A3.9 into equation A3.4 yields:

$$\sin\gamma\cos(\varepsilon + \delta) = \cos\left(\tfrac{1}{2}\gamma - \varepsilon\right)\sin\left(\tfrac{1}{2}\gamma - \delta\right) + \cos\left(\tfrac{1}{2}\gamma + \varepsilon\right)\sin\left(\tfrac{1}{2}\gamma + \delta\right) \tag{A3.16}$$

after some elementary trigonometry resulting in:

$$\sin\gamma\cos(\varepsilon + \delta) = \sin\gamma\cos(\varepsilon + \delta) \tag{A3.17}$$

which concludes the proof.

A 3.2 Proof of κ and γ circles

In this appendix, analytical proof will be given of the fact that the dynamically equivalent point of application can be found at the intersection of two circles. One of these circles is the locus of this point as a function of the inclined angle γ, the other is the locus of this point as a function of $\kappa = F_1 / F_2$.

First, figure A3.3a is used to find the locus of point $P_r(x, y)$, under the condition that $\gamma = \angle P_1 P_r P_2$ is constant. By inspection, one finds:
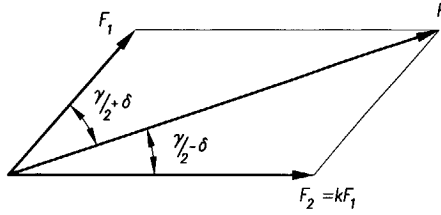
$$\tan\psi = (y - a)/x \tag{A3.18}$$

Figure A3.2 Triangle of forces.

$$\tan(\psi + \gamma) = (y + a)/x \tag{A3.19}$$

Substituting equations A3.18 and A3.19 into the trigonometric relation

$$\tan(\psi + \gamma) = \frac{\tan\psi + \tan\gamma}{1 - \tan\psi\tan\gamma} \tag{A3.20}$$

yields:

$$y - a + x\tan\gamma = y + a - \frac{(y-a)(y-a)}{x}\tan\gamma \tag{A3.21}$$

Multiplying by x, and rearranging results in:

$$\left(x - \frac{a}{\tan\gamma}\right)^2 + y^2 = a^2\left(1 + \frac{1}{\tan^2\gamma}\right) \tag{A3.22}$$

This is the equation of a circle with center $M_\gamma = (a/\tan\gamma, 0)$ and radius $R_\gamma = a/\sin\gamma$.

Figure A3.3b will now be used to find the locus of point $P_r(x, y)$ such that the ratio $\kappa = \sin\gamma_1/\sin\gamma_2$ is constant, where $\gamma_1 = \angle OP_1 P_r$, and $\gamma_2 = \angle OP_2 P_r$. From the figure, it is seen that:

$$\sin\gamma_1 = \frac{x}{\sqrt{x^2 + (a + y)^2}} \tag{A3.23}$$

$$\sin\gamma_2 = \frac{x}{\sqrt{x^2 + (a - y)^2}} \tag{A3.24}$$

so that

$$\kappa = \frac{\sin\gamma_1}{\sin\gamma_2} = \frac{\sqrt{x^2 + (a - y)^2}}{\sqrt{x^2 + (a + y)^2}} \tag{A3.25}$$

Squaring this expression results in:

230
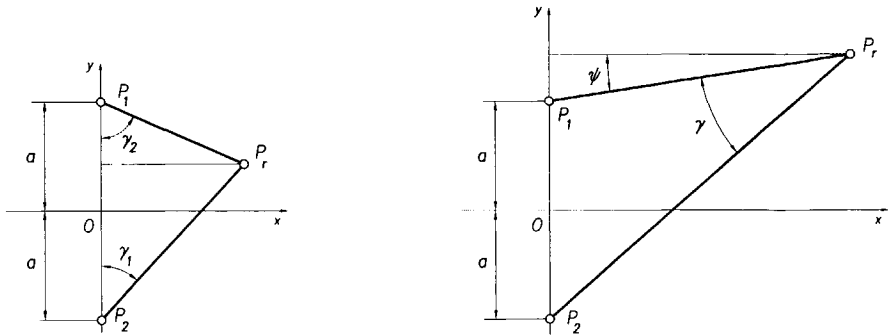
Figure A3.3   Proof of circle constructions: (a) the circle of constant γ, (b) the circle of constant κ.

$$\kappa^2 x^2 + \kappa^2 a^2 + 2ay\kappa^2 + \kappa^2 y^2 = x^2 + a^2 - 2ay + y^2 \qquad (A3.26)$$

which can be rearranged into:

$$x^2 + \left(y + \frac{a(\kappa^2 + 1)}{(\kappa^2 - 1)} \right)^2 = \frac{4a^2\kappa^2}{(\kappa^2 - 1)^2} \qquad (A3.27)$$

This is indeed the representation of a circle. Its center is given by: $K_\kappa = \left(0, a(\kappa^2 + 1)/(\kappa^2 - 1) \right)$ and it radius by $R_\kappa = 2a\kappa /(\kappa^2 - 1)$.
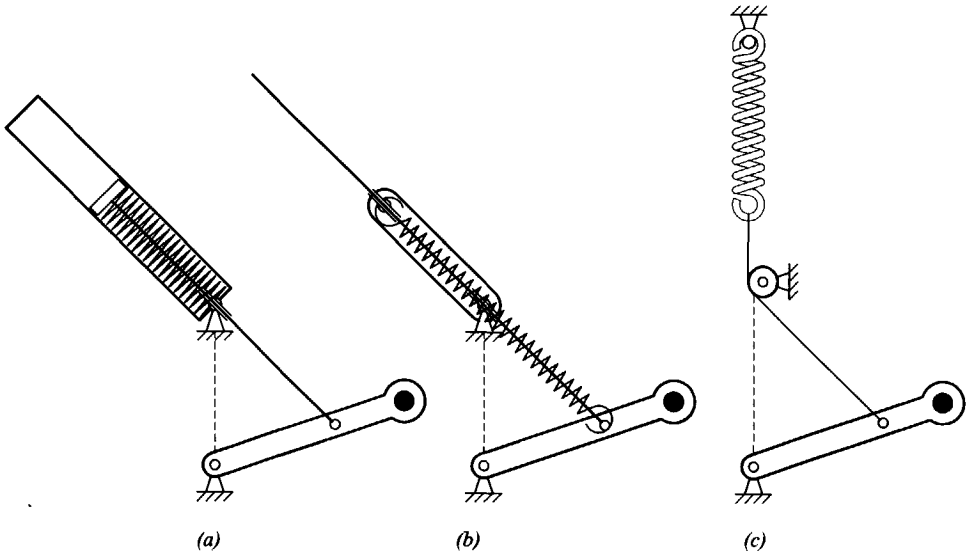
Figure A4.1   Ideal spring embodiments in the basic equilibrator: (a) compression spring with guiding elements (Haupt and Grewolls, 1963), (b) tension spring with guiding elements (Carwardine, 1932; Streit and Gilmore, 1989), (c) pulley and string arrangement (Carwardine, 1934; Hain, 1952).

A4.1   Ideal spring embodiments

Several ways to achieve zero-free-length behavior have been mentioned in the text. Details were provided in endnote 4.2. This section will provide some additional diagrams. Most of the ideal spring embodiments are published in conjunction with the basic gravity equilibrator (figure A4.1). As guiding elements are present, some friction is introduced.

Another noteworthy construction is described by Van der Hoek (1986) to achieve increased initial tension (figure A4.2). A compression spring of sufficient pitch is mounted on two linked brackets. Together these brackets correspond exactly with initial length L_0 of the spring. As the distance between the loops is equal to the compression of the spring, ideal behavior is obtained from the point where the loops leave the spring until the spring is fully pressed together.

Solutions of a different kind can be obtained by using other than helical springs. A few examples are given. If not deflected excessively, the bending of prismatic bars is linear enough to provide zero free length spring behavior (figure A4.3a; Haupt and Grewolls, 1963). In general, however, their use will
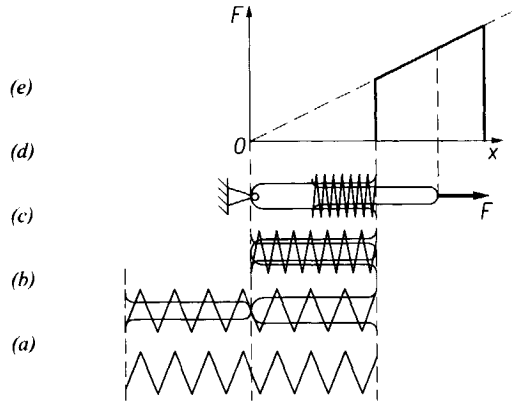
Figure A4.2 Spring arrangement with zero effective free length (Van der Hoek 1986): (a) unloaded helical compression spring of large pitch, (b) two U-brackets inserted, (c) the eye of the moving bracket is about to leave the coils, (d) spring in usable working range, (e) characteristic.

require much more spring mass (and space) than helical springs due to the lower energy storage capacity per weight ratio (Cool, 1987). In this respect, prismatic elements outperform helical springs, so when weight and volume are critical, rubber springs could be considered. In the Wilmer elbow orthosis (figure 2.6), an O-ring accomplishes the desired approximate gravity balance. Some rubber springs having a characteristic as suggested in figure A4.3b may even provide quite an accurate balancing quality (Ruina, 1998; Papadopoulos, 1997).
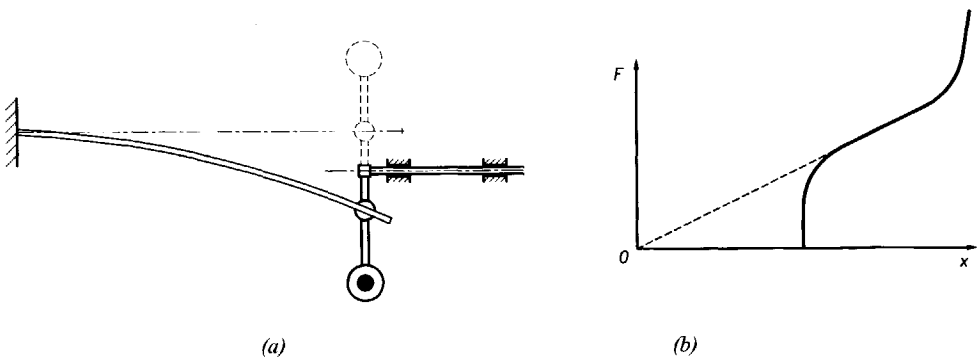

(a)   *(b)*

Figure A4.3   Ideal spring behavior by other than helical springs: (a) bending of a prismatic bar (after Haupt and Grewolls, 1963), (b) profitable use of a part of a non-linear characteristic.
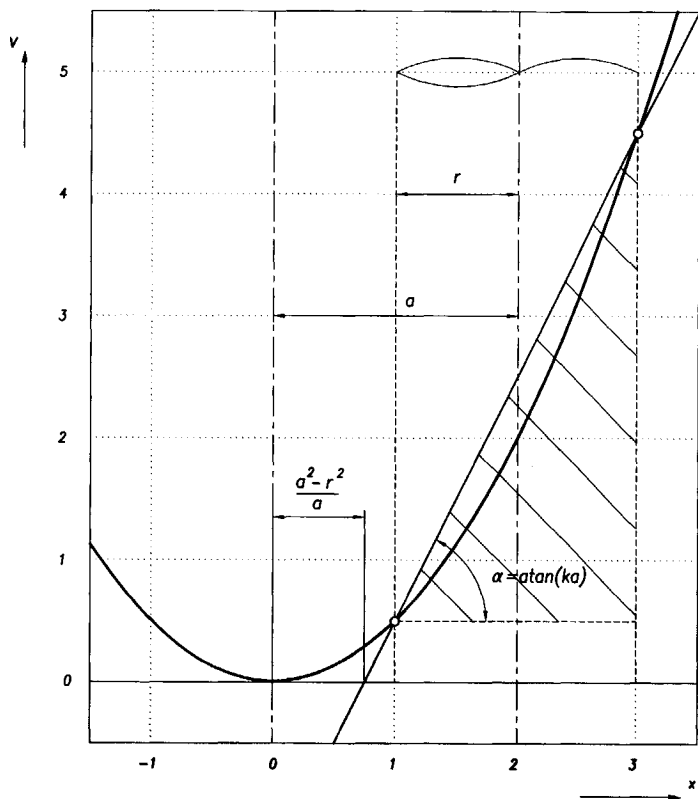
233

Figure A4.4   Intersection of the potential-paraboloid of an ideal spring and the cylinder above a rotatable link.

A4.2   Intersection of paraboloid and cylinder

The intersection of a paraboloid and a cylinder with parallel lines of symmetry is found as follows. First the equations of the potential-paraboloid of an ideal spring k and the cylinder above a rotatable link r hinged at $(a,0)$ are given (figure A4.4):

$$z = \tfrac{1}{2}k\left(x^2 + y^2\right) \tag{A4.1}$$

$$(x - a)^2 + y^2 = r^2 \tag{A4.2}$$

Isolating $\left(x^2 + y^2\right)$ from equation A4.1 and substituting the result into equation A4.2 yields:

234

$$z = ka \cdot x + \tfrac{1}{2}k\left(r^2 - a^2\right)$$ (A4.3)

So, as point $Q(x, y)$ traces a circle in the ground plane, point P describes an ellipse on the potential-paraboloid of the spring. The angle of inclination α of the plane containing the ellipse is therefore given by:

$$\tan \alpha = ka$$ (A4.4)

which, remarkably enough, is independent of r. Using this equation, the amplitude K_s of the potential energy function is readily found from the hatched triangle:

$$\tan \alpha = \frac{2K_s}{2r} = ka$$ (A4.5)

so:

$$K_s = rka$$ (A4.6)

The plane intersects the ground plane at a distance of $\left(a^2 - r^2\right)/a$ from the origin, which, remarkably enough, is independent of k.

A5.1 Rolling-link medical forceps

This section will provide some background on the medical forceps project. The project was initiated when it was found that the mechanical efficiency of current instruments was insufficient for accurate force feedback (Sjoerdsma *et al.*, 1997). The 10mm-shaft rolling version was the first result (see [5.15]). A 5mm version (Van der Pijl and Herder, 2001), and a version based on balanced springs (see [5.16]) are under development.

The rolling-link design was based upon a single-sided movable jaw, attached to a single roller. This roller is to be supported in such a manner that minimal reaction forces are generated. Figure A5.1a shows the force directed design of the movable jaw. Two of the forces are roughly known: the grasping force F_{grasp}, and the driving force from the shaft F_{rod}. Static equilibrium demands that the working lines of the three forces intersect at one point, labeled S. Possible working lines for the supporting force $F_{support}$ must contain point S, and must be located outside the hatched areas in order to result in equilibrium. It is advantageous to place the support plane perpendicular to the working line of $F_{support}$, in order to keep shear forces small, leading to a favorable support location as indicated. The remainder of the shear forces was supported by flexible bands, (Godden, 1968; NASA, 1985). Flexible bands of stainless steel with a thickness of 35 µm were selected,
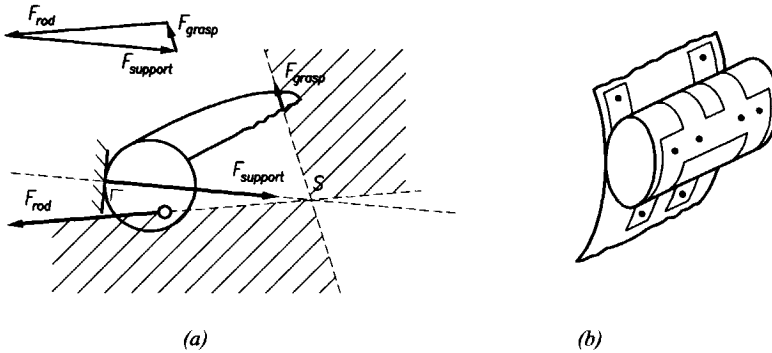
Figure A5.1   Force directed design of laparoscopic forceps: (a) movable jaw, (b) flexible bands.

yielding the best compromise between internal bending stress and normal stress. With these bands, the desired grasping force of 30N is attainable.

The demand for a constant force transmission function was satisfied by the application of a symmetrical construction. Figure A5.2 presents a schematic view of the mechanism, with somewhat exaggerated dimensions to illustrate the working principle. Two small rollers with the same radius are placed opposite each other against two support areas, one at each end of the frame. Two rods connect these rollers. The support areas of the rollers are parts of an imaginary central cylinder, dashed the figure, and they are fixed rigidly to the frame of the instrument. The pivots at the ends of the connecting rods are also designed to roll: its contact areas are furnished such that the little pins fixed to the rollers roll on the inside of an imaginary ring (drawn with dashed lines in figure A5.2a) keeping these pins at constant distance. The cross in the middle of the imaginary cylinder is the center of symmetry during motion. When the grasper is being closed, both rollers roll clockwise over their support areas, from the drawn positions towards the dashed situation. Meanwhile, the rods' ends roll over the small pins fixed to the rollers. In principle, all dimensions can be selected freely, as long as the rollers are equal and the connecting rods have equal length. Note that the center of the central cylinder need not be collinear with the centers of the rollers. Placing it eccentric does not affect the kinematics of the mechanism, but does influence the force distribution between the connecting rods.

The rods are prestressed so as to pull the rollers against the central cylinder. Thus, unforeseen forces and moments below the preload are prevented from lifting the rollers from the central cylinder in any direction. Prestressing also eliminates backlash in the mechanism. In order to prestress the rods, the central cylinder was divided into two parts so that the length of the frame could be
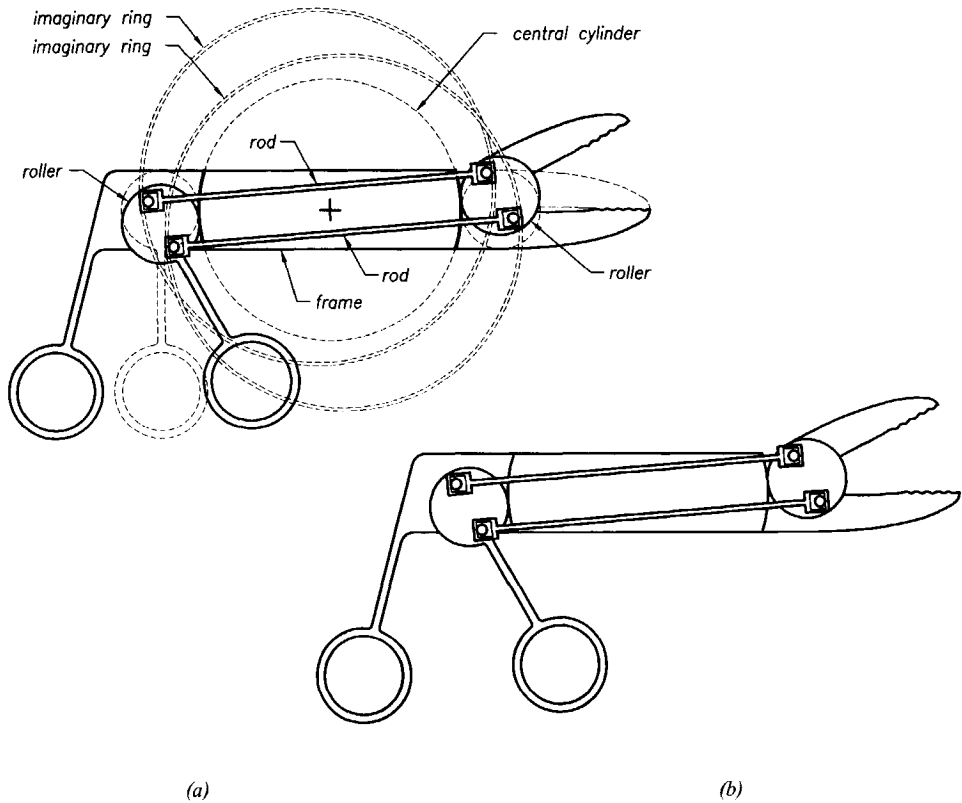
236

Figure A5.2 Working principle of laparoscopic forceps: (a) schematic representation, (b) without dashed lines (Patented, Herder and Horward, 1998).

adjusted. As an additional protection for the bands, the rollers are flanked by guidance planes, which conduct the excess of unforeseen forces and moments exceeding the preload in the rods. Figure A5.3 shows photographs of the first and second prototypes. The ergonomic handgrip was designed by Maase (1996).

The specifications of first prototype are as follows. The rollers' diameter was maximized at 7mm to fit in the 10mm shaft, whereas the diameter of the central cylinder is 392mm. The effective length of the shaft is 291mm. The prototype weighs 256g, but it is estimated that this can be reduced by a factor of at least two in the final design phase. The mechanical efficiency, defined as the ratio of output energy and input energy during one cycle of opening and closing, amounts to 96%. The force transmission characteristic shows a maximum deviation of 3% of the calculated curve. A second prototype featuring a shaft diameter of 5mm is under development (figure A5.3, Van der Pijl and Herder, 2001).
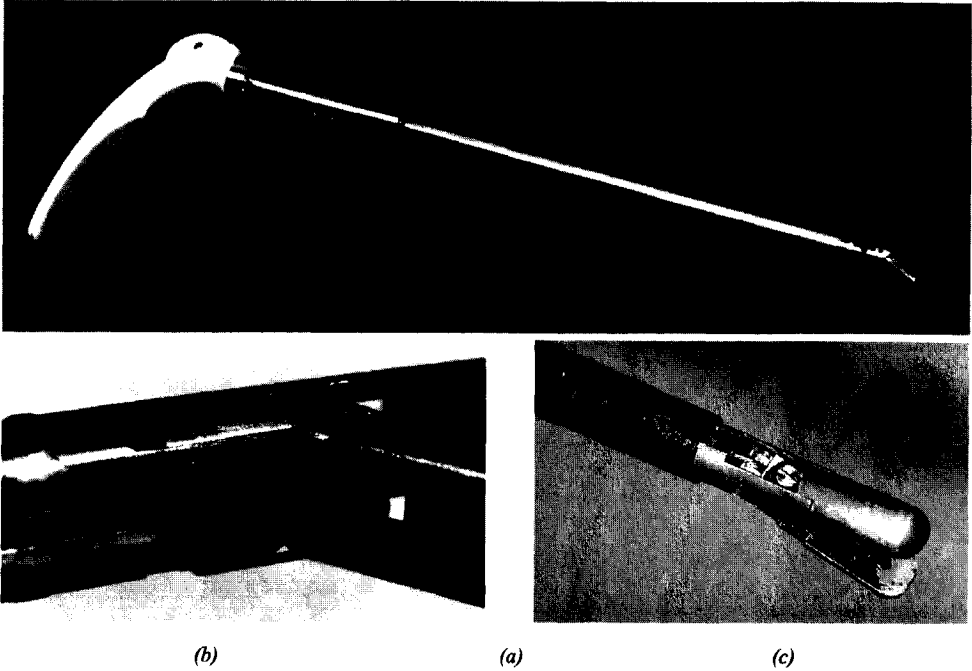
(b)　　　　　　　　　*(a)*　　　　　　　　　*(c)*

Figure A5.3　Photographs of rolling forceps: (a) overview of first prototype, (b) close-up of first prototype, (c) close-up of second prototype.

In addition to the mechanical measurements, the subjective sensitivity was assessed. An experimental set-up has been developed which meant to simulate a pulsating artery. By using an oscillator, pulses of varying amplitude could be guided through a thin-walled silicon tube. As a measure for the sensitivity, the absolute sensory threshold was used, defined as the minimal amplitude of the pulse necessary to perceive it (Gescheider, 1976). The absolute sensory threshold has been determined for bare fingers, for the low friction prototype, and for three laparoscopic forceps commercially available. If the sensitivity threshold for bare fingers is normalized as unity, the threshold of the prototype amounts to 2, approximately, whereas the other instruments have threshold values of about 10 to more than 20 (Den Boer *et al.*, 1998). In practice, it means that the pulse in an artery can be perceive with the rolling mechanism, whereas this sensation is absent in commercially available forceps.

Summary

Work in the field of rehabilitation engineering has initiated the desire to design mechanical systems with high energy-efficiency and good force transmission quality. Statically balanced systems provide continuous equilibrium, constant potential energy, and neutral stability. Therefore, they are particularly suited to meet the demands of low operating effort in the presence of (undesired) forces, especially when springs are used to avoid the weight and inertia associated with counterweights. These systems are called energy-free systems.

Investigation of the stability of a rigid body under the influence of forces led to a procedure for the composition of two forces in such a way that a point of application can be assigned to the resultant force. Consideration of the contribution of two forces to the stability of a rigid body yields an equation in addition to the resultant force and the resultant moment equations. This equation, called the stability equation, determines the location of the point of application on the line of action of the resultant force for dynamic equivalence (rather than instantaneous equivalence). For constant forces, the point of application of the resultant force of two given forces, is located on the circle circumscribing the points of application of the original forces and the intersection of their lines of action. In the case of central linear forces, different stability equations are found, and an additional translation along the resultant line of action was found to be required. Reducing the force system to a system of two forces while making use of the points of application of the dynamically equivalent resultant forces, provides a strategy to judge the stability of a given rigid body under the influence of forces. Using this theory, an elementary statically balanced system incorporating two zero-free-length springs is derived.

Several modification rules are presented which allow the elementary configuration to be altered and extended while maintaining its state of static balance. Together with guidelines for the proper application of these rules, the elementary configuration and the modification rules constitute a general framework for the conceptional design of statically balanced spring mechanisms. Many examples are given, including floating balanced systems with no physical pivots at all, to illustrate the versatility of the procedure, and to demonstrate the insight the procedure provides in the subsequent steps taken during the conceptional design phase, which may benefit the future design of mechanisms. It was further shown that when the use of normal springs is

required, the zero-free-length spring designs can function as initial estimates in optimization procedures. Several examples are provided.

Although the framework is primarily based on the perspective of constant potential energy, the inspection of the equilibrium of forces turns out to be very valuable. Force directed design, which takes desired force configurations as point of departure rather than desired motion objectives, has lead to profitable design solutions. The examples given include medical forceps for minimally invasive surgery, and a hand prosthesis. Undesired forces, due to the elasticity of compliant mechanism or cosmetic covering are statically balanced while friction is reduced by the design of rolling links, resulting in excellent force transmission quality, while the hand prosthesis features uniform force distribution on any object.

Just Herder, 2001

Samenvatting

Werk in het veld van de revalidatie heeft geleid tot de wens mechanische systemen te ontwerpen met een hoog energetisch rendement en een goede krachtoverdracht. Statisch gebalanceerde systemen zijn in elke stand in evenwicht, bezitten een constante potentiële energie, en zijn randstabiel. Dankzij deze eigenschappen zijn ze uitermate geschikt om systemen onder de invloed van (ongewenste) krachten een lage bedieningsinspanning te geven, vooral wanneer veren worden gebruikt om de massa en traagheid van contragewichten te vermijden. Deze systemen worden energie-vrije systemen genoemd.

Onderzoek naar de stabiliteit van een star lichaam onder de invloed van krachten heeft geleid tot een procedure voor het samenstellen van twee krachten zodanig dat een aangrijpingspunt kan worden aangewezen voor de resultante. Het beschouwen van de bijdrage aan de stabiliteit van een star lichaam levert de extra voorwaarde die naast de kracht- en momentvergelijkingen nodig is. Deze voorwaarde, de stabiliteitsvergelijking, bepaalt de locatie van het aangrijpingspunt van de resultante op zijn werklijn voor dynamische (in plaats van statische) equivalentie. Voor constante krachten is het dynamisch equivalente aangrijpingspunt van twee gegeven krachten gelegen op de cirkel door de aangrijpingspunten van de gegeven krachten en het snijpunt van hun werklijnen. In het geval van centraal lineaire krachten worden andere stabiliteitsvergelijkingen gevonden en is ten opzichte van het gevonden punt bij konstante krachten een additionele verschuiving van het dynamisch equivalente aangrijpingspunt langs de resultante werklijn noodzakelijk. Het reduceren van het krachtenspel tot een configuratie met twee krachten levert een aanpak om de stabiliteit van een star lichaam onder de invloed van krachten te beoordelen. Toepassing van deze theorie op een lichaam met twee centraal lineare krachten heeft een elementair statisch gebalanceerd systeem opgeleverd met twee veren die een ongespannen lengte gelijk aan nul bezitten.

Een aantal modificatieregels wordt gepresenteerd die het mogelijk maken het elementaire statisch gebalanceerde systeem te veranderen en uit te breiden met behoud van de statische balans. Samen met richtlijnen voor de juiste toepassing, vormen het elementaire systeem en de modificatieregels een raamwerk voor het conceptueel ontwerp van statisch gebalanceerde veermechanismen. Een reeks voorbeelden wordt gegeven, inclusief zonder enig scharnier zwevende gebalanceerde systemen, om de veelzijdigheid en

praktische toepasbaarheid te illustreren, en om het inzicht aan te tonen dat wordt verkregen tijdens het stapsgewijs uitvoeren van het conceptueel ontwerp, dat vervolgens ten goede kan komen aan nieuwe ontwerpen. Verder wordt aangetoond dat ook indien gewone veren dienen te worden toegepast, de concepten met de speciale veren als uitgangspunt en beginschatting kunnen dienen voor optimalisatieprocedures. Verschillende voorbeelden worden gegeven.

Ofschoon het raamwerk voornamelijk gebruik maakt van het perspectief van de constante potentiaal, blijkt dat de analyse van het krachtevenwicht zeer nuttig is. Krachtgestuurd ontwerpen, waarbij gewenste krachtconfiguraties als uitgangspunt dienen voor het ontwerp, in tegenstelling tot de gebruikelijke bewegingsdoelstellingen, heeft tot gunstige praktische uitvoeringen geleid. Onder de gegeven voorbeelden bevinden zich een paktang voor minimaal invasieve chirurgie en een handprothese. Ongewenste krachten, ten gevolge van de stijfheid van elastische mechanismen of de cosmetische handschoen worden statisch gebalanceerd, terwijl wrijving wordt verminderd door het toepassen van rollende scharnieren, wat samen tot een uitstekende krachttransmissie leidt, en bij de handprothese bovendien tot een uniforme krachtverdeling op vastgehouden voorwerpen met een verscheidenheid aan vormen.

Trefwoorden: statische balans, indifferent evenwicht, stabiliteit, dynamisch equivalente kracht, veermechanisme, zwaartekrachtscompensatie, conceptueel ontwerp, rollende scharnieren, krachtgestuurd ontwerpen, krachtterugkoppeling, handprothese, laparoscopische paktang.

Just Herder, 2001

Acknowledgement

Two opposite desks form the center of our study, the best room of the house with large windows, a french balcony, and atmospheric lighting for after sunset, including, of course, an Anglepoise desk lamp. The combined foot space under these desks provided an opportunity for physical contact during the numerous hours Monika and I spent there, each deeply entrenched in thoughts abouts our theses. As a soul mate and higly critical running mate, she has been of vital significance to the completion of this thesis. As I write this, she is close-reading the most recent and almost final version, but more than her sharp comments or shoulder massages, she gives meaning to this work.

Much of what has been put to paper has evolved as described in the preface. This is the place to express my gratitude to my supervisor Prof. Jan Cool for offering me the opportunity to do this project. I hope to have learned from his well-developed 'Möglichkeitssinn', and to continue the development of this ability. I owe special thanks to him, as well as to Prof. dr ir J.F. Besseling en Arend Schwab, for their contribution to chapter three (see endnote [3.1]). Furthermore, I thank Prof. Shigeo Hirose [2.6; 2.11], who stimulated rolling-link and pulley-and-string designs during my visit to his lab, Prof. Andy Ruina for suggesting the generalization of the Floating Suspension [5.7], and Prof. Clément Gosselin who stimulated research into statically balanced systems in general and the conception of the general suspension unit in particular [5.24].

Others, many of them graduate students of various background, were no less of a stimulus to this project. Of those who were active in the field of static balancing I am particularly grateful to Gabriëlle Tuijthof [5.26] and others [5.27] for their work on the anthropomibile arm, Sérgio Tomázio and Luis Cardoso who are developing an arm support for the physically challenged [5.25], and Victor van Passel for his spring force balancer [6.6]. The project on the hand prosthesis with Hans de Visser was particularly rewarding [6.18], as is the associated project on psychophysics [6.15], which started with Marten Munneke. The same holds true for the development of several laparoscopic forceps with Marcel Horward, Wouter Sjoerdsma, Karen den Boer, and Albert van der Pijl [5.15], while other projects are still on their way [5.16]. Finally I gladly mention Fred van den Berg, who falls outside the above categories, as he devised statically balanced laparoscopic forceps [6.21]. This project also continues, by Jacco Drenth, and by Marc Brinkman, who also created a number

of the drawings in this thesis [4.3]. The contributions of these and others, such as Johan Surentu who posed sharp questions on stability every now and then, were a great stimulus for the completion of this work, not only by their professional efforts but perhaps even more so at the social level. As to this aspect, not meaning to disregard their professional achievements, I couldn't fail to mention Michiel Oderwald and Maarten de Bruijne, the poineers of the Delft Finger Group, and Arno Kemner, the first in our group to explore intrument-tissue interaction.

Jan Verbeek deserves special mention for the detailed design of many of the prototypes [5.6; 5.21; 6.5] and others not mentioned. John Dukker and Ad van der Geest transformed the drawings into material with such accuracy that it is hard to familiarize onself with tolerances, while ir J. van Rhee (Roveron BV) supplied the specially made springs for free. As mentioned in [6.11], the collaboration with rehabilitation centers De Hoogstaat and Maartenskliniek is much appreciated.

The stimulating environment in which the presented work came to being was initially formed by the Wilmer group and currently by the HuMan-Machine Systems group. I look forward to reintegrating the findings of this thesis into their field of origin together with my much valued collegues Dick Plettenburg and André Sol. I am specially grateful to Prof. dr ir Henk Stassen, who created an assitant professor position in times of budget cuts, and to the other staff for accepting me so naturally. The feeling of being at home at the office is perhaps best illustrated by the development of close friendships with colleagues: Hans Poulis and Marianne Groot, Bachtiar Arif, Arthur Aalsma, and Gabriëlle Tuijthof, other great collegues to spend survival weekends with notably Hans de Visser, Petr Havlik and Martijn Heijkens from the Equipe Zebra, and the others of MISIT, MICAB, DIPEX and DBL (including Richard van der Linde who beat me in obtaining the degree by a couple of hours), the Sweden-gang, and of course the Cyclosportive d'Epaule heroes, who all come from this environment. A similar home sensation applies to my ISPO friends Sam Landsberger, Bob Radocy, Debbie Zarubick and others, as well as my ASME friends including Clément Gosselin, Suresh Ananthasuresh, Karim Abdel-Malek, Sunil Agrawal, Mary Frecker, and Steve Canfield. Anyone I didn't mention yet? Oh yes, Nils van Leerdam, Eelco Kunst, Daan Schutte, Joris Jaspers, Marco Hoefman, and many others, who in some way helped keeping the project going. I thank them all.

A special corner is reserved for my family, to thank my grandmother, for thinking of me more than I thought of myself, to thank my mother who always stimulated my self-fulfillment even if it implied low visiting frequencies, and

Curriculum vitae

23 Aug 1966	Born in Hengelo (O.), the Netherlands.
1985-1992	MSc study Mechanical Engineering at Delft University of Technology. Graduated with honours at the Laboratory for Measurement and Control, Wilmer group, headed by Prof. ir J.C. Cool. Title of MSc-thesis: Methods for reducing energy dissipation in cosmetic gloves.
1992-1993	Civil service.
1993-1998	PhD study at the Wilmer group under supervision of Prof. ir J.C. Cool. Involved in courses Mechanical Design in Medical Technology (graduate), and Mechanical Systems (undergraduate). Supervision of MSc students.
1998-present	Assistant Professor at Delft University of Technology, HuMan-Machine Systems Group, headed by Prof. dr ir H.G. Stassen, succeeded by Prof. dr ir P.A. Wieringa. Involved in courses Mechanical Design in Medical Technology (graduate), HuMan-Machine Systems (graduate), Mechanical Systems (undergraduate), Theme Projects (undergraduate): Transportation (Vehicles, Dredging) and Energy (Turbines), and the new courses Biomechatronics (graduate), and Haptic Interface practical (graduate). Supervision of MSc and PhD students. Publications include three patents, six peer reviewed journal articles, eight peer reviewed conference papers, and over fifteen conference contributions. Awarded the GM/Freudenstein Young Investigators award at the 2000 ASME Design Engineering Technical Conference. Review coordinator for the 2001 ASME DETC.